
Properties of Tire-Derived Aggregate

For Civil Engineering Applications



California Department of Resources Recycling and Recovery

May 14, 2013

Contractor's Report
Produced Under Contract By:



Arcata, CA

Brad Finney, Ph.D., Professor
Zack H. Chandler, Jessica L. Bruce and Brian Apple
Environmental Resources Engineering

STATE OF CALIFORNIA

Edmund G. Brown Jr.
Governor

Matt Rodriguez
Secretary, California Environmental Protection Agency

DEPARTMENT OF RESOURCES RECYCLING AND RECOVERY

Caroll Mortensen
Director

Department of Resources Recycling and Recovery
Public Affairs Office
1001 I Street (MS 22-B)
P.O. Box 4025
Sacramento, CA 95812-4025
www.calrecycle.ca.gov/Publications/
1-800-RECYCLE (California only) or (916) 341-6300

Publication # DRRR-2014-1489

 To conserve resources and reduce waste, CalRecycle reports are produced in electronic format only. If printing copies of this document, please consider use of recycled paper containing 100 percent postconsumer fiber and, where possible, please print images on both sides of the paper.

Copyright © 2013 by the California Department of Resources Recycling and Recovery (CalRecycle). All rights reserved. This publication, or parts thereof, may not be reproduced in any form without permission.

Prepared as part of contract number DRR 10066 for \$230,000.

The California Department of Resources Recycling and Recovery (CalRecycle) does not discriminate on the basis of disability in access to its programs. CalRecycle publications are available in accessible formats upon request by calling the Public Affairs Office at (916) 341-6300. Persons with hearing impairments can reach CalRecycle through the California Relay Service, 1-800-735-2929.

Disclaimer: This report was produced under contract by Humboldt State University. The statements and conclusions contained in this report are those of the contractor and not necessarily those of the Department of Resources Recycling and Recovery (CalRecycle), its employees, or the State of California and should not be cited or quoted as official Department policy or direction.

The state makes no warranty, expressed or implied, and assumes no liability for the information contained in the succeeding text. Any mention of commercial products or processes shall not be construed as an endorsement of such products or processes.

Abstract

Properties of Tire-Derived Aggregate for Civil Engineering Applications

Disposal costs of scrap tires have prompted researchers to investigate beneficial reuses. One important application is the use of tire chips as tire-derived aggregate (TDA), which can be a substitute for rock aggregate in civil engineering applications.

Properties of TDA were investigated through a series of experiments using type A TDA (maximum 8-in. length), type B TDA (maximum 12-in. length) and a type A/type B TDA mixture. Three areas of testing were completed on TDA, which included physical properties, substitution of rock aggregate by TDA in leach fields, and exothermic properties of TDA.

A small and large magnitude dynamic vertical compression test was completed using tri-axial cylinders to measure the compressibility of TDA. Density, weight specific gravity, void ratio, and porosity were also calculated during testing.

During compression testing, TDA initially exhibited plastic compression under load, but after the material was subjected to compressive loads it behaved like an elastic material. A constant-head permeameter, under loads up to 95 psi, was used to measure the hydraulic conductivity of tested TDA. The hydraulic conductivity varied for all tests by TDA type, applied pressure, and hydraulic gradient. Implications of substituting TDA for gravel were also investigated using simulated septic leach fields.

Results indicated that TDA was a viable substitute for rock aggregate for onsite septic systems, in regards to wastewater treatment and durability. The TDA experimental leach field had increased microbiological growth occurring within the media and the effluent quality significantly differed for some constituents when compared to the rock aggregate leach field. A thermal analysis was completed for temperature changes of type A TDA in (1) a septic leach field, (2) a 20-ft.-tall column of packed TDA, and (3) an underground earthen pit, where the TDA was installed within 12 hours of manufacturing.

In all of the thermal experiments, type A TDA did not react hazardously via exothermic oxidation reactions.

This page is intentionally left blank.



Table of Contents

Abstract.....	i
Properties of Tire-Derived Aggregate for Civil Engineering Applications	i
List of Acronyms	ix
Introduction.....	1
Background.....	3
TDA and Parent Tire Characteristics	3
Water Quality and Biological Implications of Using TDA	4
Studies on Exothermic Reactions in TDA Fills	6
Studies on Compression Testing of TDA	7
Hydraulic Conductivity of TDA	8
Methodology and Application	11
Sieve Analysis for TDA.....	11
Suitability of TDA as a Septic Leach Field Media	12
Exothermic Behavior of Deep TDA Fills	16
Exothermic Behavior of TDA Under Immediate Fill Conditions.....	23
Compression Testing of TDA for Varied Loads.....	28
Determining Physical Properties of TDA Under Moderate Load.....	34
Determining Hydraulic Conductivity of TDA Under Large Loads	41
Results and Discussion	44
Comparison of Rock Aggregate and TDA as Leach Field Media	45
Exothermic Behavior of Deep TDA Fill.....	71
Exothermic Behavior of TDA Under Immediate Fill Conditions.....	74
Sieve Analysis for TDA.....	80
Compression Testing of TDA for Varied Loads.....	80
Physical Properties of TDA	85
Conclusions and Recommendations	93
Conclusions.....	93
Recommendations for Further Work	95
References.....	97

List of Tables

Table 1. Type A and type B specifications for TDA used in project experiments.	3
Table 2. The compositional components of a typical rubber tire.....	4
Table 3. Components of a typical tire from the Goodyear Tire Company.....	4
Table 4. Cases of observed self-combustion incidents in TDA fills.....	6
Table 5. Typical untreated domestic wastewater composition	12
Table 6. Physical characteristic values for the 20 mil linear low density polyethylene	13
Table 7. Comparative statistics for the leach field media and air temperature	48
Table 8. Water quality constituents that had no detectable concentrations observed.....	51
Table 9. Regulatory water quality parameter values compared to maximum values found	52
Table 10. Results from a Student’s t-Test for water quality parameters.....	54
Table 11. Comparative statistics for temperature over a 20 ft. tall cylinder filled.....	71
Table 12. Physical Parameters of type A, B, and A/B mixed TDA.....	87
Table 13. Physical properties of TDA reported in the literature.....	88
Table 14. Literature values for the hydraulic conductivity of TDA materials.....	90
Table 15. Parameter values for a predictive model of hydraulic conductivity	92

List of Figures

Figure 1. Cross section of the experimental fill used by Humphrey and Katz (2000).....	5
Figure 2. A schematic diagram of the permeameter used by Edil and Bosscher (1994)	8
Figure 3. A cross section (A) and plan view (B) of the leach fields	14
Figure 4. Leach field setup of the geomembrane layer (A) and the top soil (B).....	15
Figure 5. Leach field influent piping arrangement (A) and central extraction points.....	17
Figure 6. Short weirs in the middle of the leach field.....	18
Figure 7. Temperature data was collected in the middle of the leach fields	19
Figure 8. Side view (A) and plan view (B) of the 20 ft. tall tower filled with type A TDA.	20
Figure 9. Vertical temperature differences of type A TDA	21
Figure 10. A cross sectional view of the 20 ft. tall tower shown in Figure 9	22
Figure 11. An illustration of the earthen pit filled with type A TDA	24
Figure 12. The 1000 ft ³ earthen pit excavated below ground level.....	25
Figure 13. The vibratory compacter used (A) and general location of temperature probes	26
Figure 14. Electronic equipment was powered by the three solar panels	27

Figure 15. Experimental device used to compress TDA.....	30
Figure 16. The cast iron latching mechanism (A) connects the steel cylinder.....	31
Figure 17. Pressure transducer locations inside the 29.7 in. diameter compression cylinder	32
Figure 18. The apparatus used to test large magnitude compressions of TDA.....	33
Figure 19. Bottom section of the small magnitude hydraulic conductivity experiment	37
Figure 20. Full setup of the small magnitude hydraulic conductivity experiment.....	38
Figure 21. Measurement distance used for the vertical displacement of the type A TDA	39
Figure 22. An experimental run of a static load hydraulic conductivity test for type A TDA.....	40
Figure 23. Control valve illustration and setup of large magnitude hydraulic conductivity tests..	43
Figure 24. Microorganism growth on rock aggregate after 7, 10, and 17 months.....	46
Figure 25. Microorganism growth on TDA after 7, 10, and 14 months	47
Figure 26. Effluent water clarity is shown for rock and TDA leach fields initially (A) and	47
Figure 27. Average daily media and air temperature for the experimental leach fields containing rock and TDA (gaps in data are a result of temperature probe failure).	49
Figure 28. First seven weeks of average daily temperature within/outside the leach fields	50
Figure 29. Iron concentrations in the rock and TDA leach fields.....	56
Figure 30. Manganese concentrations in the rock and TDA leach fields	57
Figure 31. Zinc concentrations in the rock and TDA leach fields	58
Figure 32. Sulfate concentrations in the rock and TDA leach fields	63
Figure 33. Nitrate (as N) concentrations in the rock and TDA leach fields.....	64
Figure 34. Ammonia (as N) concentrations in the rock and TDA leach fields.....	65
Figure 35. Influent and effluent ammonia + nitrate concentrations.....	66
Figure 36. COD concentrations in the rock and TDA leach fields	67
Figure 37. Total phosphate (as P) concentrations in the rock and TDA leach fields.....	68
Figure 38. Methylene chloride concentrations in the rock and TDA leach fields.	69
Figure 39. Toluene concentrations in the rock and TDA leach fields.	70
Figure 40. Daily average temperature changes of confined type A TDA.....	72
Figure 41. The 1st week of temperature results for confined type A TDA	73
Figure 42. Native soil and ambient temperatures at the Keifer landfill	75
Figure 43. TDA temperatures at 1.3 feet below the ground surface.....	76
Figure 44. TDA temperatures at 4.5 feet below the ground surface.....	77
Figure 45. TDA temperatures at 9 feet below the ground surface.....	78
Figure 46. Changes in temperature with depth, five feet from the wall of the earthen pit	79

Figure 47. Particle size distribution of TDA used in six different experiments.....	81
Figure 48. Vertical strain on type A TDA resulting from a static load of about 2.95 psi	82
Figure 49. Vertical strain versus stress for various types of TDA	83
Figure 50. Type B TDA before (A) and after (B) a large magnitude compression experiment	84
Figure 51. Hydraulic conductivity is shown against the hydraulic gradient for TDA	89
Figure 52. Hydraulic conductivity of type A TDA vs. load at various hydraulic heads.....	91
Figure 53. Hydraulic conductivity of type A TDA vs. hydraulic head at various loads.....	91
Figure 54. Hydraulic conductivity of type A and B TDA vs. loading at various hydraulic heads	92

List of Appendix Figures

Figure C-1. Iron concentrations in the rock and TDA leach fields	117
Figure C-2. Lead concentrations in the rock and TDA leach fields.....	118
Figure C-3. Manganese concentrations in the rock and TDA leach fields	119
Figure C-4. Zinc concentrations in the rock and TDA leach fields	120
Figure C-5. Chloromethane concentrations	121
Figure C-6. Methylene Chloride concentrations in the rock and TDA leach fields.....	122
Figure C-7. Chloroform concentrations in the rock and TDA leach fields.....	123
Figure C-8. Toluene concentrations in the rock and TDA leach fields	124
Figure C-9. Naphthalene concentrations in the rock and TDA leach fields	125
Figure C-10. Trichlorobenzene (1,2,3) concentrations	126
Figure C-11. Surrogate for trichlorobenzene (1,2,3): 1,2-dichloroethane-d4 concentrations.....	127
Figure C-12. Surrogate for trichlorobenzene (1,2,3): dibromofluoromethane concentrations	128
Figure C-13. Surrogate for trichlorobenzene (1,2,3): toluene-d8 concentrations	129
Figure C-14. Sulfate concentrations in the rock and TDA leach fields	130
Figure C-15. Ammonia (as N) concentrations in the rock and TDA leach fields.....	131
Figure C-16. Nitrate (as N) concentrations in the rock and TDA leach fields.....	132
Figure C-17. BOD concentrations in the rock and TDA leach fields	133
Figure C-18. Non-filterable residue concentrations.....	134
Figure C-19. pH in the rock and TDA leach fields	135
Figure C-20. COD concentrations in the rock and TDA leach fields	136
Figure C-21. Total phosphate (as P) concentrations	137
Figure C-22. Fecal coliform in the rock and TDA leach fields	138
Figure C-23. Total coliform in the rock and TDA leach fields.....	139

Figure C-24. Total Kjeldahl nitrogen concentrations	140
Figure D-1. Plan view of the rock and tire-derived aggregate leach fields (Wright, 2011).....	143
Figure D-2. Side view of the rock and TDA leach fields (Wright, 2011).....	144
Figure D-3. Cross-sectional and plan view of the effluent setup for rock TDA leach fields.....	145
Figure D-4. Side view of the tower containing type A TDA (Wright, 2011).	146
Figure D-5. Plan view of the tower containing type A TDA (Wright, 2011)	147
Figure E-1. Native soil and ambient temperatures for the Keifer landfill.....	150
Figure E-2. Temperatures at 1.3 ft. below the ground surface in the TDA pit.	151
Figure E-3. Temperatures at 2.5 ft. below the ground surface in the TDA pit.	152
Figure E-4. Temperatures at 3.7 ft. below the ground surface in the TDA pit.	153
Figure E-5. Temperatures at 4.5 ft. below the ground surface in the TDA pit.	154
Figure E-6. Temperatures at 6.0 ft. below the ground surface in the TDA pit.	155
Figure E-7. Temperatures at 7.0 ft. below the ground surface in the TDA pit.	156
Figure E-8. Temperatures at 9.0 ft. below the ground surface in the TDA pit.	158

Appendices

Appendix A. Leach Field Water Quality Parameters	101
Appendix B. Lab Analysis Results For Leach Fields	103
Appendix C. Water Quality Graphs-Leach Fields	116
Appendix D. Computer Aided Design Drawings	141
Appendix E. Temperature Results From TDA Pit.....	148

This page is intentionally left blank.

List of Acronyms

ASTM	American Society for Testing and Materials
AWWTP	Arcata Wastewater Treatment Plant
BOD	Biological oxygen demand
CalRecycle	California Department of Resources Recycling and Recovery
COD	Chemical oxygen demand
EPA	U.S. Environmental Protection Agency
HSU	Humboldt State University
LLDPE	Linear low density polyethylene
MCL	Maximum contaminant level
PVC	Polyvinyl chloride
TDA	Tire-derived aggregate
TGA	Thermo-gravimetric analysis
TSS	Total suspended solids
TTC	TDA Technology Center
VOC	Volatile organic compounds

This page is intentionally left blank.



Introduction

Vehicle usage has led to disposal concerns for waste tires in many regions of the world (waste tires are used tires unsuitable for use on vehicles). In California, there were approximately 41.1 million waste tires generated in 2010 and about 7.8 million of those waste tires were deposited in landfills (CalRecycle, 2010). Approximately 250,000 waste tires remain in stockpiles throughout California, posing a potential threat to public health, safety, and the environment (CalRecycle, 2012).

Recycling is an alternative to landfilling or stockpiling waste tires. One method for waste tire recycling is the use of tire-derived aggregate (TDA) as a lightweight construction material. TDA is composed of recycled waste tires that are shredded to a standard size for use in a range of civil engineering applications. Recycling scrap tires, through the manufacturing of TDA, can reduce the volume of waste tires that are stored or scrapped in landfills.

While there have been some successful construction projects that have used the material, additional knowledge of TDA properties may result in more widespread adoption of this valuable resource in construction applications.

This report provides results from experiments that determined material properties relevant to the use of TDA in a variety of engineering applications. Testing was completed with type A TDA, type B TDA, and a type A/type B TDA mixture. Type A and type B TDA contain tire fragments with maximum lengths of 8 in. and 12 in., respectively.

TDA was investigated through a series of experiments to determine the (1) compressibility, (2) physical properties, (3) suitability of TDA use in a leach field, and (4) the tendency of TDA to self-combust due to exothermic reactions in static piles. A small and large magnitude dynamic vertical compression test was completed using tri-axial cylinders to measure the compressibility of TDA.

A constant-head permeameter was then used to measure the hydraulic conductivity of type A and type B TDA. To test the suitability of replacing rock with TDA in leach fields, leachate effluent water quality was determined over a 14-month period.

In the past, numerous cases of self-ignited fires have occurred within TDA fills. Self-ignited fires are considered to be a result of increased temperatures from exothermic reactions in TDA material.

Therefore, temperature changes of static TDA fills were analyzed in several settings:

1. A septic leach field filled with type A TDA to analyze the temperature of TDA in a simulated septic leach field.
2. A 20-ft.-tall column of packed type A TDA to provide a thermal analysis of a static TDA fill.
3. A 1000 ft³ earthen pit below the ground surface to provide information on the thermal properties of a type A TDA fill directly after being produced.

This page is intentionally left blank.

Background

A background analysis of tire-derived aggregate (TDA) was completed to assess the validity of results and create quantifiable experiments. The properties of TDA were reviewed in the literature for the following topics: water quality of leachate from leach fields, temperature analyses, compressive behaviors, and hydraulic conductivities. The background should provide an understanding of previous experimental activities completed by researchers and their relation to the methods conducted in the Methodology and Application section.

TDA and Parent Tire Characteristics

TDA is categorized by the materials aggregate size, which can vary depending on different manufacturing techniques. The American Society for Testing and Materials (ASTM) (2012) define dimensions for tire chips as 0.472-1.97 in., dimensions for tire shreds as 1.97-12 in., and dimensions for tire granulated rubber as 0.0167-0.472 in. Tire fragments have been classified in construction practice as type A or B. Type A, and type B TDA contain tire fragments with maximum lengths of 8 in. and 18 in., respectively (see Table 1 for specifications). The manufacturing process requires sharp knives to shear tires into a predefined size (Humphrey, 2003). However, the manufacturing process does not produce homogeneous mixtures of TDA with size classifications specified in Table 1; therefore, TDA may contain any proportion of tire shreds, chips or granulated rubber.

Table 1. Type A and type B specifications for the tire-derived aggregate used in project experiments.

Parameter Tested	Type A TDA Specification	Type B TDA Specification
Maximum (Max.) Percent Free Steel (%)	1	1
Max. Longest Shred (in.)	8	18
Max. Weight of Shreds >12 in. of total (%)	0	10
Maximum Passing No. 4 sieve (0.187 in.) (%)	5	1
Maximum Number of Sidewall Shreds in Mixture	1	1
Max. Weight of Shreds >2 in. wire exposed (%)	10	10
Max. Weight of Shreds >1 in. wire exposed (%)	25	25

Source: Values taken from Scardaci et al. 2012

Passenger car tires have similar physical and chemical characteristics, but with so many subtle material differences between brands, it is impossible to know the exact composition of any tire within a TDA sample (Grimes et al., 2003). A few investigators have provided general chemical and physical characteristics of tires. The Texas Natural Resource Council Commission (1999) found that tires typically contain 85 percent carbon, 10-15 percent ferric material, and 0.9-1.25 percent sulfur. An analysis by Dodds et al. (1983) showed that the following components are in tires: a vulcanized rubber, a rubberized fabric reinforced with textile cords, a mass of steel or fabric belts, and a mass of steel-wire reinforced rubber beads. Vulcanization is a chemical process for converting rubber or related polymers into more durable materials via the addition of additives. Compounds that make up the components presented by Dodds et al. (1983) follow the typical weight percentages shown in Table 2. A more recent tire

composition analysis was presented by Amoozegar and Robarge (2006) (Table 3) Components that make up tires provide various functions including: (1) carbon black, which acts as a strengthening element and adds abrasion resistance to rubber; (2) sulfur molecules, which harden rubber; (3) accelerators, which act as a catalyst for vulcanization; (4) extender oil, which softens rubber; and (5) zinc oxide/stearic acid, which act as aids in vulcanization (Dodds et al., 1983).

Table 2. The compositional components of a typical rubber tire

Component	Weight %
Styrene Butadiene Copolymer	62.1
Carbon Black	31
Extender Oil	1.9
Zinc Oxide	1.9
Stearic Acid	1.2
Sulfur	1.1
Accelerator	0.7
Total	99.9

Source: Dodds et al., 1983

Table 3. Components of a typical tire from the Goodyear Tire Company

Component	Weight %
Carbon Black	28
Synthetic Rubber	27
Natural Rubber	14
Steel Wire	10
Extender Oil	10
Other Petrochemicals	4
Organic Fabric	4
Sulfur, Zinc Oxide and Other Compounds	3
Total	100

Amoozegar and Robarge, 2006

Water Quality and Biological Implications of Using TDA

Studies on the substitution of rock aggregate with TDA have been completed for septic system leach fields. These studies have focused on water quality and biological analyses above the groundwater table. Chenette Engineering, Inc. (1993), in Montpelier, Vt., built two leach fields for a four-bedroom residential septic system. Each trench was 4 ft. by 70 ft. with a 12-in. thick layer of tire shreds placed

around the drainpipes. Two lysimeters were used to sample effluent at a depth of 36 in. below tire shreds used in the leach fields. Sampling was performed monthly for about seven months. Of the 12 metals analyzed, all were present at negligible concentrations except for iron and lead, which were initially measured at 0.43 mg/L and 0.038 mg/L, respectively (Chenette Engineering, Inc., 1993). Metal concentrations dropped below iron and lead groundwater standards within one to two months of the initial study. No rock aggregate leach fields were built for a control analysis, therefore the source of iron and lead concentrations were unknown.

Humphrey and Katz (2000) created an experiment beneath a state highway to investigate the water quality effects of tire shred fills placed above the groundwater table. Both filtered and unfiltered water samples were collected in geomembrane-lined locations beneath the shoulder of a road (Figure 1). Approximately 2 ft. of tire shreds, with a maximum 3 in. size, were covered by a granular soil. They found negligible concentrations of 82 volatile organic compounds and 69 semi-volatile organic compounds in their sampling results. Inorganic constituent samples were taken quarterly from January 1994 through June 1999 and three samples of volatile and semi-volatile organic compounds were also taken. When compared with natural background levels in the groundwater, they found no evidence that the presence of tire shreds altered chromium, lead, selenium, cadmium, barium, aluminum, zinc, chloride, or sulfate concentrations. Iron and manganese levels exceeded secondary standards in a few samples but were not considered a critical concern because these metals are categorized under secondary drinking water standards.

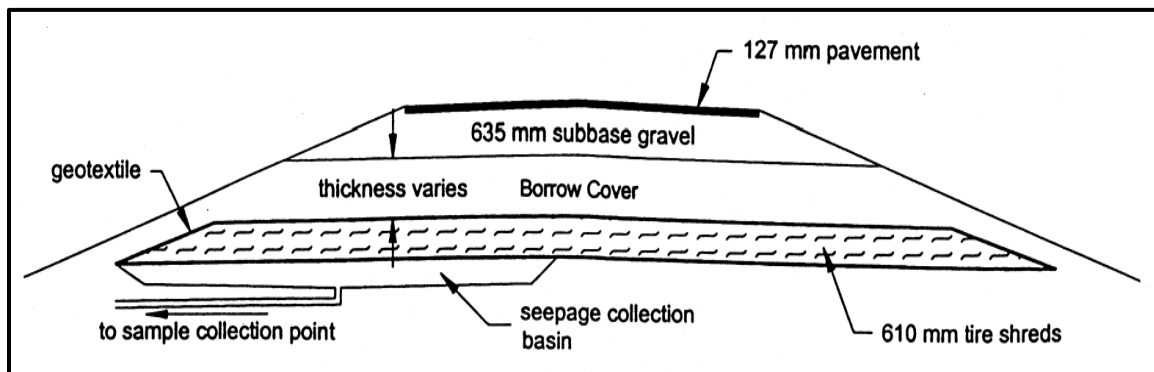


Figure 1. Cross section of the experimental fill used by Humphrey and Katz (2000).

Sengupta and Miller (2000) installed three leach fields in Chelsea, MA, which were dosed with septic tank effluent. The septic tank effluent was piped to a distribution box, which sent effluent to the leach fields on a timed cycle. Samples of wastewater were collected approximately every 14 days for about seven months from each leach field and the distribution box. They found that under typical septic system conditions, both tire chip leachate and stone aggregate leachate contained high concentrations of iron. Iron concentrations, however, did not surpass any maximum contaminant levels (MCL) for water quality and therefore did not pose a health threat. Grimes et al. (2003) found that the media in TDA leach fields have, in the presence of iron and other unknown factors, enhanced macro-biological growth. Spagnoli et al. (2001) also found that manganese was higher in the tire chip leachate than in the rock aggregate leachate. However, Sengupta and Miller (2000) showed that manganese concentration was of equivalent concentrations in rock and TDA leach fields, and although the concentration fluctuated, effluent concentrations of manganese were higher than influent concentrations and higher than the secondary drinking water MCL. Zinc concentrations in the leachate were also found to be lower than secondary drinking water standards for both rock and TDA (Sengupta and Miller, 2000).

Grimes et al. (2003) found that wastewater treatment efficiency using TDA was equivalent to rock aggregate in leach fields. Water quality constituents considered in their study included: biological oxygen demand, chemical oxygen demand, total suspended solids, ammonia, nitrate, fecal coliforms, and pH. Wastewater treatment efficiency in TDA leach fields may take several months to reach the same rates as rock aggregate trenches (Robinson (2000); Sengupta and Miller (1999, 2000); Spagnoli et al. (2001)). Spagnoli et al. (2001) and Gunasekara et al. (2000) found that volatile and semi-volatile compounds do not enter leachate and that the ground rubber and tire chip material actually removed some organic compounds.

Macrobiology of tire chips, in comparison to rock aggregate systems, have previously been examined in North Carolina and South Carolina (Grimes et al., 2003; Amoozegar and Robarge, 2006). Results from past studies revealed that a thick biological material covered tire material over time and invertebrates were also actively present within the media. Nematodes were found in two-year-old septic systems and trophic levels of microorganisms and macroorganisms were present in eight-year-old septic systems. These results demonstrated that additional wastewater treatment was occurring in TDA leach fields, via organismic growth, which provided an ecologically suitable environment. The organisms found in TDA leach fields included grazers, saprophytic feeders, protozoa, and filter feeders (Grimes et al., 2003). The diversity of organisms in TDA leach fields demonstrates the potential for additional levels of wastewater treatment.

Studies on Exothermic Reactions in TDA Fills

Several incidents of self-combustion have been observed from using TDA as a construction material (Table 4). In these incidents, TDA self-ignited after construction without any known external cause. Careful study of self-combustion cases resulted in design guidelines to avoid the problem. Avoidance guidelines included: (1) tire shreds should be free of contaminants such as oil, grease, gasoline, and diesel fuel that could create fires; (2) tire shreds should not contain the remains of tires that have been previously subjected to a fire (liquid remnants of tires may cause a fire); and (3) TDA layers should be limited to a 3 m thickness unless an intermediate non-combustible layer is present (Ad Hoc Civil Engineering Committee, 2002). Exothermic reactions were identified as the main problem in regards to self-combustion, but the oxidation of steel belts and/or oxidation of rubber were also possible causes (Arroyo et al., 2011). Other contributing factors included increased oxygen concentrations from free air intrusion, increased water presence, very thick layers of TDA, and a large amount of air exposed steel belt exposed to the air (Arroyo et al., 2011).

Table 4. Cases of observed self-combustion incidents in TDA fills

Case	TDA Fill Height (ft.)	Time between Construction and Self Combustion (months)
Road Embankment, Ilwaco, WA	16.4	5
Road Embankment in Garfield County, CO	39.4	6-8
Retaining Wall in Glenwood Canyon, CO	19.7-26.2	10-12

Source: Humphrey, 2003; Wappett and Zornberg, 2006.

Aydilek et al. (2006) investigated the self-combustion of tire chips in a landfill leachate collection system. Approximately 3.28 ft. of TDA, with about a 1-4 in. size distribution, was used to test spontaneous combustion properties. Aydilek et al. (2006) found insignificant combustion hazards due to low

background values of carbon monoxide, oxygen, and temperature. The primary mechanisms responsible for non-self-combustion were determined to be small thicknesses of TDA layers and a lack of oxygen in the testing cells used. The temperature of the top TDA layer was consistently near the ambient air temperature, while lower TDA layers had 50-68 °F warmer temperatures than ambient conditions during winter months (Aydilek et al., 2006).

To determine the thermal stability of scrap tires in air, Moo-Young (2003) performed a thermo-gravimetric analysis (TGA), a thermal analysis technique used to measure changes in the weight mass of a sample as a function of temperature and/or time. TGA is commonly used to determine degradation temperatures, residual solvent levels, absorbed moisture content, and the amount of inorganic non-combustible filler in material composition (Moo-Young, 2003). Moo-Young (2003) found that, in general, tire shreds were stable up to temperatures of about 392 °F. This high temperature stability indicates that other mechanisms may be attributed to exothermic reactions in self-combusting tire fills (such as reasons described previously that were postulated by Arroyo et al., 2011).

Studies on Compression Testing of TDA

Compressional testing has been completed by a number of researchers. Ahmed (1993) completed compressibility tests on tire chips alone and with soil/tire chip mixes. Testing materials included Ottawa sand and Crosby till, tire chips varying in sizes from 0.5-2 inch, and a 12-inch diameter compression device. Ahmed (1993) showed that varying rubber/soil mixtures increased the total compression with increasing percent of tire chips—where the highest value of compression was observed when using 100 percent tire chips. Ahmed (1993) also found that mixed blends of rubber-soil provide lower void ratios and less future settlement of overhead fill material over time (also known as creep). A rubber-sand mixture was suggested for use as a lightweight geomaterial where structural settlements need to be minimized.

Edil and Bosscher (1994) implemented compaction tests based on ASTM test D698 and ASTM test D1557. These procedures involve the use of 4-inch or 6-inch diameter experimental compressional devices. Edil and Bosscher (1994) described the mechanism of compression for tire chips as: (1) reorientation of tire chips into compact arrangements, and (2) compression of individual tire chips under stress. Compressibility of tire chips was found to be high compared to soils and would be a foremost design factor in any fill applications.

Edil and Bosscher (1994) showed that initial plastic compression was exhibited by tire chip/soil mixtures under load, which was as high as 40 percent of the initial thickness. They showed that once the material was subjected to compressive loads, it behaved as an elastic material. Bressette (1984) confirmed that used tire materials are capable of extreme deformation when subjected to static loading. Bressette (1984) found a 25 percent change in height for 2-in. shredded tire material and a 12 percent change in height for 2-inch square tire material. When vibrated for eight minutes, the tire materials underwent further deformation (an additional 3 percent change for 2-inch shredded tires and 2 percent change for 2-inch square tires). Edil and Bosscher (1994) explained that constant overhead pressures above tire chip fills would limit the elastic behavior after compression.

Humphrey and Manion (1992) also tested the compressibility of 2-inch (maximum size) tire aggregate using ASTM test D698 and ASTM test D1557. They used a 10-in. diameter compaction mold with a 10-inch height in a thick-walled cast aluminum bucket. Compressibility testing revealed that tire chips were highly compressible, but compressibility decreased as the stress level increased. They found a maximum vertical strain of nearly 50 percent. Humphrey and Manion (1992) agreed that side friction was a significant factor in compression testing because it caused the vertical stress to decrease from top-down in the compressional device, which was measured to be 10-40 percent of the total applied load.

Hydraulic Conductivity of TDA

TDA has generally been used as a drainage material due to its relatively high hydraulic conductivity compared to most soils. Previous studies have indicated this in different experimental settings. Bressette (1984) evaluated the hydraulic conductivity of three different types of compacted and non-compacted TDA material. The TDA materials and test equipment included: 2-inch square chopped tires; 2-in. shredded tires; Class 3 coarse aggregate; and an 11.8 inch diameter constant head permeameter. The range of hydraulic conductivities found for non-compacted samples was 0.160-1.94 ft/s, and for compacted samples the values varied from 0.0949-0.721 ft/s. The results indicate that compaction of tire does have a significant impact on hydraulic conductivities.

Edil and Bosscher (1994) measured the hydraulic conductivity under varying pressures using a special constant-head, rigid-wall permeameter. The device was constructed of a rigid steel ring with a diameter of approximately 11.2 inch (Figure 2). They calculated the hydraulic conductivity values without any correction for equipment resistance, which they determined may provide lower values for hydraulic conductivities by as much as an order of magnitude. Edil and Bosscher (1994) found that the hydraulic conductivity of pure tire chips, without loaded pressure, depended on the hydraulic gradient.

Results from their testing provided hydraulic conductivities of approximately 0.0148 to 0.0197 ft/s for confining pressures of 0 to 14.5 psi, respectively. However, the hydraulic conductivity varied significantly with various tire chip and sand mixtures. They also found that applied pressures reduced porosity and caused reductions in the hydraulic conductivity of tire chips. Nevertheless, the material was found to have a relatively high hydraulic conductivity, compared to rock, under typical drainage applications.

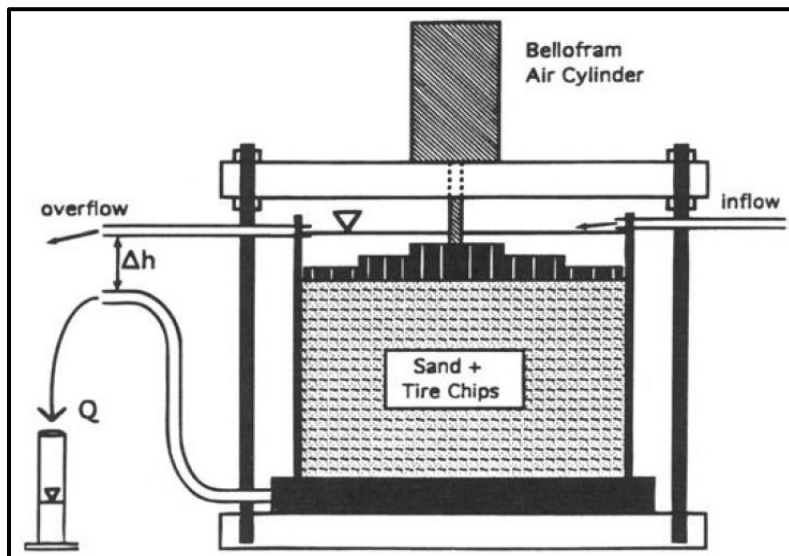


Figure 2. A schematic diagram of the permeameter used by Edil and Bosscher (1994).

Reddy and Saichek (1998a) determined the hydraulic conductivity of shredded tire chips with an average chip size of 3 in. using an 11.8 in. diameter compressional cylinder. They found that as the normal stress increased, tire chip compression increased. This occurred until the hydraulic conductivity decreased by three orders of magnitude at a maximum compression of 21,000 lb_f/ft² (146 psi). The results showed that shredded tires performed effectively as a drainage medium.

The ASTM has developed many standards and practices in material testing for engineering design. For TDA, the hydraulic conductivity can be estimated using ASTM test D2434 using a constant head permeameter for particle sizes smaller than 0.75 inch (ASTM, 2006). However, TDA generally has particles greater than 0.75 inch therefore, larger hydraulic conductivity testing apparatus' are needed. The ASTM has developed appropriate testing procedures for TDA resulting in ASTM test D6270. This test describes measuring the hydraulic conductivity with a constant head permeameter that has a diameter several times greater than the maximum particle size of the TDA, or 8 and 18 inches for type A and B TDA, respectively (ASTM, 2012).

This page is intentionally left blank.

Methodology and Application

A series of experiments were conducted to determine several physical properties of TDA, the suitability of TDA to act as a substitute for rock aggregate in a leach field, and the potential for dangerous exothermic behavior in a static pile of TDA. A sieve analysis was completed to determine the classification (e.g. type A or B) of the tire material used in all of the experiments. Rock and TDA leach fields were constructed and loaded with wastewater for 14 months to determine the differences in behavior and effluent quality between the two media. Temperature changes in TDA fills were analyzed in a 20 ft. tall tower and a 1000 ft³ excavated earthen pit. Temperature variations within the leach fields were also tested at several depths. Lastly, the hydraulic conductivity, density, and compressibility of TDA under a variety of loading conditions were determined. The methods and procedures used for each of these experiments are presented in the sections that follow.

Sieve Analysis for TDA

A sieve analysis was completed to determine the particle size distribution for a sample of each batch of TDA used in this project. Gradation studies were performed to determine whether the tire material met type A or B TDA specifications. A sample of each batch of tire material used in the experiments was tested by the TDA Technology Center (TTC) at California State University, Chico. Two batches had been characterized by the TDA supplier as type A, and two batches as type B. A third batch was prepared by mixing equal parts of the purported type A and B material. Evaluation of type A and type B TDA specifications was accomplished by using a gradation process and physical data from the maximum TDA size, the percent of exposed wires, and the unconnected free steel in samples (results are shown in Figure 47).

The gradation process involved a gradation standard created by the TTC. The procedure was completed by the TTC for type A, type B and a type A/type B mixture using the following process (Scardaci et al., 2012; Winter and Cheng, 2012):

1. Measure the total weight of the sample.
2. Check and measure the weight of tire pieces with average metal that protrude more than one inch from the cut edge of the TDA samples.
3. Check and measure the weight of tire pieces with average metal that protrude more than two inches from the cut edge of the TDA samples.
4. Measure the weight and number of pieces for each TDA sample which have a maximum dimension, measured in any direction, of 18 inches or greater.
5. Measure the weight and number of pieces for each TDA sample which have a maximum dimension, measured in any direction, between eight and 12 inches.
6. Measure the weight and number of pieces for each TDA sample which have a maximum dimension, measured in any direction, of eight inches or less.
7. Check and measure if any pieces are retained on an eight inch square mesh sieve.
8. Measure the weight retained on a four inch square mesh sieve.
9. Measure the weight retained on a three inch square mesh sieve.
10. Measure the weight retained on a 1.5 inch square mesh sieve.

11. Measure the weight retained on a 0.015 inch sieve.
12. Measure the weight retained in a pan and the weight of unconnected free steel.

Suitability of TDA as a Septic Leach Field Media

Construction of a septic tank leach field was completed to allow comparison of TDA as a substitute for rock aggregate media. The leach field was constructed adjacent to an oxidation pond at the city of Arcata’s wastewater treatment plant. Typical domestic wastewater sewage is characterized by the parameter values shown in Table 5. The oxidation pond water had already received primary treatment (screening and settling) and was chosen because it was assumed to best simulate the quality of water leaving a normal septic tank.

The leach field dimensions were roughly 40 ft. x 2 ft. x 2 ft. (Figure 3) and it was covered with two feet of top soil (Figure 4B). Two leach lines were built parallel to each other, one trench using rock aggregate and the other trench using type A TDA (Figure 3). Each trench was lined with a 20 mil linear low density polyethylene (LLDPE) geomembrane liner to prevent wastewater from permeating surrounding soil. Physical properties of the geomembrane liner were provided by the manufacturer (Table 6). Perforated 4-inch polyvinyl chloride (PVC) distribution piping was used in the leach field (Figure 4A). Effluent from both leach fields flowed through outlet pipes into a catchment basin (Figure 3A and Figure 5A), where sump pumps returned the effluent back into the oxidation pond.

Approximately equal volumes of influent from the same oxidation pond were pumped through each trench for 17 months. Flow in each trench was measured with an accuracy of ± 0.001 gpm using a Signet 2551 magnetic flow meter (Georg Fischer Signet, 2011) to maintain consistency in the volume of water entering both leach fields (Figure 5B). The delivery system was designed to be similar to the discharge from a household septic tank. Pumps ran on a set time schedule for approximately 4.5 hours per day to mimic household peak wastewater discharge, with loading from 7:30 a.m.-9 a.m., 1 p.m.-2:30 p.m., and 5 p.m.-6:30 p.m.

Table 5. Typical untreated domestic wastewater composition

Constituent	Weak	Medium	Strong
Ammonia (as Nitrogen) (mg/L)	10	25	50
BOD ₅ (as O ₂) (mg/L)	100	200	300
COD (as O ₂) (mg/L)	250	500	1,000
Total Suspended Solids (mg/L)	120	210	400
Sulfate (mg/L)	20	30	50
Total Kjeldahl (mg/L) (as Nitrogen)	20	40	80
Total Phosphorus (as P) (mg/L)	5	10	20

Source :
Adapted from Davis, 2011.

Table 6. Physical characteristic values for the 20 mil linear low density polyethylene geomembrane liner used.

Property	Test Method	Minimum Roll Averages	Typical Roll Averages
Nominal Thickness (mil)	ASTM D 5199	20	21
Density (g/cm ³)	ASTM D 1505	0.92	0.92
Carbon Black Content (%)	ASTM D 1603*	2	2.5
Min. Tensile Strength at Break (lb _f /in. of width)	ASTM D638	76	95
Min. Tensile Elongation at Break (%)	ASTM D638	800	875
Tear Resistance (lb _f)	ASTM D 1004	11	13
Puncture Resistance (lb _f)	ASTM D 4833	30	39
Bonded Seam Strength (lb _f /in. of width)	ASTM D4545*	40	45
Seam Peel Adhesion (lb _f /in. of width)	ASTM D4545*	30	36
Hydrostatic Resistance (psi)	ASTM D751	118	122

Source: Raven Industries Inc., 2003.

Note: *Modified

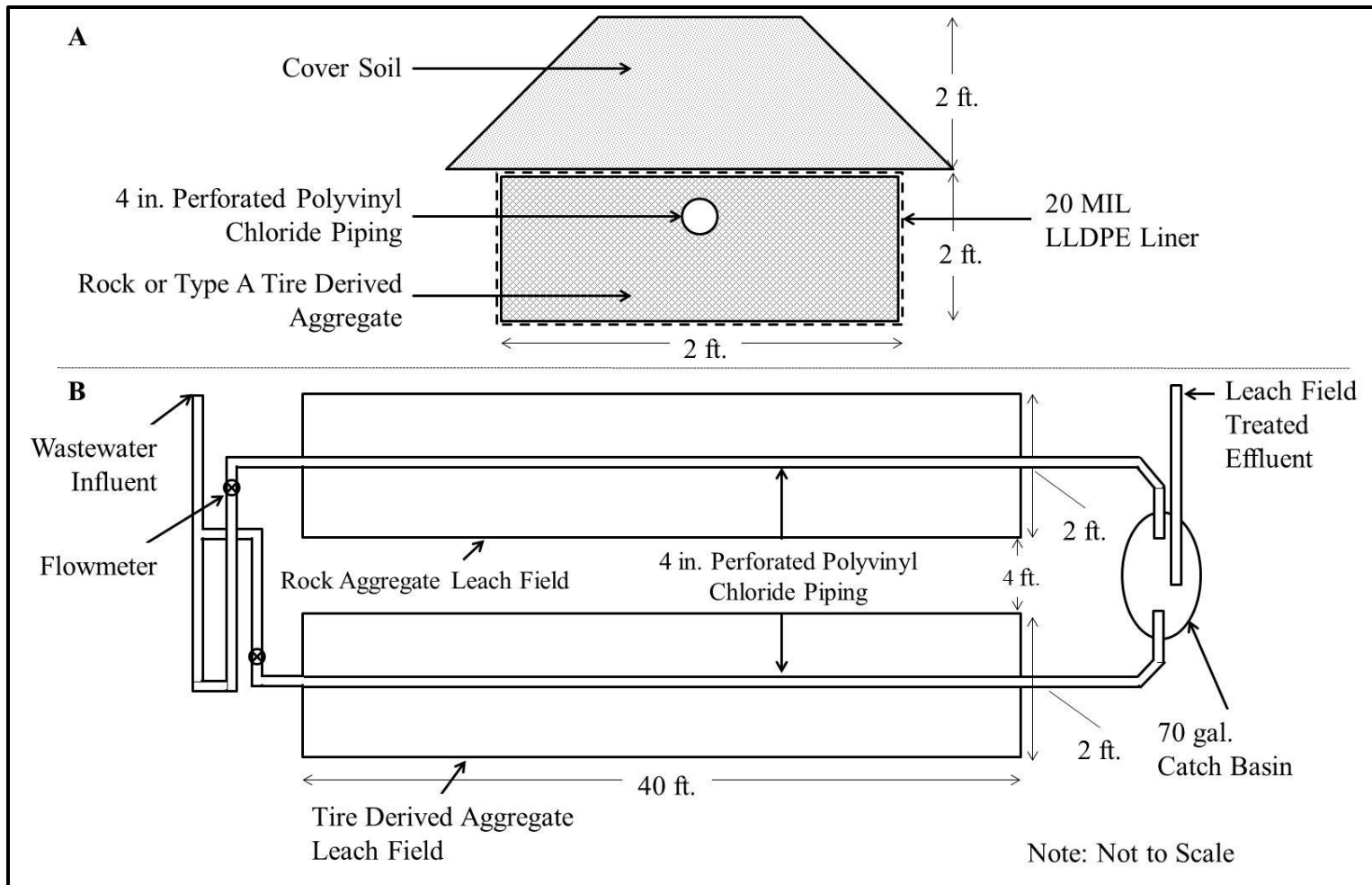


Figure 3. A cross section (A) and plan view (B) of the leach fields that used rock and tire-derived aggregate material.



Figure 4. Leach field setup of the geomembrane layer (A) and the top soil (B).

Five water sample points were built into the leach field system. Leach field wastewater influent was extracted from a single nozzle, which is shown in Figure 5A. Six feet of vertical PVC that extended to the bottom liner was used to collect leachate in the center of the leach field (Figure 5B). To accumulate leachate at the central extraction points, a short wooden weir was placed on the bottom section of the 20 mil LLDPE liner that provided enough water depth upstream to allow sampling through the vertical pipe with a small hand pump (Figure 6A).

Rock and TDA leach field effluent was sampled as it exited through a 1.5 inch PVC pipe into a 70 gallon catchment basin (Figure 6B). Two submersible sump pumps (0.3 hp pumps with a flow rate capacity of about 43 gal/min) were used to pump effluent leachate from the catchment basin (Figure B) back to an adjacent oxidation pond. One of the effluent pumps was set further off the bottom of the catchment basin than the other pump to serve as a backup. If the lower (primary) pump malfunctioned, the backup pump was there to prevent wastewater from overtopping the catch basin. The delivery and effluent pumps were regularly checked to make sure the system was powered and that each leach field was working properly.

Leach field samples were analyzed a range of organic and inorganic compounds/elements (list is shown in Appendix A on page **Error! Bookmark not defined.**). Samples were collected and analyzed once every two weeks for the first four months of operation, and once a month for the next seven months. After 11 months, water quality testing was performed at the 14th month and once more at the end of the 17-month operational period.

Temperature Analysis of Leach Field Media

The temperature of the leach field media was monitored to determine whether exothermic behavior was occurring and to help interpret changes in effluent water quality. HOBO Pro v2 data logging temperature probes were placed at the midpoint of the simulated leach. Two temperature probes were placed in the TDA trench, one about one inch above the bottom of the 20 mil LLDPE geomembrane liner and the other directly below the four-inch diameter perforated PVC leach piping. The rock aggregate leach field probe was placed in the middle of the leach field directly below the four-inch perforated PVC leach pipe. A fourth probe was mounted four feet above ground level to record ambient air temperatures (Figure 7). The temperature was recorded every 15 minutes for about 17 months. Temperature memory storage devices for both the rock and TDA trenches had failures due to manufacturing defects, resulting in some data loss.

Exothermic Behavior of Deep TDA Fills

One possible use for TDA is as a media for filtering stormwater runoff from highways. One proposed configuration would be to direct stormwater runoff into 15 to 20 foot deep cisterns filled with TDA media. A potential concern is that exothermic reactions could raise temperatures within the media high enough to result in a fire. To provide data on potential exothermic reactions in such a setting, temperature changes were measured in a lightly compacted tower filled with type A TDA. The tower was 20 feet tall and built at Humboldt State University (HSU) in Arcata, Ca. (Figure 8 and Figure 9). The tower was constructed of three foot diameter cylindrical aluminum ducting. Approximately 450 ft³ of type A TDA was packed lightly inside the tower using a wooden rake (Figure 10A). A temperature sensor was placed approximately every four feet in elevation, directly in the radial center of the cylindrical tower (Figure 10B). An ambient temperature probe was placed approximately 12 ft. from the bottom of the tower and about two inches away from the outside of the tower (a two-inch distance limited heat gain to the ambient probe from the tower). A 180° elbow was positioned on the top of the cylindrical tower to prevent precipitation from wetting the media. Temperature readings for each probe were gathered in 15 min. intervals for approximately nine months.

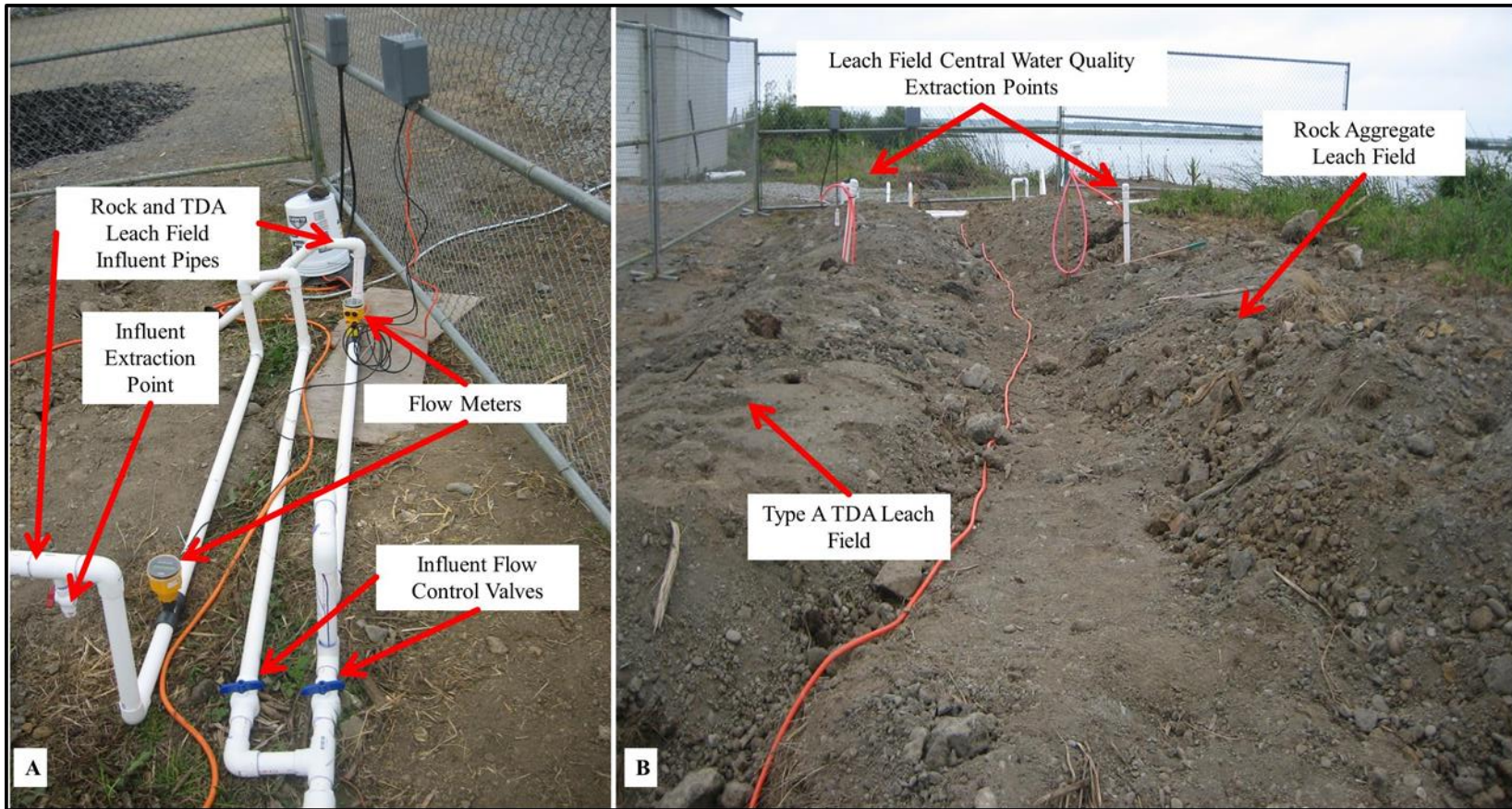


Figure 5. Leach field influent piping arrangement (A) and central extraction points (B).

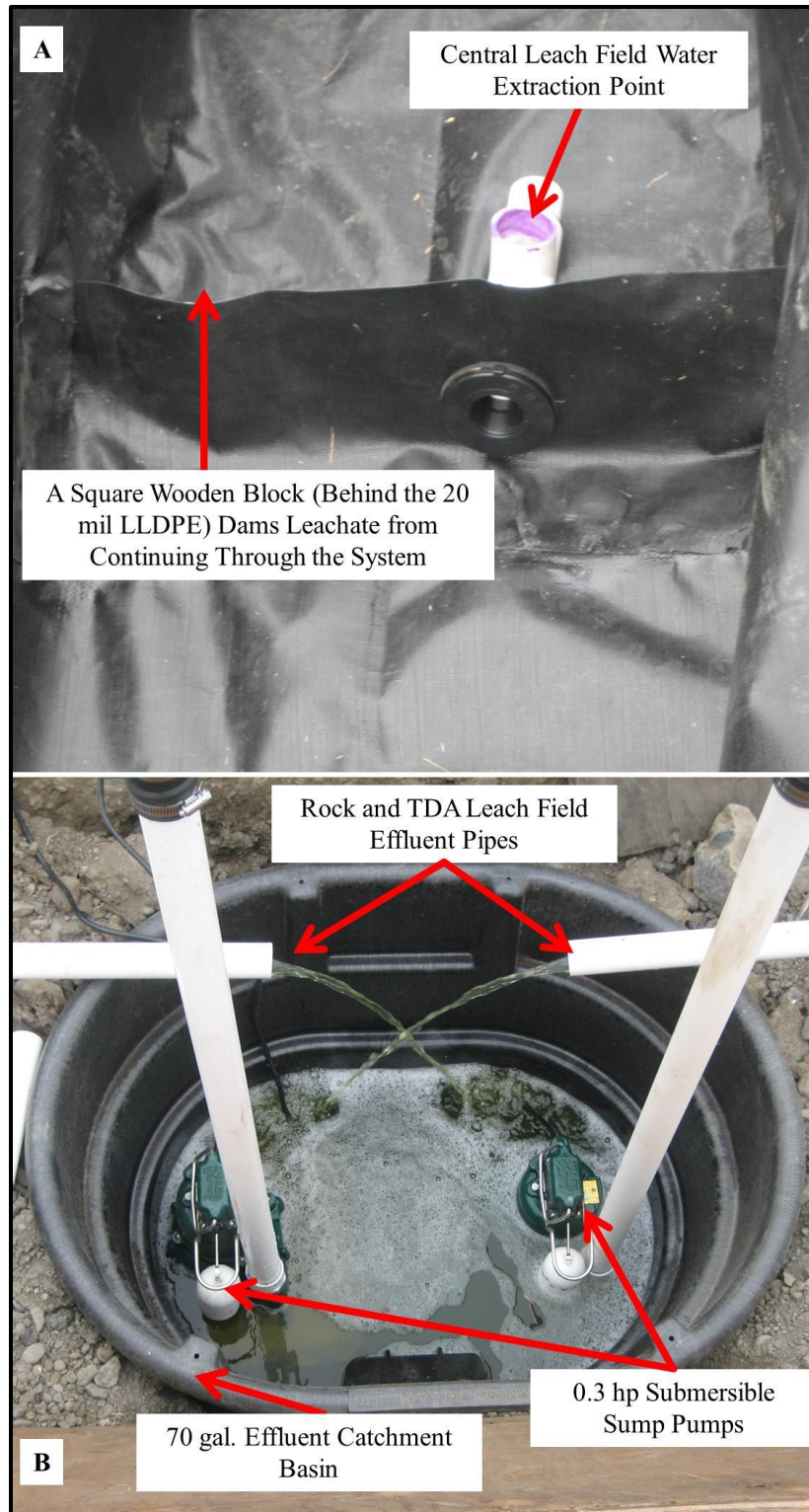


Figure 6. Short weirs in the middle of the leach field to allow sampling (A). Effluent discharging into a catchment basin (B).

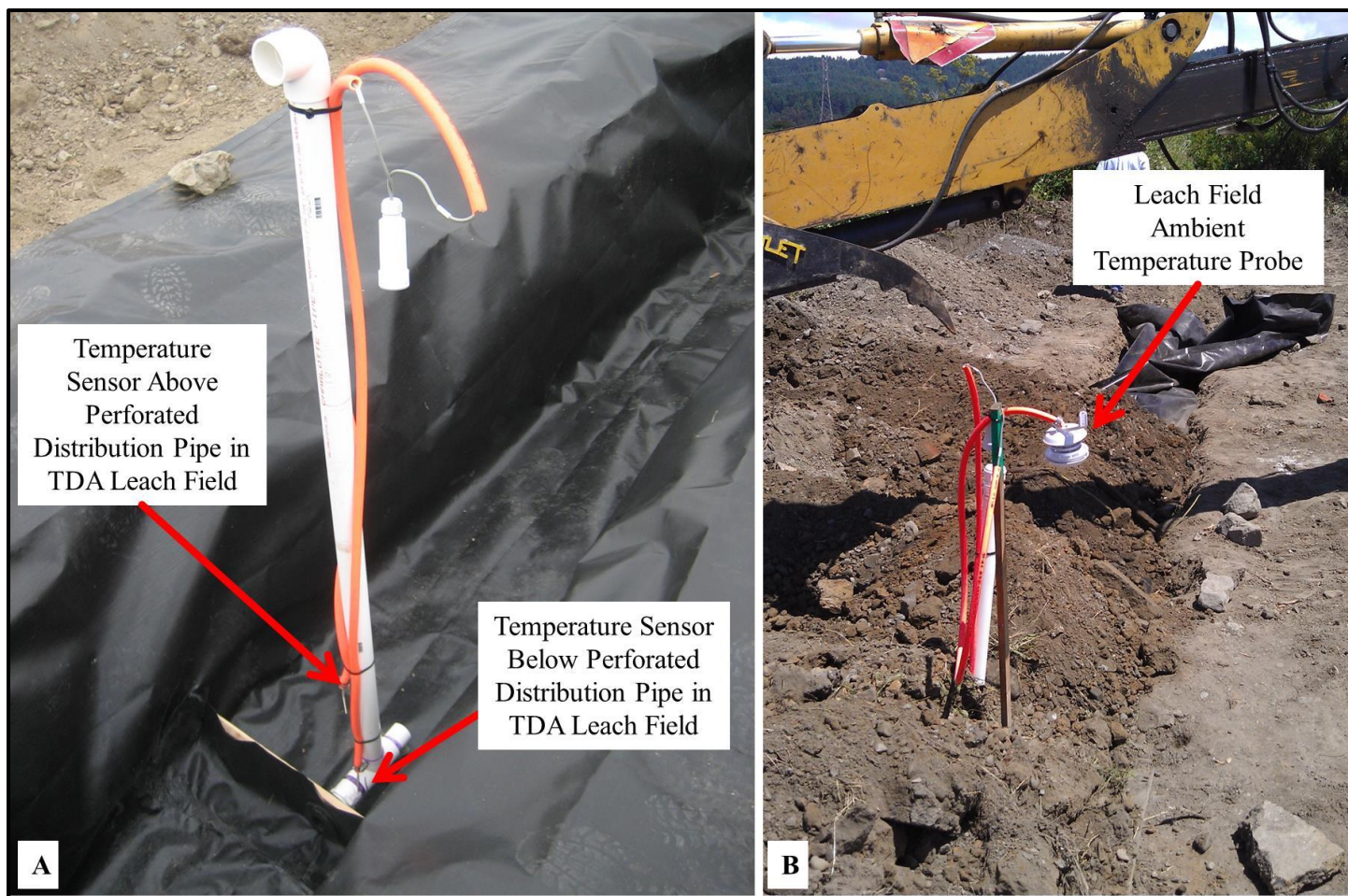


Figure 7. Temperature data was collected in the middle of the leach fields, within the media (A) and at ambient conditions (B).

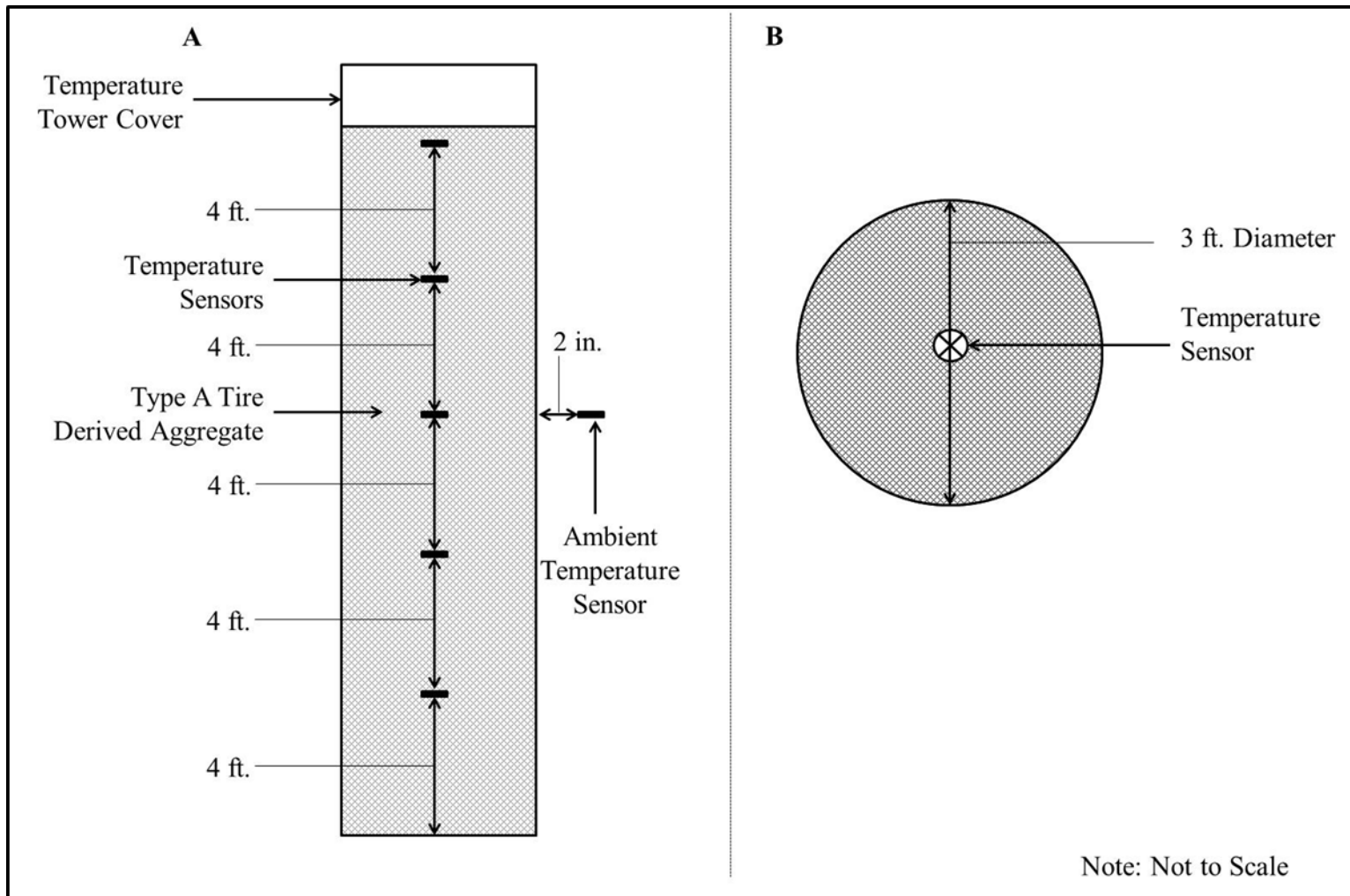


Figure 8. Side view (A) and plan view (B) of the 20-ft.-tall tower filled with type A TDA.

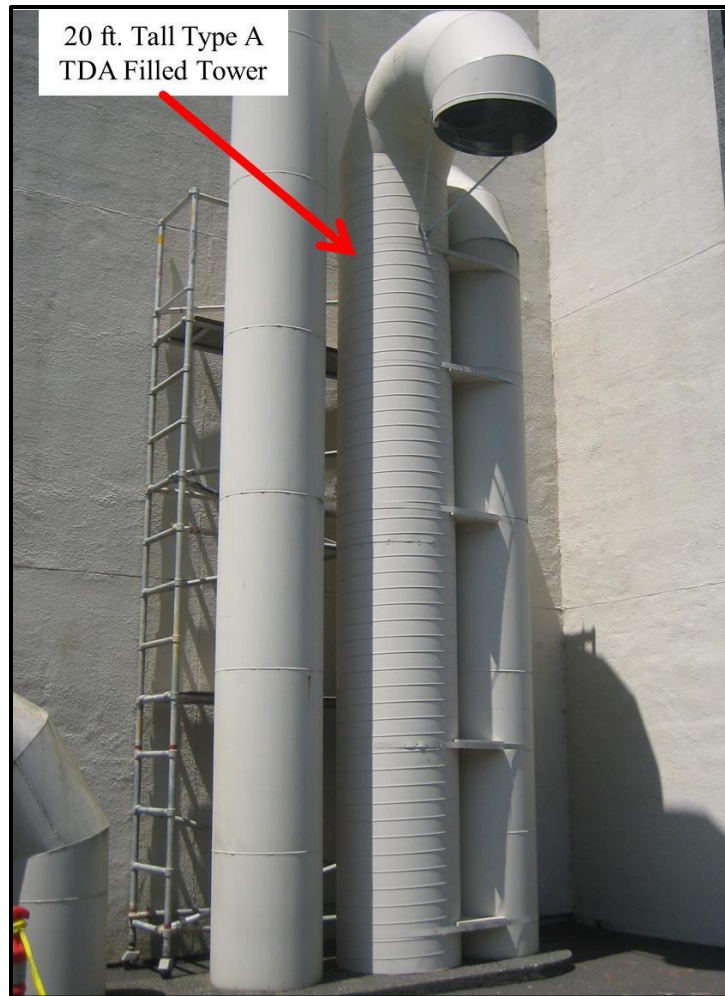


Figure 9. Vertical temperature differences of type A tire-derived aggregate were analyzed within a 20-ft.-tall tower for approximately nine months.

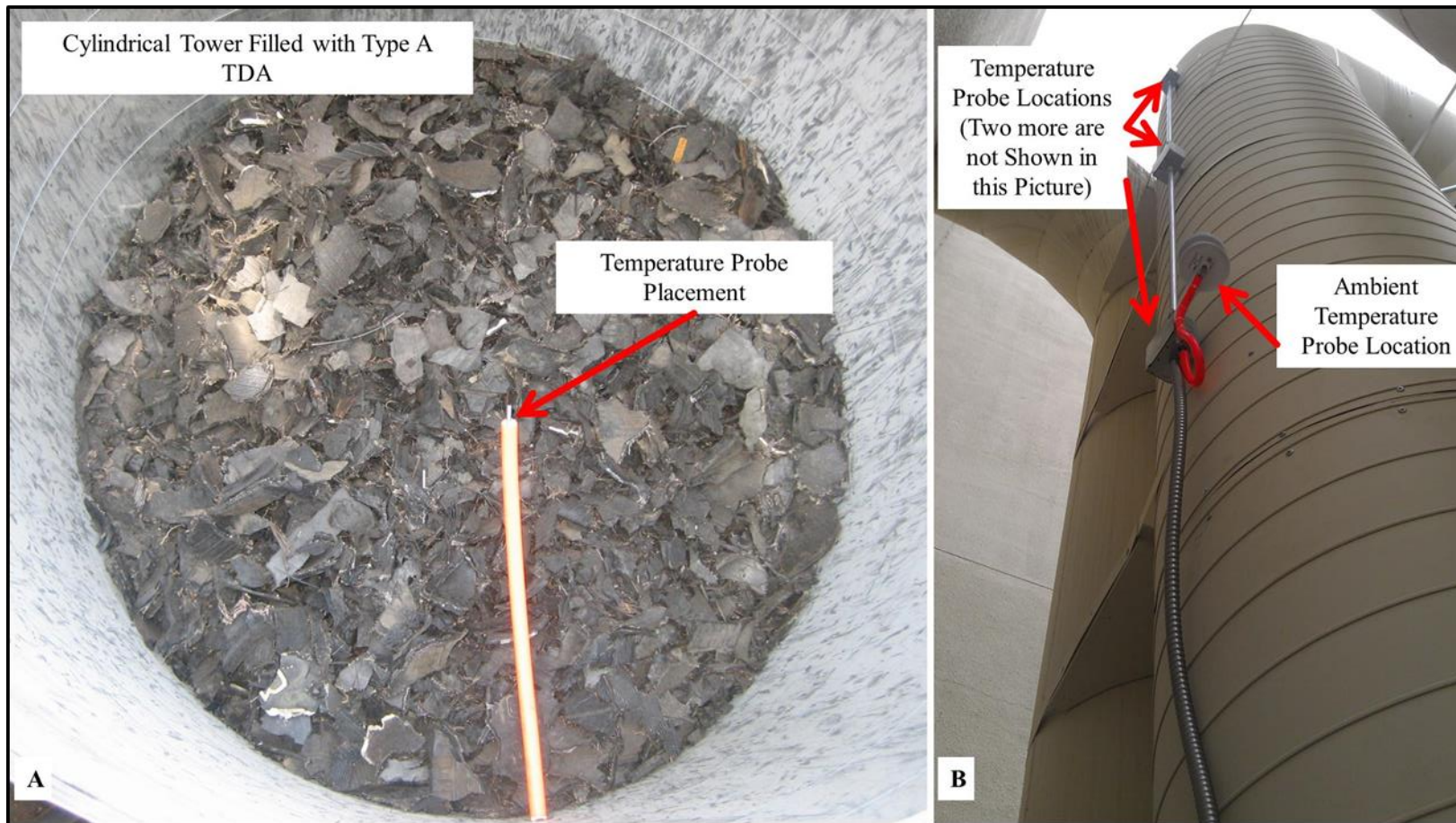


Figure 10. A cross sectional view of the 20-ft.-tall tower shown in Figure 9 (A) and the location of the temperature probes (B).

Exothermic Behavior of TDA under Immediate Fill Conditions

There is some evidence that exothermic behavior observed in TDA results, in part, from chemical “healing” that occurs following the tire shearing process used to produce TDA. To investigate the importance of this phenomenon, temperature changes in type A TDA were observed in a 10 foot x 10 foot x 10 foot earthen pit constructed at the Kiefer Landfill in Sloughouse, Ca. The TDA had been cut from scrap tires less than six hours before placement (Figure 11). The TDA temperature was recorded every 15 minutes at 28 different locations in the earthen pit over a five-month period. The ambient air and soil temperature was also recorded, and daily precipitation data was obtained from a nearby weather station. Site preparation and the experimental procedures are listed below:

1. Excavation was completed to produce a 10-by-10-by-10 foot cube immediately below ground level (Figure 12A). The native soil was a dry, solid, clayey material.
2. Line the excavated earthen pit with an eight ounce non-woven geotextile fabric to prevent soil from entering the TDA (Figure 12B).
3. Place approximately 42 ft³ of type A TDA in the ground cavity in a 5-inch deep layer.
4. Run a Rammax RW1504HF vibratory compactor over the surface area of the type A TDA at least six times (Figure 13A).
5. Place 4 temperature sensors in the middle of the earthen pit across the compacted TDA (Figure 13B).
6. Perform Steps 3-5 with the addition of 258, 100, 150, 83, 116, 116, and 133 ft³ of type A TDA before temperature probes were placed in the pit.
7. Cover the top of the tire earthen pit with 8 oz. non-woven geotextile fabric.
8. Place a two-foot layer of soil on top of the earthen pit.
9. Place an ambient soil temperature probe two feet to the east of the pit and two feet below the ground.
10. Place an ambient temperature sensor approximately six feet above ground.
11. Connect the temperature sensor wires to HOBO U30 Cellular Data Loggers and three solar panels (Figure 14).

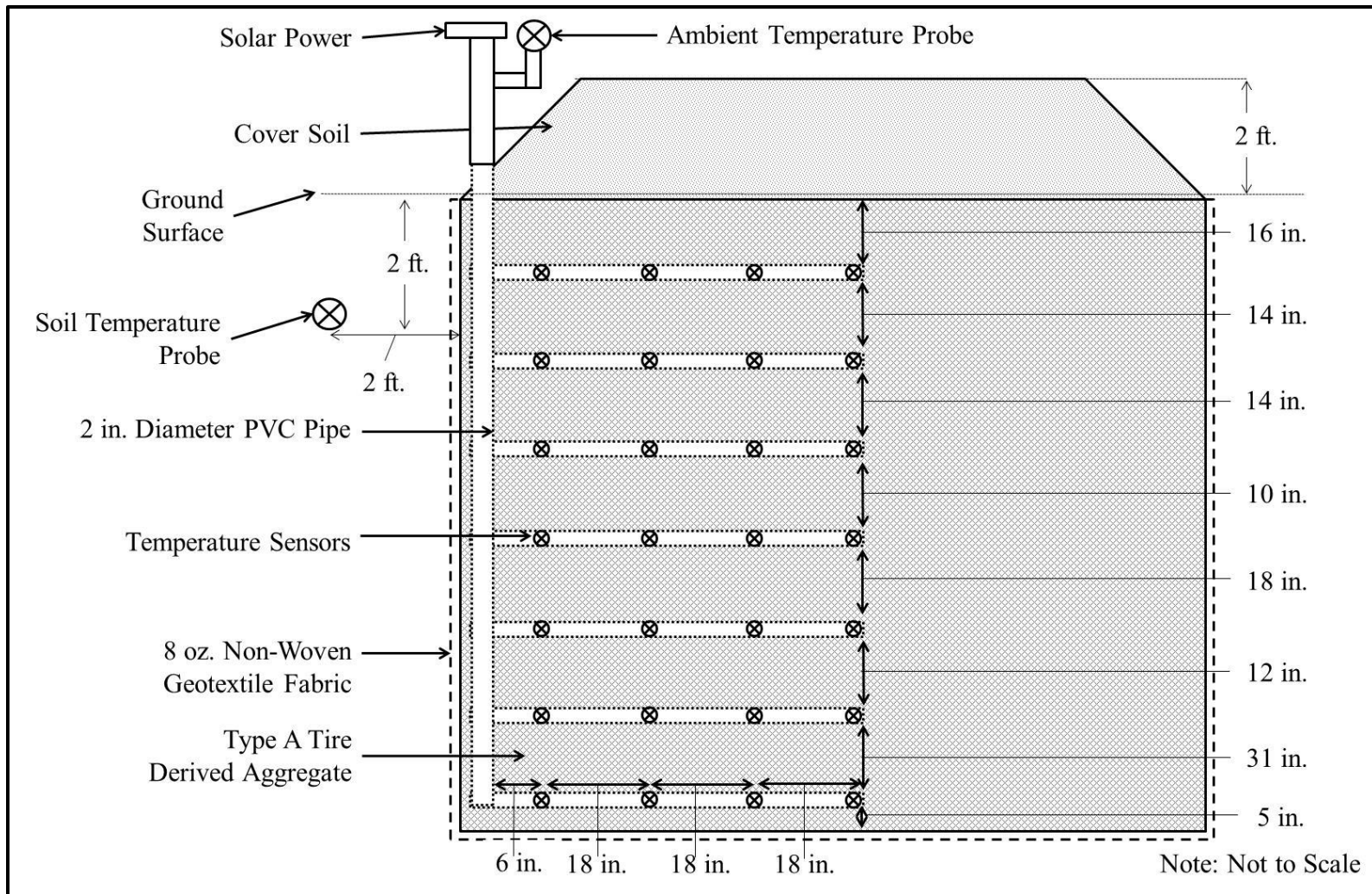


Figure 11. An illustration of the earthen pit filled with type A tire-derived aggregate and the location of temperature sensors within the pit.



Figure 12. The 1000 ft³ earthen pit excavated below ground level (A) and an 8 oz. non-woven geotextile fabric (B) used to contain type A TDA.

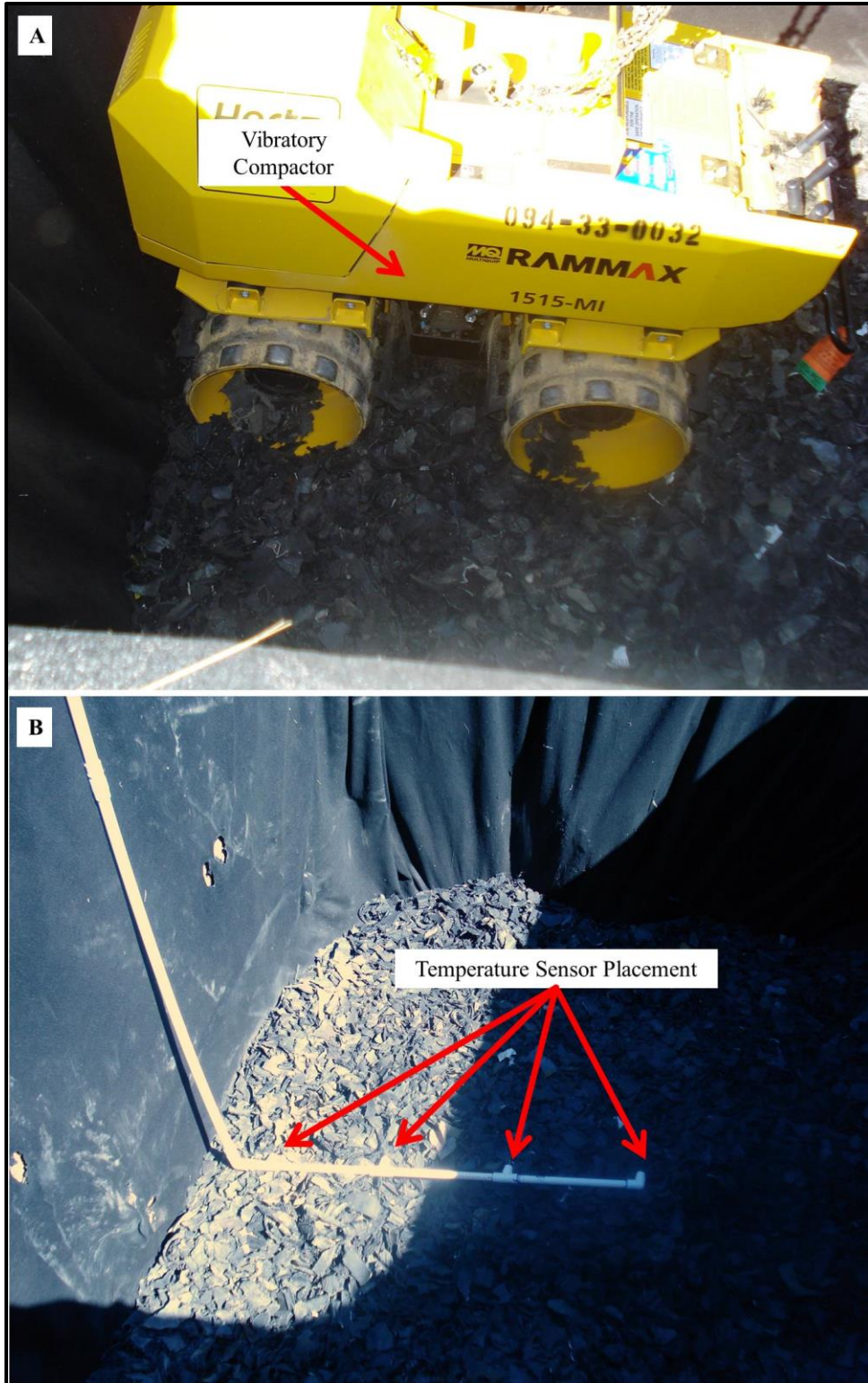


Figure 13. The vibratory compactor used (A) and general location of temperature probes within the earthen pit (B) (see Figure 11 for a cross sectional reference).

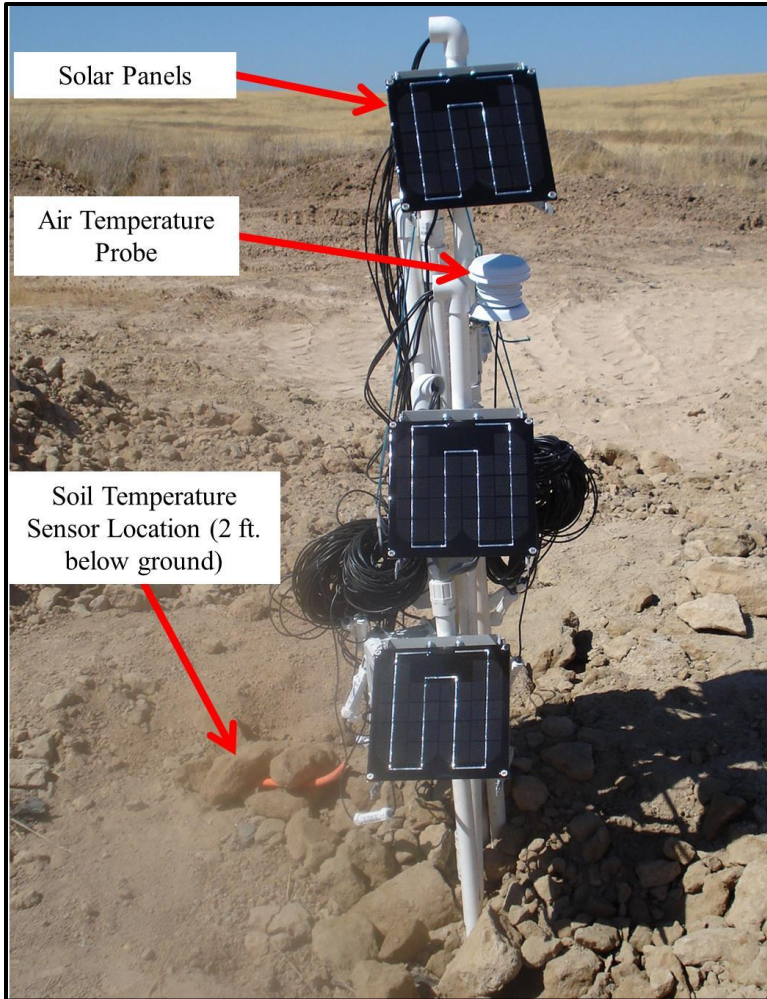


Figure 14. Electronic equipment was powered by the three solar panels.

Compression Testing of TDA for Varied Loads

Previous investigators have attempted to determine the compressibility of TDA using test apparatus that was designed for small grain size soil particles. The diameter of compression cylinders that contain the samples typically range from 6 to 12 inches, which is smaller than tire pieces commonly found in TDA. In this experiment, a large diameter compression apparatus was designed and fabricated specifically for testing type A and type B TDA under loads equivalent to 80-100 feet of soil fill (115 psi) (Figure 15). The apparatus can also be used to determine the density, porosity, and hydraulic conductivity of a TDA sample.

The compression cylinder has a 29.7 in. inside diameter, and can hold a 30-inch-deep layer of TDA. The loading force is provided by manually operated hydraulic bottle jacks that drive a steel piston. The vertical loading force is measured by four pressure transducers, each with a 30,000 lb_f capacity. The pressure transducers rest on the solid bottom of the cylinder, separated from the TDA by a perforated steel plate. The entire apparatus rests on a 4-foot-square digital scale with a 3,000 lb_f capacity and an accuracy of ±1.0 lb_f. Water enters and leaves the cylinder via a fitting near the base of the unit.

The typical test procedure is as follows:

1. Place the steel cylinder on the large capacity scale.
2. Place the pressure transducers on the bottom of the cylinder (Figure 17A).
3. Place a perforated steel plate on top of the pressure transducers (Figure 17B). The plate was used to contain the TDA while allowing distribution of the load to the transducers and to allow the passage of water through the system.
4. Place and weigh a 30-inch-deep layer of TDA (approximately 340 lb_f) on top of steel plate described in Step 3.
5. Slowly add water (from below to help drive out air bubbles) to the cylinder up to the top of the TDA. The water was added to lubricate cylinder walls, minimize shear friction, and allow calculation of TDA porosity.
6. Record weight of the water added.
7. Place the steel piston on the TDA (Figure 18A).
8. Place latching mechanism on the cylinder (Figure 18A).
9. Place three wooden blocks on each of the four platforms located on the piston (Figure 18B). (
10. Place four 20-ton jacks on the wooden blocks from Step 10 (Figure 18).
11. Raise the jacks until the maximum extension of the jack pistons is reached.
12. Fasten the latching mechanism with bolts to hold the compressed position.
13. Record pressure transducer readings.
14. Place additional wooden blocks on platform below the jacks (while maintaining the previous compressed position) Figure 18B).
15. Measure the vertical displacement between the top of the cast iron cylinder and the TDA.
16. Repeat Steps 11-14 until about 100-105 psi was placed on the TDA.

17. Reverse Steps 9-14 to remove the jacks, wooden blocks, and the piston from the experimental apparatus.
18. Record the rebounding vertical displacement and pressure transducer readings for decreased pressure on the TDA.
19. Remove the piston, TDA, and latching mechanism from the cast iron cylinder.
20. Calculate the void ratio of TDA (e) at seating load using:

$$e = \frac{V_T - V_{TDA}}{V_{TDA}} \quad \text{Equation 0-1}$$

a. where:

- i. V_T (ft³) = the total volume between the plates encompassing the TDA material
- ii. V_{TDA} = the total volume of the TDA material (ft³)

21. Calculate the porosity of TDA (n) at seating load using:

$$n = \frac{V_T - V_{TDA}}{V_T} \times 100\% \quad \text{Equation 0-2}$$

22. Calculate the compressive strain (ϵ) of TDA using:

$$\epsilon = \frac{x_D - x_i}{x_i} \times 100\% \quad \text{Equation 0-3}$$

a. where:

- i. x_D = the depth of TDA loaded (in.)
- ii. x_i = the initial depth of TDA in the cast iron cylinder (in.)

23. Calculate the void ratio and porosity under load using Equations 0-1 and 0-2.
24. Repeat Steps 1-23 using about 289-304 lb_f of type B TDA in 29.9 inch layer and load with a maximum pressure of about 100 psi.
25. Repeat Steps 1-23 using 346 lb_f of a type A/type B TDA mixture in a 27.9 inch layer and tall and use a maximum loading pressure of about 114 psi.

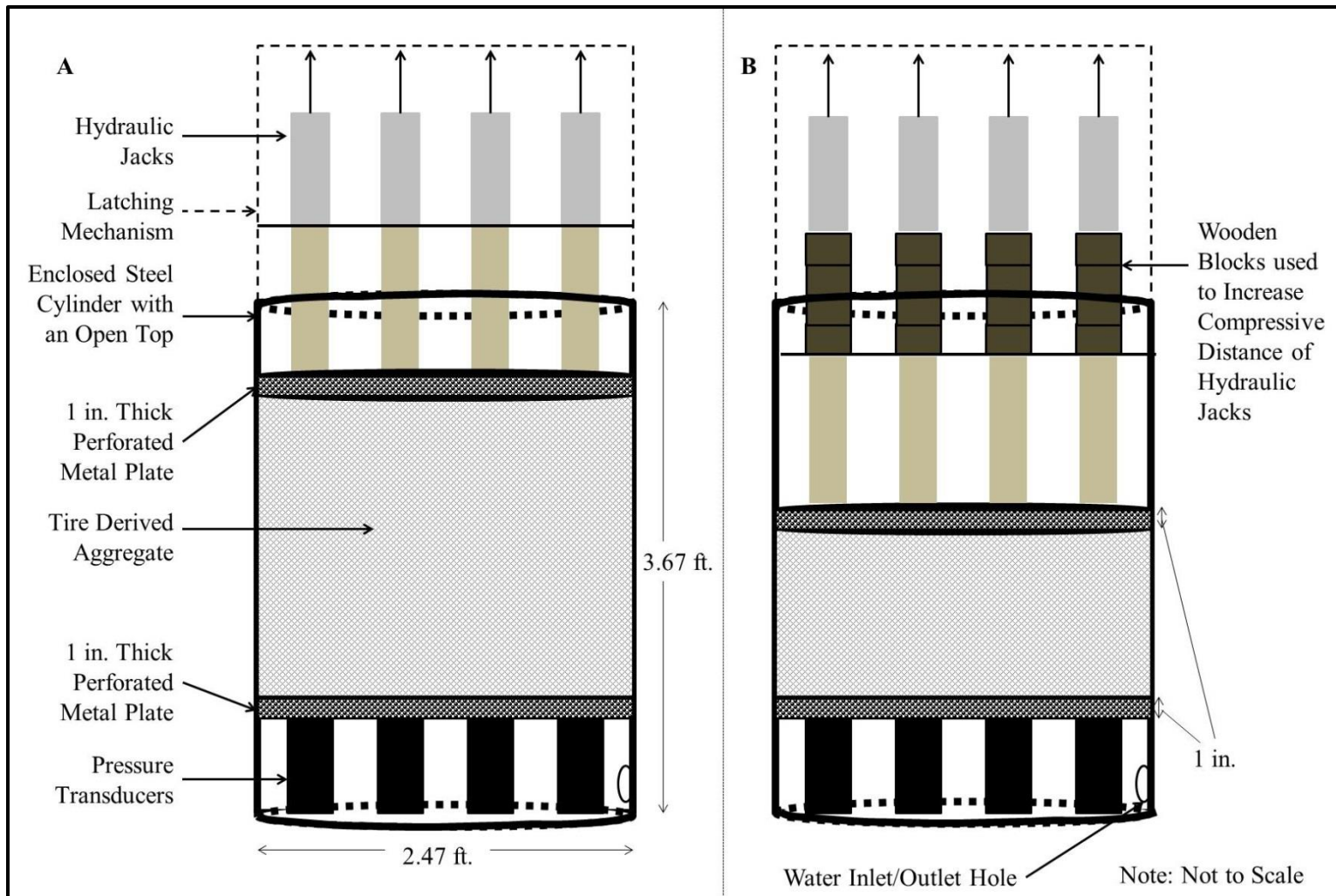


Figure 15. Experimental device used to compress tire-derived aggregate (A), where wooden blocks were placed below the hydraulic jacks to increase compression distance (B).



Figure 16. The cast iron latching mechanism (A) connects the steel cylinder to the tire crusher (B). The two pieces of equipment are shown fully setup in Figure 18.

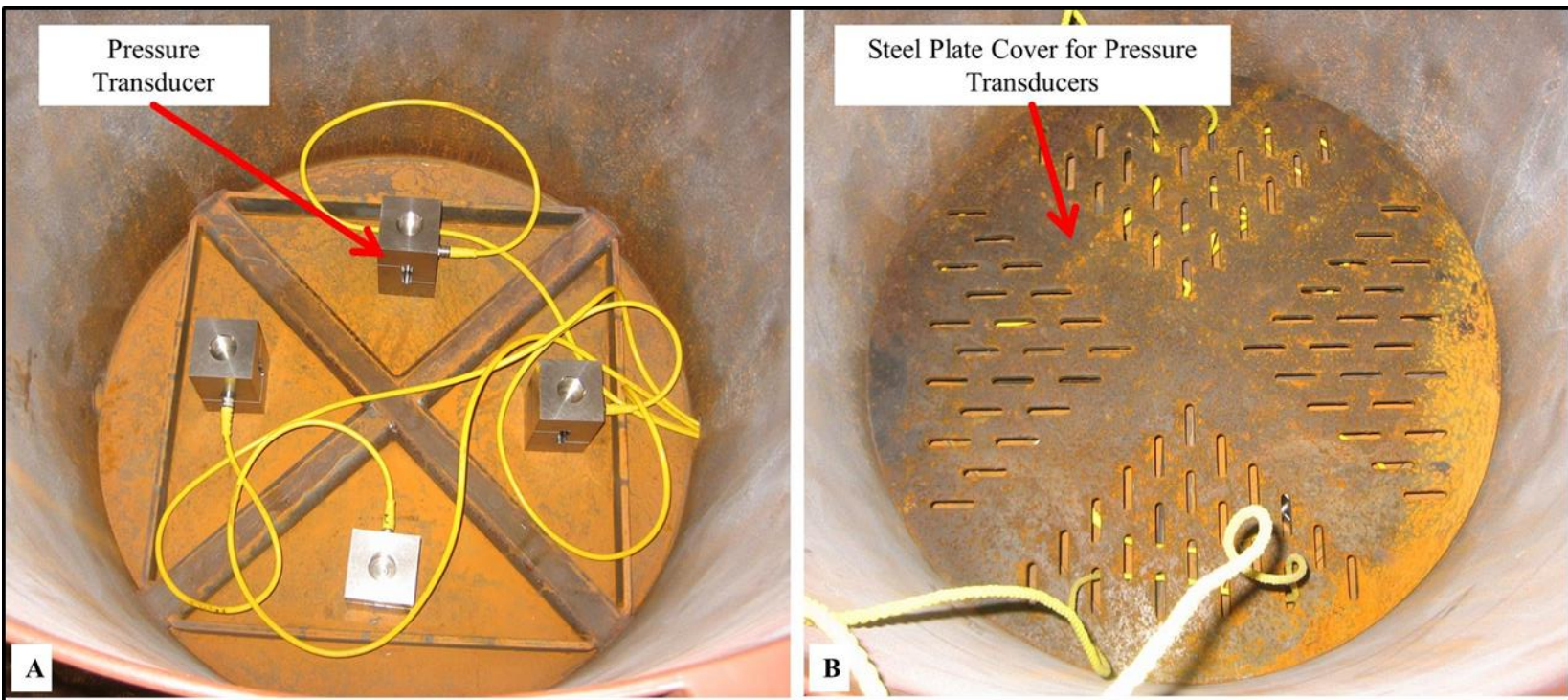


Figure 17. Pressure transducer locations inside the 29.7 in. diameter compression cylinder (A) and the perforated steel plate which was placed on top of the transducers (B).

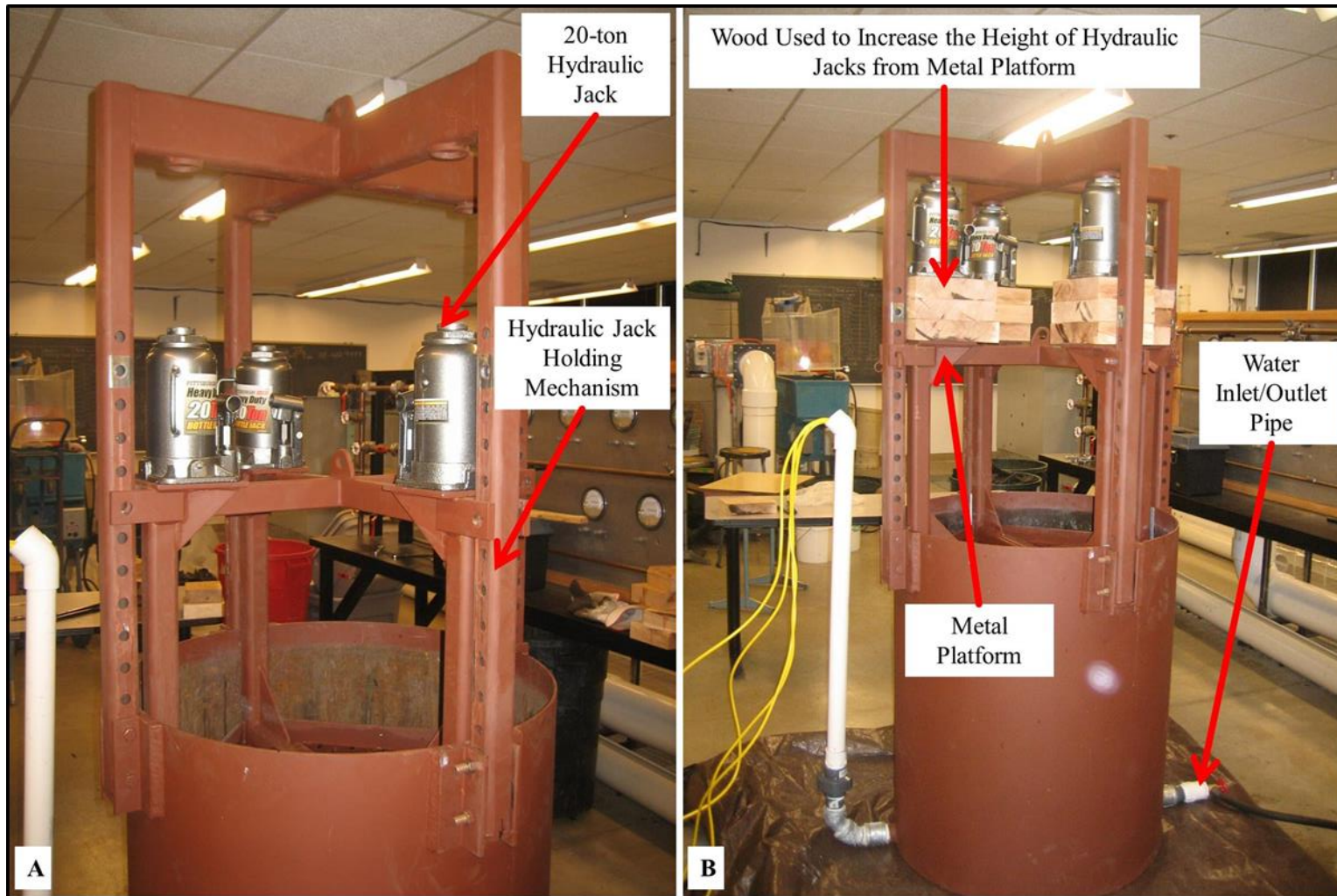


Figure 18. The apparatus used to test large magnitude compressions of tire-derived aggregate utilized a latching mechanism to hold loaded pressure (A), where wooden blocks were used to raise the jacks when a maximum hydraulic pressure was reached (B).

Determining Physical Properties of TDA under Moderate Load

The density, specific weight, specific gravity, porosity, void ratio, and hydraulic conductivity was determined for TDA subject to a constant load comparable to that of aggregate in a typical leach field (one to two feet of soil cover). A large diameter test apparatus was designed and constructed specifically for testing TDA under moderate loading conditions. The test apparatus and experimental setup is very similar to that described in the previous section, except the steel cylinder is replaced with a 30-inch-diameter polyethylene tank, and the perforated steel plates is replaced with perforated wooden plates. The load was applied using sand bags each weighing about 37 lb_f. The following materials were used for experimental setup: a set of 54 sandbags, water, a submersible sump pump, a set of four buckets, a stopwatch, a 0.3-hp submersible sump pump, two hoses, a surveying rod, two 1-inch-thick wooden plates, a 200-gallon and a 100-gallon polyethylene cylindrical tank, a large capacity scale, and three cinder blocks. The wooden plates were perforated with 635 holes (that were 0.375 in. diameter). The 200-gallon tank was approximately 5.41 ft. in height and had an outside diameter of 2.55 feet. The 100-gallon polyethylene cylindrical tank was approximately 3.11 ft. in height and had an outside diameter of 2.28 feet. The density, specific weight, specific gravity, porosity and void ratio of the TDA were calculated throughout the experimental process. The procedure used to construct and use the apparatus is listed below:

1. Cut off the top of the 200-gallon polyethylene cylindrical tank and place the tank on the large capacity scale.
2. Place three cement blocks on the bottom of the 200-gallon tank to support a platform for the TDA and allow passage of water through the exit hole on the bottom of the tank (Figure 19A).
3. Place a one inch thick perforated wooden plate on top of the cement blocks to prevent type A TDA from obstructing the exit of water from the 200-gallon tank (Figure 19B).
4. Place approximately 11 ft³ (about 36 inches deep) of type A TDA on the wooden plate from Step 3.
5. Measure the weight of the TDA (W_{TDA}) on the two wooden cylinders.
6. Place a second one-inch-thick perforated wooden plate on the TDA to act as a piston and equally distribute weight placed above the TDA and allow water to flow through the system (Figure 20A).
7. Calculate the volume of TDA between the two perforated wooden plates (V_{TDA}).
8. Calculate the specific weight (γ_{TDA}) using:

$$\gamma_{TDA} = \frac{W_{TDA}}{V_{TDA}}$$

9. Calculate the total volume between the two perforated wooden plates (V_T).

11. Calculate the TDA density using:

$$\rho = \frac{Y_{TDA}}{g}$$

where:

g= standard gravity (32.2 ft/s²)

12. Measure the vertical distance every 90° around the circumference of the 200-gallon tank, between the top of the tank and the top of the perforated wooden piston (Figure 21).
13. Fill the 200-gallon tank with water up to the top of the wooden plate acting as a platform for the TDA.
14. Fill the 200-gallon tank with water up to the bottom of the perforated wooden piston (the top of the TDA).
15. Measure the temperature of the water, and compute the volume of water knowing the weight of water added in step 13.
16. Calculate the void ratio and porosity (at the seated load) for TDA using Equations 0-1 and 0-2.
17. Cut off the top of the 100-gallon tank and place the tank inside the 200-gallon tank on top of the wooden piston described in Step 6.
18. Place 54 sandbags inside the 100-gallon tank to provide a loading of approximately 2.95 psi on the type TDA (Figure 20B).
19. Measure the vertical displacement of the TDA resulting from loading by the sandbags using the method described in Step 11.
20. Calculate the void ratio and porosity under load using Equations 0-1 and 0-2.
21. Attach a 1.5 in. diameter hose to the exit hole of the 200-gallon tank (Figure 21).
22. Place a 1.5 in. diameter hose inside the top of the 200-gallon tank and connected the hose to a submersible sump pump. The pump was set to deliver water slightly faster than it exited, allowing the overflow to maintain a constant head on the TDA (Figure 22).
23. Position the hose attached from Step 19 at various heights above a datum on a static surveying rod (Figure 22).
24. Measure and time the volume of water leaving the hose from Step 21 in five-gallon buckets at varied hydraulic heads.

25. Calculate the hydraulic conductivity and specific gravity:

$$k = \frac{Q}{iA} \quad \text{Equation 0-4}$$

$$i = \frac{h_1 - h_2}{L} \quad \text{Equation 0-5}$$

$$SG_{TDA} = \frac{\rho_{TDA}}{\rho_{water}} \quad \text{Equation 0-6}$$

where:

k = the hydraulic conductivity of tire-derived aggregate (ft/s)

Q = the flow rate passing through the tire-derived aggregate medium (ft³/s)

i = the hydraulic gradient (dimensionless)

A = the gross cross sectional area of flow (ft²)

h₁ = the highest pressure head level (ft.)

h₂ = the lowest pressure head level (ft.)

L = the height of material which water is flowing through (ft.)

SG_{TDA} = the specific gravity of TDA (dimensionless)

ρ_{TDA} = the density of the TDA (slugs/ft³)

ρ_{water} = the density of the water (slugs/ft³)

1. Repeat Step 11 for 12 days until negligible changes in the displacement are seen.
2. Remove the sandbags, 100-gallon tank, and top perforated wooden cylinder from inside the 200 gallon tank.
3. Measure the rebound distance using the method described in Step 11 for approximately two days.

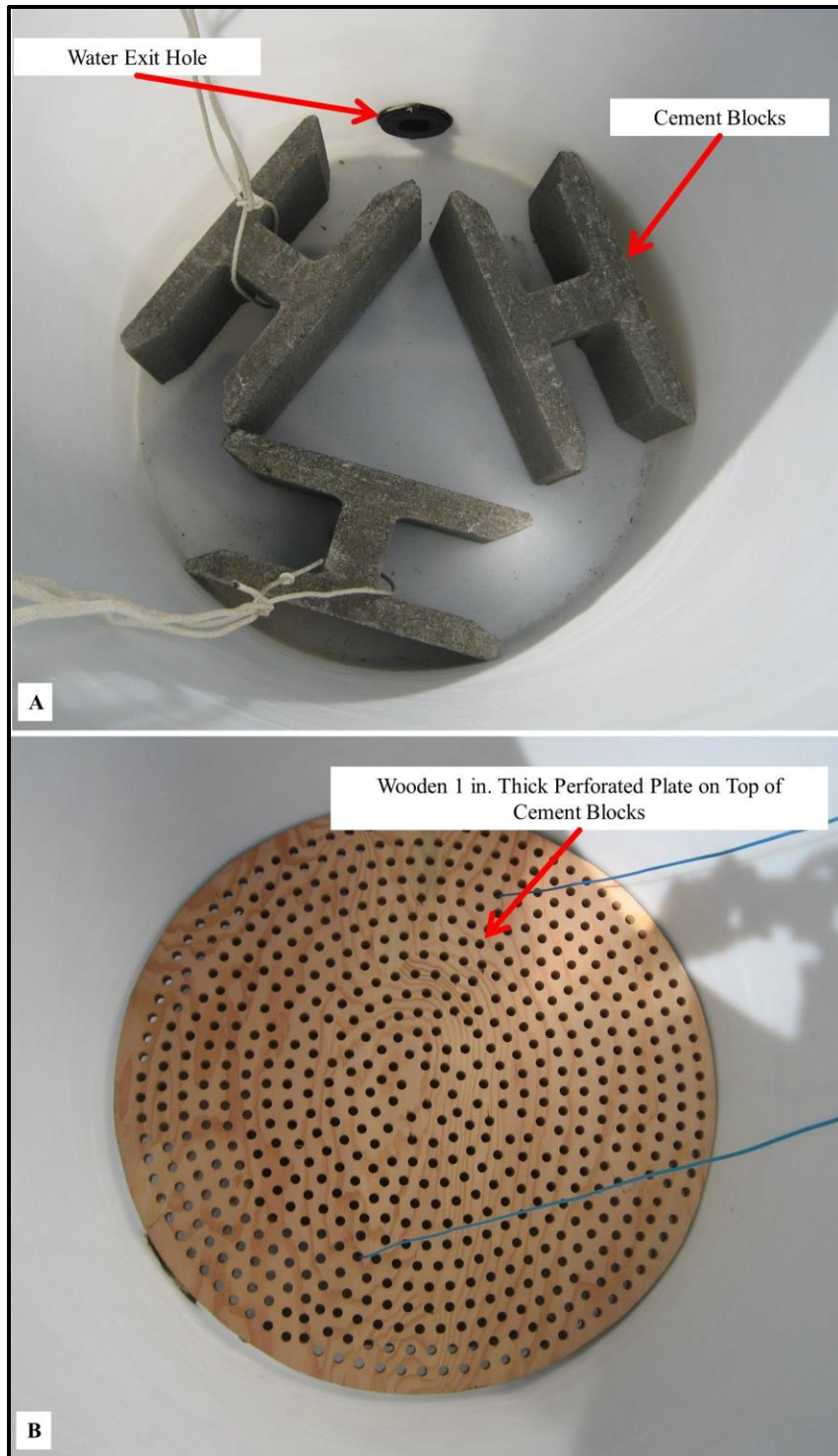


Figure 19. Bottom section of the small magnitude hydraulic conductivity experiment used to test type A TDA. Cement blocks allowed water to exit the experimental apparatus (A), while a perforated wooden plate was used to retain TDA and prevent clogging in the water exit hole (B).

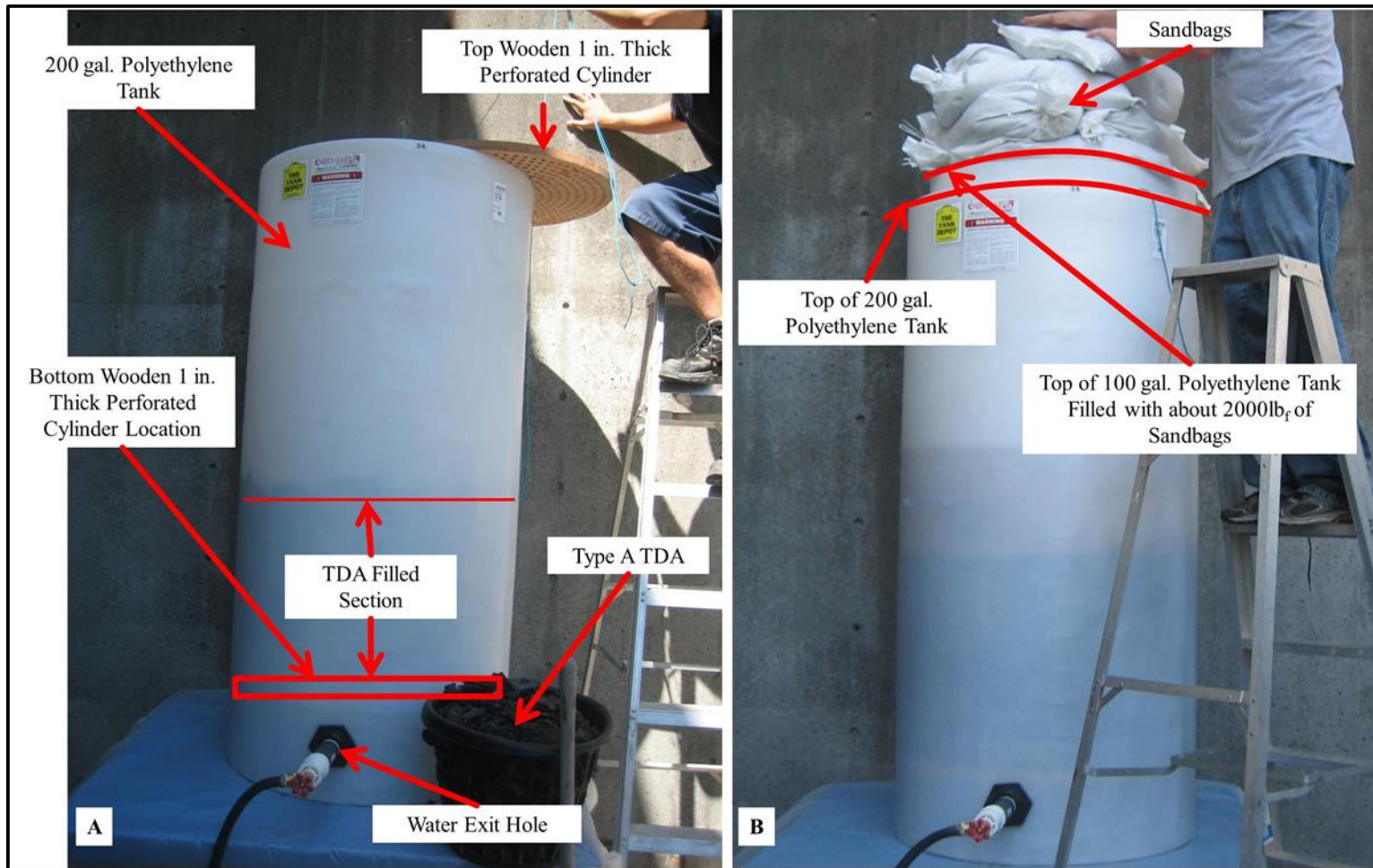


Figure 20. Full setup of the small magnitude hydraulic conductivity experiment used to test the physical properties of type A TDA. The setup after placing the TDA inside the device (A) and at full setup (B) are shown for reference.

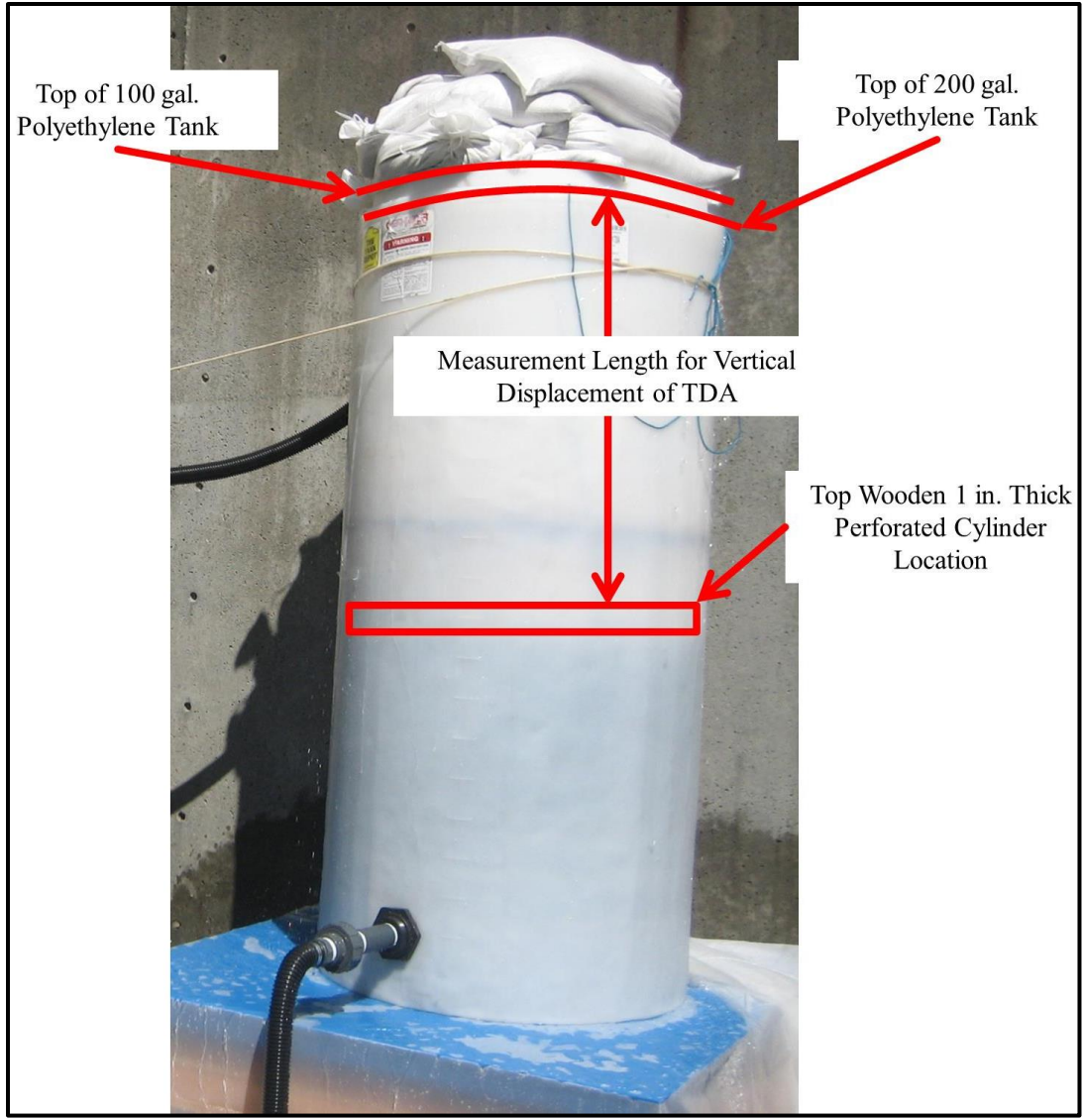


Figure 21. Measurement distance used for the vertical displacement of the type A TDA under a static load.

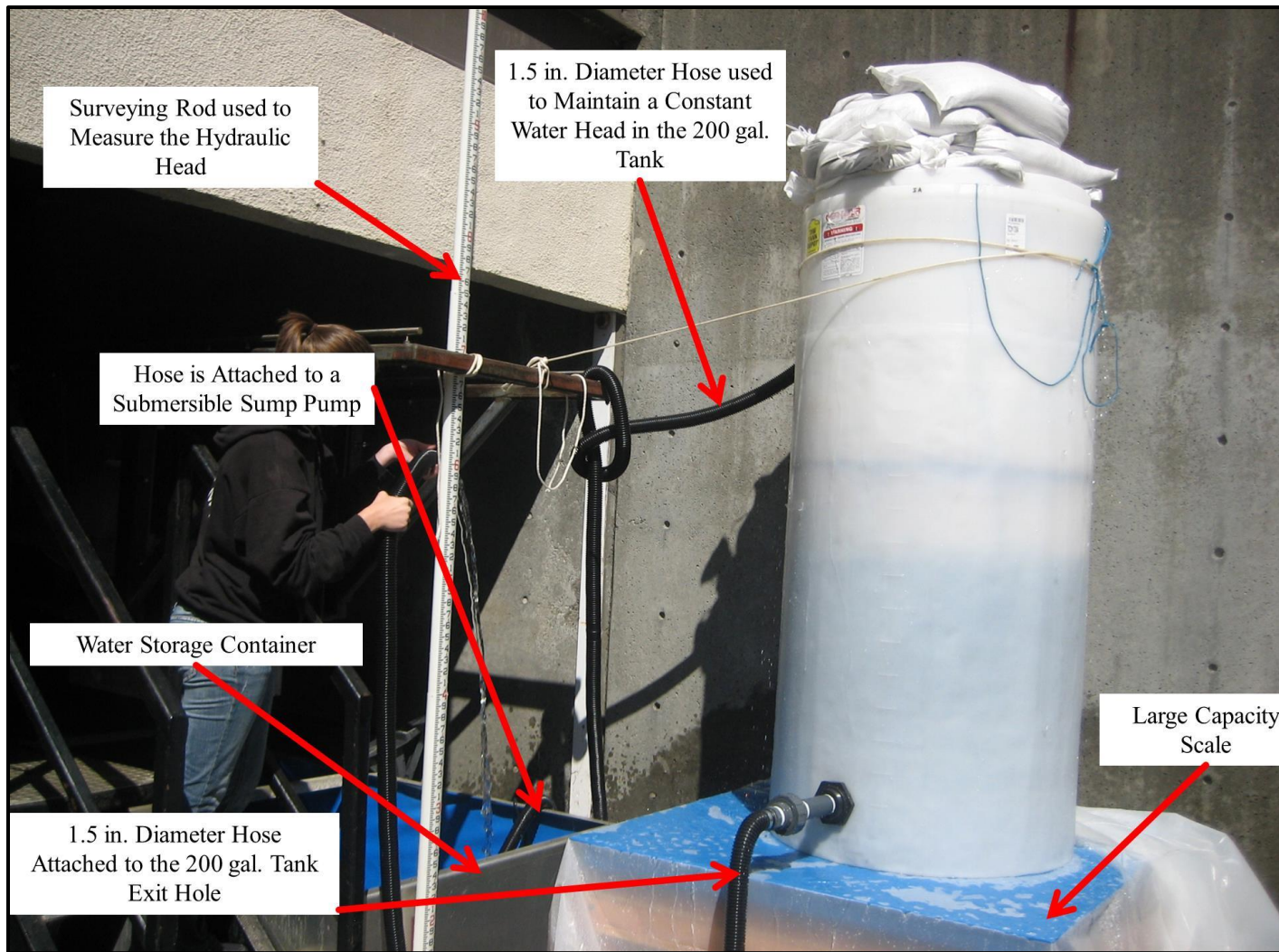


Figure 22. An experimental run of a static load hydraulic conductivity test for type A TDA.

Determining Hydraulic Conductivity of TDA under Large Loads

The hydraulic conductivity of TDA was determined in the previous section under approximately 2,000 lb_f (2.95 psi) loading. In this experiment, the hydraulic conductivity was determined under a load of more than 100 psi, equivalent to more than 80 feet of soil cover. The same apparatus used in the small magnitude hydraulic conductivity experiment was used to determine the hydraulic conductivity under large loads with the addition of: a small pool used for overflow water containment, a 0.3-hp submersible sump pump used to deliver water to the load cylinder, and a PVC manifold containing control valves for water passage (Figure 23A). The test procedure used in this experiment is described below:

1. Place a 58-inch diameter pool on the large capacity scale for water containment.
2. Place the steel cylinder on the large capacity scale and inside pool.
3. Place the pressure transducers inside the steel cylinder (Figure 17A).
4. Place the steel plate with perforations on top of the pressure transducers (Figure 17B).
5. Place approximately 336-343 lb_f of type A TDA (about 30 inches of TDA) on top of the steel plate.
6. Place the steel piston on the TDA (Figure 18A).
7. Place the steel latching mechanism on the steel piston (Figure 18A).
8. Place three wooden blocks on each of the four platforms located on the piston (Figure 18B).
9. Place four 20-ton jacks on the wooden blocks (Figure 18).
10. Connect a 1.5-inch diameter hose to the bottom of the cast iron cylinder; this hose was used to control the hydraulic head (Figure 23B).
11. Connect a 1.5-inch diameter hose from the control valve PVC attachment to the submersible sump pump (Figure 23A).
12. Connect a 1.5-inch diameter hose from the control valve PVC attachment, shown in Figure 23A, to allow the exit of excess water.
13. Connect a 1.5-inch diameter hose from the control valve PVC attachment, which was used to pump water into the steel cylinder (Figure 23A).
14. Place the sump pump into a water reservoir.
15. Turn on the sump pump and slowly fill the cylinder with water.
16. Measure the temperature of the water that was added.
17. Raise the jacks until half of their maximum working pressure is reached.
18. Fasten the latching mechanism to the piston in order to hold the compressed position.
19. Record the pressure transducer readings.
20. Position the hose attached from Step 10 at a single height above a datum on a static object.

21. Turn on the sump pump and adjust the flow rate to keep a constant filled water level in the steel cylinder.
22. Measure and time the volume of water leaving the hose from Step 21 three times in five-gallon buckets.
23. Calculate the hydraulic conductivity using Equation 3-4.
24. Repeat Steps 21-23 at different hydraulic heads under the pressure introduced in Step 17.
25. Insert more wooden blocks beneath the hydraulic jacks.
26. Raise the jacks to their maximum hydraulic pressure.
27. Fasten the latching mechanism on the piston to hold the compressed position.
28. Record the pressure transducer readings.
29. Repeat Steps 20-24 at the new pressure loading.
30. Record the pressure transducer readings.
31. Remove the wooden blocks holding the jacks to release the pressure on the TDA.
32. Remove the piston, TDA, and latching mechanism from the cast iron cylinder.
33. Repeat Steps 1-32 using type B TDA.

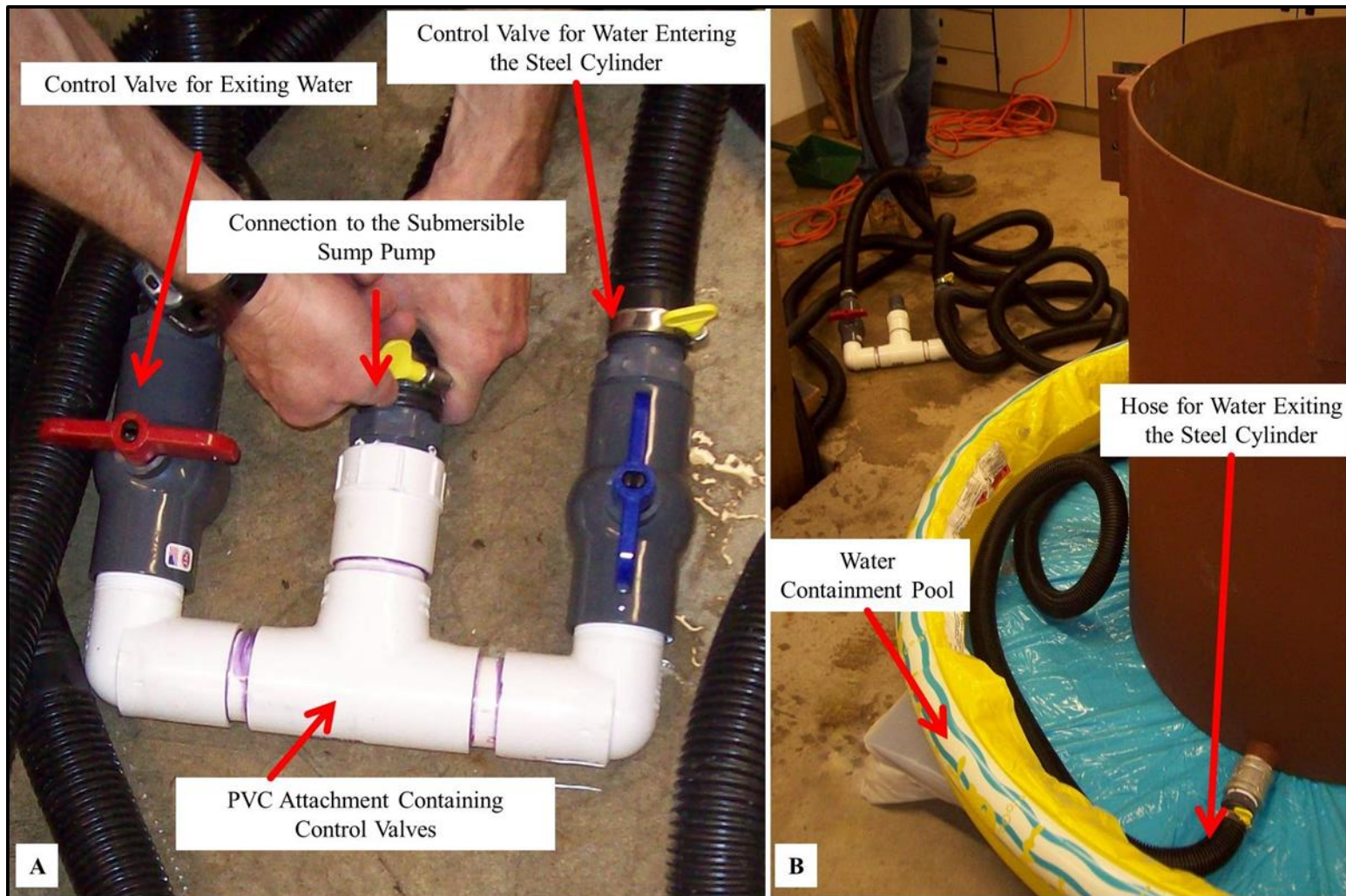


Figure 23. Control valve illustration and setup of large magnitude hydraulic conductivity tests. Image A shows a valve attachment for controlling the flow of existing water, for water entering the steel cylinder and for flow control of a submersible sump pump. Image B shows the garden hose used to control the hydraulic head of the system and the water containment pool.

This page is intentionally left blank.

Results and Discussion

The following sections present and discuss results from the experiments described in Section 3. The experiments were conducted to determine several physical properties of TDA, the suitability of TDA to act as a substitute for rock aggregate in a leach field, and the potential for dangerous exothermic behavior in a static pile of TDA. The TDA material used in the experiments included type A, type B, and a 50-50 mix of type A and B. The material used is representative of the size range most likely to be specified in civil engineering applications.

Comparison of Rock Aggregate and TDA as Leach Field Media

The rock aggregate and TDA leach fields were dosed with primary treated municipal wastewater from an oxidation pond each day for 17 months. The daily flow rate delivered to each leach field was approximately the same and was chosen to be representative of average daily household water use in the United States, which is 349 gal/day (American Water Works Association, 1999). Over the course of the experiment, the average flow rate to the rock aggregate and TDA leach fields was 416 gallons per day (gpd) and 366 gpd respectively. The difference in the delivery rate to each system was not by design, but rather due to minor differences in valve settings.

Physical Properties of Experimental Leach Fields

Physical inspections of the media within the rock and TDA leach fields were performed after approximately 4, 7, 10 and 17 months of wastewater loading to observe the presence of any organism growth. The location of the media inspection was at the mid-length point in each trench. During the final inspection, the media was also examined at the end of each trench. Besides a fresh soil type aroma, no odor was detected from either leach field during any of the media examinations. The rock aggregate leach field showed negligible signs of microorganism growth until 17 months from the start of the experiment (Figure 24). Rock aggregate that was closer to ground surface was relatively clean gravel, but the gravel's grittiness increased with depth. Below the perforated pipe in the TDA leach field, microorganism growth was observed at each inspection and the TDA media became increasingly more oxidized and covered in organic slime as time progressed (Figure 25).

During the 17-month internal media inspection of the leach fields, samples were taken of the leachate that was pooled at the bottom of the trench near the effluent pipe. The leachate samples contained solids dislodged from the media during the examination, along with solids that had settled to the bottom of the trench over the 17-month operational period. Leachate from the TDA leach field was considerably darker than the rock aggregate leach field, which may be a product of iron sulfide precipitation, decaying biological slime that had sloughed off the TDA, and/or carbon particulate matter from the TDA material itself (Figure 26). In contrast, leachate from the rock aggregate trench was brown and contained soil-like particulate matter. In both systems, the particulates responsible for the color were colloidal in nature, with poor settling characteristics.

During water quality sampling a noticeable change in the clarity of wastewater samples occurred on March 14, 2012 (approximately 12 months into the experimental trial) at the middle sampling location in the TDA leach field. Extracted leachate began to exhibit an increase in black carbon particulate that was suspended in wastewater samples. Even at the 7-month inspection, the TDA media was covered with biological slime. Biological slime in attached growth systems is constantly sloughing off and regrowing, with the sloughed solids settling to the bottom of the trench along with influent settleable solids. It would be expected that the slime layer and subsequent sloughed solids would be highest at the head end of the trench where the influent concentration of nutrients and organic material is highest. Since much of the influent solids would also settle out near the head end of the trench, a "plume" of solids along the bottom of the trench extending "downstream" from the entrance likely forms. It is possible that the March 14,

2012 sample date marked the time where the “plume” of solids had reached the midpoint sample port explaining the marked change in sample turbidity from that date forward.



Figure 24. Microorganism growth on rock aggregate after 7, 10, and 17 months of wastewater loading in leach fields.



Figure 25. Microorganism growth on TDA after 7, 10, and 17 months of wastewater loading in leach fields.

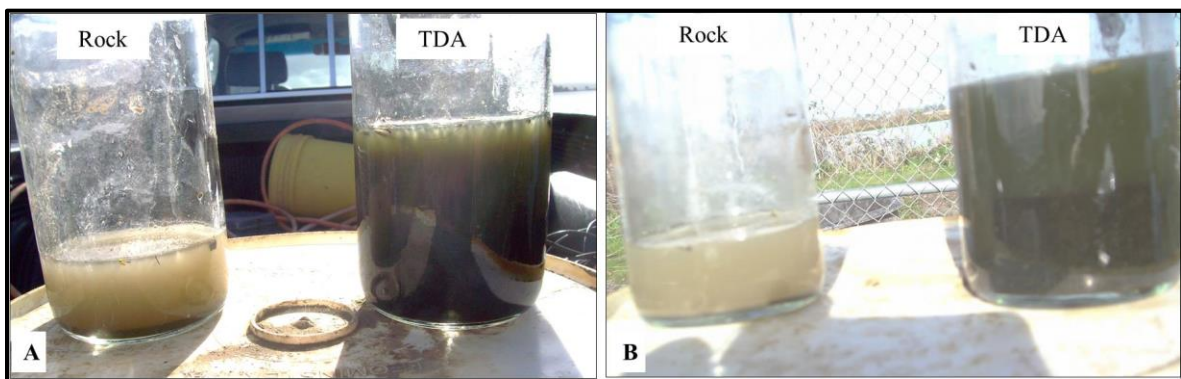


Figure 26. Effluent water clarity is shown for rock and TDA leach fields initially (A) and 15 min. later (B) for a representation of settling characteristics.

Leach Field Media Temperature

The average daily temperature of the media in both leach fields exhibited a pattern very similar to the ambient air temperature during the experimental period (Figure 27). Both materials were initially warmer than the air temperature, with the TDA more so than the rock. The rock and TDA were subject to the solar radiation during site construction, which explains the media temperature initially being higher than the air. The temperature of the rock and TDA fluctuated similarly throughout the experiment. However, temperature probes below both materials were not necessarily subject to the same degree of influence from influent wastewater loading which may account for slightly higher temperatures observed in the TDA leach field (Figure 27, Table 7).

For at least the first seven weeks of experimentation, the temperature above the TDA leach pipe was approximately 3 °F higher than the temperature below the pipe in either the TDA or rock system (Figure 28). This condition is probably due to oxidation reactions in the TDA, solar radiation warming the overlying soil, or wastewater dosing cooling media below the pipe. It is not known how long this temperature condition persisted because a temperature sensor failure occurred on Sept. 8, 2011. When the sensor was replaced on Oct. 25, 2011, temperatures above and below the TDA leach field pipes were nearly the same. The TDA media temperature above and below the pipe were nearly the same until April 2012, when warming of the overlying soil may have influenced the above pipe media temperatures. Overall, there was little difference between the rock and TDA media temperatures and there was no evidence of any hazardous temperature increases due to exothermic reactions during the experimental time period.

Table 7. Comparative statistics for the leach field media and air temperature data for matching dates.

Statistic	TDA Leach Field- Above Perforated Pipe	TDA Leach Field- Below Perforated Pipe	Rock Leach Field- Below Perforated Pipe	Ambient Temperature
Mean (°F)	64.9	63.6	63.7	55.5
Standard Deviation (°F)	6.6	5.6	6.1	8
Minimum Value (°F)	48.7	48.1	48.7	30.1
Maximum Value (°F)	75.3	71.8	73.3	82
# of Data Points	30,474	30,474	30,474	30,474

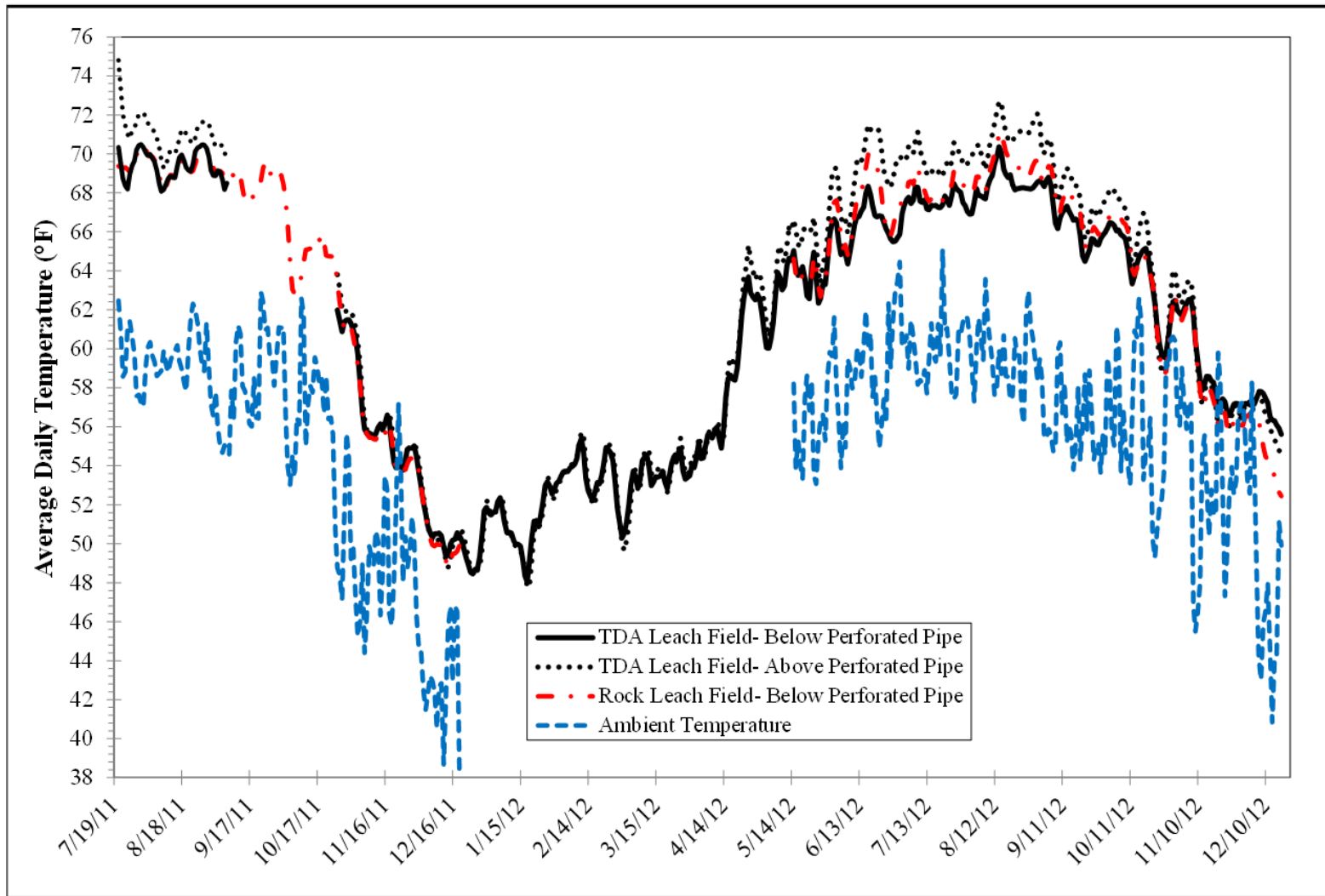


Figure 27. Average daily media and air temperature for the experimental leach fields containing rock and tire-derived aggregate (gaps in data are a result of temperature probe failure).

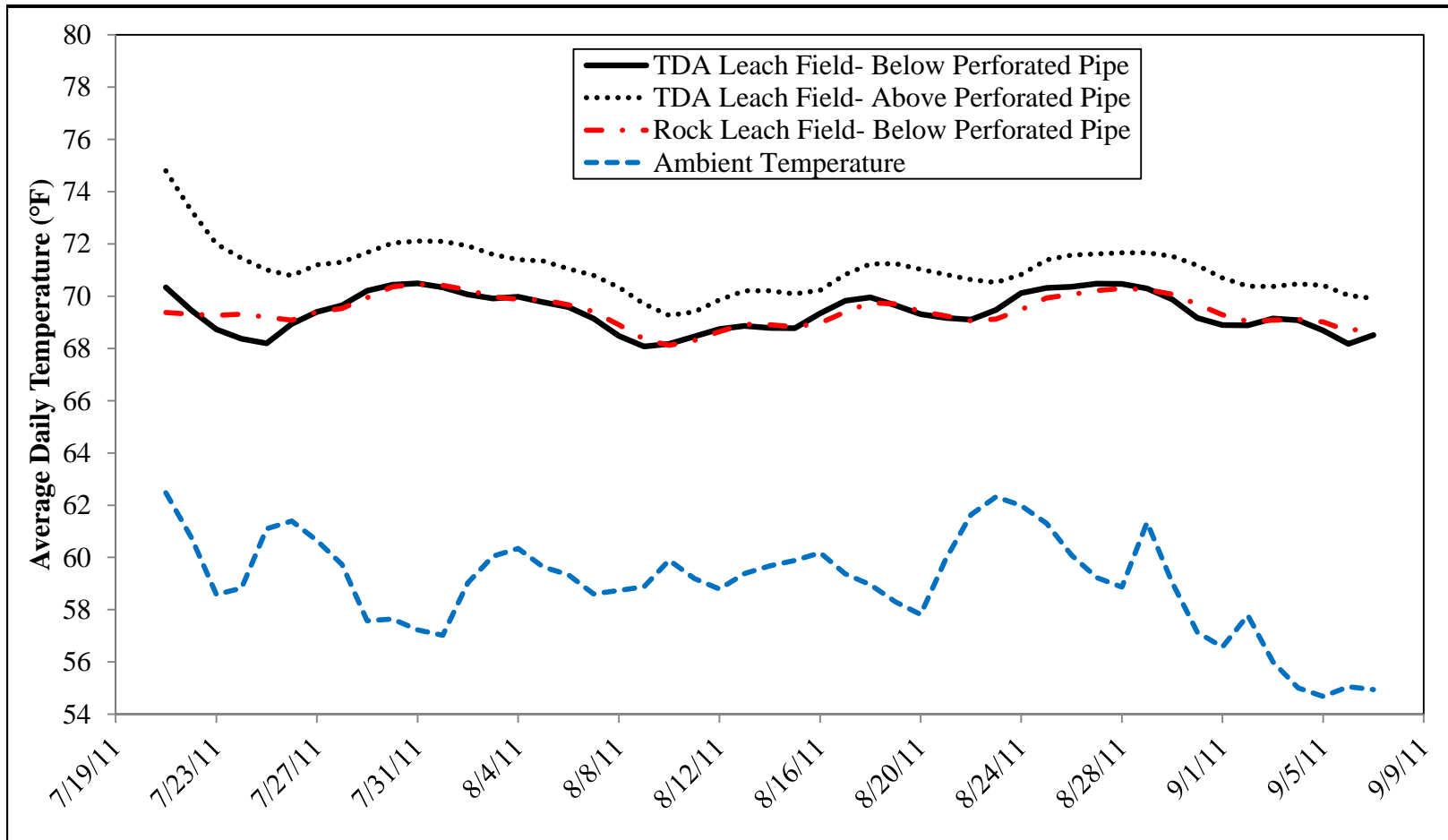


Figure 28. First seven weeks of average daily temperature within/outside the leach fields.

Water Quality Characteristics of Leachate from Leach Fields

The leachate concentration of a variety of water quality constituents for the experimental rock and TDA leach fields was measured to determine the appropriateness of substituting TDA for rock as a leach field aggregate. A total of 84 different water quality constituents were analyzed for the influent, midpoint, and effluent samples from both systems on 16 sample dates over the 17-month operational period (see Table A-1 on Page 101 for a complete list of the tested constituents). Of those tested, only 24 constituents had detectable concentrations in any of the samples. A list of the parameters with no detectable concentration is shown in Table 8.

Table 8. Water quality constituents that had no detectable concentrations observed in the experimental leach fields for the entire test period.

Water Quality Constituents Not Detected			
•1,1,1,2-Tetrachloroethane	•1,3,5-Trimethylbenzene	•Carbon tetrachloride	•n-Butylbenzene
•1,1,1-Trichloroethane	•1,3-Dichlorobenzene	•Chlorobenzene	•n-Propylbenzene
•1,1,2,2-Tetrachloroethane	•1,3-Dichloropropane	•Chloroethane	•o-Xylene
•1,1,2-Trichloroethane	•1,4-Dichlorobenzene	•cis-1,2-Dichloroethene	•sec-Butylbenzene
•1,1-Dichloroethane	•2,2-Dichloropropane	•cis-1,3-Dichloropropene	•Styrene
•1,1-Dichloroethene	•2-Chlorotoluene	•Dibromochloromethane	•Tert-amyl methyl ether (TAME)
•1,1-Dichloropropene	•4-Chlorotoluene	•Dibromomethane	•Tert-butyl ether (MTBE)
•1,2,3-Trichloropropane	•4-Isopropyltoluene	•Dichlorodifluoromethane	•tert-Butylbenzene
•1,2,4-Trichlorobenzene	•Benzene	•Di-isopropyl ether (DIPE)	•Tetrachloroethene
•1,2,4-Trimethylbenzene	•Bromobenzene	•Ethyl tert-butyl ether (ETBE)	•TPHC Gasoline
•1,2-Dibromo-3-chloropropane (DBCP)	•Bromochloromethane	•Ethylbenzene	•trans-1,2-Dichloroethene
•1,2-Dibromoethane (EDB)	•Bromodichloromethane	•Hexachlorobutadiene	•trans-1,3-Dichloropropene
•1,2-Dichlorobenzene	•Bromoform	•Isopropylbenzene	•Trichloroethene
•1,2-Dichloroethane	•Bromomethane	•m,p-Xylene	•Trichlorofluoromethane
•1,2-Dichloropropane	•Cadmium	•Methyl tert-butyl alcohol (TBA)	•Vinyl chloride

Water quality constituents that had detectable concentrations were compared to a variety of available potable water regulatory standards including: the removal action level, the maximum contaminant level, the maximum contaminant level goal, the drinking water equivalent level, and the secondary maximum contaminant level. Of the constituents examined, only the concentration of iron did not meet any regulatory standards (Table 9).

Table 9. Regulatory water quality parameter values compared to maximum values found in the leach fields tested

Parameter (µg/L unless otherwise noted)	Removal Action Level	MCL	MCLG ¹	DWEL ²	Secondary MCL	Max. Rock Effluent Value	Max. TDA Effluent Value
1,2-Dichloroethane	40	5	0	NA	NA	122	123
Ammonia (as N) (mg/L)	34,000	NA	NA	NA	NA	19	21
BOD ³ (mg/L)	NA	NA	NA	NA	NA	160	140
Chlorobenzenes	700	100	100	700	NA	0	0.52
Chloroform	100	100	0	400	NA	0	0
Chloromethane	100	NA	NA	100	NA	0	0.51
COD ⁴ (mg/L)	NA	NA	NA	NA	NA	230	220
FC ⁶ (MPN/100 mL)	NA	TT ⁷	0	NA	NA	1,300,000	1,700,000
Iron	NA	NA	NA	NA	300	1,300	12,000
Lead	15	TT ⁷	0	NA	TT ¹	0	0
Manganese	NA	NA	NA	NA	50	200	250
Methylene chloride	500	5	0	2,000	NA	2.5	1.0
Naphthalene	100	NA	NA	100	NA	0	0
Nitrate (as N) (mg/L)	10,000	10,000	10,000	56,000	NA	3.7	2.3
NFR ⁸ (mg/L)	NA	NA	NA	NA	NA	140	130
pH	NA	NA	NA	NA	6.5-8.5	7.2	7.0
Sulfate (mg/L)	250,000	500,000	500,000	NA	250,000	22	21
TC ⁹ (MPN/100 mL)	NA	≤5.0 % ¹⁰	0	NA	NA	5,400,000	5,400,000
Toluene	2,000	1,000	1,000	7,000	NA	1.90	0
Total Phosphate (as P) (mg/L)	NA	NA	NA	NA	NA	7.1	6.3
Zinc	3,000	NA	NA	10,000	5000	46	250

Source: U.S. Environmental Protection Agency, 1997) (NA= not available).

¹MCLG=maximum contaminant level goal, ²DWEL= drinking water equivalent level, ³BOD= biological oxygen demand, ⁴COD=chemical oxygen demand, ⁶FC= fecal coliform, ⁷TT=treatment technology, ⁸non-filterable residue, ⁹TC= total coliform, ¹⁰of the tested samples for total coliform this corresponds to the positive tests in a month

The differences in the effluent concentrations of detectable water quality parameters from the two leach fields were statistically analyzed using a paired sample Student's t-Test for equality of means. Since this experiment was designed to provide information on the appropriateness of substituting rock with TDA in leach fields, a one-sided, 95 percent confidence level was used ($\alpha=0.05$). Effluent water quality values

were assumed to follow a normal distribution and the difference between the TDA and rock effluent concentration on sample days was assumed to be statistically independent.

Eight parameters had significant differences in effluent water quality between the rock and TDA leach fields (Table 10); iron, manganese, zinc, methylene chloride, sulfate, nitrate, chemical oxygen demand, and total phosphate. Of these eight constituents, only iron, manganese, and zinc TDA effluent concentrations were significantly higher (positive mean difference) compared to the rock media. The results and discussions that follow are focused primarily on those eight water quality constituents that showed statistically significant differences between the TDA and rock leach field effluent. A graphical representation of all detectable parameters is shown in Appendix C (Page **Error! Bookmark not defined.**).

There are a few considerations to recognize before proceeding. Water quality parameter concentrations were graphed over time and observed values are connected with a line to aid in identifying trends and not to imply that the behavior of the system is known between observed values. Another important consideration regards the data for 1,2,3-trichlorobenzene. Testing procedures for this compound are difficult, and generally the concentration of 1,2,3-trichlorobenzene are inferred from the concentration of a surrogate. Surrogates are compounds considered similar in chemical composition to an analyte of interest (in this case 1,2,3-trichlorobenzene), and for which analytic procedures to detect the compound are available. In this experiment, the surrogates 1,2-dichloroethane-d4, dibromofluoromethane, and toluene-d8 were used for 1,2,3-trichlorobenzene, but they may not completely represent actual concentrations of the 1,2,3-trichlorobenzene. Lastly, there was a loss of electric power to the experimental site from June 27, 2012 to July 1, 2012, Aug. 1, 2012 to Aug. 5, 2012, and Aug. 15, 2012 to Sept. 1, 2012. During those time intervals, the leach fields were not loaded with wastewater, which may have contributed to changes in constituent concentrations in tested samples after July 1, 2012.

Parameter ($\mu\text{g/L}$ unless otherwise noted)	Effluent MD ¹ ($\mu\text{g/L}$)	Effluent MD SD ² ($\mu\text{g/L}$)	t Statistic	Degrees of Freedom	One Tailed p Value	Reject Null Hypothesis	95% Confidence Level
1,2,3-Trichlorobenzene	0.0325	0.130	1	15	0.167	Do Not Reject	0.0693
1,2-Dichloroethane-d ₄ ³	2.07	4.89	1.69	15	0.0556	Do Not Reject	2.61
Ammonia (as N) (mg/L)	0.212	1.76	0.482	15	0.318	Do Not Reject	0.936
BOD ⁴ (mg/L)	-4.63	15.3	1.21	15	0.122	Do Not Reject	8.14
COD ⁵ (mg/L)	-14.7	33.4	1.76	15	0.0497	Reject	17.8
Chloroform	0	0	NA	15	NA	Do Not Reject	NA
Chloromethane	0.0319	0.128	1	15	0.167	Do Not Reject	0.0679
Dibromofluoromethane ³	0.0687	3.65	0.0753	15	0.470	Do Not Reject	1.95
FC ⁶ (MPN/100 mL)	75,385	562,889	0.483	12	0.319	Do Not Reject	340,150
Iron	3,646	3,137	4.65	15	1.57x10 ⁻⁴	Reject	1,671
Lead	0	0	NA	15	NA	Do Not Reject	NA
Manganese	29.4	32.6	3.61	15	0.00130	Reject	17.4
Methylene chloride	-0.223	0.442	2.02	15	0.0309	Reject	0.236
Naphthalene	0	0	NA	15	NA	Do Not Reject	NA
Nitrate (as N) (mg/L)	-0.956	0.473	8.08	15	3.81x10 ⁻⁷	Reject	0.252
NFR ⁷ (mg/L)	2.81	12.2	0.923	15	0.185	Do Not Reject	6.50
pH (pH units)	-0.0437	0.126	1.39	15	0.0931	Do Not Reject	0.0673
Sulfate (mg/L)	-2.25	1.95	4.62	15	1.6x10 ⁻⁴	Reject	1.04
Toluene	-0.206	0.571	1.45	15	0.0845	Do Not Reject	0.304
Toluene-d ₈ ³	-0.663	3.54	0.749	15	0.233	Do Not Reject	1.89
TC ⁸ (MPN/100 mL)	346,154	1,572,432	0.794	12	0.221	Do Not Reject	950,211
TKN ⁹ (mg/L)	-0.5	4.95	0.143	1	0.455	Do Not Reject	44.5
Total Phosphate (as P) (mg/L)	-0.544	0.643	3.38	15	0.00205	Reject	0.343
Zinc	26.0	56.3	1.85	15	0.0422	Reject	30.0

Table 10. Results from a Student's t-Test for water quality parameters that had detectable effluent concentrations in experimental leach fields.

¹MD=mean difference or average tire-derived aggregate effluent minus the average rock aggregate effluent parameters for every sample tested, ²SD= standard deviation of the mean difference, ³a surrogate of 1,2,3-Trichlorobenzene, ⁴BOD= biological oxygen demand, ⁵COD=chemical oxygen demand, ⁶FC= fecal coliform, ⁷NFR= non-filterable residue, ⁸TC= total coliform, ⁹total Kjeldahl nitrogen

IRON, ZINC, AND MANGANESE

The concentration of iron, zinc, and manganese in the leachate from rock and TDA leach fields behaved similarly over the 17-month study. Very little change in concentration occurred in the rock aggregate system, with the influent and effluent concentration generally being the same (Figures 29-30). Attached growth systems are not noted as having significant metals removal, so it is not surprising that the effluent concentration of these metals was the same as the influent concentration in the rock aggregate leach field.

The situation was considerably different in the TDA system, where the effluent concentration for all three metals is generally higher than the influent concentration. The increase in iron, zinc, and manganese effluent concentration as compared to the influent value was evident from the initial sampling date, and addition of metals to the leachate from the TDA increased for the first two months (until Oct. 12, 2011). After the first two months, the behavior of the three metals was somewhat different. The percentage increase in the effluent concentration of iron and manganese compared to the influent was reasonably constant for the remaining 15 months of the study, with perhaps a slight decline the last couple of months (Figures 29-30). In contrast, the effluent zinc concentration from the TDA system appeared to be only slightly higher than the influent value after Oct. 12, 2011 for the remainder of the study period.

It is surprising that the percent increase in the effluent concentration of these three metals compared to the influent either remained constant or declined after October 2011 given the sharp increase in concentration observed at the midpoint sample location beginning with the March 13, 2012 sample. The timing of this increase in concentration of iron, zinc, and manganese at the midpoint sample location coincides with the previously discussed increase in turbidity observed at the same site on the same date. It is reasonable to assume that the black particulate material that was responsible for the increase in turbidity at this site also contained high concentration of metals. This plume of solids likely became trapped at the small weir placed at this sample location, and the material was caught in each sample extracted by the hand pump for analysis.

The increase in iron, zinc, and manganese concentration in the leach field indicates a source of these metals within the system. In this situation, the source of the metals must be the TDA media. Tires contain 1-2 percent zinc by weight, and zinc is known to leach from crumb rubber (Rhodes et al., 2012). The TDA used as leach field aggregate material had exposed steel wire visible on most tire fragments. Iron and manganese are reported as the most commonly observed metals leaching from tires (Spagnoli et al., 2001). Iron is the principal component of steel, and most steel mixtures contain from 0.1 to 1.0 percent manganese. Exposed to the air and moisture, the steel wire in the tire will oxidize, forming rust, a reddish-brown crust on the surface of the wire. Some of the rust material can break or wash off and become part of the particulates in the leachate. The rust on the TDA used in the leach field was very pronounced by the time of the first physical inspection of the media, four months into the study (Figure 25).

Rhodes et al. (2012) observed a “first flush” spike in zinc leaching from TDA when it was first exposed to water. After the first pulse, the concentration of zinc in the leachate was reduced to a more steady-state, constant value. This condition corresponds to what was observed in the TDA leach field effluent in this study. The same phenomenon would be expected with the oxidation of the steel wire in the TDA. Initially the oxidation rate would be high when all of the “fresh” exposed wire was available. Over time, the oxidation rate would slow due to the reduction in available exposed steel. Again, this condition would account for the change in the rate of iron and manganese addition observed from during study in the TDA leach field.

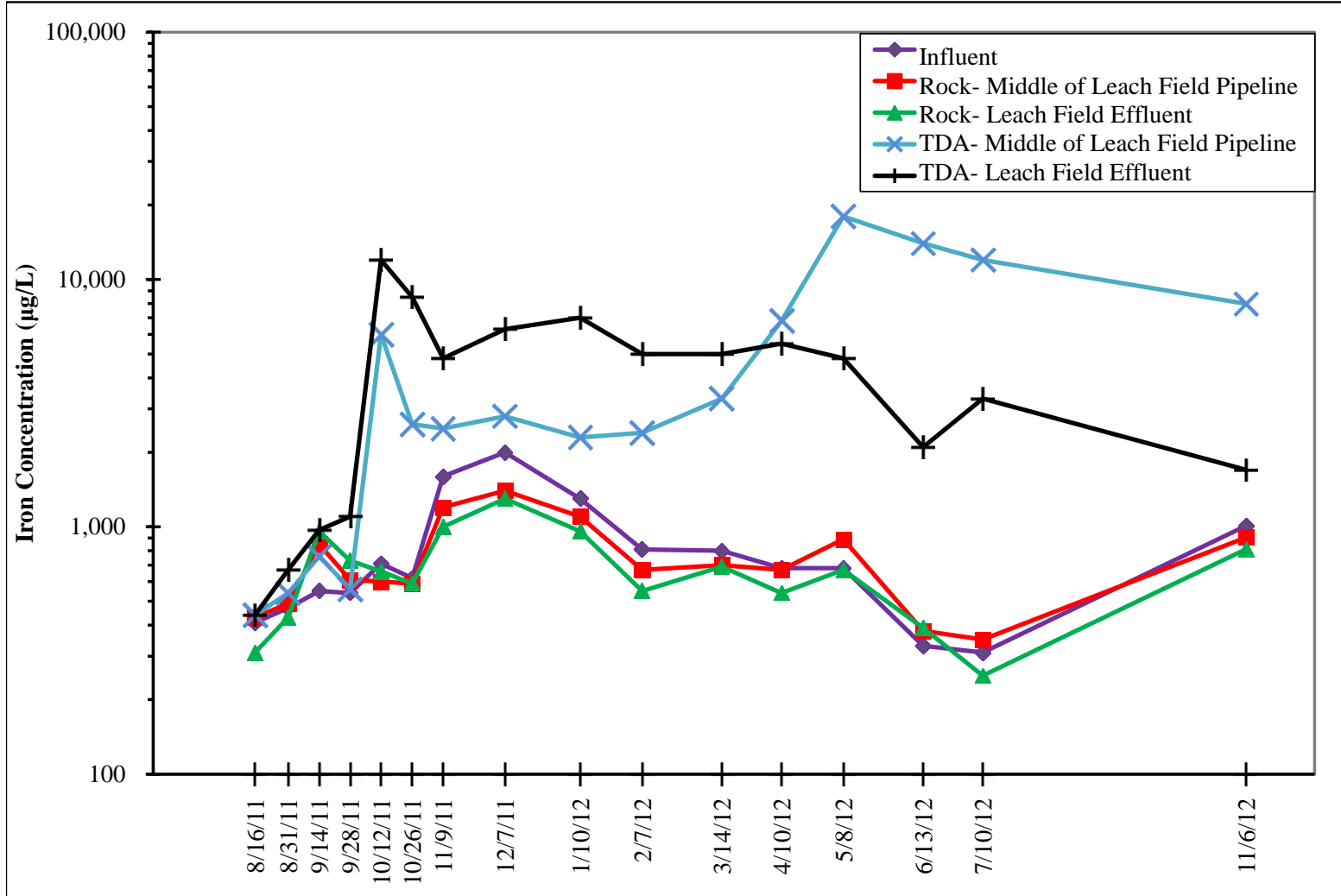


Figure 29. Iron concentrations in the rock and TDA leach fields

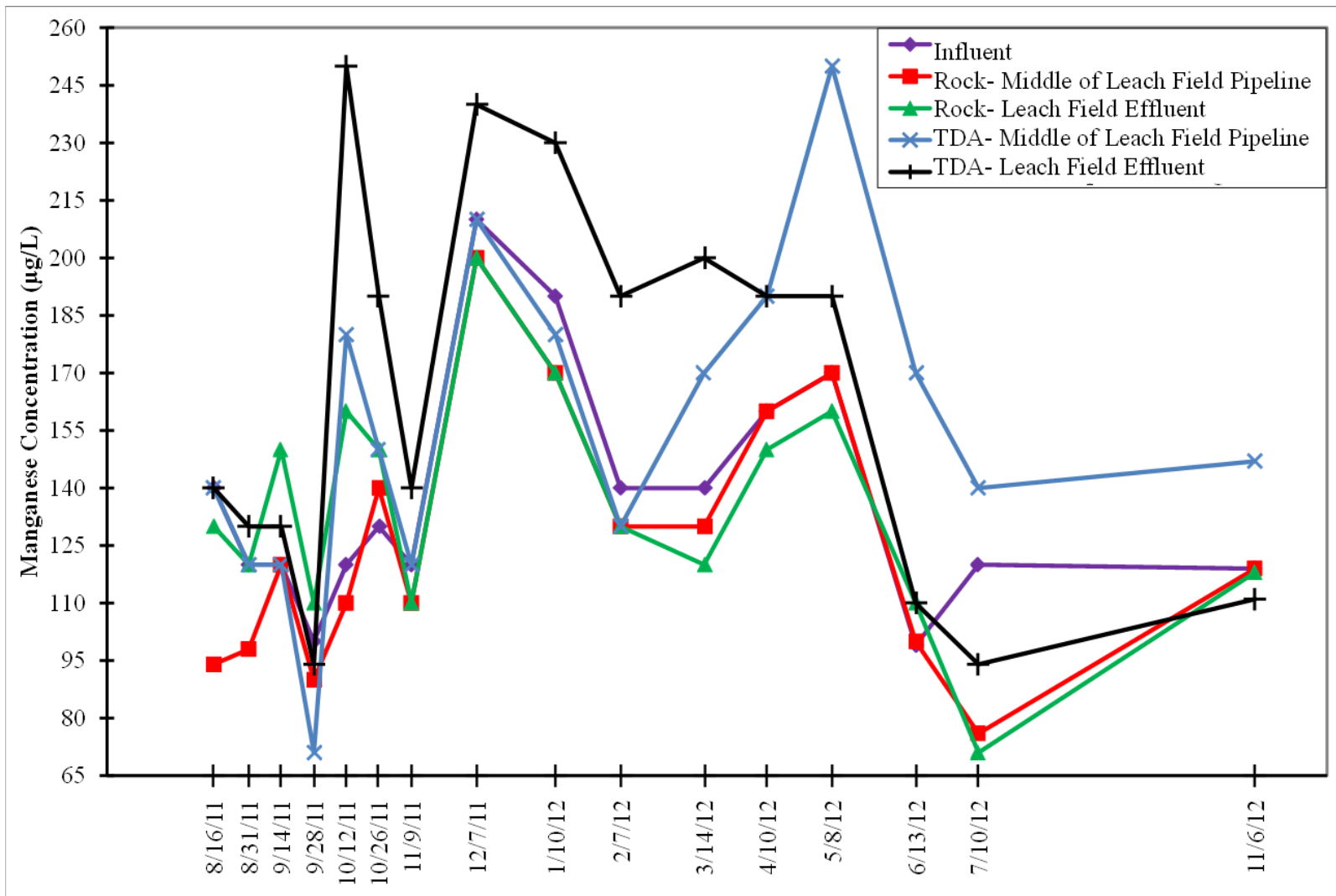


Figure 30. Manganese concentrations in the rock and TDA leach fields

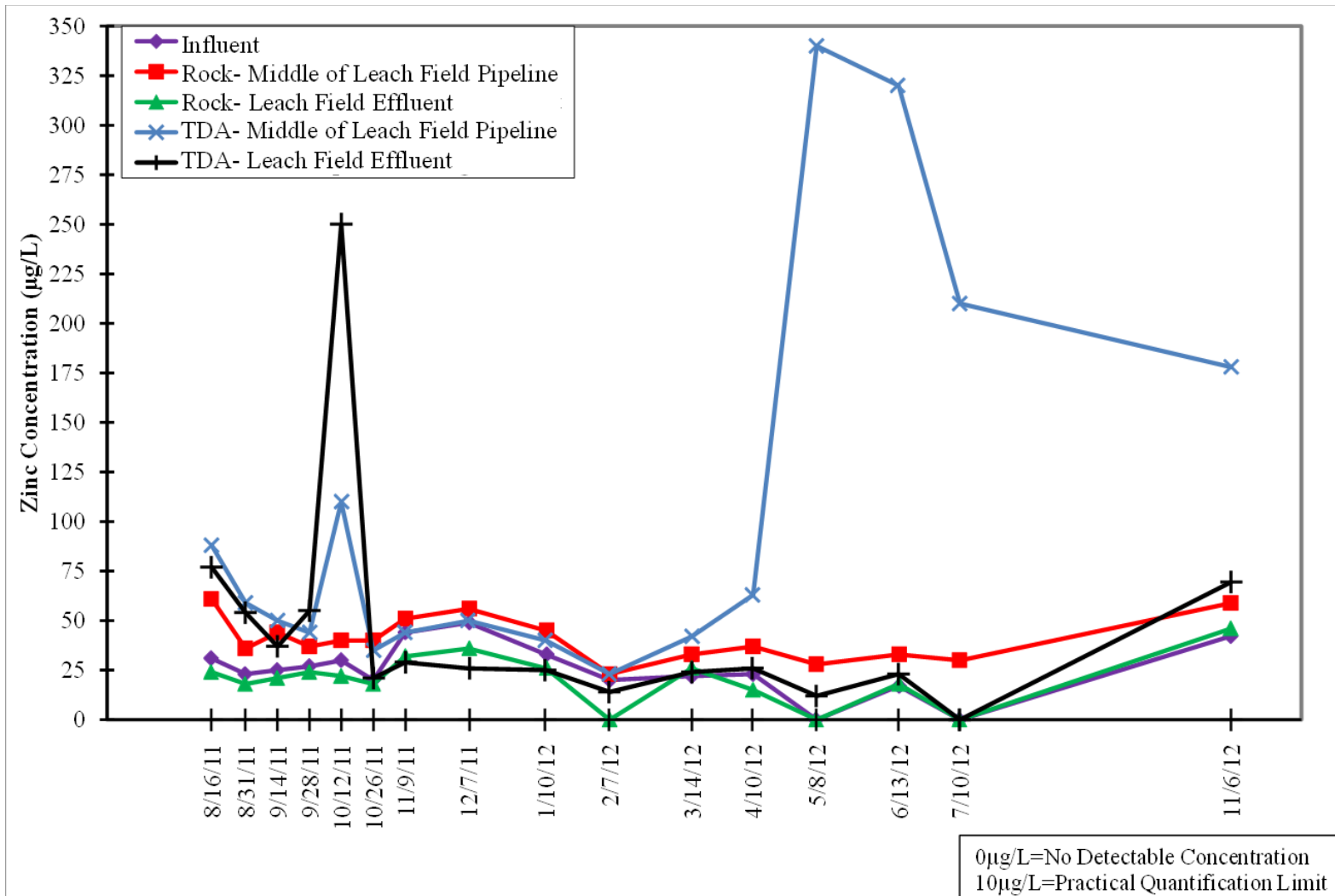


Figure 31. Zinc concentrations in the rock and TDA leach fields.

SULFATE

The sulfate concentration in the oxidation pond, which is the leach field influent source, varies throughout the year as a function of dilution from precipitation, oxidation pond pH, temperature, and a variety of other factors. Reduction in sulfate concentration generally occurred in both leach fields; however, the TDA effluent leachate had significantly lower concentrations of sulfate than the rock aggregate leachate (Figure 32). The more extensive biofilm layer noted on the TDA compared to the rock aggregate is the likely reason for the difference between sulfate concentrations in the leach fields. Attached growth anaerobic sulfate-reducing bacteria reduce sulfate to hydrogen sulfide using sulfate or other compounds such as nitrate as terminal electron acceptors (Marietou et al., 2009; Schulze and Mooney, 1994). Hydrogen sulfide can combine with metal ions to form insoluble metal sulfides. Ferrous sulfide is dark brown or black colored, and is likely the black colloidal material described earlier that was observed in the TDA effluent.

The degree of sulfate reduction in the TDA leach field was observed to decrease beginning with the Jan. 10, 2012 sample. The decrease in the sulfate reduction rate follows a rapid decrease in media temperature (60°F in November 2011 to 48°F in January 2012) which would suppress the activity of the mesophilic sulfate reducing bacteria. However, the decreased rate of sulfate reduction continued into the spring of 2012 after the media temperature increased to a more favorable range. Influent pumps were offline a few times between July and September 2012, which limited flow through the leach fields and may have starved any organisms present of essential nutrients or decreased the availability of an anaerobic environment.

NITRATE

The majority of nitrogen in raw domestic wastewater is either organic nitrogen or ammonia nitrogen, with small amounts of nitrate nitrogen. Organic nitrogen is composed of proteins and urea, and is converted to ammonia by bacterial decomposition and hydrolysis. The concentration of organic nitrogen is estimated from determining the Total Kjeldahl Nitrogen (TKN) and ammonia concentration, where TKN is the sum of the organic and ammonia nitrogen. Most of the nitrogen in the oxidation pond (the influent to the leach fields) would be in the form of ammonia. For example, the leach field influent concentration of TKN and ammonia were measured as 20.0 and 15.0 mg/l on July 10, 2012. The nitrate concentration in the leach field influent was essentially zero for the entire experimental period. Ammonia is converted by aerobic bacteria in a process known as nitrification, and nitrate is converted to nitrogen gas by anaerobic bacteria in a process known as denitrification. The conversion of organic nitrogen to ammonia, nitrification, and denitrification can all occur simultaneously in the leach field, complicating the interpretation of the nitrogen-related water quality data.

Although the differences are relatively small, the effluent nitrate concentrations were lower in the TDA leach field than the rock aggregate system throughout the experiment (Figure 33). Since the influent nitrate concentration to the leach field is zero, any nitrate measured in the effluent is the result of nitrification within the system. Review of the data shows that the midpoint and effluent sample point nitrate concentration values were nearly the same for each system, indicating that the nitrification rate is about the same as the denitrification rate (nitrate is being created as fast as it is converted to nitrogen gas). Some of the differences in the nitrate concentrations were due to the differences in the ammonia concentrations in each system. During the first few months of operation, the nitrification rate in both leach fields was low, and the influent and effluent ammonia concentrations were nearly the same (Figure 34). Beginning with the Dec. 7, 2011 sample, the nitrification rate appeared to increase and some reduction in ammonia occurred in each system for the remainder of the experimental period. Overall the rate of nitrification was slightly higher in the rock leach field, but the differences were small enough that the rates are not statistically significantly different (Table 10). The delay in the onset of measurable

ammonia removal at the beginning of the experiment is likely due to the time it takes to establish a viable colony of nitrifying bacteria in the media.

Assuming that the organic nitrogen concentration is unchanged in the both leach fields, the total nitrogen removal can be determined by comparing the sum of the ammonia and nitrate concentrations for the influent and effluent wastewater. The total nitrogen removal in both leach fields was zero or very small for all sample dates except March 14, 2012, May 8, 2012, and July 10, 2012. (Figure 35). While overall the removal of nitrogen in the TDA leach fields was greater than the rock system, the nitrification/denitrification process does not appear particularly important in either system.

CHEMICAL OXYGEN DEMAND

Chemical oxygen demand (COD) is a measure of the amount of oxygen required to completely oxidize carbon- and hydrogen-based compounds. The COD concentration of a wastewater is often used as an indicator for the relative oxygen consumptive impact a discharge will have on the receiving water. In general, it is beneficial for a treatment system to reduce the COD of the waste as much as possible prior to discharge. Often biochemical oxygen demand (BOD) is used rather than COD to quantify the organic content of a waste stream, but TDA leachate could potentially contain compounds that interfere with the BOD test. The primary mechanisms for COD (and BOD) removal in a leach field are sedimentation (settling of particles containing oxidizable material) and biological oxidation.

The COD concentration in the effluent from the rock aggregate leach field was only slightly different from the influent, indicating very little COD removal in this system (Figure 36). The minimal COD removal is not surprising given the relatively sparse biological community observed growing on the rock media. While not large, the removal rate of COD in the TDA leach field was higher than that of the rock leach field. After the first two months of operation, the effluent COD was consistently 10 to 30 percent lower than the influent value. The extensive biological growth on the TDA likely provides the bacteria responsible for COD removal.

The COD concentration at the midpoint sample location of the TDA system exhibited behavior similar to that previously discussed with other water quality constituents. Beginning with the May 8, 2012 sample, the COD concentration at the midpoint was significantly greater than the influent value (and all other sample locations) (Figure 36). This is likely due to a settled solids plume that is trapped behind a small weir at this sample point. Those settled solids were extracted along with the wastewater sample, resulting in a COD value that was not representative of the leachate at this point in the leach field. The power outages that resulted in the loss of influent pumping from June 27, 2012 to July 1, 2012, Aug. 1-5, 2012 and Aug. 15, 2012 to Sept. 1, 2012 may have contributed to this situation, allowing additional sloughing of biological material from the TDA due to the lack of nutrients. The sloughed biofilm would then contribute to the COD concentration of the leach field effluent.

PHOSPHORUS

Phosphorus is an essential nutrient used by all life forms. Phosphorus can be categorized as either organic or inorganic phosphorus where organic phosphorus is bound to plant or animal tissue. Inorganic phosphorus includes orthophosphate (which plants uptake), and polyphosphate. Total phosphate is the sum of all forms of phosphate in the soluble or particulate form. Phosphorus has a strong affinity for inorganic particulate matter; therefore, the primary mechanism for phosphorus removal in a leach field is the settling of inorganic particles containing bound phosphorus or organic material that incorporated phosphorus into its cellular structure.

The behavior of total phosphate in the leach fields was nearly identical to that of COD. There was very little total phosphate removal in the rock aggregate leach field for the entire study period and negligible removal in the TDA system for the first few months of operation (Figure 37). After the first two months

of operation, the TDA effluent total phosphate was consistently 10 to 40 percent lower than the influent value. The extensive biological growth on the TDA provides a suitable surface for enmeshment of inorganic particles containing bound phosphorus. The TDA was also likely providing the biological community necessary for phosphorus uptake and subsequent settling of the biological material to the bottom of the leach field. Note that the phosphorus was not permanently removed from the system, since it can be released and resuspended as the biofilm material decomposes.

Total phosphate concentration at the midpoint sample location of the TDA system also exhibited behavior similar to that previously discussed with other water quality constituents. Beginning with the May 8, 2012 sample, the total phosphate concentration was significantly greater than the influent value (and all other sample locations) (Figure 37). As with COD, this situation is suspected to be due to a settled solids plume that was trapped behind a small weir at this sample point. Those settled solids were extracted along with the wastewater sample, resulting in a phosphorus value that was not representative of the leachate at this point in the system.

TOLUENE AND METHYLENE CHLORIDE

Toluene and methylene chloride were detected on a few sample days in both rock and TDA leach fields. Methylene chloride is a colorless volatile liquid that is used in various industrial processes such as paint stripping, pharmaceutical manufacturing, paint remover manufacturing, metal cleaning, and metal degreasing. Toluene is usually a mixture added to gasoline to improve octane ratings (U.S. Environmental Protection Agency, 2012). Toluene is also used to produce benzene, organic chemicals, and polymers. Both of these compounds were detected in the influent, indicating their presence in the leach field samples was due to the oxidation pond water and not the rock or TDA media.

Methylene chloride was only detected at four of the 16 sample dates during the 14 month sampling period (Figure 38). Methylene chloride was first detected in the Feb. 7, 2012, seven months after system startup, and again at each of the next three sampling dates. While some reduction occurred in both leach fields, the effluent concentration of methylene chloride from the TDA leach field was always less than the effluent concentration from the rock aggregate system.

Toluene was only detected once in an influent sample, and twice in an effluent sample from each leach field (Figure 39). When detected, the concentration of toluene in all samples was near or at the practical qualification limit of 0.5 µg/l (the lowest concentration that reliable analytic data can be reported). The concentrations of toluene in the rock and TDA leach fields were not statistically significantly different, but the time when toluene was detected was different. Toluene was detected in the rock aggregate leach field a month after system startup, corresponding with the one influent sample with a detectable toluene concentration. The two sample dates when toluene was detected in the TDA leach field occurred nine months after system startup. As with methylene chloride, the TDA leach field appeared to do a better job of removing toluene than the rock media system given that toluene was only detected at the midpoint sample location in the TDA system and never in the effluent.

SUMMARY OF WATER QUALITY RESULTS

A total of 84 different water quality constituents were analyzed for the influent, midpoint, and effluent of both systems in 16 sample dates (see Table A-1 on page 101 for a complete list of the tested constituents). Of those 84 constituents tested, only 24 constituents had detectable concentrations in any of the samples over the 17-month leach field operation period. Of the constituents detected, only the concentration of iron did not meet all regulatory standards examined.

Eight constituents had statistically significant differences in effluent water quality between the rock and TDA leach fields; iron, manganese, zinc, methylene chloride, sulfate, nitrate, chemical oxygen demand, and total phosphate. Of these eight constituents, only iron, manganese, and zinc TDA effluent

concentrations were statistically significantly higher compared to the rock media, which is likely a result of oxidation steel components in the TDA. Reduction in sulfate, COD, and phosphorus concentrations generally occurred in both leach fields; however, the TDA effluent leachate had significantly lower concentrations of these constituents than the rock aggregate leachate. The more extensive biofilm layer noted on the TDA compared to the rock aggregate is a likely reason for the difference between effluent concentrations of these constituents in the leach fields. While the removal of nitrogen in the TDA leach fields was greater than the rock system, it did not appear that the nitrification/denitrification process was particularly important in either system. Finally, methylene chloride and toluene were occasionally detected in both leach fields, but the TDA system appeared to remove these compounds better than the rock media system.

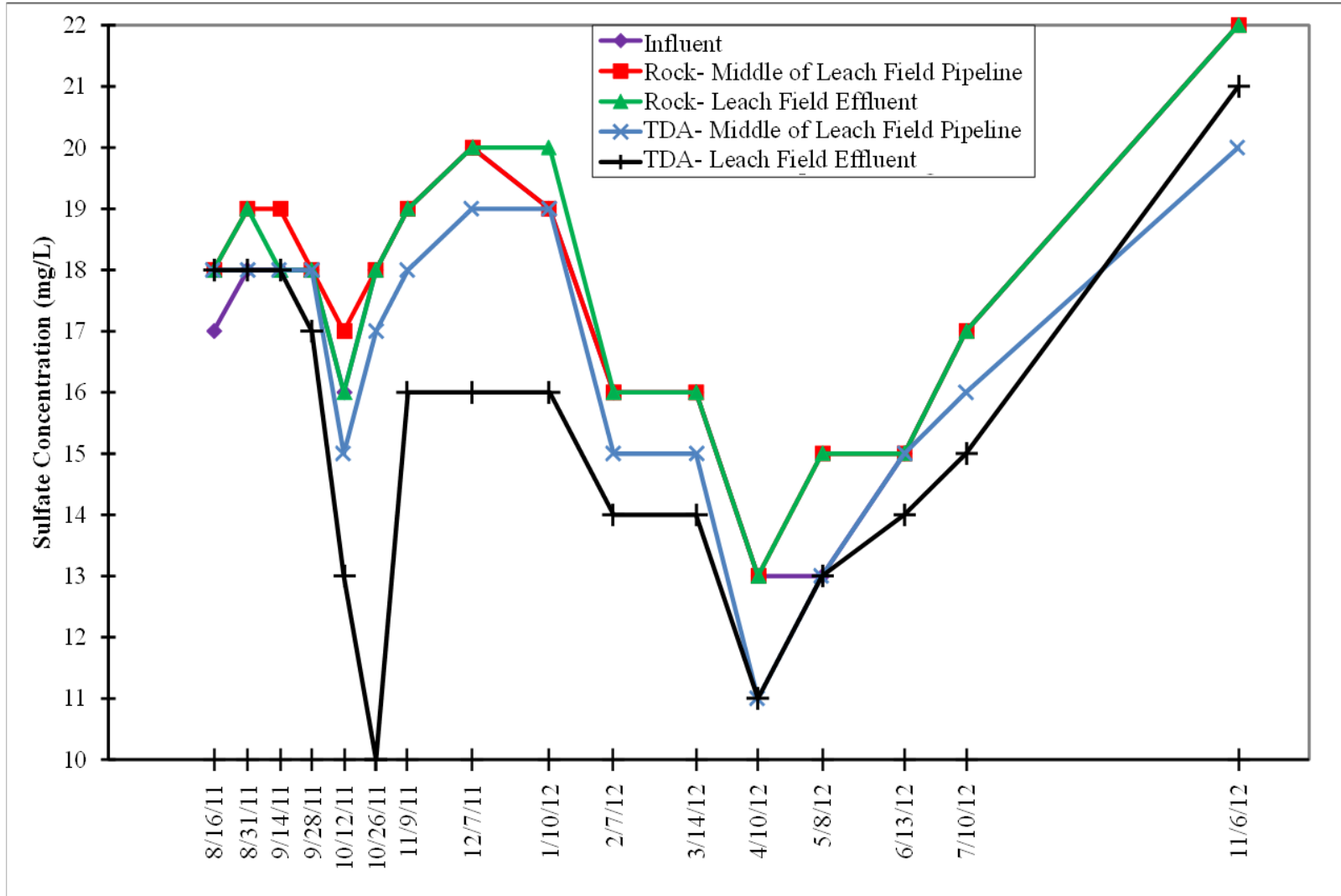


Figure 32. Sulfate concentrations in the rock and TDA leach fields.

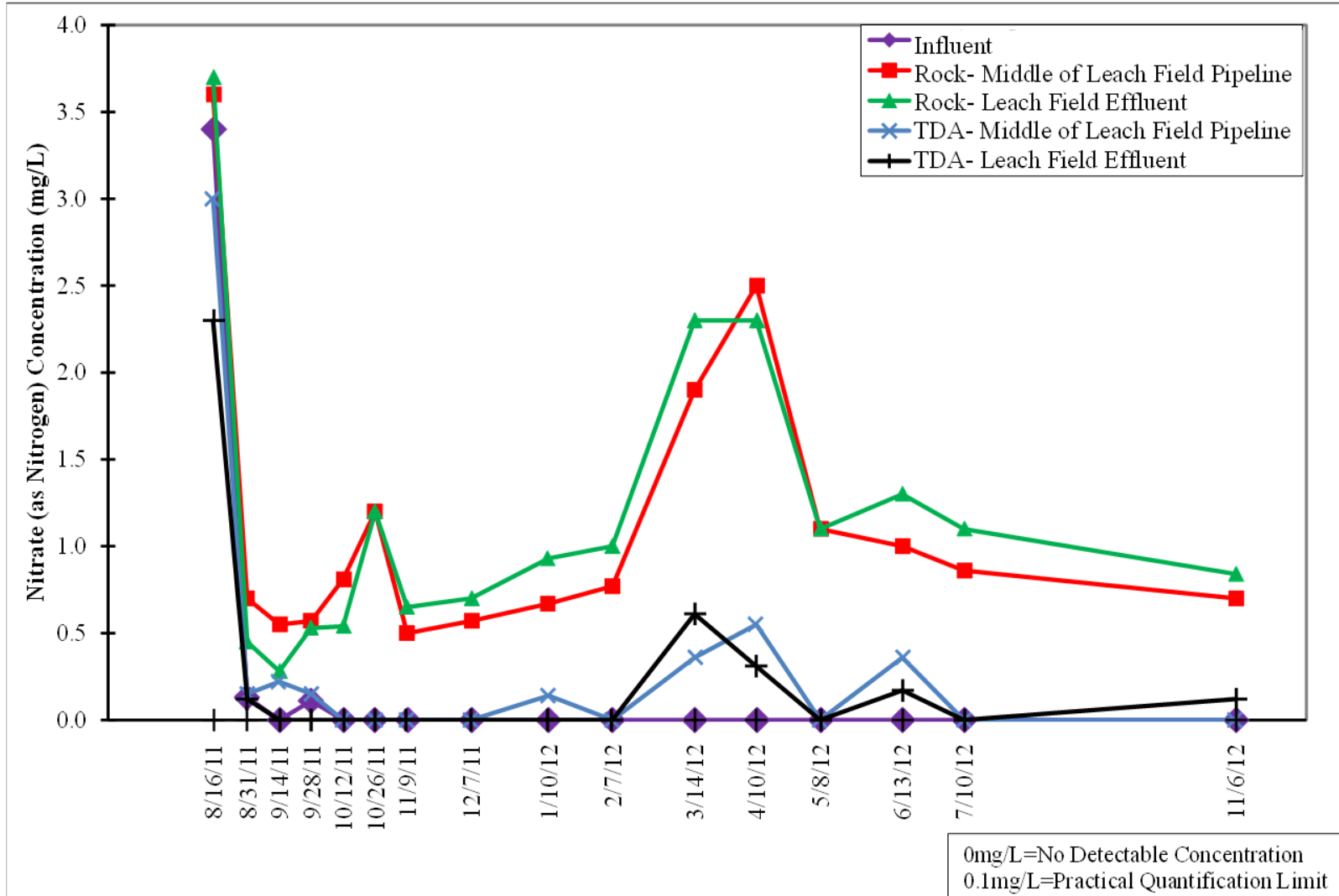


Figure 33. Nitrate (as N) concentrations in the rock and TDA leach fields

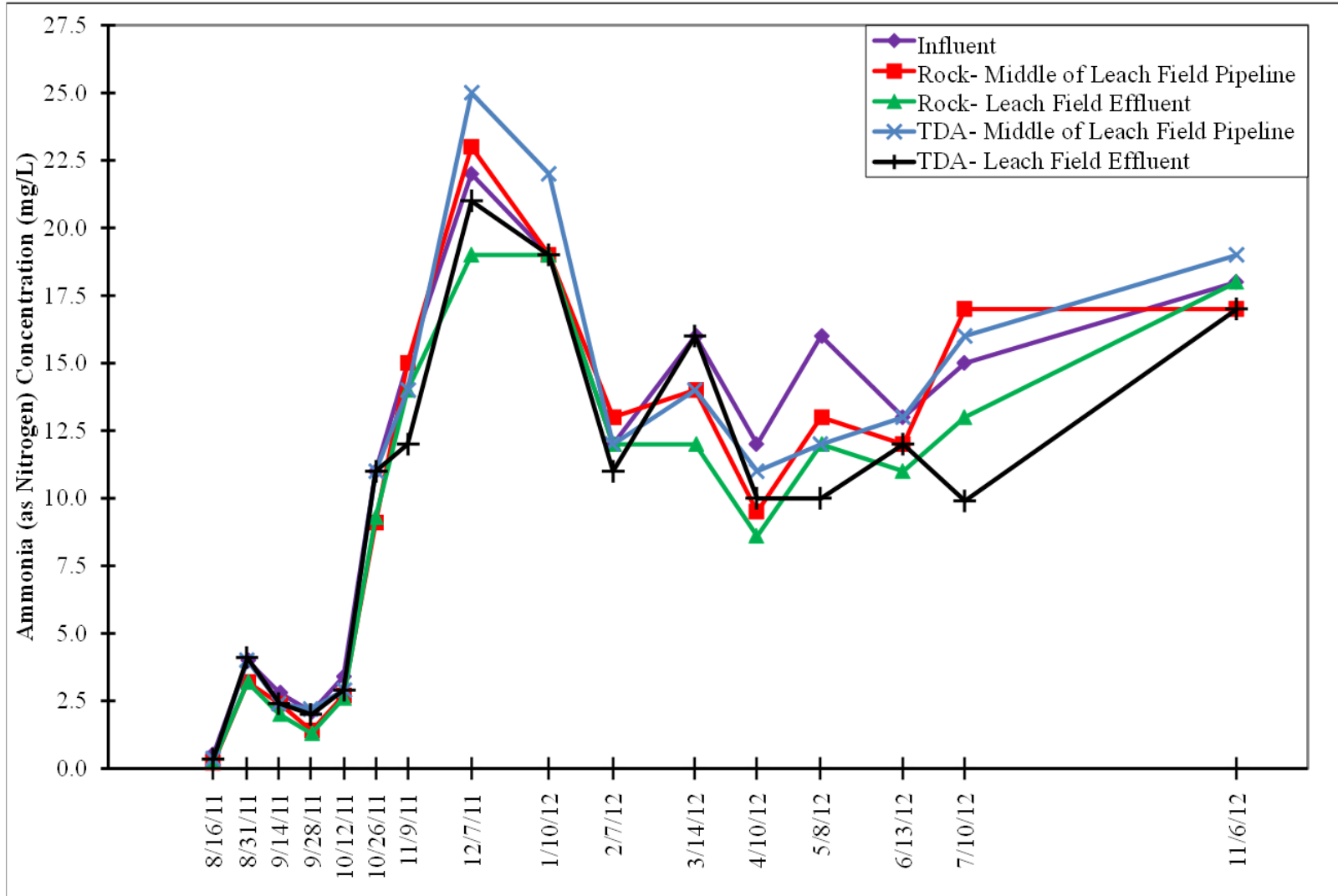


Figure 34. Ammonia (as N) concentrations in the rock and TDA leach fields.

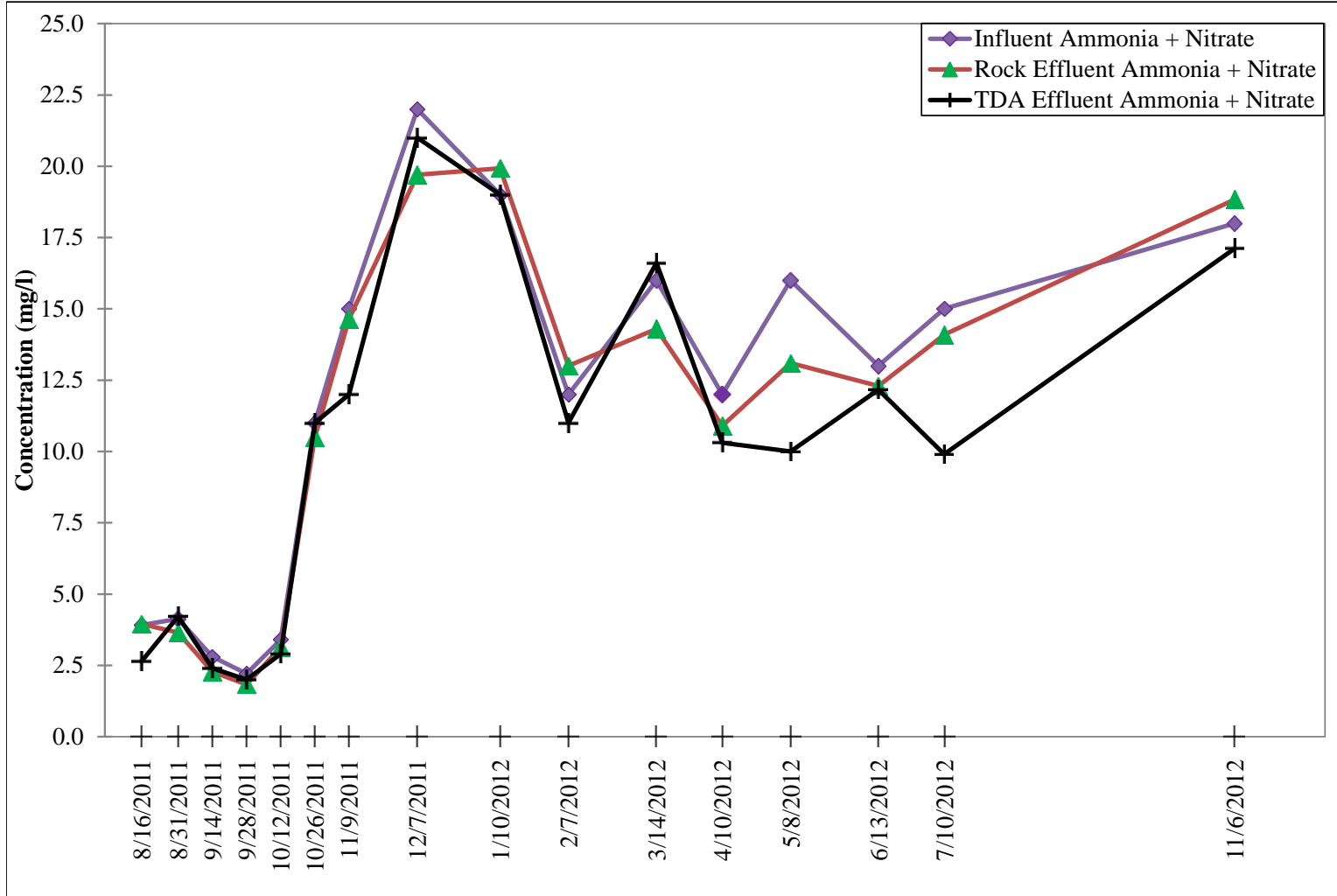


Figure 35. Influent and effluent ammonia + nitrate concentrations in rock and TDA leach fields.

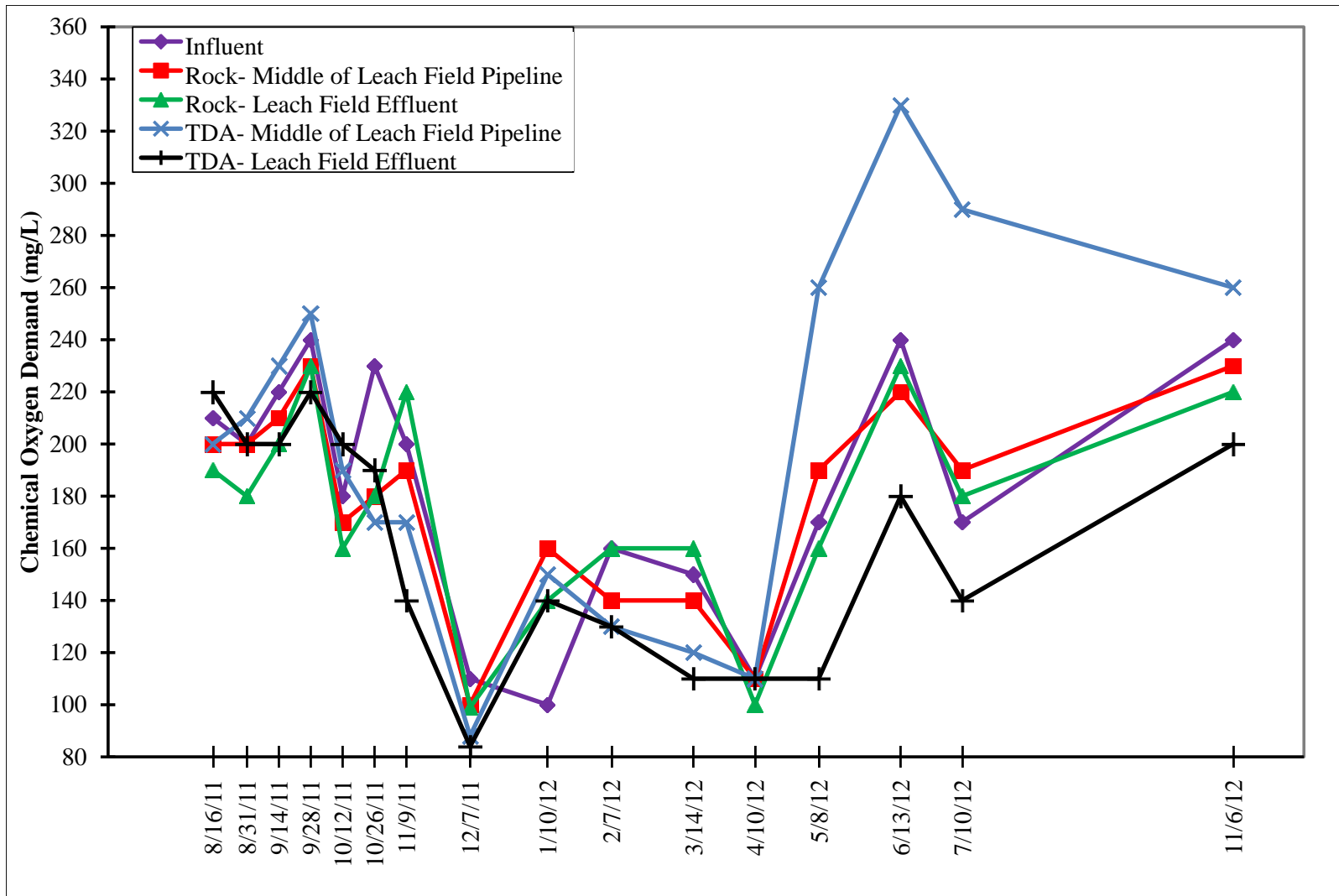


Figure 36. COD concentrations in the rock and TDA leach fields.

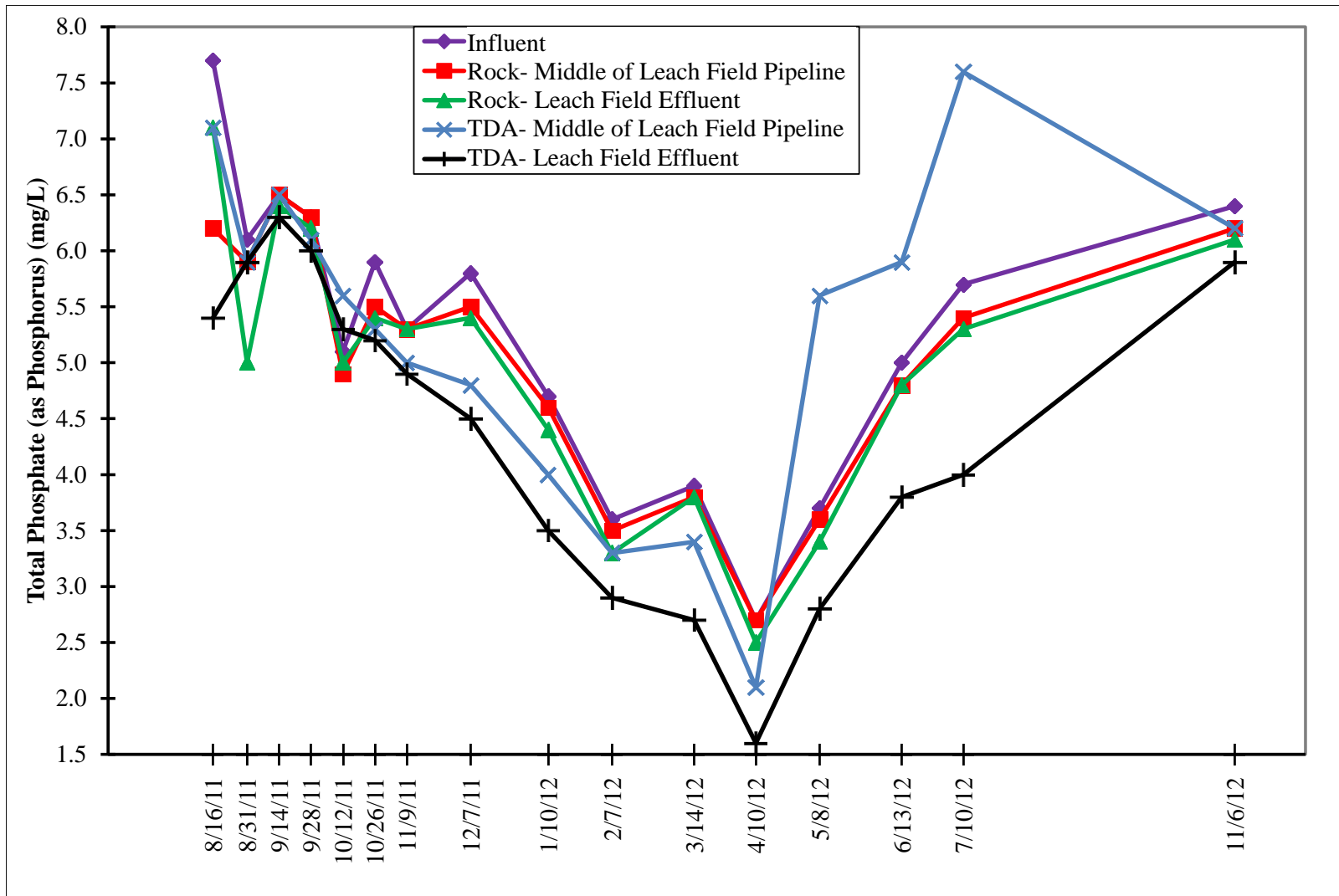


Figure 37. Total phosphate (as P) concentrations in the rock and TDA leach fields.

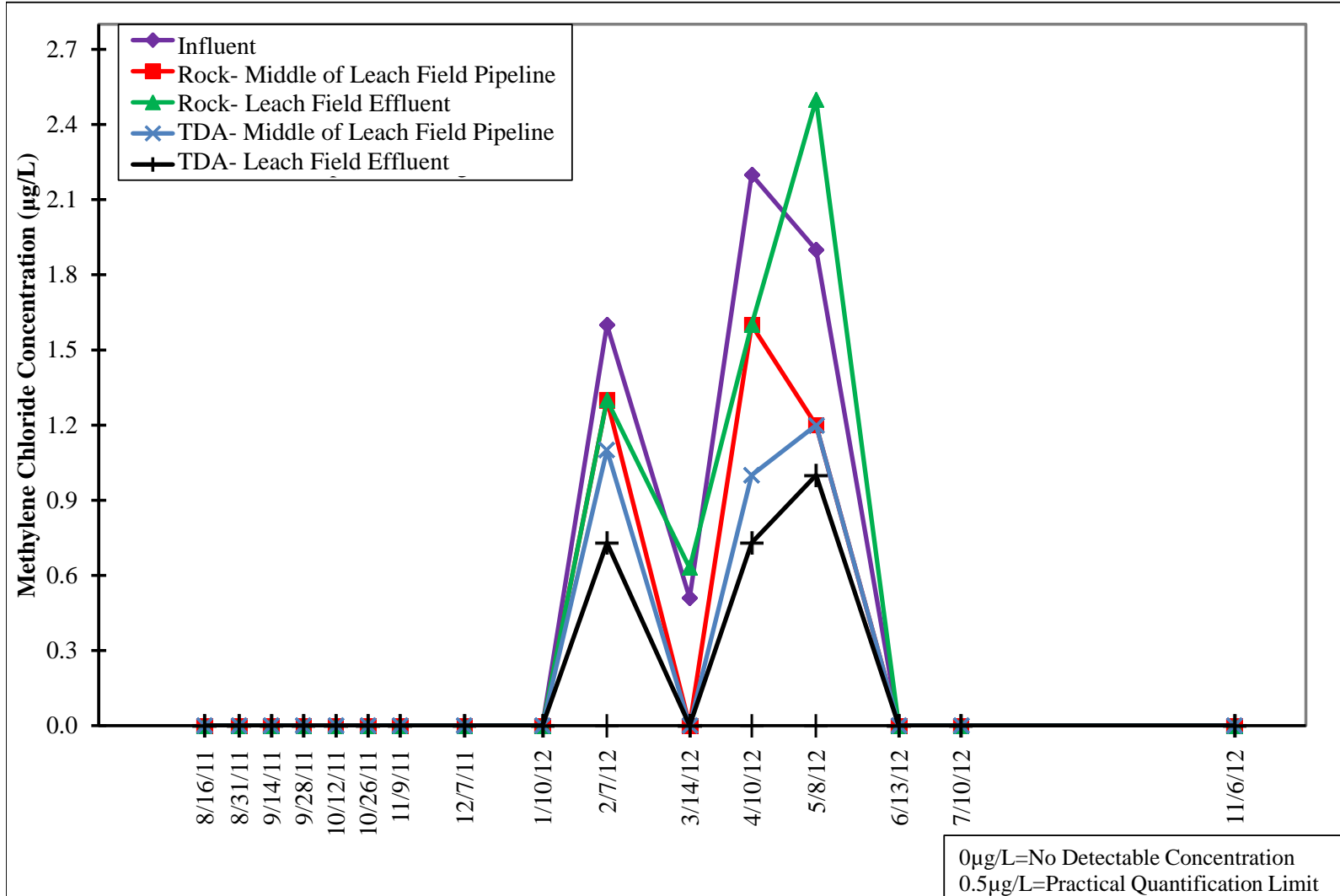


Figure 38. Methylene chloride concentrations in the rock and TDA leach fields.

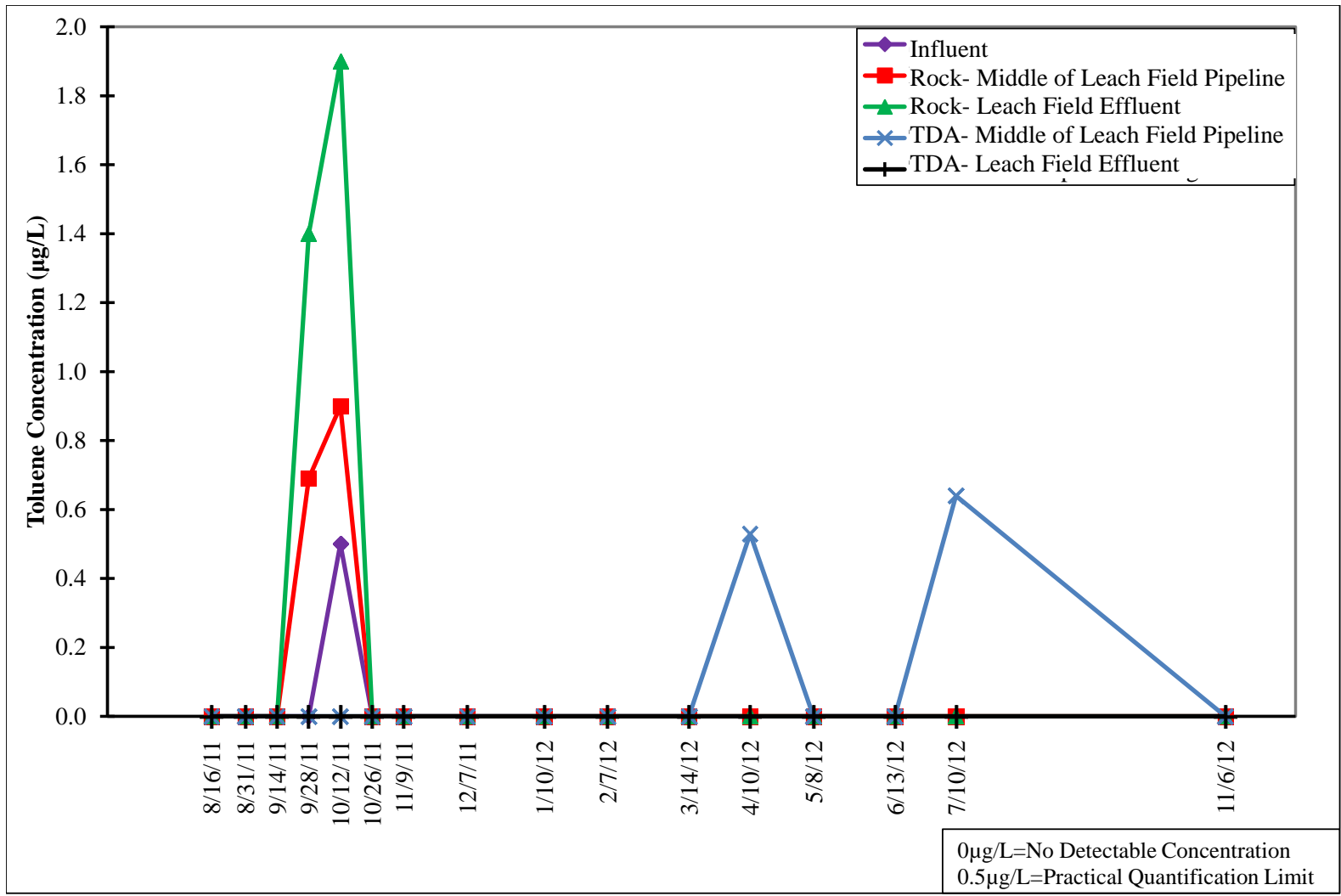


Figure 39. Toluene concentrations in the rock and TDA leach fields.

Exothermic Behavior of Deep TDA Fill

Using TDA as the media in deep fills raises concerns about possible exothermic reactions leading to temperatures high enough to result in a fire. Temperature changes were measured for a lightly compacted tower filled with TDA to provide data on potential exothermic reactions. The experiment was conducted using a 20-foot tall, 36-inch diameter above ground tower filled with type A TDA. More than 31,000 temperature measurements were made of the ambient air and at each of the five sample points in the media during the 11 month experimental period.

The average daily temperature at each sample point in the media followed the same seasonal trend as the ambient air temperature (Figure 40). The basic statistical characteristics of the TDA media temperature is very similar to that of the air temperature with the exception of a dampening of the extreme values due to the thermal mass of the TDA (Table 11). Over the entire data collection period, the temperature 4 feet from the bottom of the tower (with 16 feet of TDA above it) was approximately 3°F warmer than the coolest sample location at the top of the tower that had only a few inches of TDA cover. The TDA temperature exhibited a diurnal pattern similar to the ambient air temperature but also damped in magnitude (Figure 41).

TDA temperatures were considerably higher during the first week of testing (Figure 41) compared to the rest of the experimental period. The TDA was piled on black asphalt in direct sunlight for two days prior to placement in the tower. The TDA was noticeable warmer just before placement in the tower than it was when it was delivered to the worksite. The increase in temperature may have resulted from direct solar radiation on TDA, heat conducted to the pile from the asphalt, and/or from heat released by the oxidation of steel wire in the material. However, the highest recorded TDA temperature during the experiment was 80.7°F, suggesting that the industry guideline of limiting TDA fills to 10 feet without a noncombustible layer is unnecessarily conservative, especially when using clean type A TDA.

Table 11. Comparative statistics for temperature over a 20 ft. tall cylinder filled with type A TDA.

Statistic	Probe at 4 ft. AGL ¹	Probe at 8 ft. AGL ¹	Probe at 12 ft. AGL ¹	Probe at 16 ft. AGL ¹	Probe at 20 ft. AGL ¹	Ambient Air Probe
Mean (°F)	58.0	56.7	56.4	56.9	56.3	54.8
Standard Deviation (°F)	7.15	6.73	6.9	6.75	6.91	8.6
Minimum Value (°F)	42.1	43.6	43.6	43.9	42.9	33.2
Maximum Value (°F)	80.7	75.4	75.1	70.1	69.9	82.6
# of Data Points	31,087	31,087	31,087	31,087	31,087	31,087

¹Above Ground Level

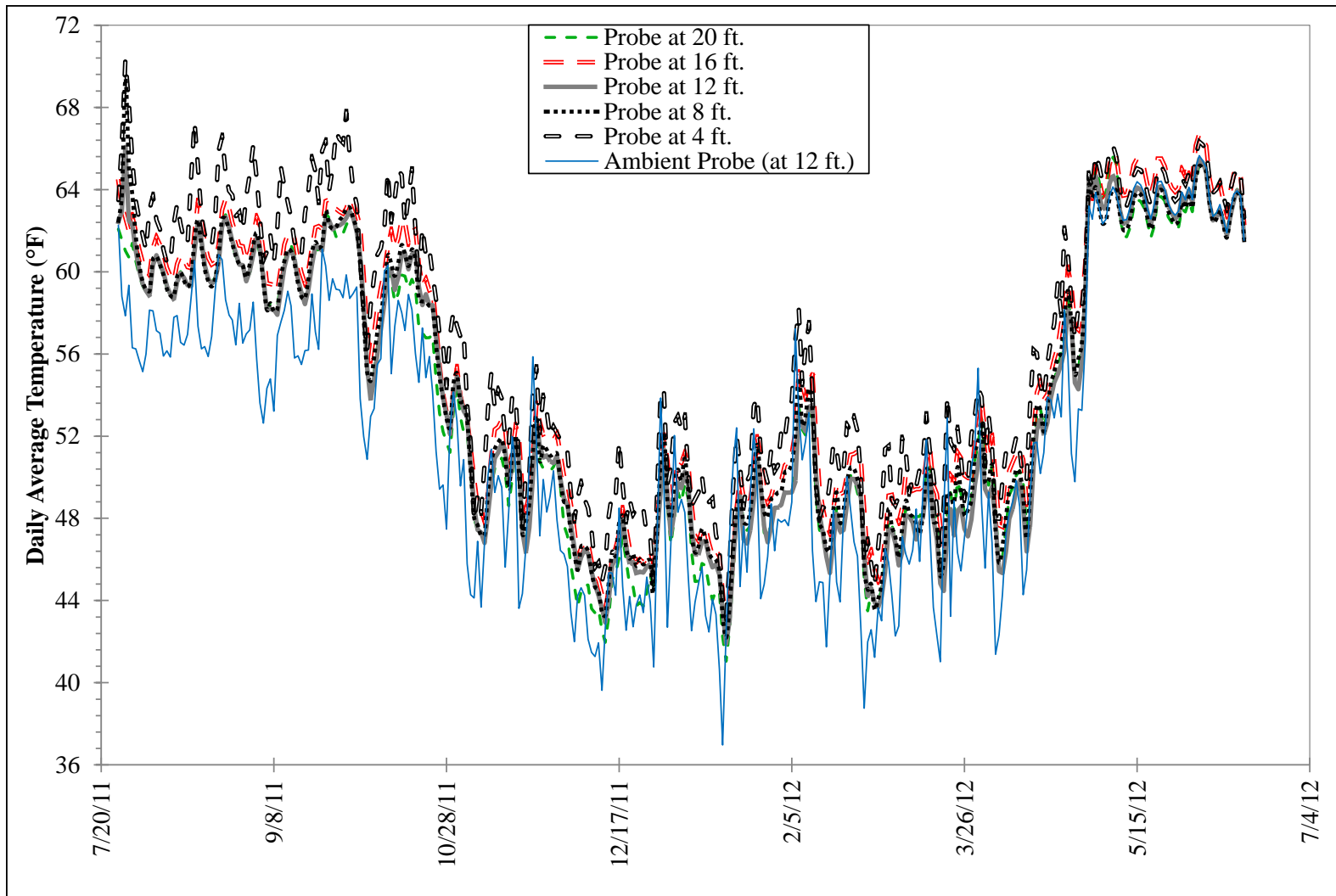
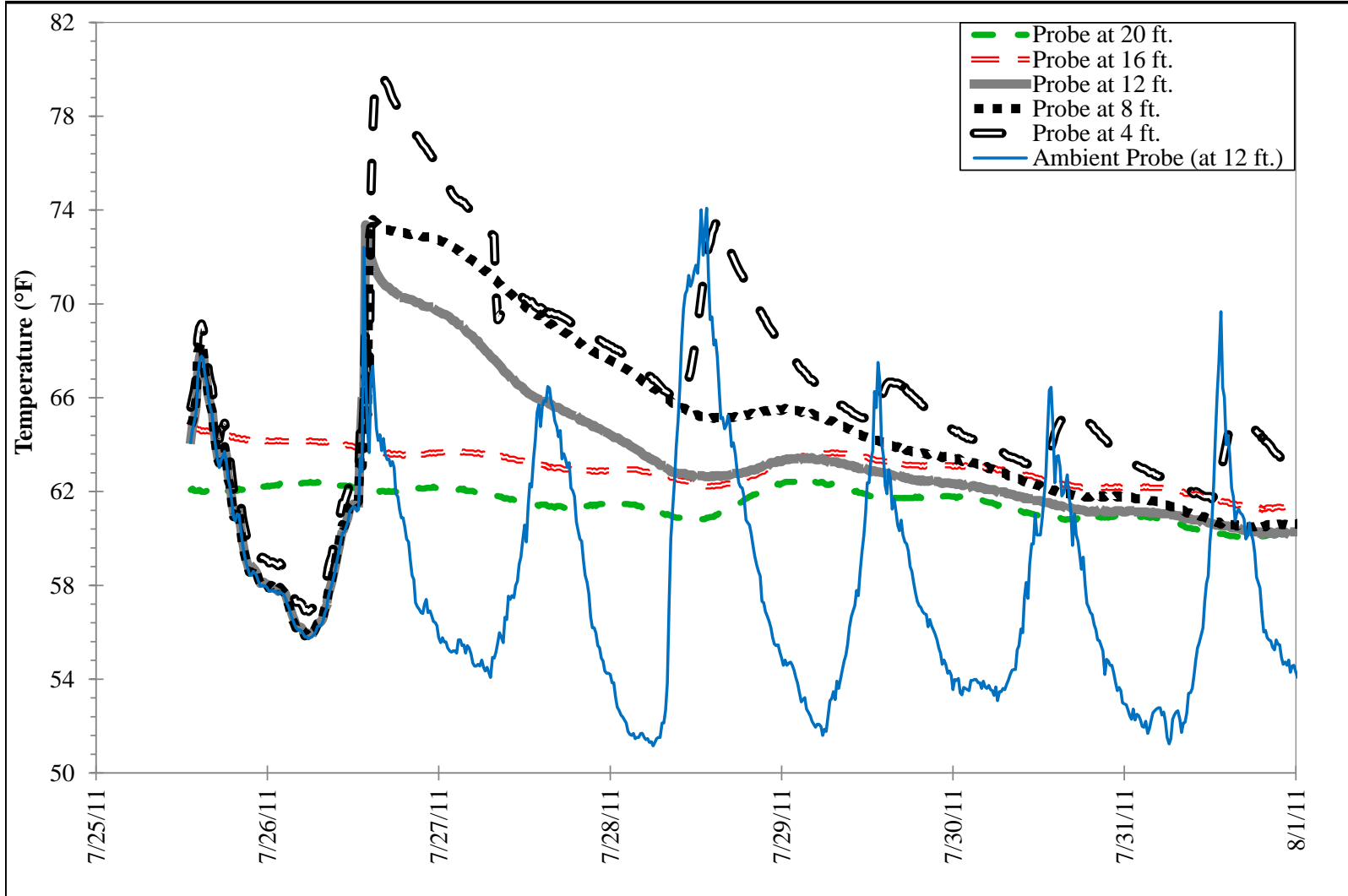


Figure 40. Daily average temperature changes of confined type A TDA recorded every 15 minutes in a 20-ft.-tall tower.



Aug. 1

Figure 41. The 1st week of temperature results for confined type A TDA recorded every 15 minutes in a 20-ft.-tall tower.

Exothermic Behavior of TDA under Immediate Fill Conditions

The highest temperatures in the tower experiment (Figure 41) were observed at the start of the experiment, suggesting that a critical time for dangerous exothermic reactions might be immediately after TDA is manufactured. A second TDA temperature experiment was designed to investigate this behavior by observing temperature changes in type A TDA placed in an earthen pit within 12 hours of being manufactured. The temperature of the TDA in the pit was measured at depths from 1.3 ft. to 9 ft. below the ground surface.

No evidence of significant exothermic activity was observed during the five months of data collection. Initial temperatures at the start of the experiment were the highest observed temperatures. The TDA was subject to ambient temperatures and direct sunlight just prior to placement in the pit, where the maximum ambient air temperature on the day of setup was 94°F. Temperatures at 1.3 feet, 4.5 feet, and 9 feet below the surface along with the ambient air/soil temperatures characterize the experimental results (Figures 42-45). To determine if precipitation had any impact on temperature changes, daily precipitation for a nearby site reported by the National Climatic Data Center (2013) are plotted alongside temperature results. The full dataset is provided in Figures E-1 through E-8 in Appendix E (page 148).

Soil temperatures and ambient temperatures followed seasonal patterns. Overall, the TDA decreased in temperature over time and appeared to follow an average between the native soil and ambient temperatures near the end data collection period (Figures 42-45). Type A TDA did not react hazardously to changes in moisture content from exothermic reactions caused by oxidation of metal wires within the tire pieces. Precipitation events tended to temporarily cool the TDA within the earthen pit. For example, a few days before Dec. 6, 2012, a series of precipitation events occurred which lowered the temperature about 2-6°F from the left to the right side of the pit, respectively (see Figure 44). Generally, TDA temperatures decreased following precipitation events, and then slowly rose in value until an equilibrium temperature was reached with surrounding soil.

Observed TDA temperatures did vary with depth and position relative to the distance from the side wall of the pit. Probes closest to the ground surface had lower temperatures than the next depth of probes (e.g., the 1.3 ft. depth probes were overall lower than the 2.5 ft. depth and so on). The temperature, with depth, increased until the central depth (4.5 ft. below ground level), where temperatures began an overall decline in value towards the bottom of the earthen pit (Figure 46). Except for the topmost sample depth, temperatures were generally higher near the wall of the earthen pit compared to that observed towards the middle of the earthen pit. This may be attributed to air movement within the wiring conduit for the probes below ground level. Since the ambient air temperature was usually higher than native soil temperatures, this could have increased temperatures near the wall of the earthen pit. The increased air movement near the side wall of the pit may have provided increased oxygen and moisture, resulting in increased oxidation reactions near the wall of the earthen pit. The thermal mass of the surrounding soil may also have reduced the heat loss after placement of the TDA nearest any edge of the earthen pit compared to the material near the center.

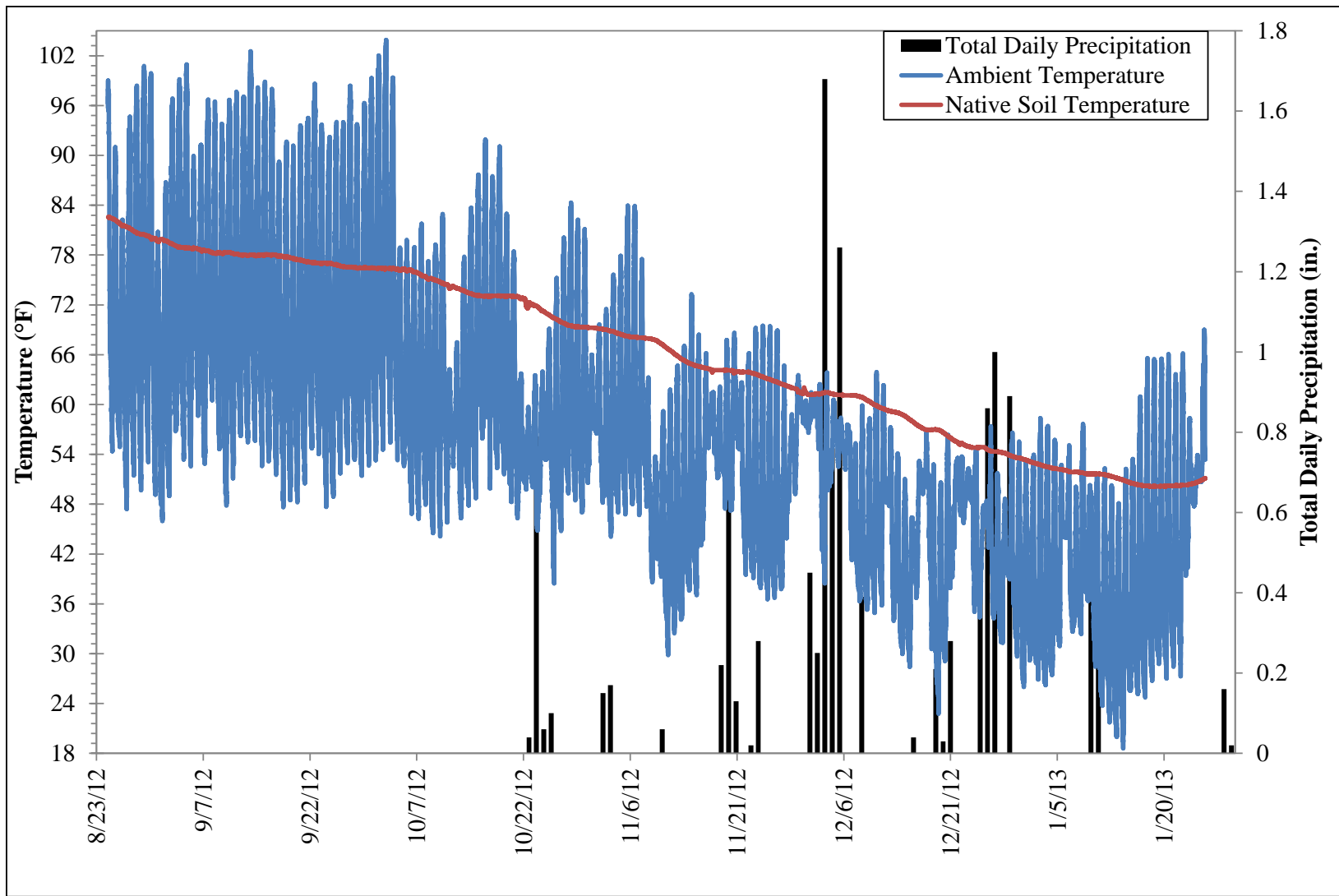


Figure 42. Native soil and ambient temperatures at the Keifer Landfill.

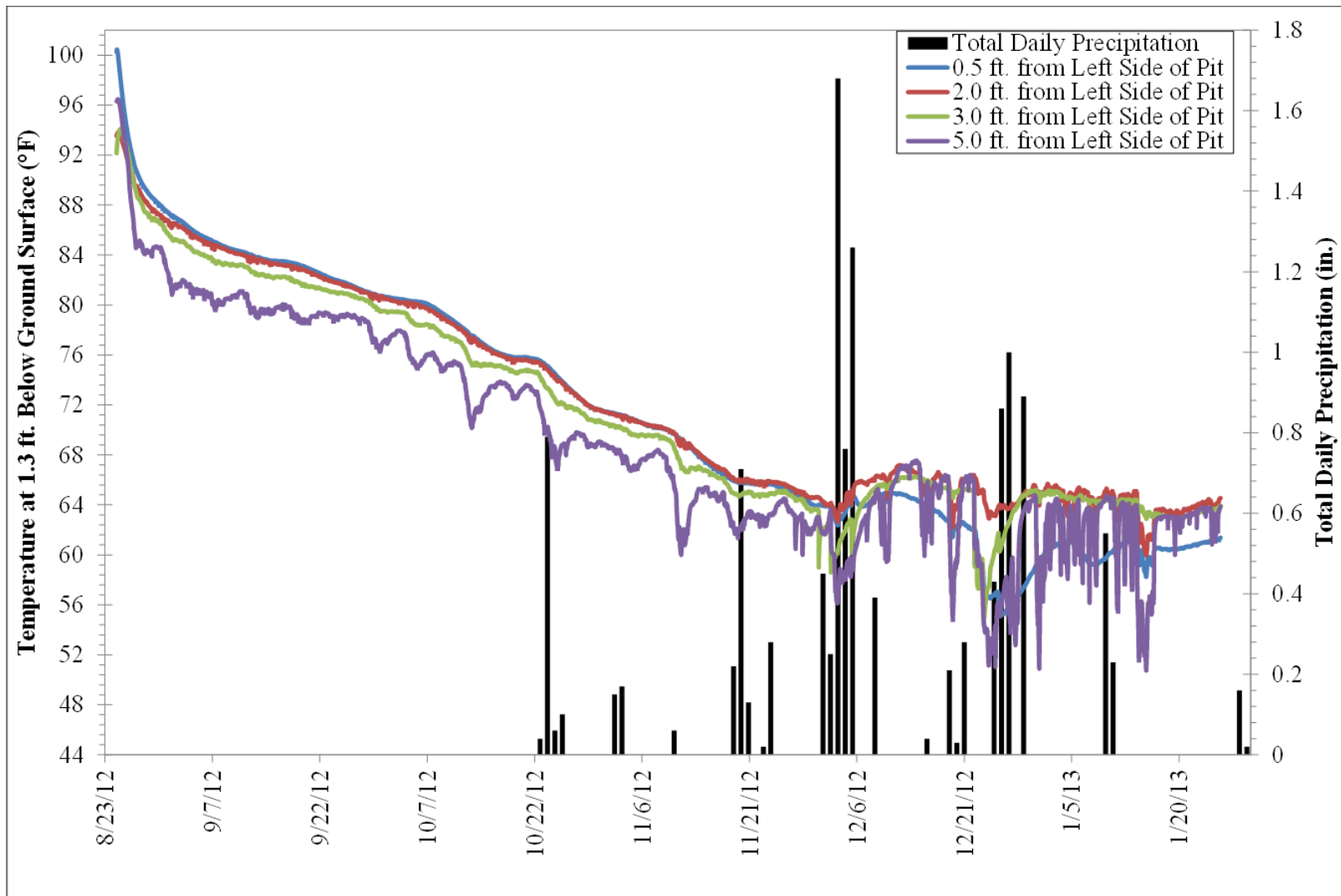


Figure 43. TDA temperatures at 1.3 feet below the ground surface.

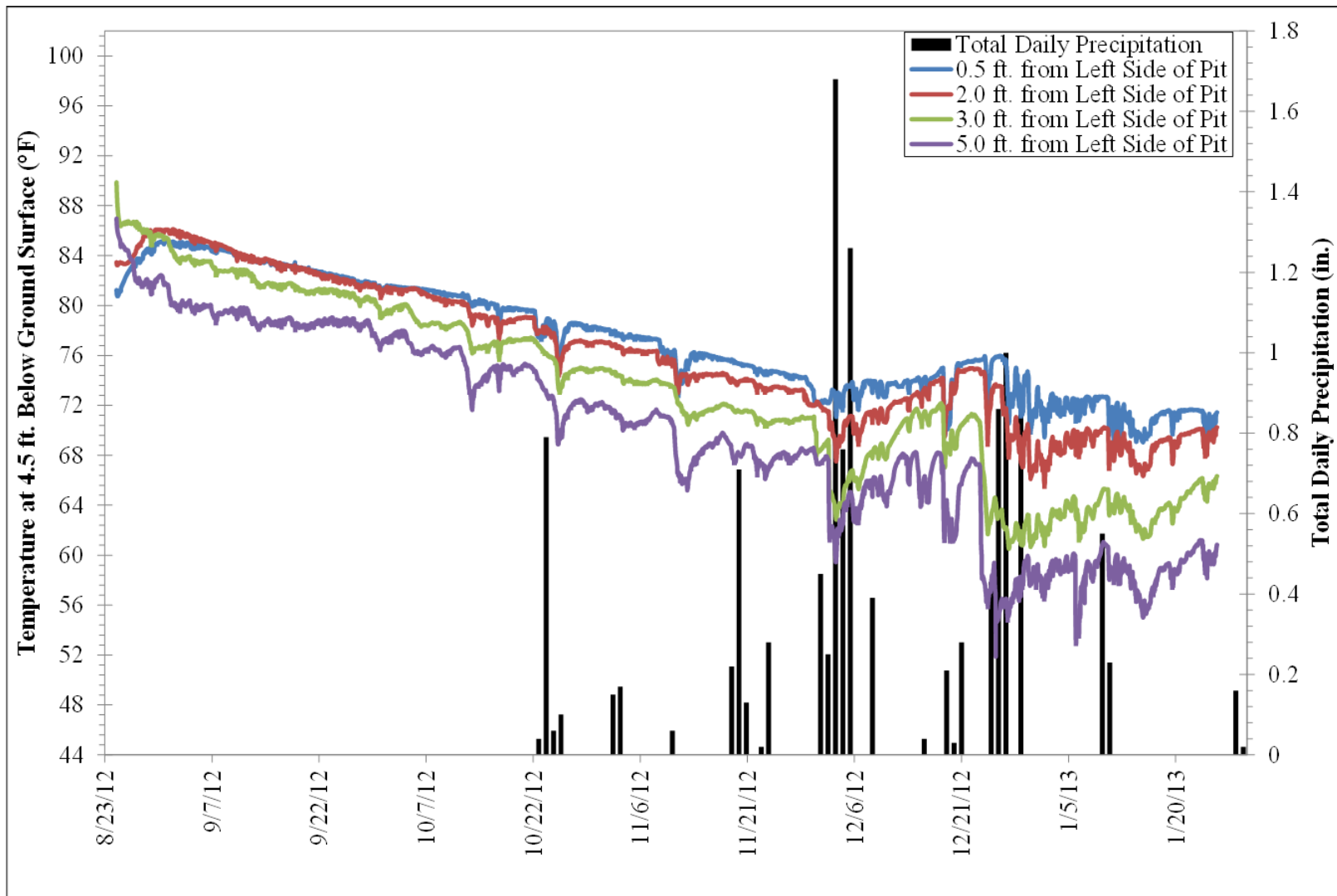


Figure 44. TDA temperatures at 4.5 feet below the ground surface.

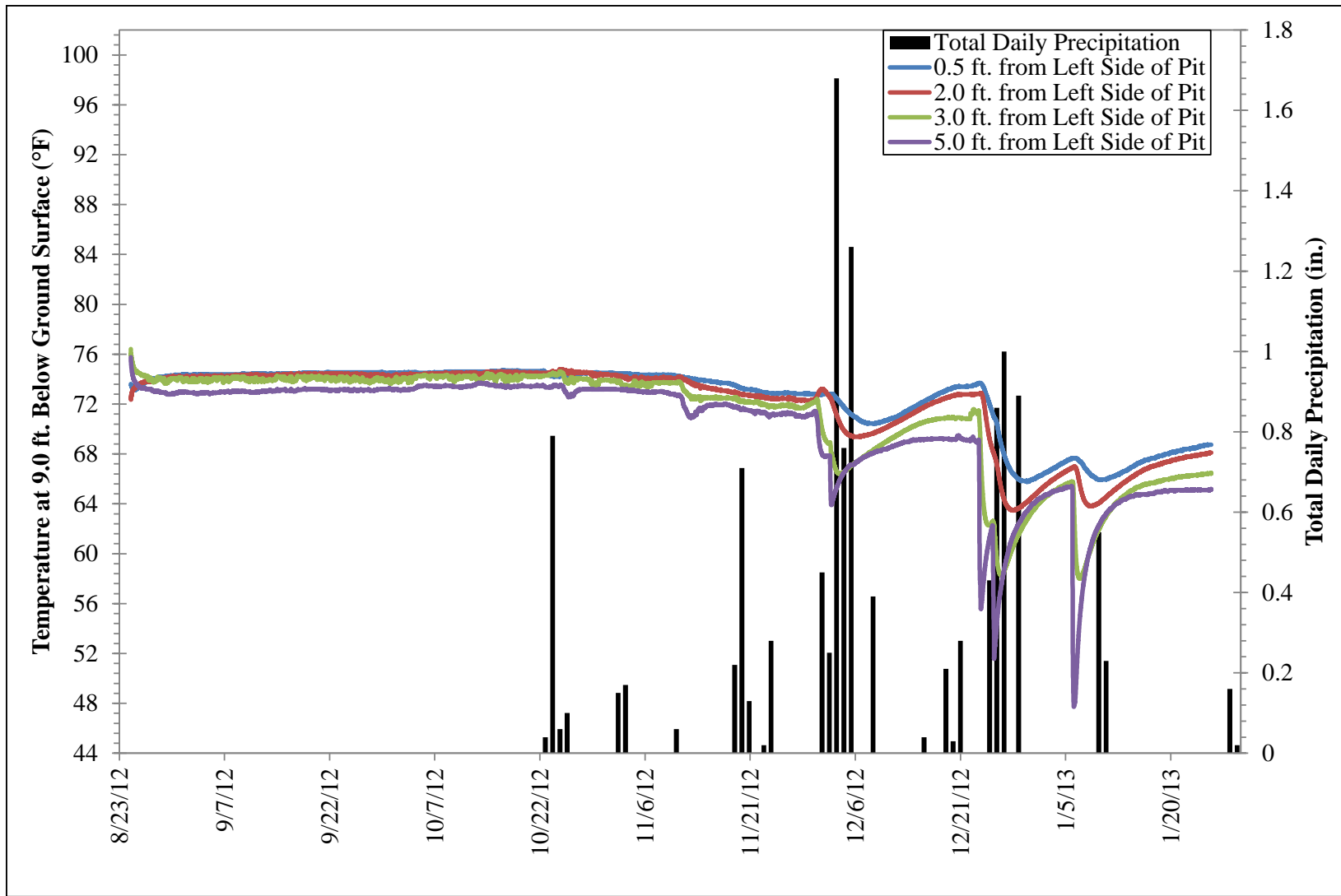


Figure 45. TDA temperatures at 9 feet below the ground surface.

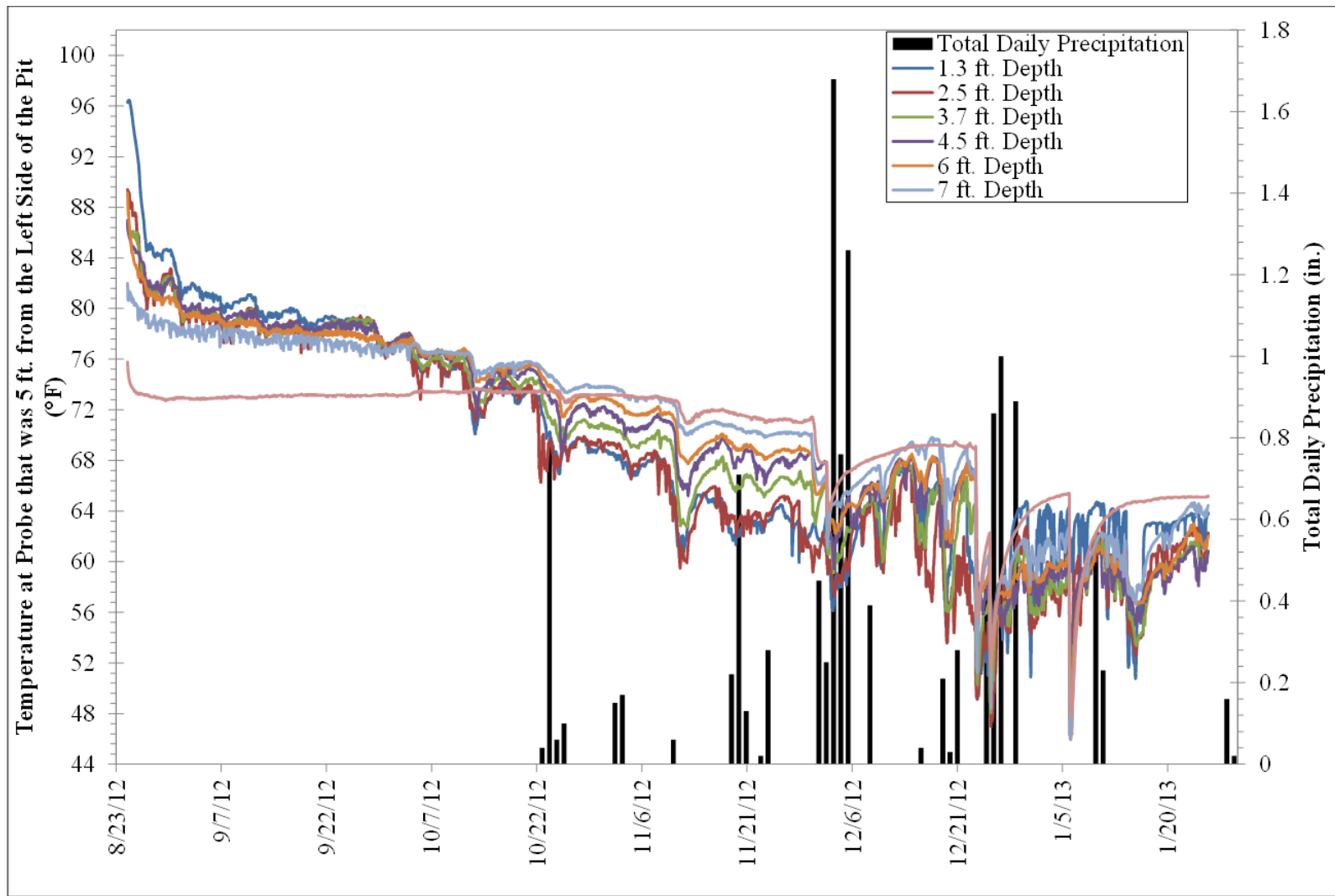


Figure 46. Changes in temperature with depth, five feet from the wall of the earthen pit.

Sieve Analysis for TDA

A sieve analysis was completed to categorize tire fragments used in experiments. The Tire-Derived Aggregate Technology Center (TTC) at California State University, Chico determined the size distribution of TDA samples from six experimental tests. Each of the six tests used a different source or type of TDA, or represented a different conditional setting for TDA use. Subsequent sections in this report will reference the test number to designate the particular TDA type and size distribution used. Type A TDA generally had a smaller particle size distribution than type B (or a type A and B mixture), and all samples provided an acceptable physical representation of the intended TDA types. The size distribution of all of the type A TDA samples were similar and contained fragments with maximum lengths of eight inches. Size distributions of the type B TDA samples were also similar to one another and the maximum length of tire fragments was 12 inches. Overall, the mixture of type A and B TDA had particle size characteristics similar to type B TDA.

Compression Testing of TDA for Varied Loads

Using the experimental setup shown in Figures 15-18, type A TDA was compacted by a static load of approximately 2.95 psi to simulate the typical loading on leach field aggregate. The TDA layer linearly compressed over the first two days, but a compressional limit was eventually reached (Figure 48). When the load was removed, the TDA returned to a thickness of about 18 percent less than its original layer thickness. Fluctuations in strain, shown in Figure 48, are likely due to measurement error or temperature changes (resulting in expansion and contraction-like properties) that happened during the first 2-5 days of experimentation.

Dynamic tests of larger magnitude loading were then completed on type A, B, and a mixture of type A/B TDA. These experiments were performed under large magnitude loads in a device larger than previous researchers have used; a 36-inch diameter steel cylinder that was 3.67 feet tall. Maximum loads for each experiment performed varied because the load was introduced to the materials using hydraulic jacks. The type B TDA appeared to have a different response to compressive forces since it experienced greater strain compared to the type A and mixed type A/B TDA under equivalent loading (Figure 49). However, since the type B TDA contained larger-sized pieces of tire, on initial fill into the compression chamber it had a larger void ratio than the type A and A/B mixture of TDA (Table 12). When the load was initially applied to the TDA, the type B sample deformed more than the type A and A/B mixture because the material reoriented and filled in void space. Once this initial compaction or compression occurred, further loading onto type A and B TDA should yield similar behavior. In experiments 2 through 5, the slope of the stress/strain curve for all TDA samples was nearly identical once the loading exceeded 2 psi, indicating that after initial deformation, type A, B, and A/B mixtures have equivalent compressive properties (Figure 49).

When a sufficient load is applied to a material it will cause the material to deform, and a temporary change in shape occurs that is reversible after removal of an applied force (elastic deformation); however, when stress is sufficient to permanently deform the material, plastic deformation can occur. In all experimental cases, TDA initially exhibited plastic compression under load, but with additional loading the TDA behaved like an elastic material as described by Edil and Bosscher (1994). Figure 50 shows type B TDA before and after compression, demonstrating the plastic and elastic behavior described. Although TDA shows elastic behavior, the deformation may also be time-dependent and thereby additional deformation of TDA may occur under long-term load conditions (Geosyntec Consultants, Inc., 2008).

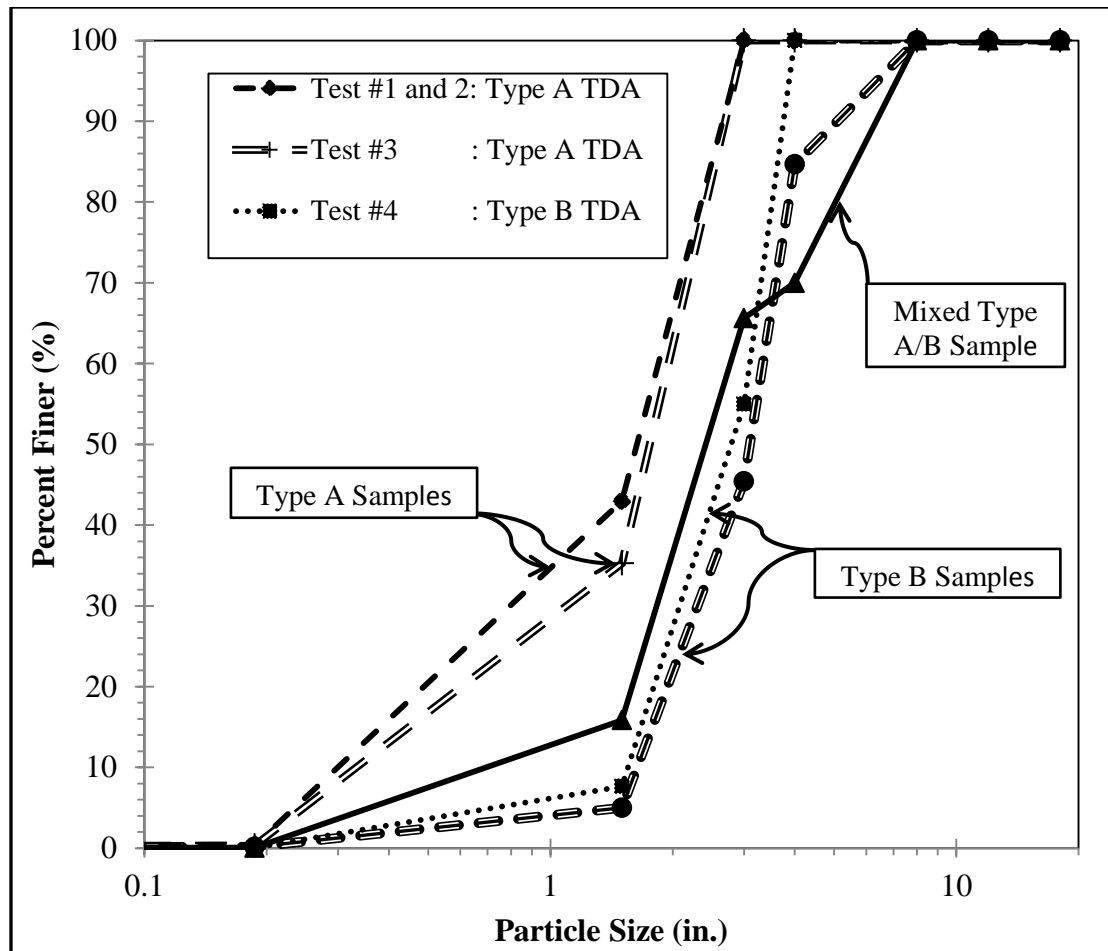


Figure 47. Particle size distribution of tire-derived aggregate used in six different experiments.

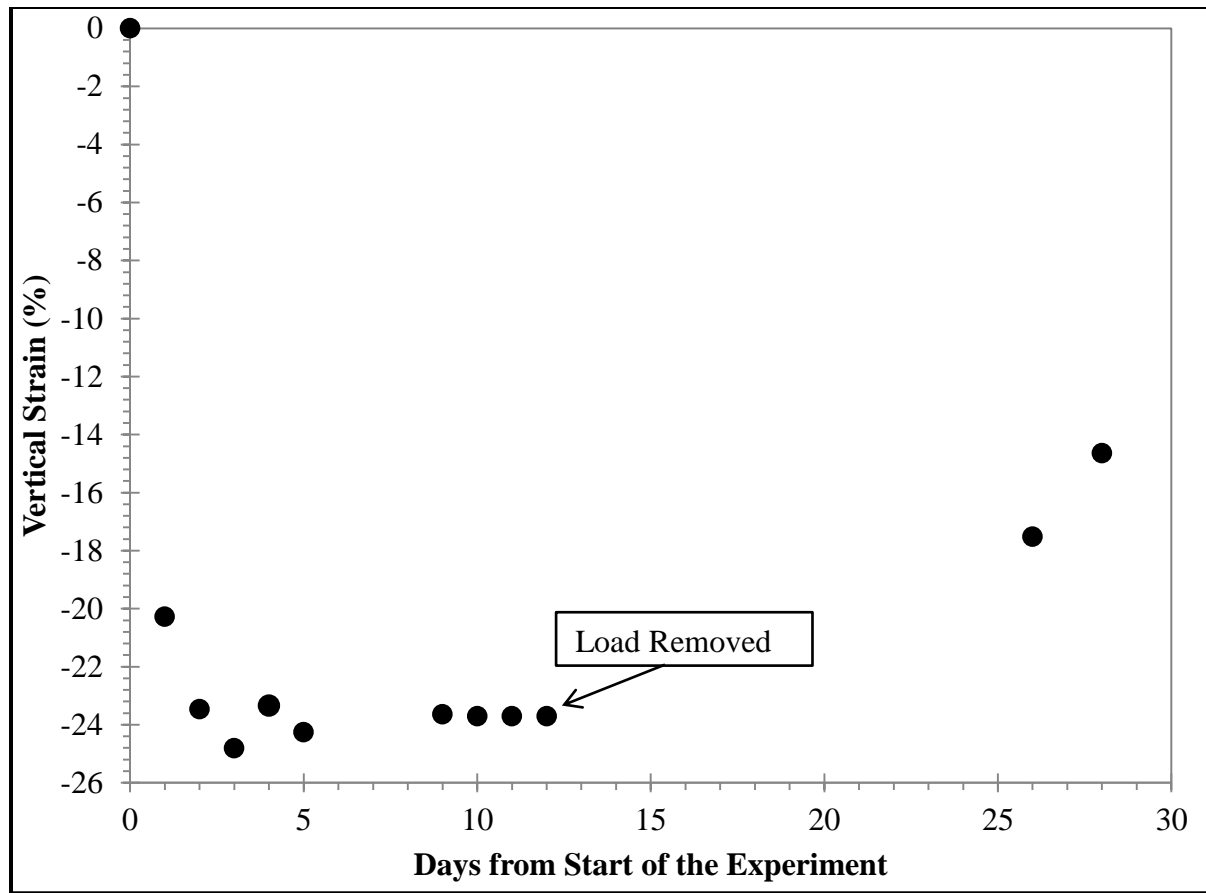


Figure 48. Vertical strain on type A TDA resulting from a static load of about 2.95 psi applied for 12 days. After 12 days, the load was removed to allow the TDA to rebound.

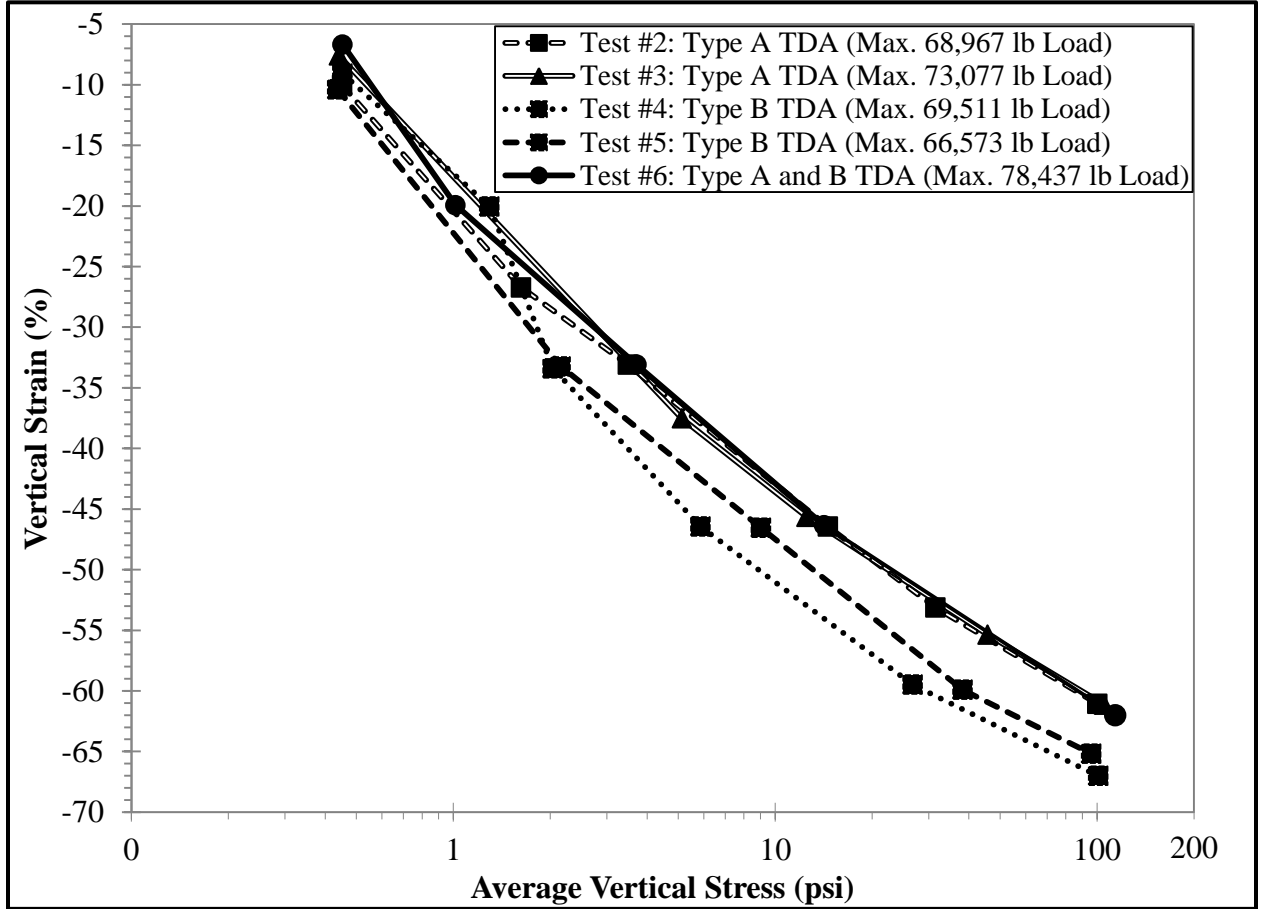


Figure 49. Vertical strain versus stress for various types of TDA.



Figure 50. Type B TDA before (A) and after (B) a large magnitude compression experiment.

Physical Properties of TDA

Understanding the physical properties of TDA such as density, hydraulic conductivity, void ratio, and porosity under various conditions can provide engineers with parameters necessary in design applications. During many of the previous experiments, the properties of types A, B, and a mixture of type A/B TDA were determined (Table 12). In some cases, TDA of one type (type A or B) was provided by a different manufacturer or produced on a different date and had different properties and distributional size characteristics. For comparative purposes, some literature values for these same properties are shown in Table 13.

There are different types of devices and procedures used to produce TDA. As a result, the quality of tire chips may vary greatly among different tire recycling plants. The physical parameters analyzed will differ depending on the manufacturing quality and consistency of TDA. Each experiment generally used TDA produced under different conditions resulting in different TDA characteristics. To assure uniformity in application of the material, a set of standards concerning the size of tire chips, length of protruding steel wires, the amount of extraneous objects (e.g., wire pieces, soil, debris, etc.), and granulated rubber should be specified to the manufacturer.

Hydraulic Conductivity of TDA

Hydraulic head is a specific measure of water pressure above a relative datum. The hydraulic gradient is the change in hydraulic head divided by the length of flow path. The capacity of a material to transmit water is referred to as the hydraulic conductivity, which is directly related to the hydraulic gradient of the water, the flow rate of the water, and the cross sectional area of the material. In general, finer grained porous media such as clay has fewer and smaller voids and a lower value of hydraulic conductivity than a coarse grained media such as sand. For the TDA material tested, increasing the loading and/or the hydraulic head resulted in a decrease in the hydraulic conductivity (Figures 51-53), the porosity, and the void ratio (Table 12). The reduction in hydraulic conductivity as the hydraulic gradient increased was probably due to an increase in fluid pore velocity at higher gradient values. As the pore velocity increased, the Reynolds number for the fluid increased and the relationship between hydraulic gradient and hydraulic conductivity became nonlinear. The results found in these experiments were comparable to those found in previous research efforts (Table 14).

The relationship between compressive load and hydraulic conductivity was observed to be nonlinear for both type A and B TDA (Figure 52 and 54). The relationship between hydraulic head and hydraulic conductivity was also observed to be nonlinear (Figure 53). The hydraulic conductivity of type A and B TDA changed similarly as the compressive load was changed. However, the rate of change in hydraulic conductivity as the load increased was smaller for type B TDA than for type A TDA. In particular, it appeared that the hydraulic conductivity of type B TDA was larger at loads above 50 to 60 psi than type A TDA. This characteristic may result from larger sized pieces of type B TDA not packing as tightly as type A TDA, where larger voids were responsible for higher conductivities. Additional testing at a wider range of loadings would help verify the results observed in this study.

The test results suggested a predictive model for hydraulic conductivity of the form,

$$k = [\alpha_1 \ln(h) + \alpha_2]p^{\alpha_3} \quad \text{Equation 0-1}$$

where h = hydraulic head (inch), p = compressive load (psi), and k = hydraulic conductivity of the TDA (in/sec). The parameters of this model were estimated using a nonlinear least squared optimization algorithm, with different parameter values found for type A and B TDA (Table 15). The differences in the behavior of type A and type B TDA are reflected in the differences in the predictive model parameters for these two materials.

TDA has often been used as a drainage material in deep fills (e.g., at landfills). Design engineers must consider the effect that the fill depth will have on the drainage properties of the material. An order of magnitude reduction in hydraulic conductivity of TDA was observed in these experiments when the compressive load was increased from 3 to 100 psi. In addition to the reduction in the hydraulic conductivity, the porosity decreased as the load increased, increasing the susceptibility of the TDA to physical clogging if fine grained material is allowed to enter TDA fills.

Table 12. Physical Parameters of type A, B, and A/B mixed TDA under various testing conditions.

Test #	TDA Type	Dry Density (slug/ft ³)	Loaded Weight (lb _t)	Pressure (psi)	Porosity at Seating Load (%)	Void Ratio at Seating Load	Porosity Under Load (%)	Void Ratio Under Load	Specific Gravity	Specific Weight (lb _f /ft ³)	Size Distribution of TDA (in.)	Met Type A or B TDA Specification
1	Type A	2.47	2,057	2.95	62.9	1.69	53.1	1.13	1.28	79.6	0.0001-7.56	Yes
2	Type A	2.72	68,967	100	63.5	1.74	15.7	0.186	1.40	87.6	0.0001-7.56	Yes
3	Type A	2.54	73,077	105	62.4	1.66	10.6	0.119	1.31	81.9	0.0001-7.88	Yes
4	Type B	2.6	69,511	101	68.2	2.14	12.3	0.14	1.34	83.8	0.0001-24.19	No
5	Type B	2.67	66,573	96	67.2	2.05	15.5	0.183	1.38	86	0.0001-41	No
6	Type A and B Mixture	2.6	78,437	114	62.9	1.70	8.88	0.0974	1.34	83.8	0.0001-17.25	No

Table 13. Physical properties of TDA reported in the literature.

	Yang et al. (2002)	Wartman et al. (2007)		Bressette (1984)	Edil and Bosscher (1994)		
Diameter of Compaction Instrument (in.)	2.50	NA	NA	6	6-12	6-12	6-12
Material Used	TDA	TDA	TDA	TDA	TDA and Outwash Sand/Casting Sand	TDA and Outwash Sand/Casting Sand	TDA and Valley Trail Clay
Soil:TDA ratio (by weight)	0:100	0:100	0:100	0:100	70:30/50:50	¹ 0:100/30:70/150:50/70:30/100:0	30:70/70:30
Moisture Content	NA	Wet	Wet	NA	Wet/dry of optimum	Dry (hygroscopic)	Wet/dry of Optimum
Density (slug/ft³)	1.13	1.28	0.938	1.10	2.35-3.28	1.09-2.83	1.68-3.32
Specific Gravity of TDA	1.15	1.07	1.31	1.18 (apparent)	1.13-1.36	1.13-1.36	1.13-1.36
TDA Particle Length (in.)	0.08-0.4	1.2 (maximum)	7.024 (maximum)	2 (shredded)	² 0.709-3.15	² 0.709-3.15	² 0.709-3.15
Seating Load (lb_f/ft²)	NA	NA	NA	NA	501	125	201
Porosity of TDA at Seating Load (%)	NA	NA	NA	NA	67	67	67
Void Ratio at Seating Load (dimensionless)	0.98	NA	NA	NA	NA	NA	NA
Pressure Under Load (lb_f/ft²)	NA	12,500	12,500	NA	0.5	0.5	0.5
Porosity Under Load (%)	NA	38	63	NA	NA	NA	NA
Void Ratio Under Load (dimensionless)	NA	0.62	1.71	NA	NA	NA	NA

¹excluding 100% sand, ²approximate range from graph in literature

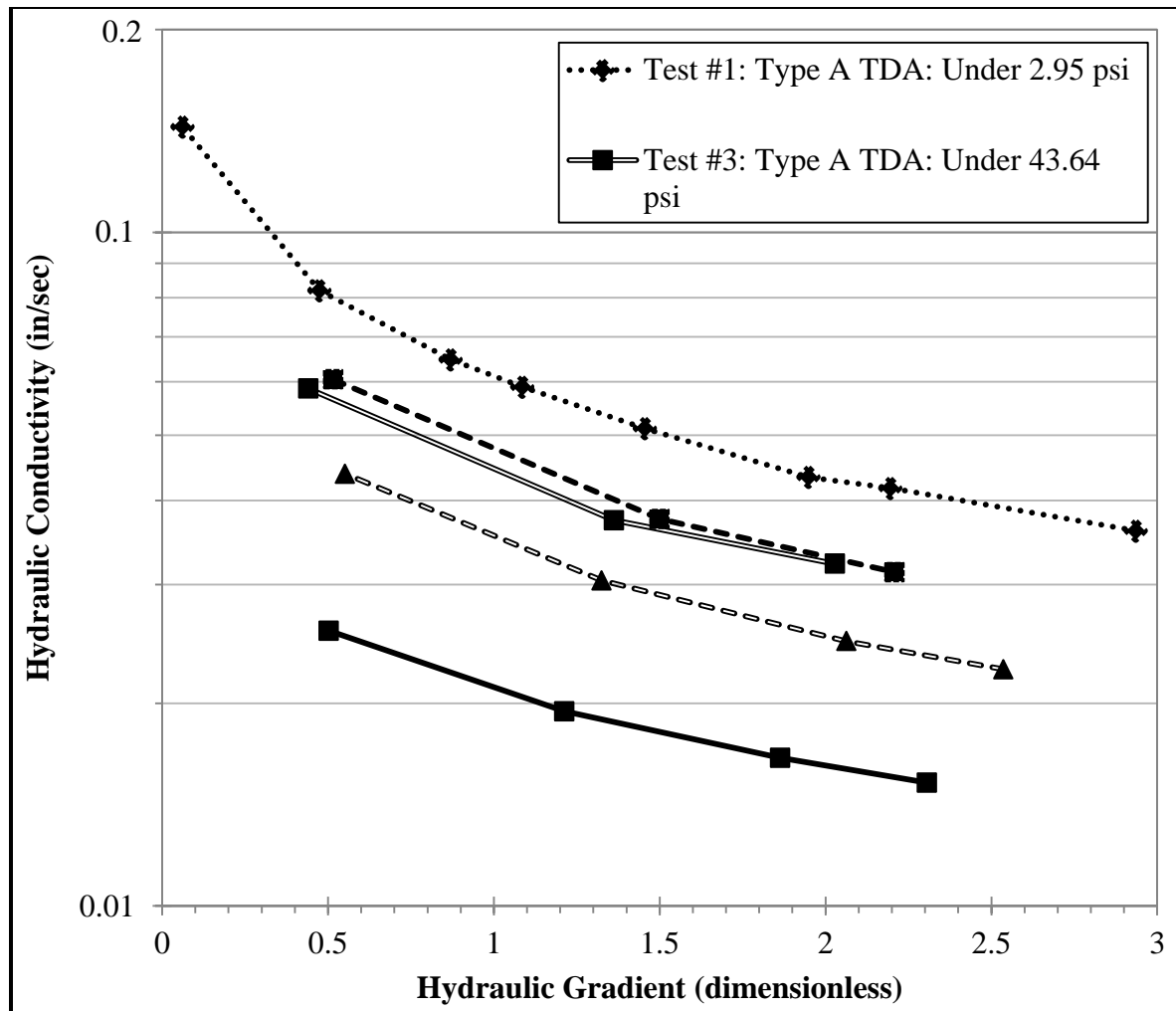


Figure 51. Hydraulic conductivity is shown against the hydraulic gradient for TDA (type A and B).

Table 14. Literature values for the hydraulic conductivity of TDA materials under various confining pressures (after Geosyntec Consultants, Inc. (2008)).

Confining Pressure (CP) (lb _f /ft ²)	Hydraulic Conductivity (k) (ft/s)	Reference	CP (lb _f /ft ²)	k (ft/s)	Reference	CP (lb _f /ft ²)	k (ft/s)	Reference	CP (lb _f /ft ²)	k (ft/s)	Reference
0.1, 100	0.02	1	0.1, 100	0.17	7	0.1, 100	0.20	3	1,100-4,400	0.15	8
	0.02	1		0.12	7		0.364	3		0.15	9
	0.02	1		0.13	7		0.581	3		0.15	9
	0.02	1		0.21	7		0.430	3		0.079	3
	0.062	2		0.581	7		0.541	3		0.18	3
	0.085	2		0.341	7		0.499	3		0.18	3
	0.039	2		0.72	7		0.2	4		0.28	3
	0.085	2		0.25	7		0.417	4		0.29	3
	0.089	2		0.771	7		0.2	4		0.11	4
	0.25	3		0.17	7		0.1	4		0.27	4
	0.535	3		0.417	7	0.092	4	0.092	4		
	0.850	3		0.22	7	0.03	2	0.02	11		
	0.863	3		0.420	7	0.072	2	0.072	8		
	0.869	3		0.16	7	0.085	2	0.069	9		
	0.25	4		1.95	7	0.046	2	0.072	9		
	0.505	4		0.404	7	0.397	8	0.33	10		
	0.22	4		0.551	7	0.31	9	0.01	11		
	0.11	5		0.075	6	0.397	9	0.049	3		
	0.1	5		0.059	6	0.062	2	0.21	3		
	0.085	6		0.1	5	1.8	10	0.21	3		
0.17	7	0.11	5	0.085	4	0.069	4				
0.358	7	0.095	5	0.079	4	0.16	4				
0.10	7	0.1	5	0.02	11	0.049	4				
0.31	7	0.082	2	0.66	10	0.2	10				
0.13	7	0.052	2	0.03	12	0.003	11				
						1,100-4,400			4,400-10,000		
									>10,000		

¹Ahmed (1993), ²Hall (1991), ³Lawrence et al. (1998), ⁴Humphrey et al. (1992), ⁵Spagnoli et al. (2001), ⁶Marella (2002), ⁷Bressette (1984), ⁸Geosyntec Consultants, Inc. (1997), ⁹Geosyntec Consultants, Inc. (2004), ¹⁰Narejo and Shettima (1995), ¹¹Duffy (1996), ¹²Reddy and Saichek (1998)

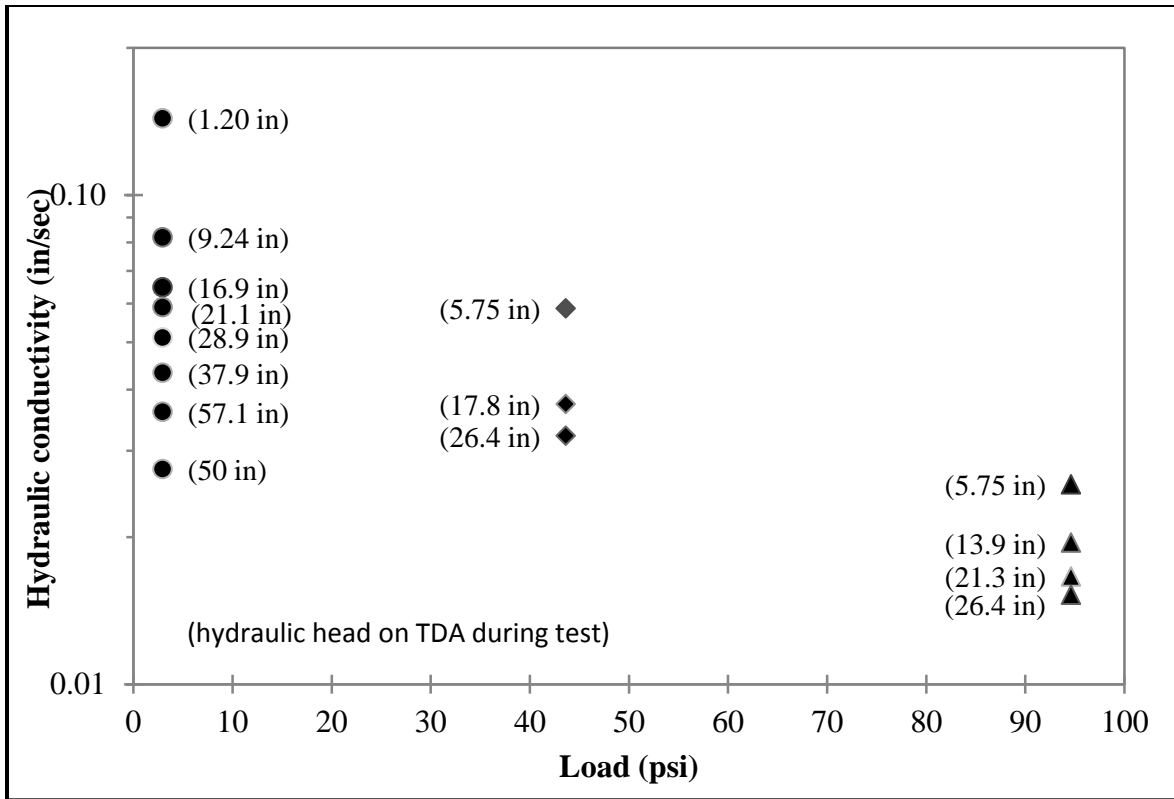


Figure 52. Hydraulic conductivity of type A TDA vs. load at various hydraulic heads.

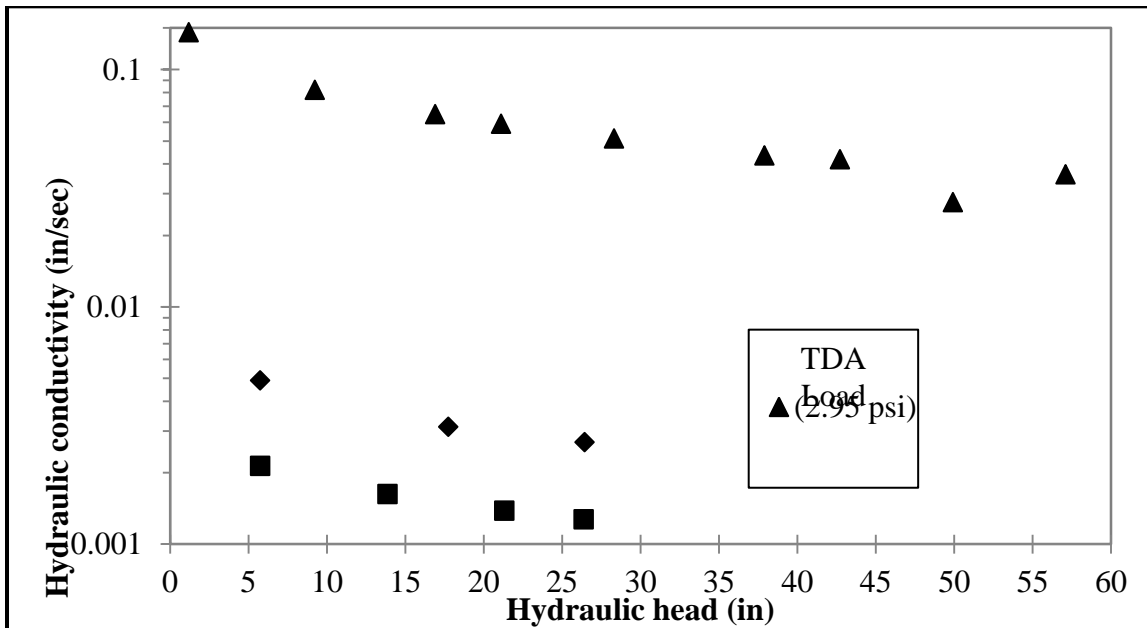


Figure 53. Hydraulic conductivity of type A TDA vs. hydraulic head at various loads.

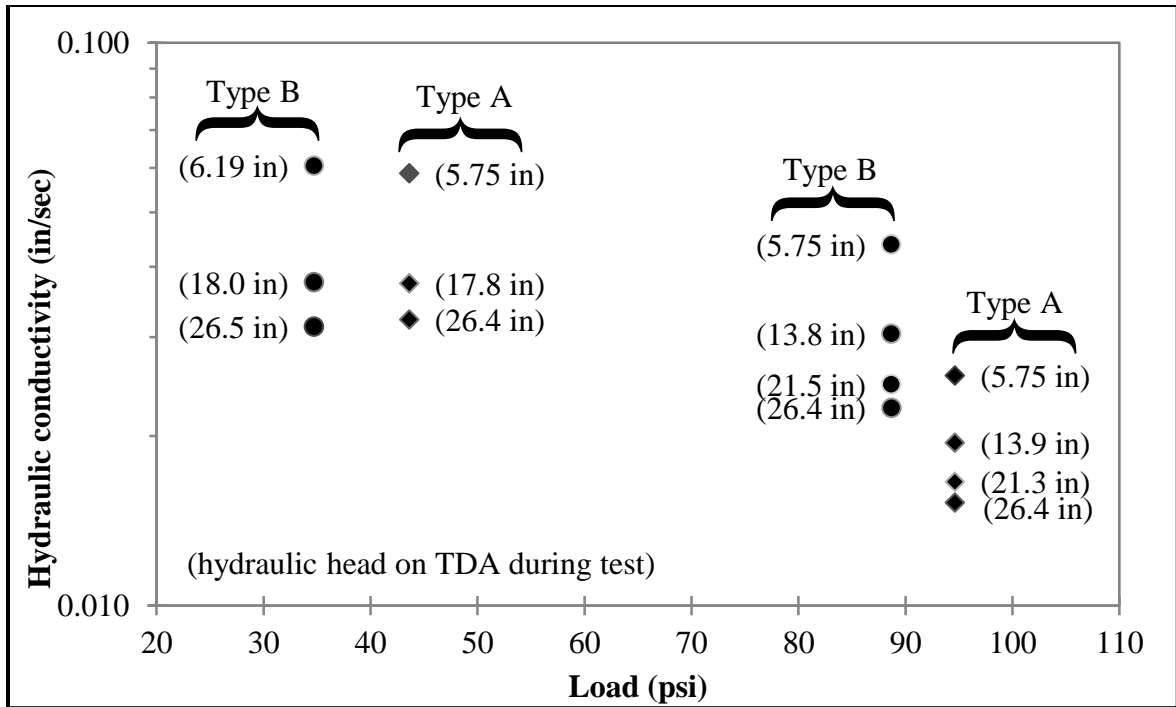


Figure 54. Hydraulic conductivity of type A and B TDA vs. loading at various hydraulic heads.

Table 15. Parameter values for a predictive model of hydraulic conductivity for TDA as a function of load and hydraulic head.

Parameter	Type A TDA	Type B TDA
α_1	-0.0675	-0.00621
α_2	0.3452	0.02979
α_3	-1.0194	-0.36789

Conclusions and Recommendations

Conclusions

A series of experiments were performed to examine exothermic tendencies of TDA and determine several physical properties of TDA and relevant for use in construction applications. The appropriateness of substituting TDA for gravel in a leach field was also investigated. Based on results, the following conclusions were made:

Size Distribution of TDA Types

- A sieve analysis showed that type A TDA had a smaller particle size distribution than type B (or a type A and B mixture).
- The size distribution of all type A TDA samples were comparable to one another as were the size distributions of all type B TDA samples.

Substituting TDA for gravel in a septic tank leach field

- TDA appeared to retain its integrity during contact with wastewater that was equivalent to septic tank effluent.
- Biofilm was much more extensive on the TDA media than on the rock aggregate media.
- Steel wires in the TDA started oxidizing immediately upon use and much of the biofilm was a reddish-brown color.
- For nearly all water quality constituents examined, the TDA and rock leach field effluents were statistically similar. The TDA system had a higher removal rate for methylene chloride, sulfate, nitrate, chemical oxygen demand, and total phosphate. Removal rates for these constituents were likely higher due to the extensive biofilm on the TDA media.
- Iron, manganese, and zinc effluent concentrations were much higher in the TDA system compared to the rock system due to the oxidation of steel wire in the tire pieces.
- While nitrate concentrations were lower in the TDA system compared to the rock system, overall nitrogen removal in both systems was negligible.
- Type A TDA is a suitable alternative substitute for rock aggregate in onsite septic systems in regards to wastewater treatment and durability.

Exothermic behavior of TDA

- Temperature changes in the simulated septic leach field over a 17-month operational period showed that TDA had slightly higher temperatures than rock aggregate, but temperatures were not considered high enough to cause dangerous exothermic reactions to occur.
- The largest temperature difference between the TDA in the 20-foot-tall tower and the ambient air occurred during the first week of the 11-month experiment, which was likely due to pre-warming of the TDA during construction of the tower.
- TDA placed in a 10-foot-deep earthen pit immediately after being produced slowly cooled over the 5-month experiment period and mirrored similar declines in the ambient air and native soil temperatures. Precipitation entering the earthen pit reduced the TDA temperature,

which suggests that oxidation of the wire in the TDA had a negligible effect on temperature variations.

- In three settings, depth of fill, degree of compaction, and degree of wetting did not appear to be significant factors in producing an exothermic reaction in the TDA.
- In each experiment, the highest recorded TDA temperature were observed at the time of placement, suggesting that the industry guideline of limiting TDA fills to six feet without a noncombustible layer is overly conservative for clean, type A material.

Compressibility of TDA

- Type A TDA linearly compressed over the first two days of 2.5 psi static loading before a compressional limit was reached. Upon removal of the load, the TDA only returned to 82 percent of the original layer thickness, indicating the degree to which material reorientation and self-packing occurred.
- Dynamic tests of compressional loading showed that type B TDA was consistently strained more under different stresses than the type A and mixture of types A/B TDA under light loading (less than 2 psi). Because type B TDA contained larger sized fragments of tire, the initial fill of the material in the compressional device had a greater void volume and porosity than type A TDA. However, once the initial media reorientation was complete, additional loading resulted in type A, B, and A/B mixed TDA having nearly identical stress/strain response curves (i.e., the same slope).
- In all experimental cases, TDA initially exhibited plastic compression under load, but after the material was subjected to additional loading it behaved like an elastic material.

Physical Properties of TDA

- There are different types of devices and procedures used to produce TDA. As a result, the quality of tire chips may vary greatly among different tire recycling plants. The physical parameters analyzed will differ depending on the manufacturing quality and consistency of TDA.
- To assure uniformity in using TDA, a set of standards concerning the size of tire chips, length of protruding steel wires, and the amount of extraneous objects (e.g., wire pieces, soil, trash etc.) and granulated rubber should be specified to the manufacturer.

Hydraulic Conductivity Testing

- Increased compressive loading results in a reduction in hydraulic conductivity.
- Under light loading, type A TDA had smaller porosities, void ratios, and hydraulic conductivities than type B TDA.
- At loading above 2 psi, the hydraulic conductivity of type A and B TDA appeared to be nearly identical.
- Careful attention is required when using TDA as a drainage material in areas subject to high overburden pressures due to resulting small values of hydraulic conductivity and the opportunity for plugging to occur from loose material in the fill.

Recommendations for Further Work

The following additional experimental work is suggested to address concerns associated with TDA use in civil engineering and construction applications:

- An experimental analysis of the surface degradation of TDA over time in leach fields. There may have been particulate release from the surface of the material, but no further analysis besides visual inspection of effluent turbidity was completed.
- An analysis of the film thickness stability for the biological growth formed on TDA surfaces in leach fields.
- The ability of TDA in leach fields to withstand shock loading, in terms of water quantity (rapid changes to high flow rates) and water quality (rapid changes in pH, BOD, nitrogen, and other water quality parameters).
- A determination of the time required for protruding wire in the TDA to completely oxidize and the release of iron, zinc, and manganese to cease.
- Guidelines or regulations used to address the extent/amount of protruding wire strands.
- Long-term compressibility behavior in laboratory and field settings should be analyzed to determine the time dependence of TDA material expansions and contractions.
- Determine the potential for a reduction in the hydraulic conductivity of TDA due to physical clogging in applications with high clogging potential.
- Characterize the tendency for creep (slow, permanent deformation) to occur in TDA that is heavily loaded.
- Determine more realistic guidelines than currently practiced for maximum fill depths without a noncombustible layer to avoid excessive temperature increases from exothermic behavior in TDA.

This page is intentionally left blank.

References

- Ad Hoc Civil Engineering Committee (1997). "Design Guidelines to Minimize Internal Heating of Tire Shred Fills." Scrap Tire Management Council, Washington, D.C., 1997.
- Ahmed, I. (1993). "Laboratory Study on Properties of Rubber-Soils," Ph.D. Thesis, School of Civil Engineering, Purdue University, W. Lafayette, IN.
- American Society for Testing and Materials (2006). "ASTM D2434 - 68(2006) Standard Test Method for Permeability of Granular Soils (Constant Head)." *ASTM International*, West Conshohocken, PA.
- American Society for Testing and Materials (2012). "ASTM D6270 - 08(2012) Standard Practice for Use of Scrap Tires in Civil Engineering Applications." *ASTM International*, West Conshohocken, PA.
- American Water Works Association (1999). *Design and Construction of Small Water Systems: An AWWA Small Systems Resource Book*.
- Amoozegar, A. and Robarge, W. P. (2006). "Evaluation of Tire Chips as a Substitute for Gravel in the Trenches of Septic Systems." Soil Science Department, North Carolina Agricultural Research Service, College of Agriculture and Life Sciences, North Carolina State University, Raleigh, North Carolina.
- Arroyo, M., San Martin, I., Olivella, S. and Saaltink, M. W. (2011). "Evaluation of Self-Combustion Risk in Tire-Derived Aggregate Fills." *Waste Management*, 31 (9-10), pp. 2133-2141.
- Aydilek, A. H., Madden, E. T. and Demirkan, M. M. (2006). "Field Evaluation of a Leachate Collection System Constructed with Scrap Tires." *Journal of Geotechnical and Geoenvironmental Engineering*, 132 (8), pp. 990-1000.
- Bressette, T. (1984). "Used Tire Material as an Alternate Permeable Aggregate." State of California, Department of Transportation, Division of Engineering Services, Office of Transportation Laboratory, Sacramento, CA.
- CalRecycle (2010). "California Waste Tire Market Report: 2010." Produced by SAIC Energy, Environment & Infrastructure, LLC, Sacramento, CA, pp. 3-33.
- CalRecycle (2012). "Tire Management Overview." <[http://www.calrecycle.ca.gov/Tires/ Overview.htm](http://www.calrecycle.ca.gov/Tires/Overview.htm)> (Accessed on: 9/17/2012).
- Chenette Engineering, Inc. (1993). "Tire Shred Leaching Systems, Demonstration Project Report for Palmer Shredding, Inc." Montpelier, VT.
- Davis, M. L. (2011). *Water and Wastewater Engineering: Design Principles and Practices*. Hash, D. B. and Neyens, L. (eds.), McGraw Hill, New York, NY, p. 12-9.
- Dodds, J., Domenico, W. P., Evans, D. R., Fish, L. W., Lusahn, P. L., and Toth, W. J. (1983). "Scrap Tires: A Resource and Technology Evaluation of Tire Pyrolysis and Other Selected Alternative Technologies." Idaho Falls, Idaho, 1-51.
- Duffy, D. P. (1996). "The Potential for Use of Shredded Tire Chips as a Leachate Drainage and Collection Medium: Design, Construction and Performance Considerations." Proceedings, Landfill Design Seminar Using Tire Shreds, Texas Natural Resource Conservation Commission, Arlington, TX.
- Edil, T. B. and Bosscher, P. J. (1994). "Engineering Properties of Tire Chips and Soil Mixtures." *Geotechnical Testing Journal*, 17(4), pp. 453-464.

- Geosyntec Consultants, Inc. (1997). "Report of Tire Chip Protective Layer Monitoring System Installation, Scrap Tire Demonstration Project, Newland Park Landfill, Wicomico County, Maryland." Prepared for the Maryland Environmental Service, Annapolis, MD.
- Geosyntec Consultants, Inc. (2004). "Report of Tire Chip Excavation and Laboratory Testing, Scrap Tire Demonstration Project, Newland Park Landfill, Wicomico County, Maryland." Prepared for Maryland Environmental Service, Annapolis, MD.
- Geosyntec Consultants, Inc. (2008). "Guidance Manual for Engineering Uses of Scrap Tires." Maryland Department of the Environment, Baltimore, MD.
- Grimes, B. H., Steinbeck, S., and Amoozegar, A. (2003). "Analysis of Tire Chips as a Substitute for Stone Aggregate in Nitrification Trenches of Onsite Septic Systems: Status and Notes on the Comparative Microbiology of Tire Chip Versus Stone Aggregate Trenches." *Small Flows Quarterly*, 4(4), 18–23.
- Georg Fischer Signet LLC (2011). "Signet 2551 Magmeter Flow Sensor Manual."
- Gunasekara, A. S., Donovan, J. A., and Xing, B. (2000). "Ground Discarded Tires Remove Naphthalene, Toluene, and Mercury from Water." *Chemosphere*, 41(8), pp. 1155-60.
- Hall, T. J. (1991). "Reuse of Shredded Tire Material for Leachate Collection Systems." Proceedings, Fourteenth Annual Madison Waste Conference, University of Wisconsin-Madison, Madison, WI.
- Humphrey, D. N. (2003). "Civil Engineering Applications Using Tire-Derived Aggregate (TDA)." University of Maine, pp. 1-142.
- Humphrey, D. N. and Katz, L. E. (2000). "Five-Year Study of the Water Quality Effects of Tire Shreds Placed Above the Water Table." Maine Department of Transportation and Scrap Tire Management Council Paper No. 00-0892.
- Humphrey, D. N. and Manion, W. P. (1992). "Properties of Tire Chips for Lightweight Fill." *Grouting, Soil Improvement, and Geosynthetics; Proceedings of the Conference*, Vol. 2, pp. 1344-1355.
- Humphrey, D. N., Sandford, T. C., Cribbs, M. M., Gharegrat, H., and Manion, W. P. (1992). "Tire Chips as Lightweight Backfill for Retaining Walls—Phase I" Prepared for the New England Consortium.
- Lawrence, B. K., Chen, L. H., and Humphrey, D. N. (1998). "Use of Tire Chip/Soil Mixtures to Limit Frost Heave and Pavement Damage of Paved Roads." A Study for the New England Transportation Consortium, by the Department of Civil and Environmental Engineering, University of Maine, Orono, ME.
- Marella, A. (2002). "Use of Shredded Scrap Tires as Drainage Material in Landfill Covers." M. S. Thesis, University of Illinois at Chicago, Chicago, IL.
- Marietou, A., L Griffiths, and J. Cole (2009). "Preferential Reduction of the Thermodynamically Less Favorable Electron Acceptor, Sulfate, by a Nitrate-Reducing Strain of the Sulfate-Reducing Bacterium *Desulfovibrio desulfuricans* 27774." *Journal of Bacteriology*, 191(3), pp. 882-889.
- Moo-Young, H., Sellasie, K., Zeroka, D. and Sabnis, G. (2003). "Physical and Chemical Properties of Recycled Tire Shreds for Use in Construction." *Journal of Environmental Engineering*, 129 (10), pp. 921-929.
- Narejo, D. B. and Shettima, M. (1995). "Use of Recycled Automobile Tires to Design Landfill Components." *Geosynthetics International*, 2 (3), pp. 619-625.

- National Climatic Data Center (2013). "Quality Controlled Local Climatological Data." <<http://cdo.ncdc.noaa.gov/qclcd/QCLCD>> (Accessed on: 1/27/2013).
- Raven Industries Inc. (2003). "Rufco 2000B Mono-layer Membrane Product Description." Sioux Falls, SD, pp. 1-2.
- Reddy, K. R. and Saichek, R. E. (1998). "Assessment of Damage to Geomembrane Liners by Shredded Scrap Tires." *Geotechnical Testing Journal*, 21 (4), pp. 307-316.
- Reddy, K. R. and Saichek, R. E. (1998a). "Characterization and Performance Assessment of Shredded Scrap Tires as Leachate Drainage Material in Landfills." The Fourteenth International Conference on Solid Waste Technology and Management, Philadelphia, PA.
- Rhodes, E. P., Z. Ren, and D. C. Mays (2012). "Zinc Leaching from Tire Crumb Rubber." *Environmental Science Technology*, 46(23), pp. 12856-12863.
- Robinson, S. J. (2000). "The Use of Chipped Tires as Alternate Aggregate in Septic System Leach Fields." M.S. Thesis in Civil Engineering, State University of New York, Syracuse, p. 234.
- Scardaci, A., Cheng, D., and Van Atta, D. (2012). "Tire-Derived Aggregate Gradation Analysis for Humboldt State University TDA Project." TDA Technology Center, California State University, Chico, CA, pp. 1-9.
- Schulze, E.-D., and Mooney, H. A. (1994). "Desulfurication." *Biodiversity and Ecosystem Function*, Springer Verlag, New York, pp. 88-89.
- Sengupta, S. and Miller, H. (1999). "Preliminary Investigation of Tire Shred for Use in Residential Subsurface Leaching Field Systems: A Field Scale Study." Technical Report #12, Chelsea Center for Recycling and Economic Development, University of Massachusetts, Lowell, p. 12.
- Sengupta, S. and Miller, H. (2000). "Investigation of Tire Shred for Use in Residential Subsurface Leaching Field Systems: A Field Scale Study." Technical Report #32, Chelsea Center for Recycling and Economic Development, University of Massachusetts, Lowell, p. 33.
- Spagnoli, J., Weber, A. S., and Zicari, L. P. (2001). "The Use of Tire Chips in Septic System Leach Fields." Center for Integrated Waste Management, University at Buffalo, NY, p. 92.
- The Texas Natural Resource Council Commission (1999). "Using Tire Shreds in On-site Sewage Facilities (Septic Systems)."
- U.S. Environmental Protection Agency (1997). "Numeric Removal Action Levels for Contaminated Drinking Water Sites." Office of Solid Waste and Emergency Response, Washington, D.C.
- U.S. Environmental Protection Agency (2012). "Toluene Hazard Summary." <<http://www.epa.gov/ttnatw01/hlthef/toluene.html>> (Accessed on: 1/26/2013).
- (2012a) "Water: Monitoring and Assessment- Phosphorus." <<http://water.epa.gov/type/rsl/monitoring/vms56.cfm>> (Accessed on: 1/26/2013).
- Wappett, H. L., Zornberg, J. G. (2006). "Full Scale Monitoring for Assessment of Exothermal Reactions Waste Tires." Recycled Materials Resource Center, Project No.27, University of Texas at Austin.
- Wartman, J., Natale, M. F., and Strenk, P. M. (2007). "Immediate and Time-Dependent Compression of Tire-Derived Aggregate", *Journal of Geotechnical and Geoenvironmental Engineering*, 133 (3), pp. 245-256.

- Winter, B. and Cheng, D. (2012). "Tire-Derived Aggregate Gradation Analysis for CalRecycle." TDA Technology Center, California State University, Chico, CA, pp. 1-10.
- Wright, J. (2011). AutoCAD Drawings for Tire-Derived Aggregate Experiments.
- Yang, S., Lohnes, R. A., and Kjartanson, B. H. (2002). "Mechanical Properties of Shredded Tires." *Geotechnical Testing Journal*, 25(1), pp. 44-52.

Appendix A: Leach Field Water Quality Parameters

Table A-1. Water quality parameters analyzed in the rock and TDA leach fields.

Parameter (µg/L unless noted otherwise)	Parameter (µg/L unless noted otherwise)	Parameter (µg/L unless noted otherwise)
1,1,1,2-Tetrachloroethane	1,2-Dichloroethane	Bromochloromethane
1,1,1-Trichloroethane	1,2-Dichloropropane	Bromodichloromethane
1,1,1,2-Tetrachloroethane	1,3,5-Trimethylbenzene	Bromoform
1,1,2-Trichloroethane	1,3-Dichlorobenzene	Bromomethane
1,1-Dichloroethane	1,3-Dichloropropane	Cadmium
1,1-Dichloroethene	1,4-Dichlorobenzene	Carbon tetrachloride
1,1-Dichloropropene	2,2-Dichloropropane	Chemical Oxygen Demand (mg/L)
1,2,3-Trichlorobenzene	2-Chlorotoluene	Chlorobenzene
1,2,3-Trichloropropane	4-Chlorotoluene	Chloroethane
1,2,4-Trichlorobenzene	4-Isopropyltoluene	Chloroform
1,2,4-Trimethylbenzene	Ammonia (as Nitrogen) (mg/L)	Chloromethane
1,2-Dibromo-3-chloropropane (DBCP)	Benzene	cis-1,2-Dichloroethene
1,2-Dibromoethane (EDB)	Biochemical Oxygen Demand (mg/L)	cis-1,3-Dichloropropene
1,2-Dichlorobenzene	Bromobenzene	Dibromochloromethane
Dibromomethane	Naphthalene	Tert-butyl ether (MTBE)
Dichlorodifluoromethane	n-Butylbenzene	tert-Butylbenzene
Di-isopropyl ether (DIPE)	Nitrate(as Nitrogen) (mg/L)	Tetrachloroethene
Ethyl tert-butyl ether (ETBE)	Non-Filterable Residue (TSS) (mg/L)	Toluene
Ethylbenzene	n-Propylbenzene	Total Coliform (MPN/100 mL)
Fecal Coliform (MPN/100 mL)	o-Xylene	Total Kjeldahl nitrogen (mg/L)
Hexachlorobutadiene	pH (pH units)	Total Phosphate Phosphorus (mg/L)
Iron	sec-Butylbenzene	TPHC Gasoline
Isopropylbenzene	Styrene	trans-1,2-Dichloroethene
Lead	Sulfate (mg/L)	trans-1,3-Dichloropropene
m,p-Xylene	Surrogate: 1,2-Dichloroethane-d4	Trichloroethene
Manganese	Surrogate: Dibromofluoromethane	Trichlorofluoromethane
Methyl tert-butyl alcohol (TBA)	Surrogate: Toluene-d8	Vinyl chloride

Parameter (µg/L unless noted otherwise)	Parameter (µg/L unless noted otherwise)	Parameter (µg/L unless noted otherwise)
Methylene chloride	Tert-amyl methyl ether (TAME)	Zinc

Appendix B: Lab Analysis Results For Leach Fields

Table B-1 represents water quality results from a 17-month operational period of wastewater flowing through a rock and TDA media leach field using representative domestic wastewater loading rates. The parameters tested are shown in Appendix A and only the parameters that had detectable values are provided in Table B-1. The volatile organic compound dilutions were changed on Feb. 7, 2012, which may affect the values of the results shown after this date.

Table B-1. Detectable organic and inorganic compounds/elements from rock and TDA leach fields.

Sample Date	Influent	Rock- Middle of Leach Pipeline	Rock- Leach Pipeline Ending Effluent	TDA- Middle of Leach Pipeline	TDA- Leach Pipeline Ending Effluent
Iron (µg/L)					
8/16/2011	410	430	310	440	440
8/31/2011	470	490	430	540	670
9/14/2011	550	850	960	760	970
9/28/2011	540	610	730	560	1,100
10/12/2011	710	600	660	6,000	12,000
10/26/2011	620	590	590	2,600	8,500
11/9/2011	1,600	1,200	1,000	2,500	4,800
12/7/2011	2,000	1,400	1,300	2,800	6,300
1/10/2012	1,300	1,100	960	2,300	7,000
2/7/2012	810	670	550	2,400	5,000
3/14/2012	800	700	690	3,300	5,000
4/10/2012	680	670	540	6,800	5,500
5/8/2012	680	890	670	18,000	4,800
6/13/2012	330	380	390	14,000	2,100
7/10/2012	310	350	250	12,000	3,300
11/6/2012	1,010	906	811	7,970	1,700
8/16/2011	0	0	0	0	0
8/31/2011	0	0	0	0	0
9/14/2011	0	0	0	0	0
9/28/2011	0	0	0	0	0
10/12/2011	0	0	0	0	0
10/26/2011	0	0	0	0	0

Sample Date	Influent	Rock- Middle of Leach Pipeline	Rock- Leach Pipeline Ending Effluent	TDA- Middle of Leach Pipeline	TDA- Leach Pipeline Ending Effluent
11/9/2011	0	0	0	0	0
12/7/2011	0	0	0	0	0
1/10/2012	0	0	0	0	0
2/7/2012	0	0	0	0	0
3/14/2012	0	0	0	0	0
4/10/2012	0	0	0	0	0
5/8/2012	0	0	0	7.0	0
6/13/2012	0	0	0	5.4	0
7/10/2012	0	0	0	0	0
11/6/2012	0	0	0	0	0
Manganese (µg/L)					
8/16/2011	140	94	130	140	140
8/31/2011	120	98	120	120	130
9/14/2011	120	120	150	120	130
9/28/2011	100	90	110	71	94
10/12/2011	120	110	160	180	250
10/26/2011	130	140	150	150	190
11/9/2011	120	110	110	120	140
12/7/2011	210	200	200	210	240
1/10/2012	190	170	170	180	230
2/7/2012	140	130	130	130	190
3/14/2012	140	130	120	170	200
4/10/2012	160	160	150	190	190
5/8/2012	170	170	160	250	190
6/13/2012	99	100	110	170	110
7/10/2012	120	76	71	140	94
11/6/2012	119	119	118	147	111
Zinc (µg/L)					
8/16/2011	31	61	24	88	77
8/31/2011	23	36	18	59	54
9/14/2011	25	44	21	50	37
9/28/2011	27	37	24	44	55

Sample Date	Influent	Rock- Middle of Leach Pipeline	Rock- Leach Pipeline Ending Effluent	TDA- Middle of Leach Pipeline	TDA- Leach Pipeline Ending Effluent
10/12/2011	30	40	22	110	250
10/26/2011	20	40	18	35	21
11/9/2011	44	51	32	44	29
12/7/2011	49	56	36	50	26
1/10/2012	33	45	26	40	25
2/7/2012	20	23	0	23	14
3/14/2012	22	33	26	42	24
4/10/2012	23	37	15	63	26
5/8/2012	0	28	0	340	12
6/13/2012	17	33	18	320	23
7/10/2012	0	30	0	210	0
11/6/2012	42.2	58.9	46	178	69.4

Chloromethane (µg/L)

8/16/2011	0	0	0	0	0
8/31/2011	0	0	0	0	0
9/14/2011	0	0	0	0	0
9/28/2011	0	0	0	0	0
10/12/2011	0	0	0	0	0
10/26/2011	0	0	0	0	0
11/9/2011	0	0	0	0	0
12/7/2011	0	0	0	0	0
1/10/2012	0	0	0	0	0
2/7/2012	0	0	0	0	0.51
3/14/2012	0	0	0	0	0
4/10/2012	0	0	0	0	0
5/8/2012	0	0	0	0	0
6/13/2012	0	0	0	0	0
7/10/2012	0	0	0	0	0
11/6/2012	0	0	0	0	0

Methylene chloride (µg/L)

8/16/2011	0	0	0	0	0
8/31/2011	0	0	0	0	0

Sample Date	Influent	Rock- Middle of Leach Pipeline	Rock- Leach Pipeline Ending Effluent	TDA- Middle of Leach Pipeline	TDA- Leach Pipeline Ending Effluent
9/14/2011	0	0	0	0	0
9/28/2011	0	0	0	0	0
10/12/2011	0	0	0	0	0
10/26/2011	0	0	0	0	0
11/9/2011	0	0	0	0	0
12/7/2011	0	0	0	0	0
1/10/2012	0	0	0	0	0
2/7/2012	1.6	1.3	1.3	1.1	0.73
3/14/2012	0.51	0	0.63	0	0
4/10/2012	2.2	1.6	1.6	1.0	0.73
5/8/2012	1.9	1.2	2.5	1.2	1.0
6/13/2012	0	0	0	0	0
7/10/2012	0	0	0	0	0
11/6/2012	0	0	0	0	0

Chloroform (µg/L)

8/16/2011	0	0	0	0	0
8/31/2011	0	0	0	0	0
9/14/2011	0	0	0	0	0
9/28/2011	0	0	0	0	0
10/12/2011	0	0	0	0	0
10/26/2011	0	0	0	0	0
11/9/2011	0	0	0	0	0
12/7/2011	0	0	0	0	0
1/10/2012	0	0	0	0	0
2/7/2012	0.50	0	0	0	0
3/14/2012	0	0	0	0	0
4/10/2012	0	0	0	0	0
5/8/2012	0	0	0	0	0
6/13/2012	0	0.65	0	0	0
7/10/2012	0	0	0	0	0
11/6/2012	0	0	0	0	0

Toluene (µg/L)

Sample Date	Influent	Rock- Middle of Leach Pipeline	Rock- Leach Pipeline Ending Effluent	TDA- Middle of Leach Pipeline	TDA- Leach Pipeline Ending Effluent
8/16/2011	0	0	0	0	0
8/31/2011	0	0	0	0	0
9/14/2011	0	0	0	0	0
9/28/2011	0	0.69	1.4	0	0
10/12/2011	0.50	0.90	1.9	0	0
10/26/2011	0	0	0	0	0
11/9/2011	0	0	0	0	0
12/7/2011	0	0	0	0	0
1/10/2012	0	0	0	0	0
2/7/2012	0	0	0	0	0
3/14/2012	0	0	0	0	0
4/10/2012	0	0	0	0.53	0
5/8/2012	0	0	0	0	0
6/13/2012	0	0	0	0	0
7/10/2012	0	0	0	0.64	0
11/6/2012	0	0	0	0	0
Naphthalene (µg/L)					
8/16/2011	0	0	0	0	0
8/31/2011	0	0	0	0	0
9/14/2011	0	0	0	0	0
9/28/2011	0	0	0	0	0
10/12/2011	0	0	0	0	0
10/26/2011	4.1	0	0	0	0
11/9/2011	0	0	0	0	0
12/7/2011	0	0	0	0	0
1/10/2012	0	0	0	0	0
2/7/2012	0	0	0	0	0
3/14/2012	0	0	0	0	0
4/10/2012	0	0	0	0	0
5/8/2012	0	0	0	0	0
6/13/2012	0	0	0	0	0
7/10/2012	0	0	0	0	0

Sample Date	Influent	Rock- Middle of Leach Pipeline	Rock- Leach Pipeline Ending Effluent	TDA- Middle of Leach Pipeline	TDA- Leach Pipeline Ending Effluent
11/6/2012	0	0	0	0	0
1,2,3-Trichlorobenzene (µg/L)					
8/16/2011	0	0	0	0	0
8/31/2011	0	0	0	0	0
9/14/2011	0	0	0	0	0
9/28/2011	0	0	0	0	0
10/12/2011	0	0	0	0	0
10/26/2011	0	0	0	0	0
11/9/2011	0	0	0	0	0
12/7/2011	0	0	0	0	0
1/10/2012	0	0	0	0	0
2/7/2012	0	0	0	0	0
3/14/2012	0	0	0	0	0
4/10/2012	0	0	0	0	0.52
5/8/2012	0	0	0	0	0
6/13/2012	0	0	0	0	0
7/10/2012	0	0	0	0	0
11/6/2012	0	0	0	0	0
Surrogate: 1,2-Dichloroethane-d4 (µg/L)					
8/16/2011	117	119	119	123	118
8/31/2011	90.9	92.3	86.1	91.8	88.3
9/14/2011	93.3	92.0	92.6	112	111
9/28/2011	98.2	101	100	100	100
10/12/2011	94.1	93.9	93.6	93.5	96.3
10/26/2011	94.8	92.9	93.4	94.0	93.2
11/9/2011	98.7	101	100	99.1	102
12/7/2011	99.4	98.3	98.7	103	102
1/10/2012	100	101	100	99.1	99.2
2/7/2012	107	110	109	106	107
3/14/2012	166	162	88.5	89.5	91.9
4/10/2012	116	116	117	120	120
5/8/2012	173	189	122	121	123

Sample Date	Influent	Rock- Middle of Leach Pipeline	Rock- Leach Pipeline Ending Effluent	TDA- Middle of Leach Pipeline	TDA- Leach Pipeline Ending Effluent
6/13/2012	113	108	115	120	112
7/10/2012	100	102	92.6	95.6	97.6
11/6/2012	98.5	98.8	100	98.8	99.6
Surrogate: Dibromofluoromethane (µg/L)					
8/16/2011	102	100	101	103	101
8/31/2011	97.6	97.4	95.6	98.4	95.5
9/14/2011	104	102	104	104	103
9/28/2011	104	103	104	106	104
10/12/2011	98.6	98.7	100	99.3	100
10/26/2011	98.5	98.5	99.4	96.9	98.2
11/9/2011	106	108	108	107	107
12/7/2011	94.6	92.0	88.2	94.0	95.3
1/10/2012	102	102	101	100	101
2/7/2012	107	110	108	107	110
3/14/2012	121	124	94.3	93.9	95.6
4/10/2012	104	103	106	107	109
5/8/2012	134	134	121	112	117
6/13/2012	112	110	118	118	109
7/10/2012	89.2	91.5	92.3	93.9	98
11/6/2012	100	101	101	101	99.5
Surrogate: Toluene-d8 (µg/L)					
8/16/2011	100	100	101	98.7	98.2
8/31/2011	100	102	103	98.7	106
9/14/2011	93.8	91.3	93.1	95.3	95.6
9/28/2011	92.2	93.1	96.2	94.9	93.7
10/12/2011	103	105	101	100	99.1
10/26/2011	97.1	96.0	97.9	95.8	95.6
11/9/2011	100	98.5	98.9	97.8	96.6
12/7/2011	119	109	119	112	114
1/10/2012	96.4	95.2	96.5	94.6	96.3
2/7/2012	100	96.4	100	98.5	98.6
3/14/2012	84.1	83.4	111	104	102

Sample Date	Influent	Rock- Middle of Leach Pipeline	Rock- Leach Pipeline Ending Effluent	TDA- Middle of Leach Pipeline	TDA- Leach Pipeline Ending Effluent
4/10/2012	98.7	99.3	100	102	100
5/8/2012	97.3	93.8	97.0	100	98.9
6/13/2012	105	111	107	96.1	109
7/10/2012	108	106	102	104	108
11/6/2012	101	104	103	103	104
Sulfate (mg/L)					
8/16/2011	17	18	18	18	18
8/31/2011	18	19	19	18	18
9/14/2011	18	19	18	18	18
9/28/2011	18	18	18	18	17
10/12/2011	16	17	16	15	13
10/26/2011	18	18	18	17	10
11/9/2011	19	19	19	18	16
12/7/2011	20	20	20	19	16
1/10/2012	19	19	20	19	16
2/7/2012	16	16	16	15	14
3/14/2012	16	16	16	15	14
4/10/2012	13	13	13	11	11
5/8/2012	13	15	15	13	13
6/13/2012	15	15	15	15	14
7/10/2012	17	17	17	16	15
11/6/2012	22	22	22	20	21
Nitrate(as Nitrogen) (mg/L)					
8/16/2011	3.4	3.6	3.7	3.0	2.3
8/31/2011	0.13	0.70	0.45	0.15	0.12
9/14/2011	0	0.55	0.28	0.22	0
9/28/2011	0.11	0.57	0.53	0.15	0
10/12/2011	0	0.81	0.54	0	0
10/26/2011	0	1.2	1.2	0	0
11/9/2011	0	0.50	0.65	0	0
12/7/2011	0	0.57	0.70	0	0
1/10/2012	0	0.67	0.93	0.14	0

Sample Date	Influent	Rock- Middle of Leach Pipeline	Rock- Leach Pipeline Ending Effluent	TDA- Middle of Leach Pipeline	TDA- Leach Pipeline Ending Effluent
2/7/2012	0	0.77	1.0	0	0
3/14/2012	0	1.9	2.3	0.36	0.61
4/10/2012	0	2.5	2.3	0.55	0.31
5/8/2012	0	1.1	1.1	0	0
6/13/2012	0	1.0	1.3	0.36	0.17
7/10/2012	0	0.86	1.1	0	0
11/6/2012	0	0.70	0.84	0	0.12
Biochemical Oxygen Demand (mg/L)					
8/16/2011	170	170	160	170	130
8/31/2011	160	150	150	180	140
9/14/2011	100	96	99	100	120
9/28/2011	120	120	120	140	130
10/12/2011	110	110	87	110	120
10/26/2011	110	110	100	110	100
11/9/2011	110	100	100	98	88
12/7/2011	35	35	36	36	28
1/10/2012	28	34	32	27	26
2/7/2012	47	53	50	49	46
3/14/2012	38	38	35	36	28
4/10/2012	36	36	34	38	30
5/8/2012	43	46	43	45	33
6/13/2012	92	84	100	130	80
7/10/2012	71	72	86	92	69
11/6/2012	140	130	130	130	120
Non-Filterable Residue (TSS) (mg/L)					
8/16/2011	130	140	120	140	130
8/31/2011	140	120	100	130	120
9/14/2011	130	130	120	130	120
9/28/2011	150	140	140	130	130
10/12/2011	110	84	68	100	100
10/26/2011	120	120	100	110	100
11/9/2011	150	130	130	130	130

Sample Date	Influent	Rock- Middle of Leach Pipeline	Rock- Leach Pipeline Ending Effluent	TDA- Middle of Leach Pipeline	TDA- Leach Pipeline Ending Effluent
12/7/2011	110	96	90	70	88
1/10/2012	76	76	64	70	64
2/7/2012	76	68	58	60	54
3/14/2012	66	58	60	81	59
4/10/2012	22	22	24	74	42
5/8/2012	67	68	60	110	64
6/13/2012	64	66	64	240	54
7/10/2012	68	72	60	250	64
11/6/2012	150	130	110	230	94
H (pH units)					
8/16/2011	7.0	7.1	7.0	6.8	6.8
8/31/2011	7.0	7.0	7.0	6.9	6.9
9/14/2011	7.1	7.0	7.0	7.0	6.9
9/28/2011	7.2	7.0	7.0	6.9	6.8
10/12/2011	7.1	6.9	6.8	7.0	7.0
10/26/2011	7.1	7.0	6.9	7.0	7.0
11/9/2011	7.3	7.0	7.0	7.0	6.9
12/7/2011	7.2	7.1	7.0	7.0	7.0
1/10/2012	7.1	7.0	6.9	6.9	6.9
2/7/2012	7.0	6.9	6.8	6.9	6.9
3/14/2012	7.2	6.8	6.8	6.8	6.8
4/10/2012	7.0	6.7	6.6	6.8	6.7
5/8/2012	7.2	6.8	6.8	6.9	6.8
6/13/2012	7.7	7.3	7.2	7.1	7.0
7/10/2012	7.3	7.1	7.0	6.9	6.8
11/6/2012	7.2	7.0	7.0	6.9	6.9
Ammonia (as Nitrogen) (mg/L)					
8/16/2011	0.51	0.21	0.25	0.36	0.34
8/31/2011	4.0	3.2	3.2	4.0	4.1
9/14/2011	2.8	2.4	2.0	2.4	2.4
9/28/2011	2.1	1.4	1.3	2.2	2.0
10/12/2011	3.4	2.7	2.6	2.9	2.9

Sample Date	Influent	Rock- Middle of Leach Pipeline	Rock- Leach Pipeline Ending Effluent	TDA- Middle of Leach Pipeline	TDA- Leach Pipeline Ending Effluent
10/26/2011	11	9.1	9.3	11	11
11/9/2011	15	15	14	14	12
12/7/2011	22	23	19	25	21
1/10/2012	19	19	19	22	19
2/7/2012	12	13	12	12	11
3/14/2012	16	14	12	14	16
4/10/2012	12	9.5	8.6	11	10
5/8/2012	16	13	12	12	10
6/13/2012	13	12	11	13	12
7/10/2012	15	17	13	16	9.9
11/6/2012	18	17	18	19	17
Chemical Oxygen Demand (mg/L)					
8/16/2011	210	200	190	200	220
8/31/2011	200	200	180	210	200
9/14/2011	220	210	200	230	200
9/28/2011	240	230	230	250	220
10/12/2011	180	170	160	190	200
10/26/2011	230	180	180	170	190
11/9/2011	200	190	220	170	140
12/7/2011	110	100	99	88	84
1/10/2012	100	160	140	150	140
2/7/2012	160	140	160	130	130
3/14/2012	150	140	160	120	110
4/10/2012	110	110	100	110	110
5/8/2012	170	190	160	260	110
6/13/2012	240	220	230	330	180
7/10/2012	170	190	180	290	140
11/6/2012	240	230	220	260	200
Total Phosphate Phosphorus (mg/L)					
8/16/2011	7.7	6.2	7.1	7.1	5.4
8/31/2011	6.1	5.9	5.0	5.9	5.9
9/14/2011	6.5	6.5	6.4	6.5	6.3

Sample Date	Influent	Rock- Middle of Leach Pipeline	Rock- Leach Pipeline Ending Effluent	TDA- Middle of Leach Pipeline	TDA- Leach Pipeline Ending Effluent
9/28/2011	6.3	6.3	6.2	6.1	6.0
10/12/2011	5.1	4.9	5.0	5.6	5.3
10/26/2011	5.9	5.5	5.4	5.3	5.2
11/9/2011	5.3	5.3	5.3	5.0	4.9
12/7/2011	5.8	5.5	5.4	4.8	4.5
1/10/2012	4.7	4.6	4.4	4.0	3.5
2/7/2012	3.6	3.5	3.3	3.3	2.9
3/14/2012	3.9	3.8	3.8	3.4	2.7
4/10/2012	2.7	2.7	2.5	2.1	1.6
5/8/2012	3.7	3.6	3.4	5.6	2.8
6/13/2012	5.0	4.8	4.8	5.9	3.8
7/10/2012	5.7	5.4	5.3	7.6	4.0
11/6/2012	6.4	6.2	6.1	6.2	5.9
Fecal Coliform (MPN/100 mL)					
8/16/2011	>1600	>1600	>1600	>1600	>1600
8/31/2011	>160,000	>160,000	>160,000	>160,000	>160,000
9/14/2011	210,000	330,000	330,000	330,000	790,000
9/28/2011	330,000	330,000	330,000	110,000	490,000
10/12/2011	>160000	>160000	>160000	>160000	>160000
10/26/2011	790,000	170,000	330,000	790,000	330,000
11/9/2011	490,000	790,000	230,000	790,000	1,700,000
12/7/2011	790,000	700,000	1,300,000	1,100,000	790,000
1/10/2012	790,000	230,000	790,000	490,000	490,000
2/7/2012	490,000	170,000	330,000	130,000	330,000
3/14/2012	330,000	700,000	490,000	330,000	490,000
4/10/2012	230,000	1,100,000	1,300,000	330,000	330,000
5/8/2012	790,000	1,300,000	330,000	1,300,000	700,000
6/13/2012	2,400,000	700,000	1,100,000	1,100,000	1,300,000
7/10/2012	490,000	340,000	490,000	790,000	490,000
11/6/2012	790,000	1,100,000	1,300,000	490,000	1,400,000
Total Coliform (MPN/100 mL)					
8/16/2011	>1600	>1600	>1600	>1600	>1600

Sample Date	Influent	Rock- Middle of Leach Pipeline	Rock- Leach Pipeline Ending Effluent	TDA- Middle of Leach Pipeline	TDA- Leach Pipeline Ending Effluent
8/31/2011	>160,000	>160,000	>160,000	>160,000	>160,000
9/14/2011	3,500,000	3,500,000	2,400,000	1,100,000	5,400,000
9/28/2011	1,100,000	790,000	2,400,000	790,000	1,300,000
10/12/2011	>160000	>160000	>160000	>160000	>160000
10/26/2011	1,300,000	790,000	1,300,000	2,400,000	1,100,000
11/9/2011	2,400,000	2,400,000	2,200,000	5,400,000	3,500,000
12/7/2011	3,500,000	5,400,000	5,400,000	5,400,000	3,500,000
1/10/2012	3,500,000	1,700,000	2,400,000	1,200,000	3,500,000
2/7/2012	1,300,000	1,700,000	790,000	700,000	1,100,000
3/14/2012	490,000	1,700,000	1,300,000	1,300,000	1,300,000
4/10/2012	3,500,000	3,500,000	2,400,000	9,200,000	790,000
5/8/2012	2,400,000	5,400,000	1,100,000	3,500,000	1,700,000
6/13/2012	2,400,000	1,400,000	3,500,000	5,400,000	2,400,000
7/10/2012	1,700,000	2,400,000	2,400,000	1,300,000	3,500,000
11/6/2012	2,400,000	9,200,000	2,400,000	3,500,000	5,400,000
Total Kjeldahl nitrogen (mg/L) (not available is defined by N/A)					
8/16/2011	N/A	N/A	N/A	N/A	N/A
8/31/2011	N/A	N/A	N/A	N/A	N/A
9/14/2011	N/A	N/A	N/A	N/A	N/A
9/28/2011	N/A	N/A	N/A	N/A	N/A
10/12/2011	N/A	N/A	N/A	N/A	N/A
10/26/2011	N/A	N/A	N/A	N/A	N/A
11/9/2011	N/A	N/A	N/A	N/A	N/A
12/7/2011	N/A	N/A	N/A	N/A	N/A
1/10/2012	N/A	N/A	N/A	N/A	N/A
2/7/2012	N/A	N/A	N/A	N/A	N/A
3/14/2012	N/A	N/A	N/A	N/A	N/A
4/10/2012	N/A	N/A	N/A	N/A	N/A
5/8/2012	N/A	N/A	N/A	N/A	N/A
6/13/2012	29	25	24	31	27
7/10/2012	20	21	18	21	14
11/6/2012	N/A	N/A	N/A	N/A	N/A

Appendix C: Water Quality Graphs-Leach Fields

Figures C-1 through C-24 represents the data in Appendix B from a 17-month operational period. The volatile organic compound dilutions were changed on Feb. 7, 2012, which may affect the values of the results shown after this date.

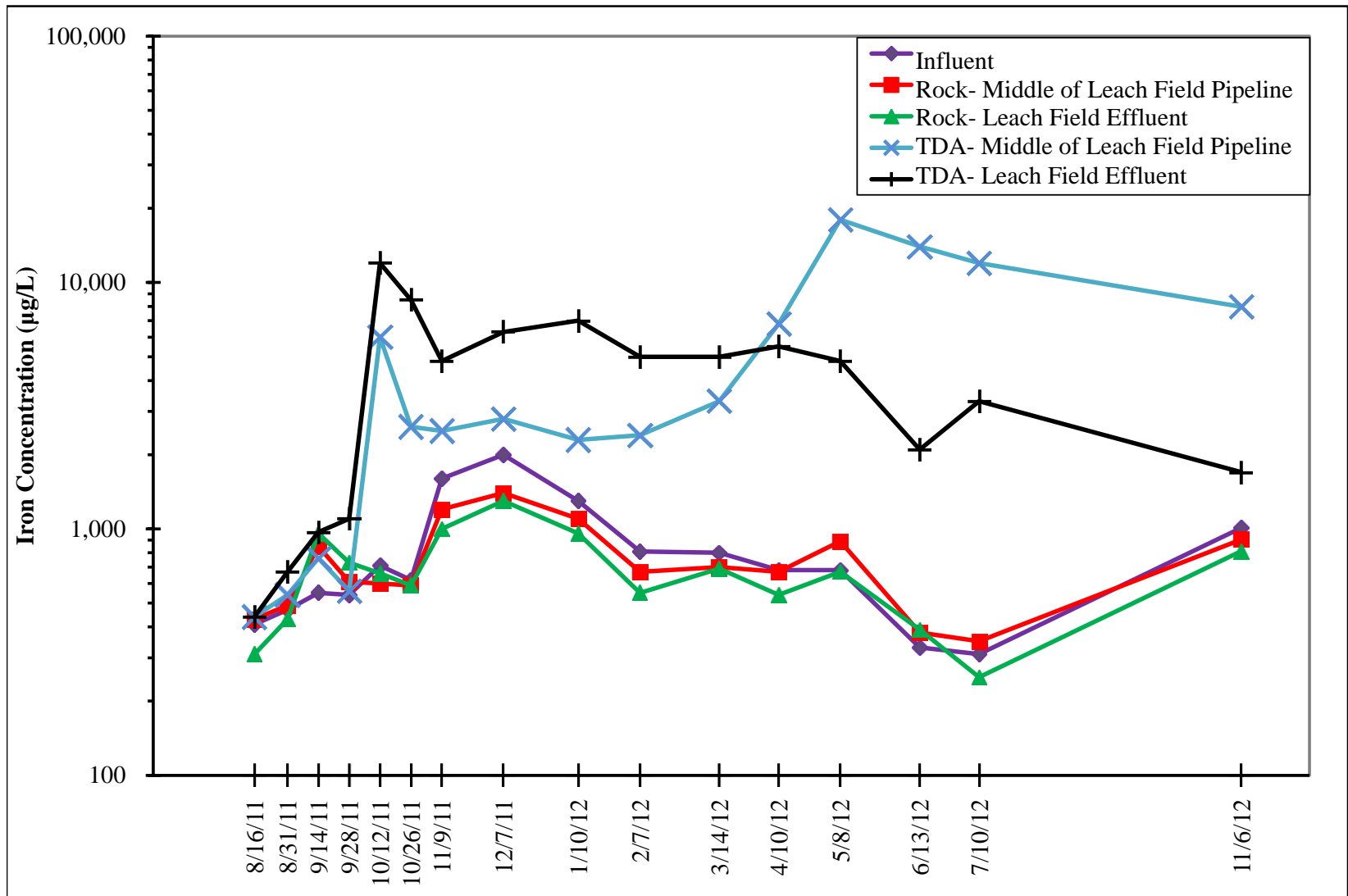


Figure C-1. Iron concentrations in the rock and TDA leach fields.

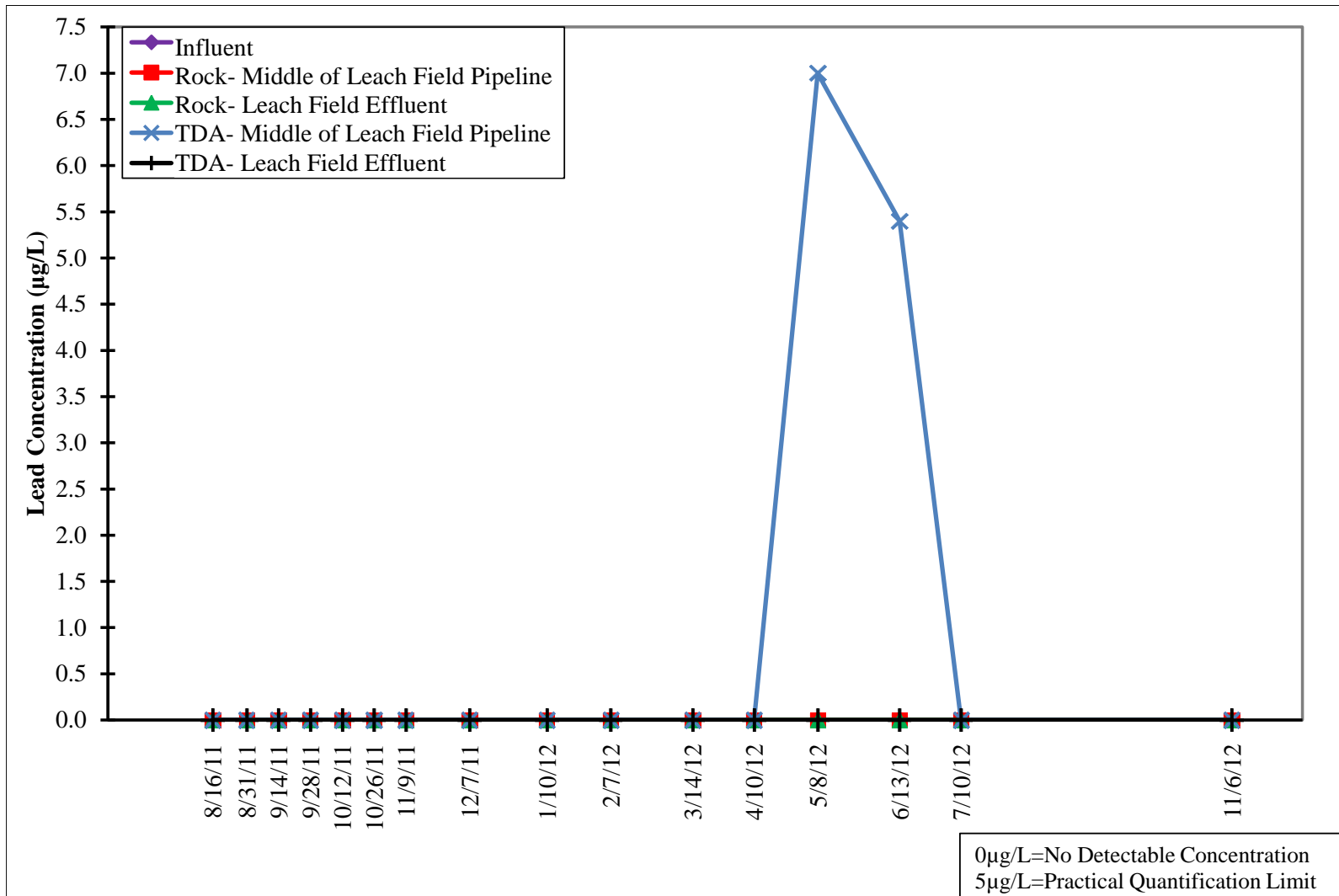


Figure C-2. Lead concentrations in the rock and TDA leach fields.

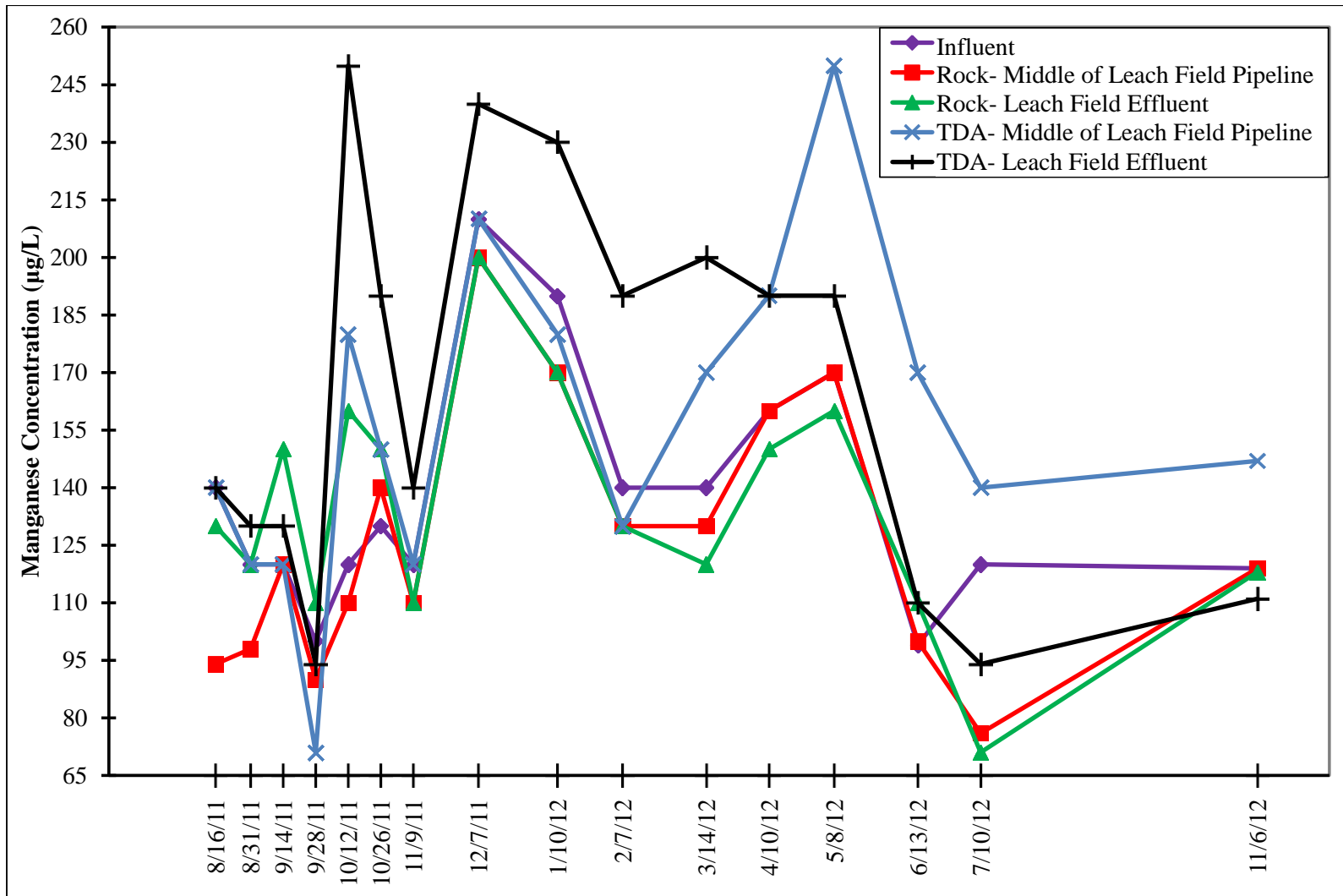


Figure C-3. Manganese concentrations in the rock and TDA leach fields.

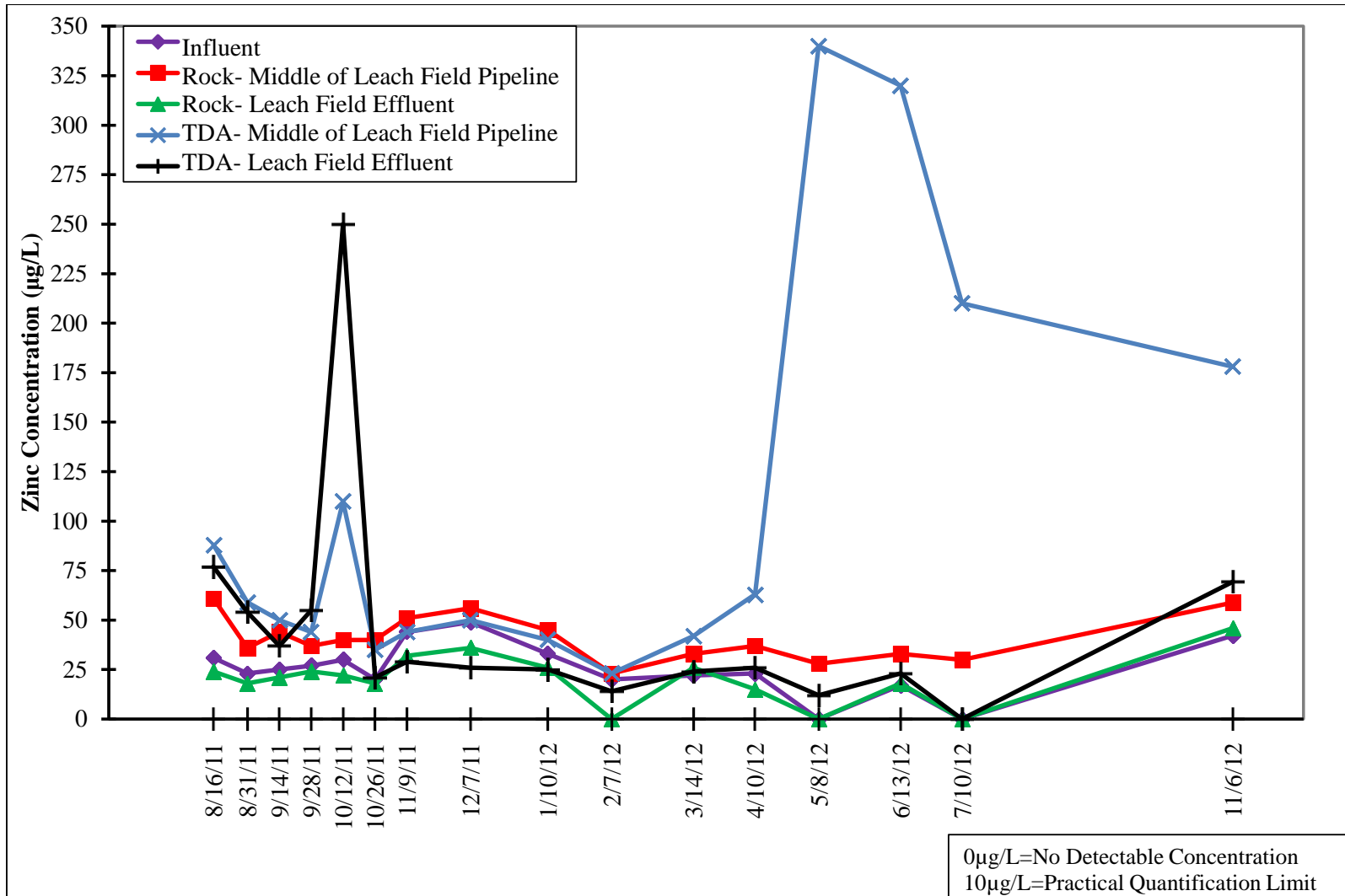


Figure C-4. Zinc concentrations in the rock and TDA leach fields.

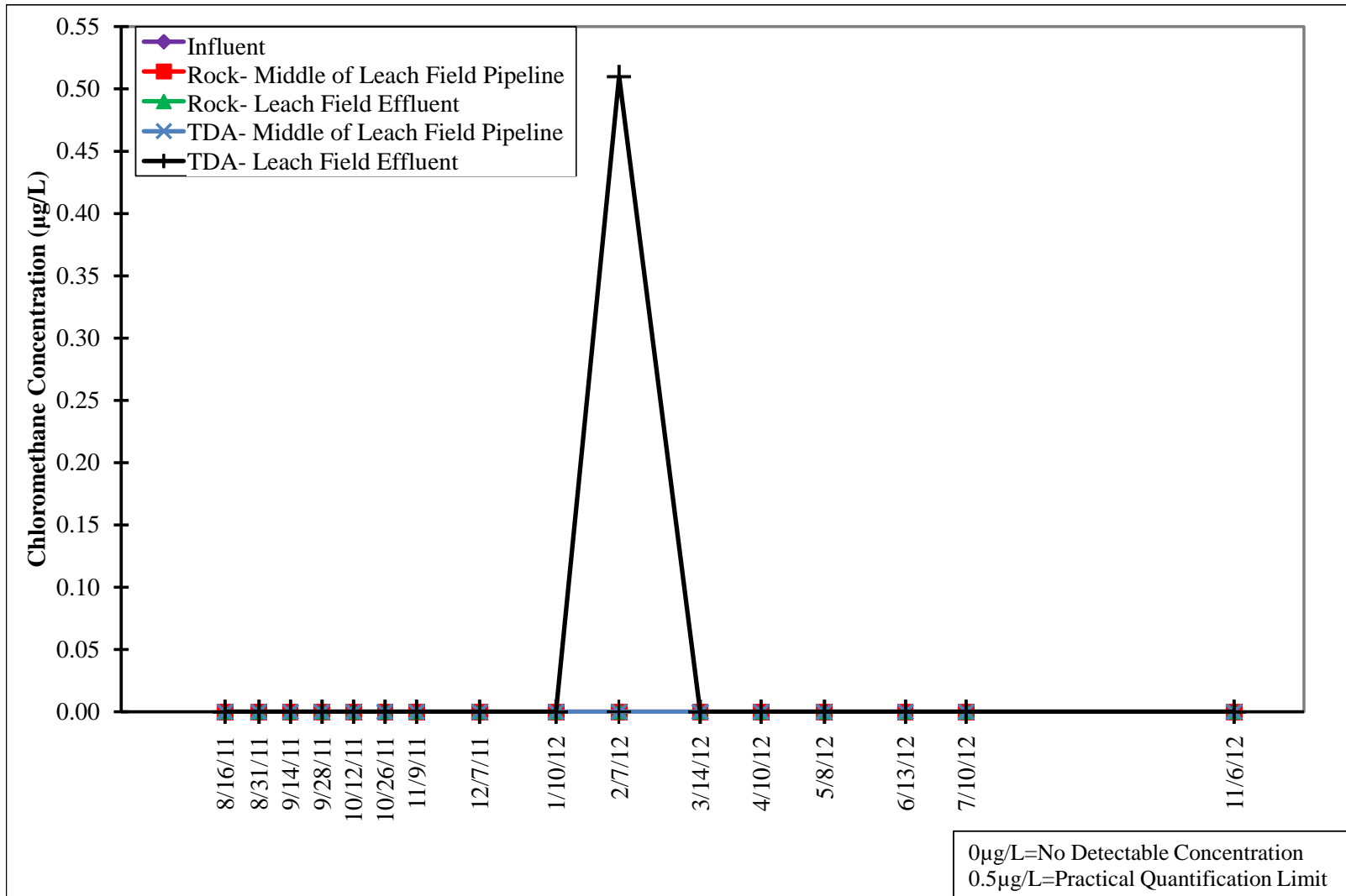


Figure C-5. Chloromethane concentrations in the rock and TDA leach fields.

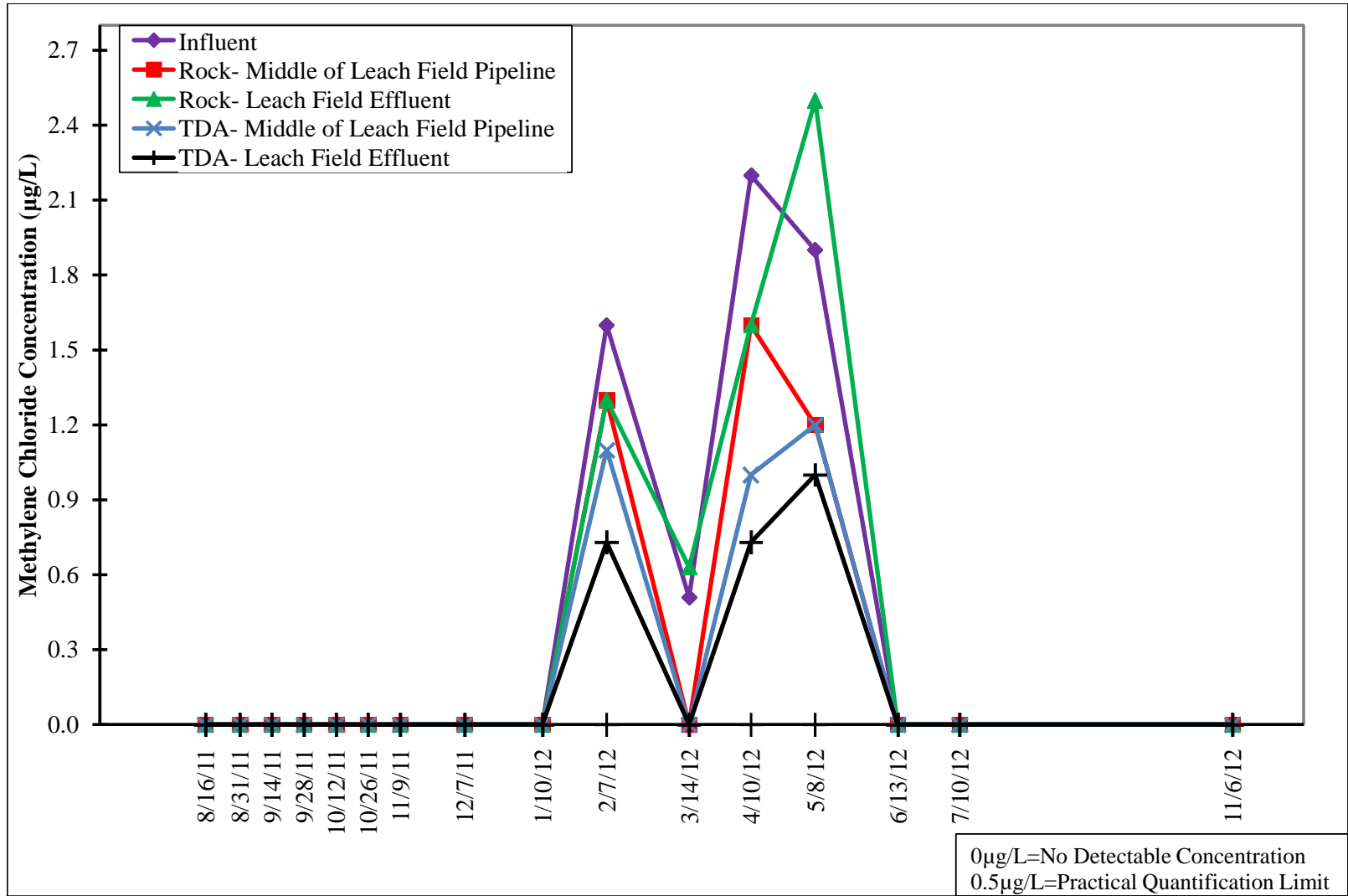


Figure C-6. Methylene Chloride concentrations in the rock and TDA leach fields.

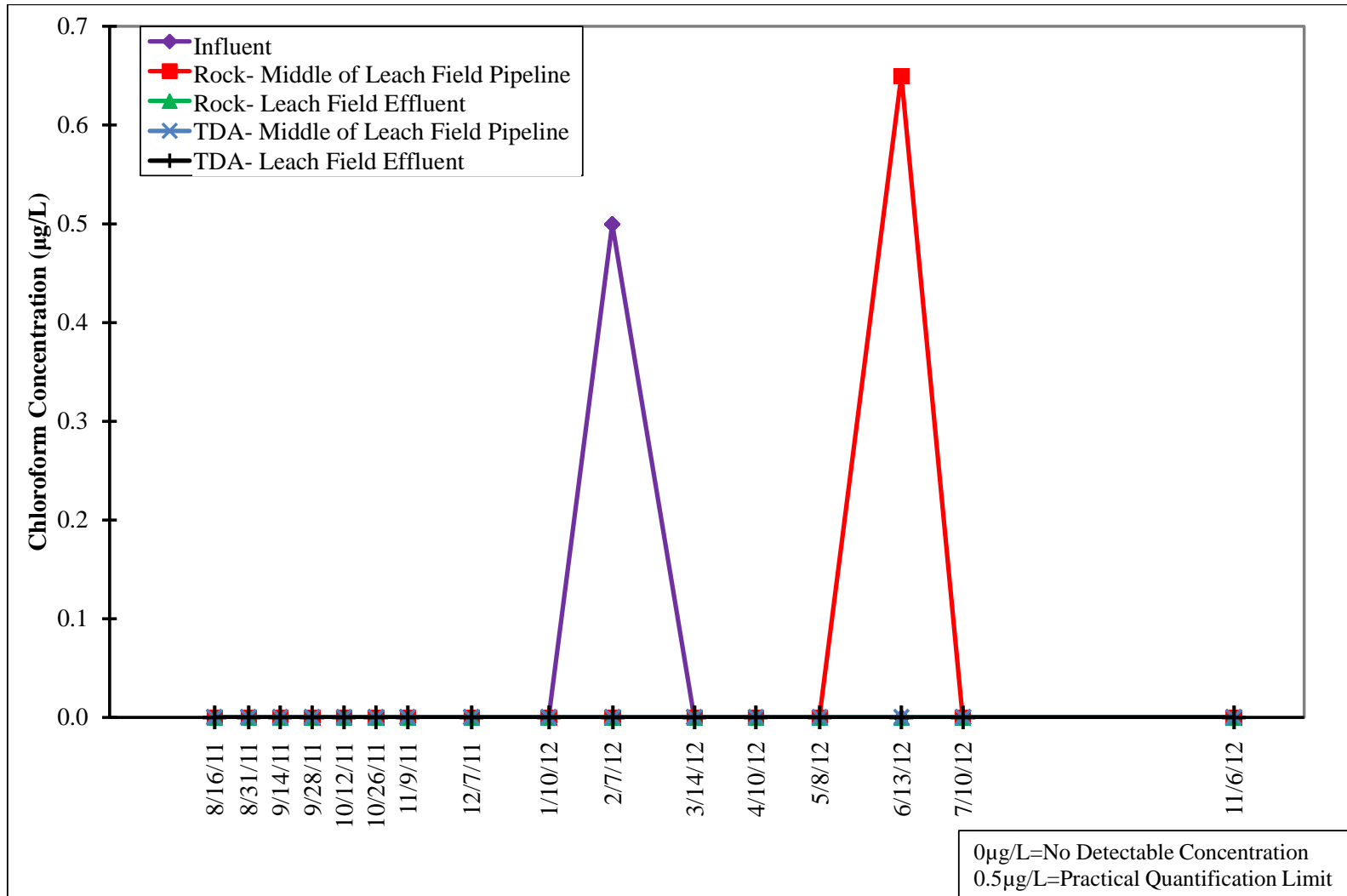


Figure C-7. Chloroform concentrations in the rock and TDA leach fields.

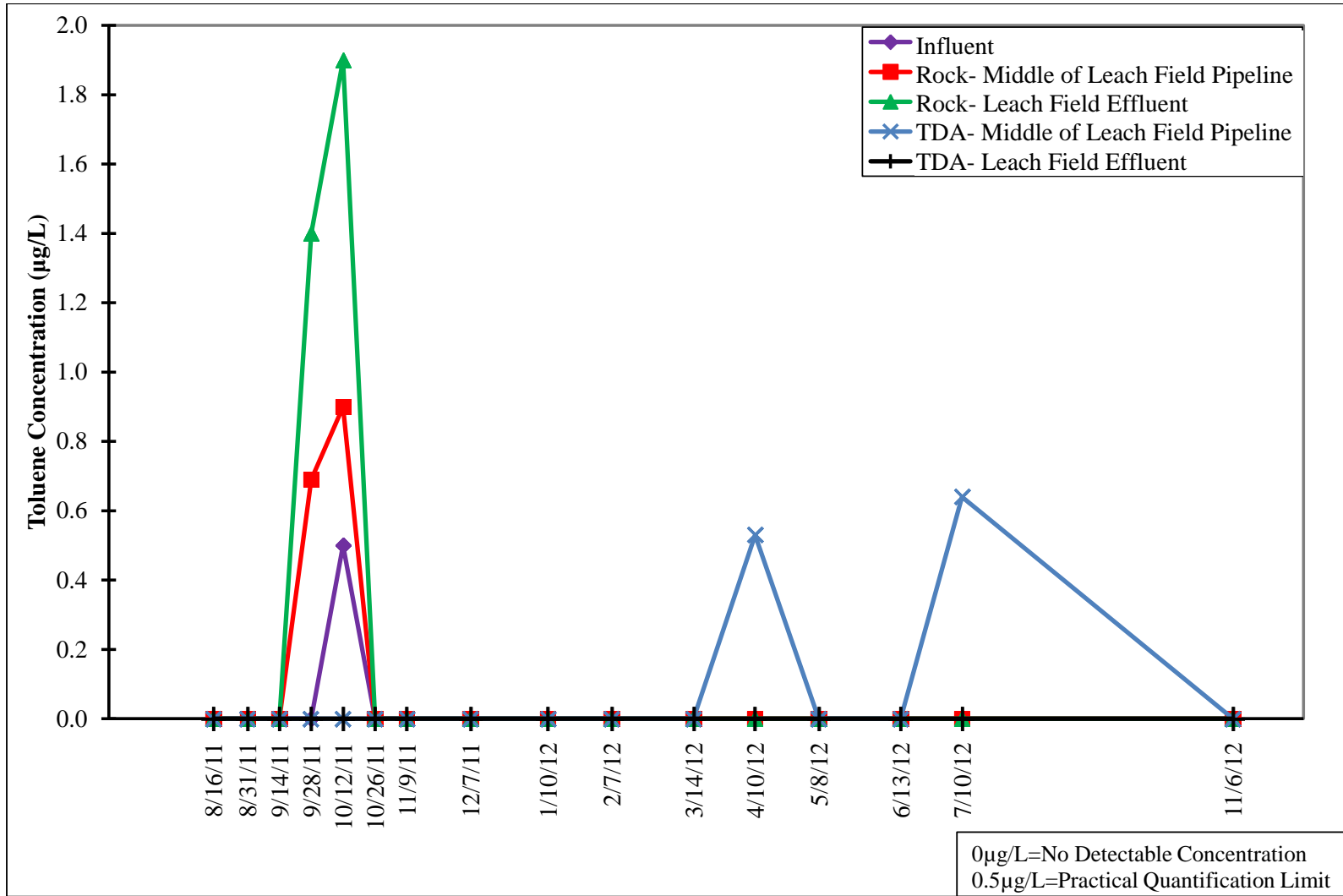


Figure C-8. Toluene concentrations in the rock and TDA leach fields.

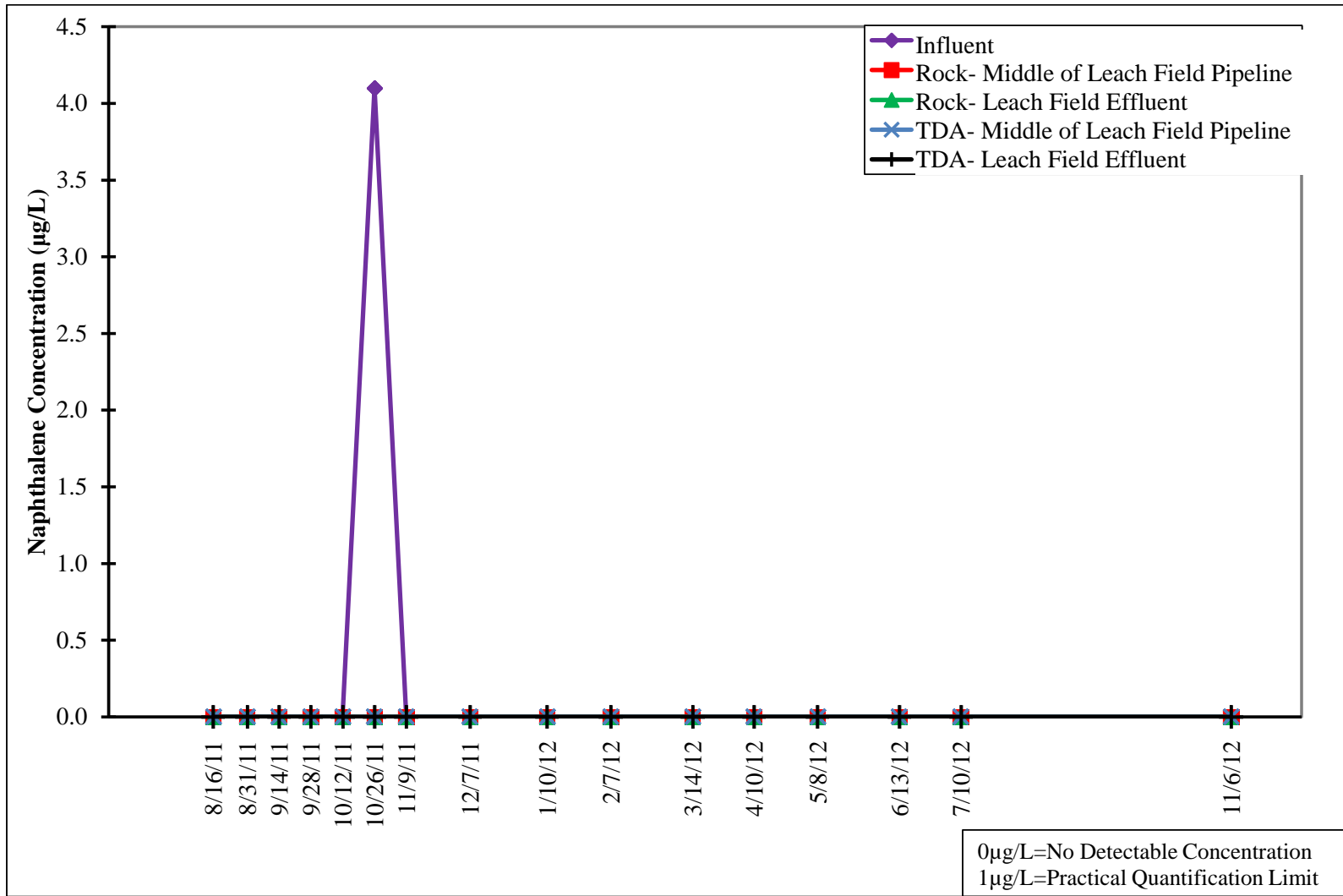


Figure C-9. Naphthalene concentrations in the rock and TDA leach fields.

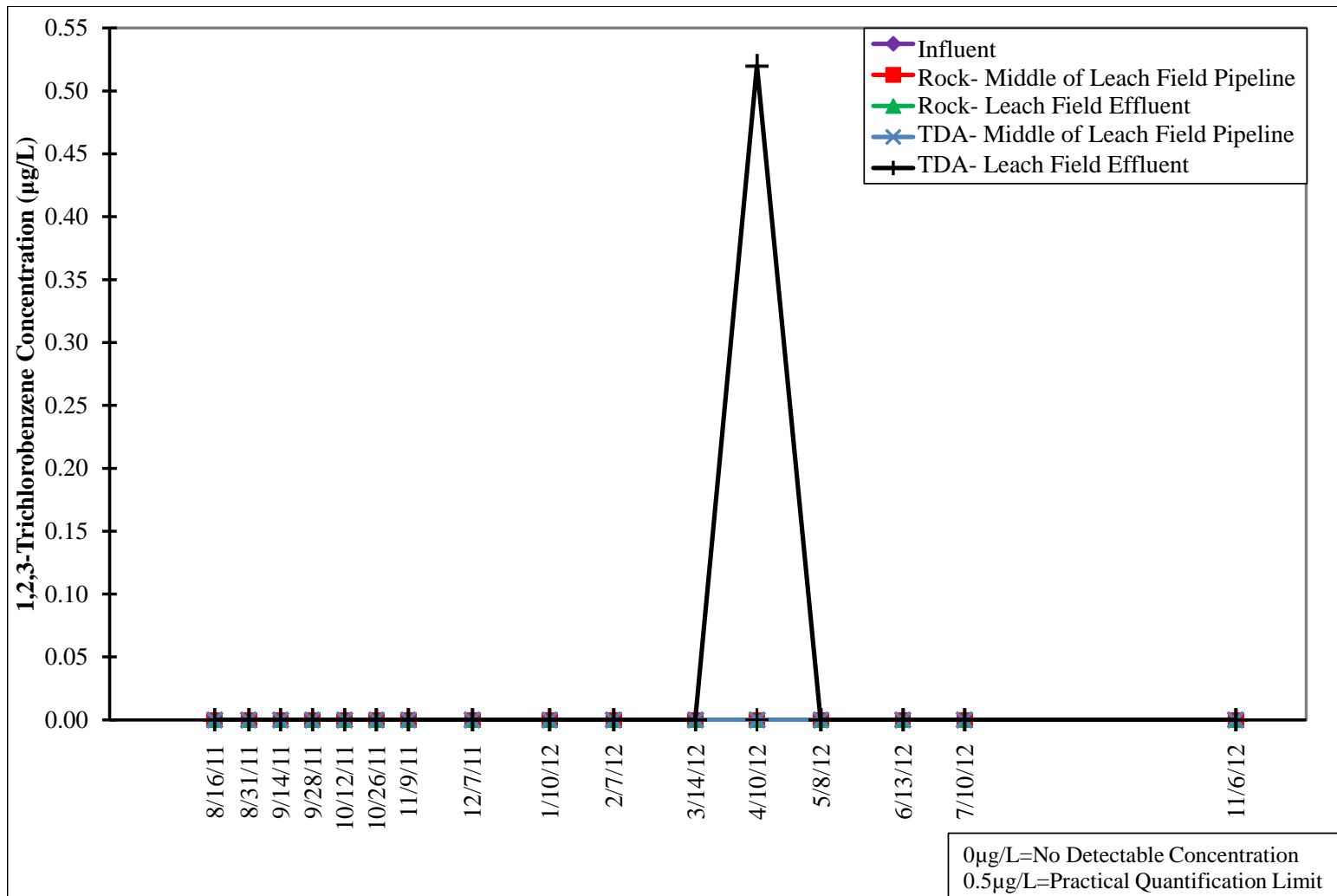


Figure C-10. Trichlorobenzene (1,2,3) concentrations in the rock and TDA leach fields.

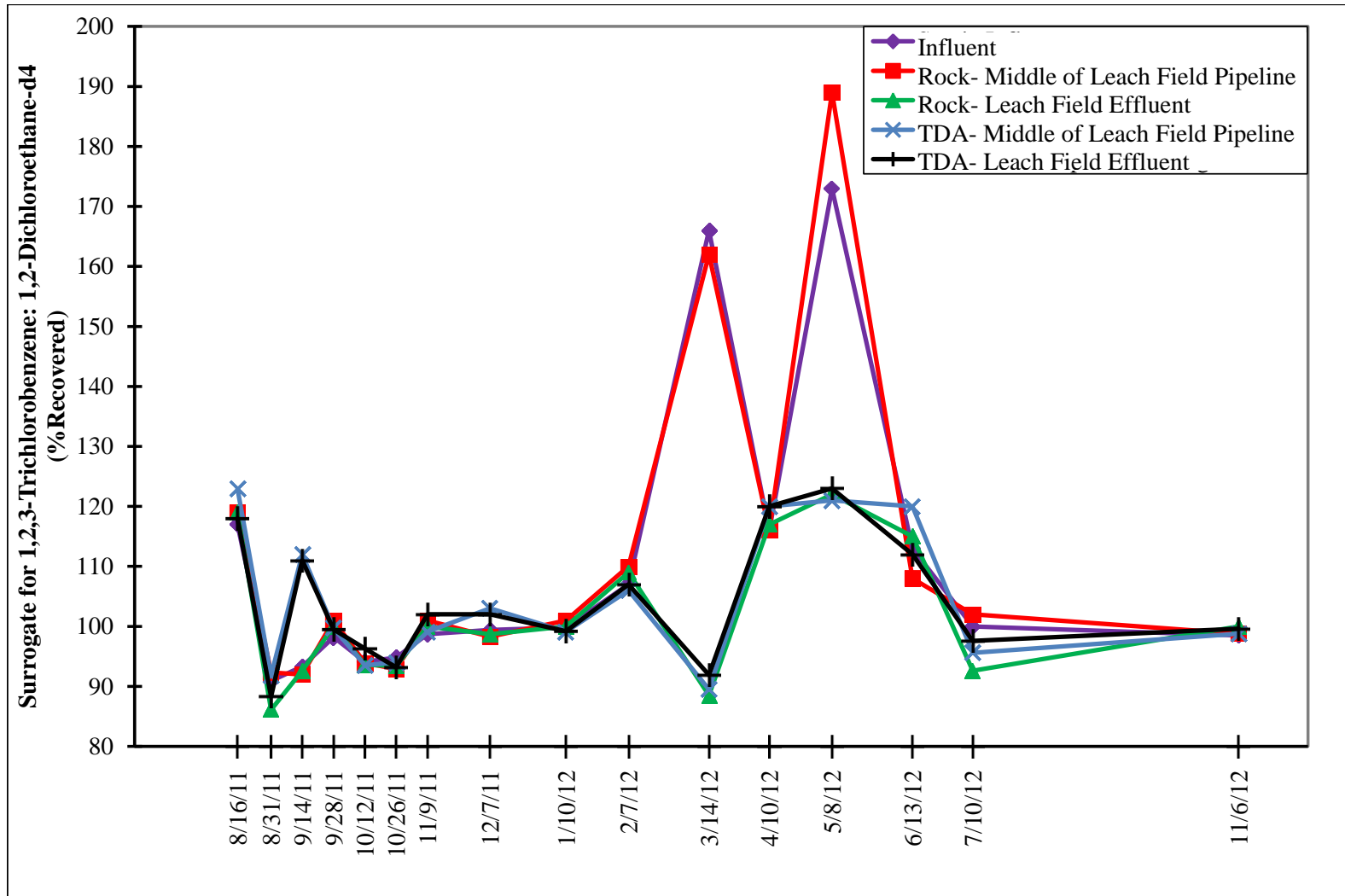


Figure C-11. Surrogate for trichlorobenzene (1,2,3): 1,2-dichloroethane-d4 concentrations in the rock and TDA leach fields..

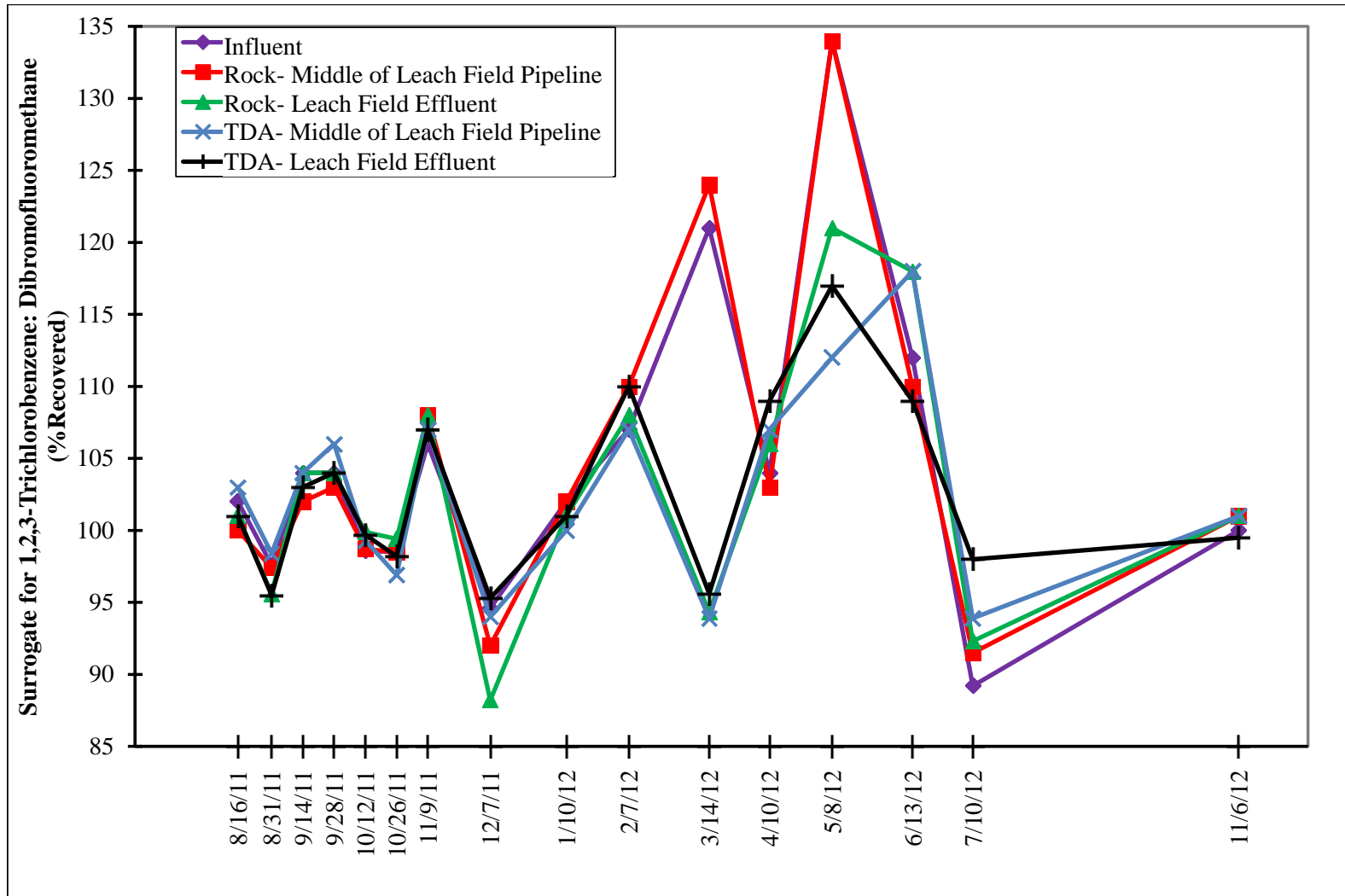


Figure C-12. Surrogate for trichlorobenzene (1,2,3): dibromofluoromethane concentrations in the rock and TDA leach fields.

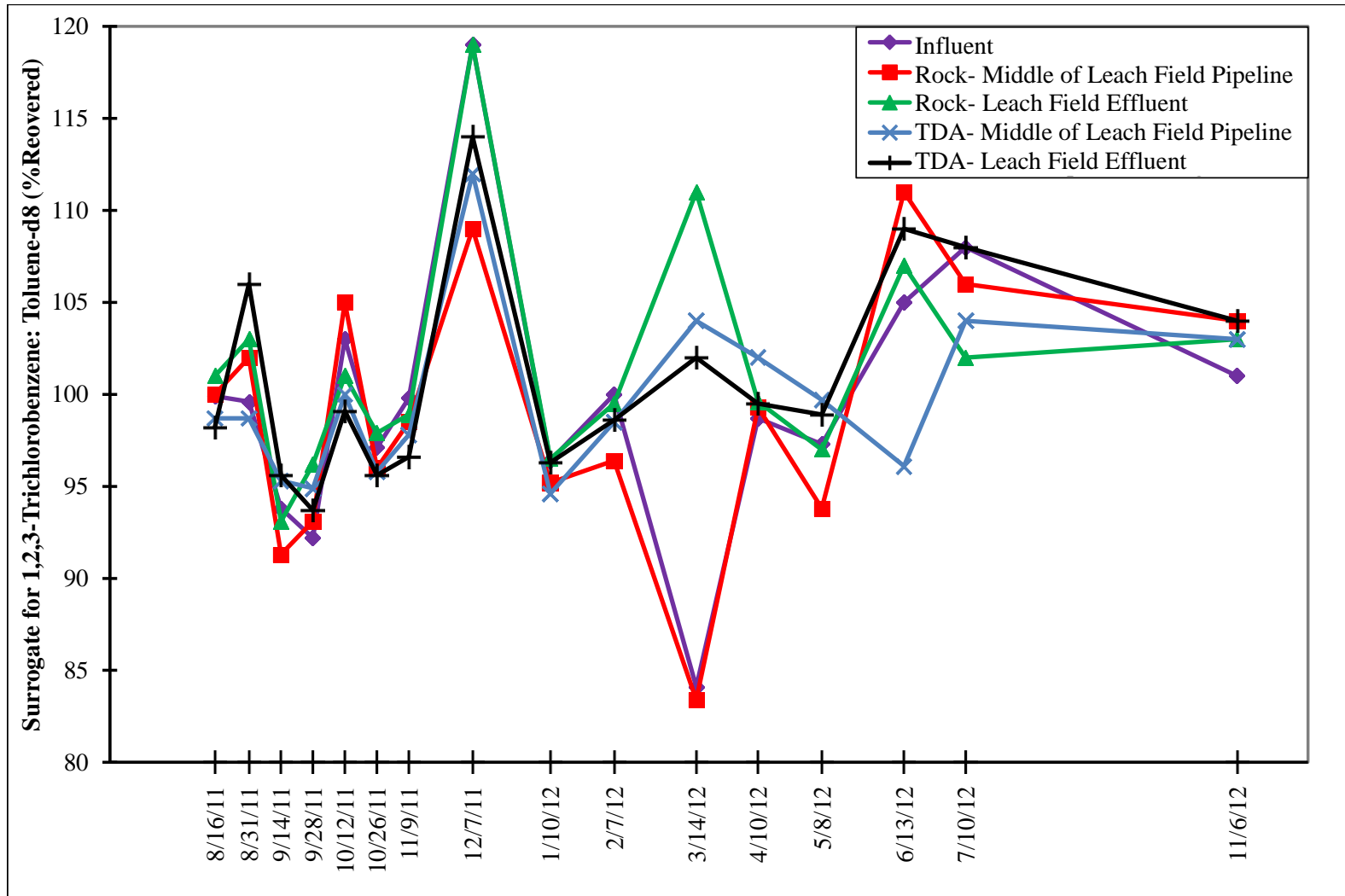


Figure C-13. Surrogate for trichlorobenzene (1,2,3): toluene-d8 concentrations in the rock and TDA leach fields.

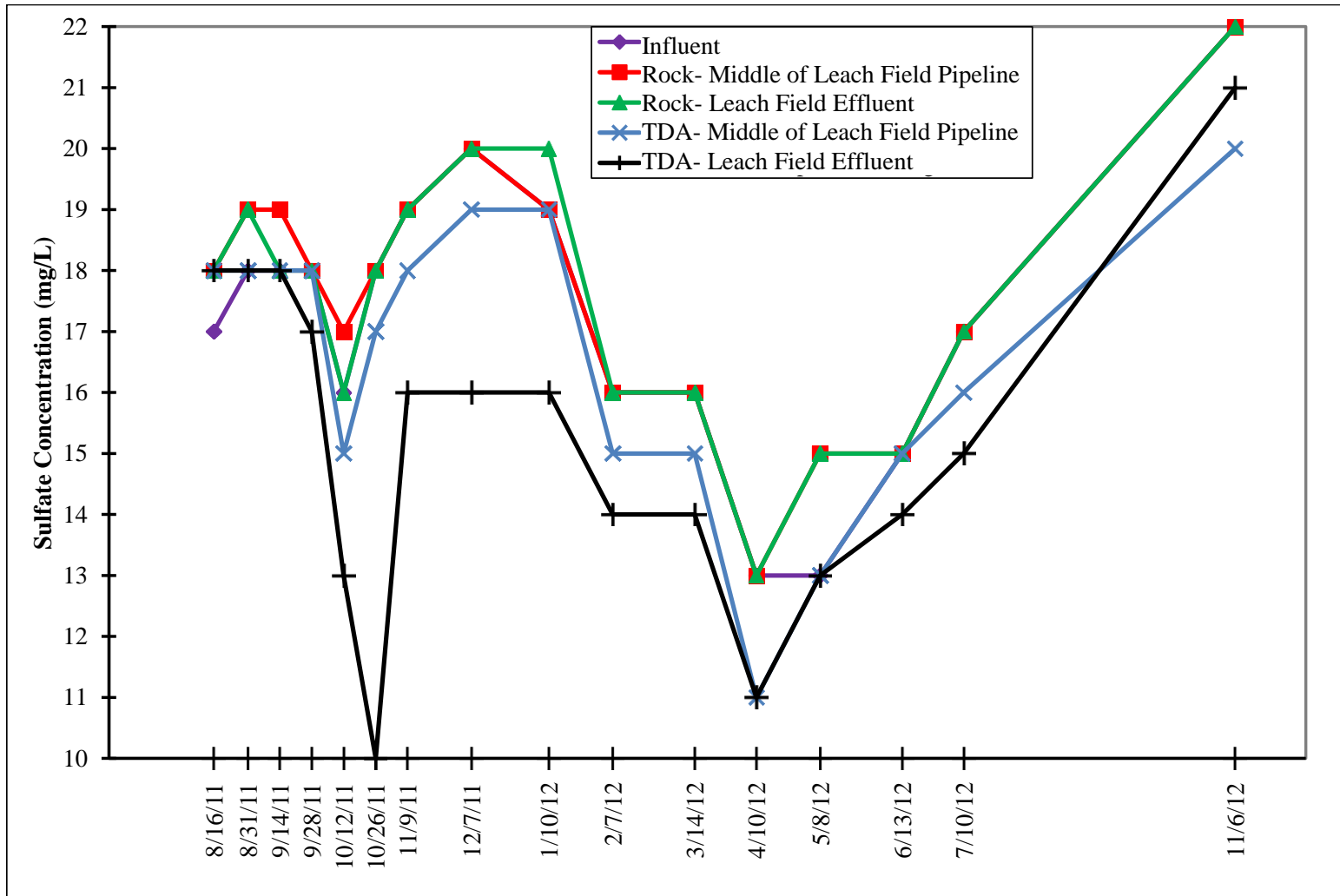


Figure C-14. Sulfate concentrations in the rock and TDA leach fields.

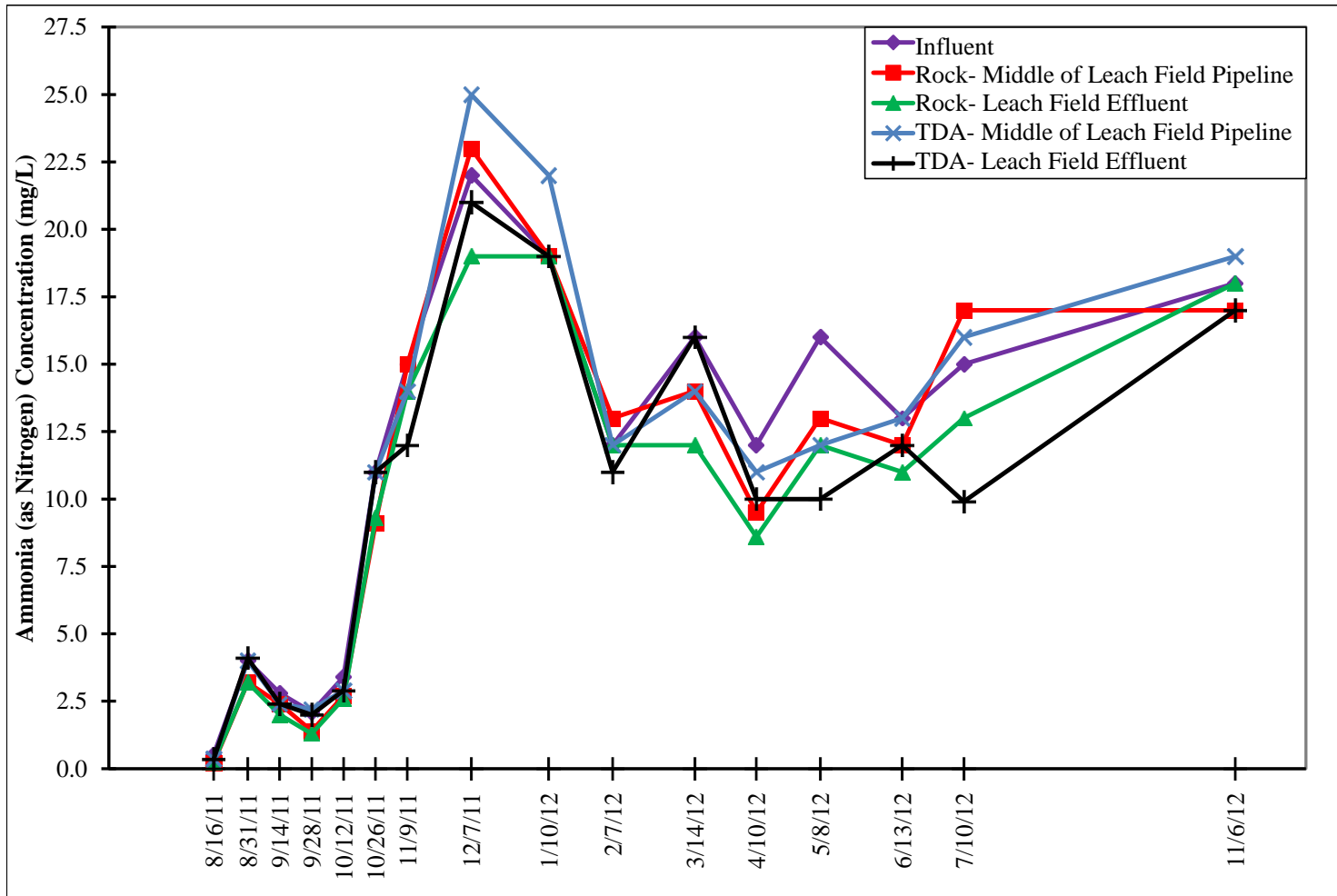


Figure C-15. Ammonia (as N) concentrations in the rock and TDA leach fields.

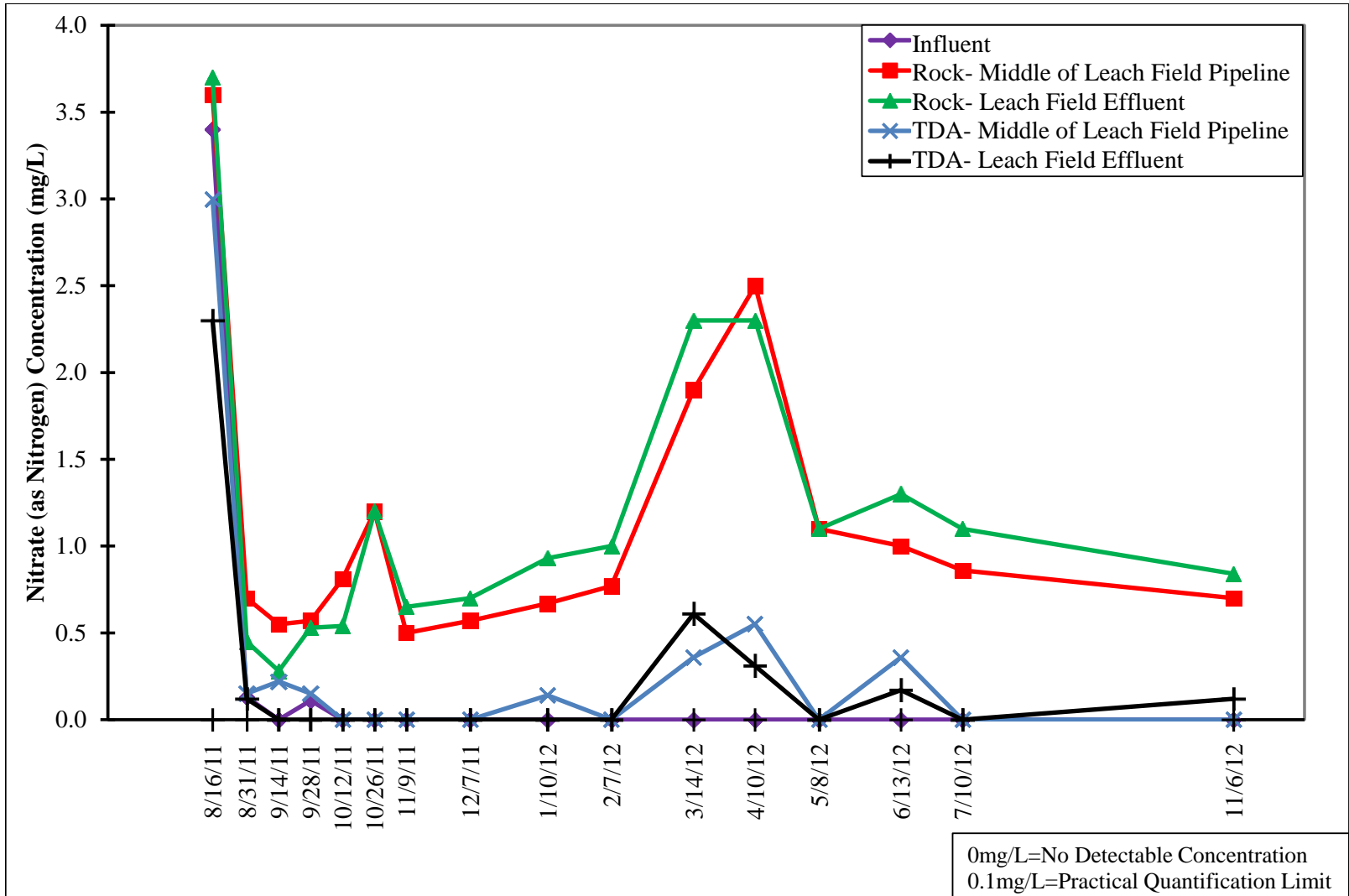


Figure C-16. Nitrate (as N) concentrations in the rock and TDA leach fields.

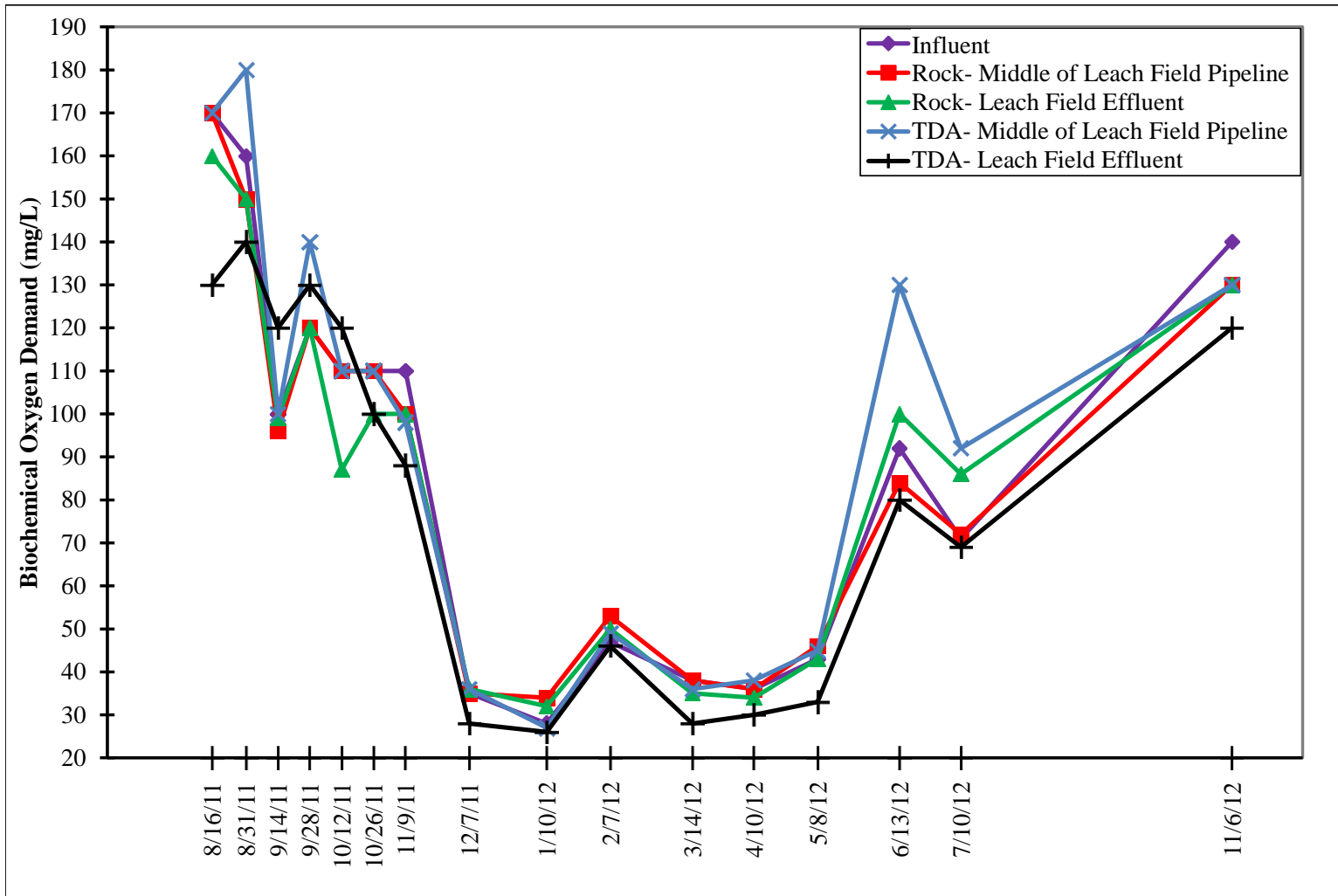


Figure C-17. BOD concentrations in the rock and TDA leach fields.

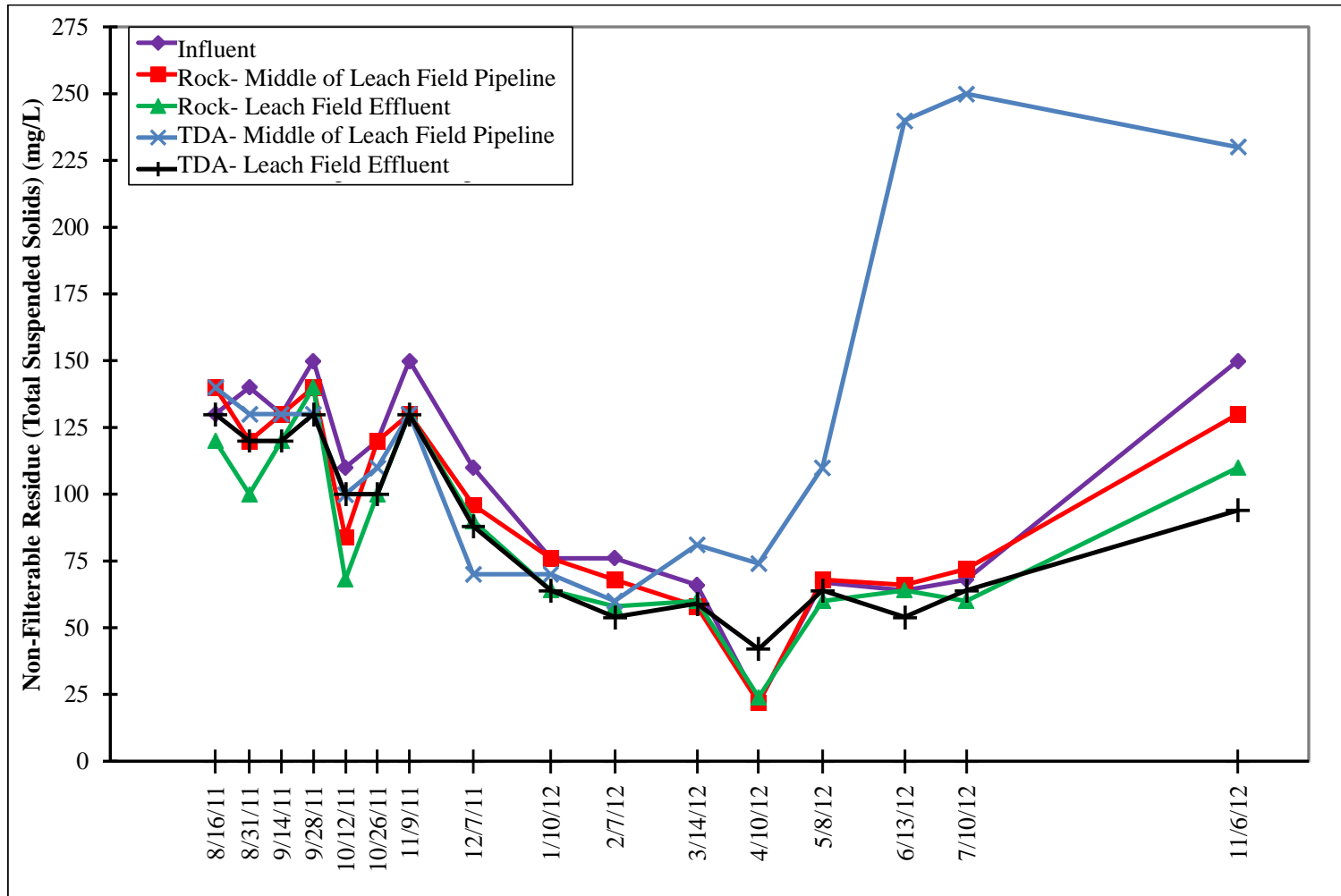


Figure C-18. Non-filterable residue concentrations in the rock and TDA leach fields.

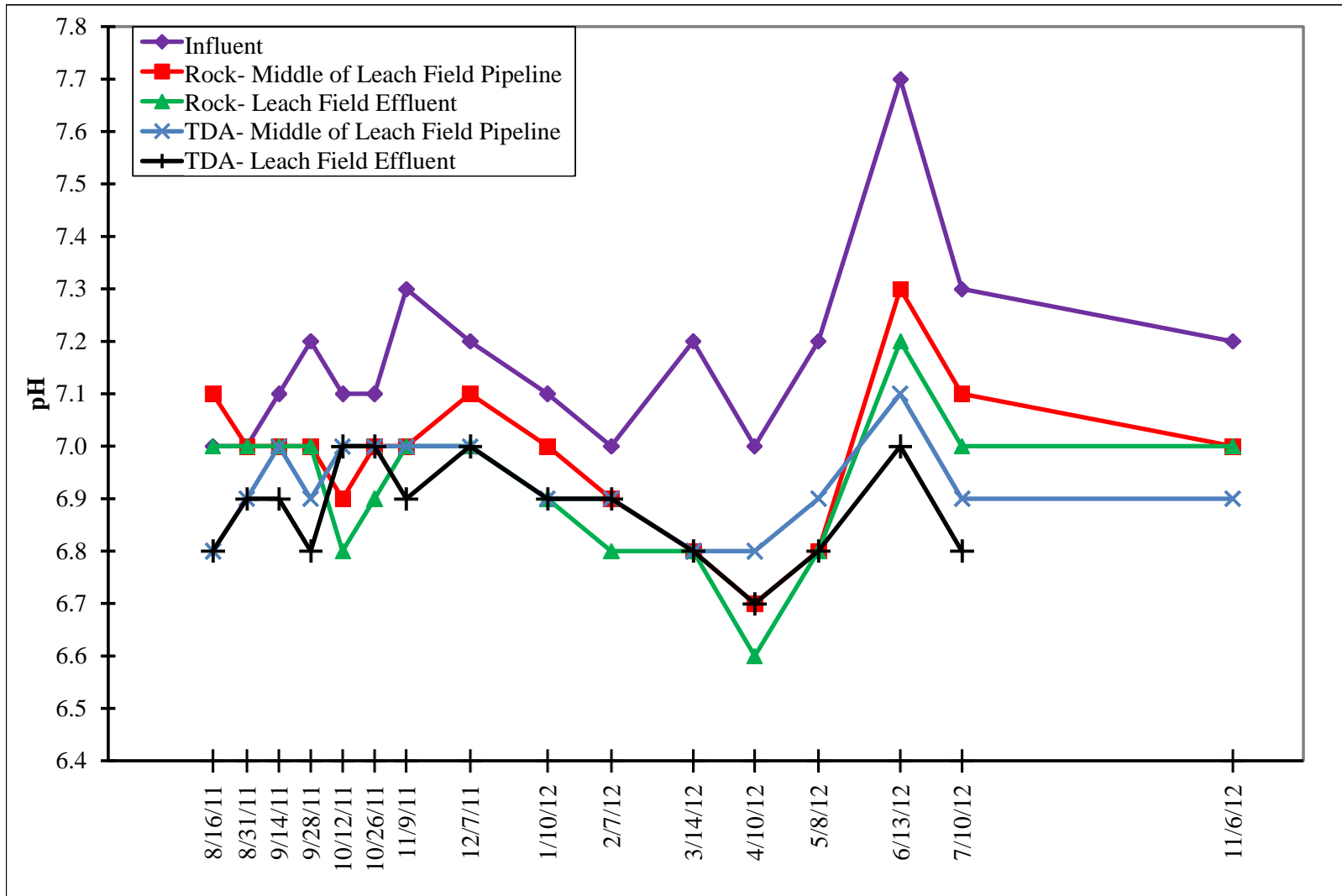


Figure C-19. pH in the rock and TDA leach fields.

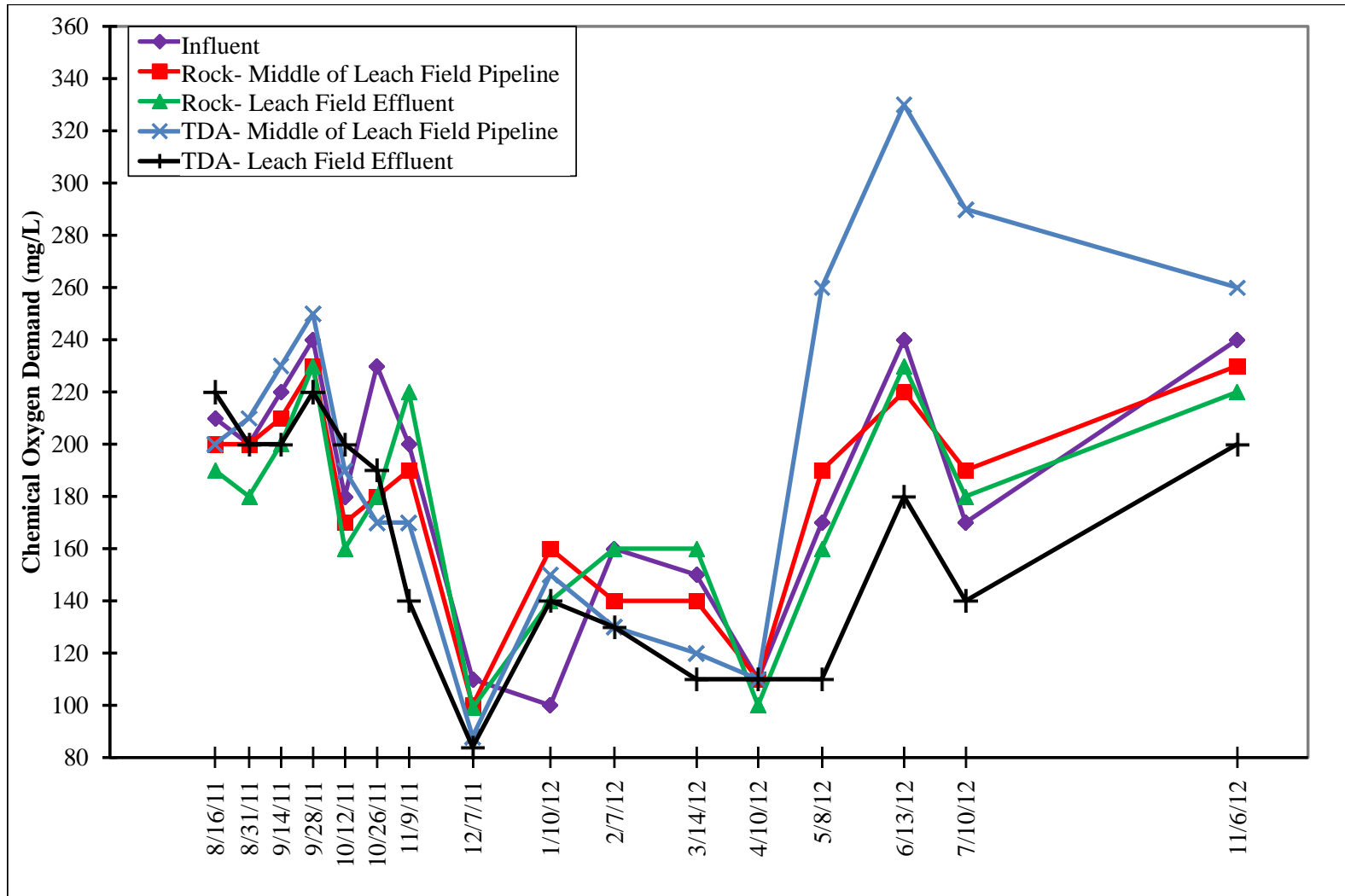


Figure C-20. COD concentrations in the rock and TDA leach fields.

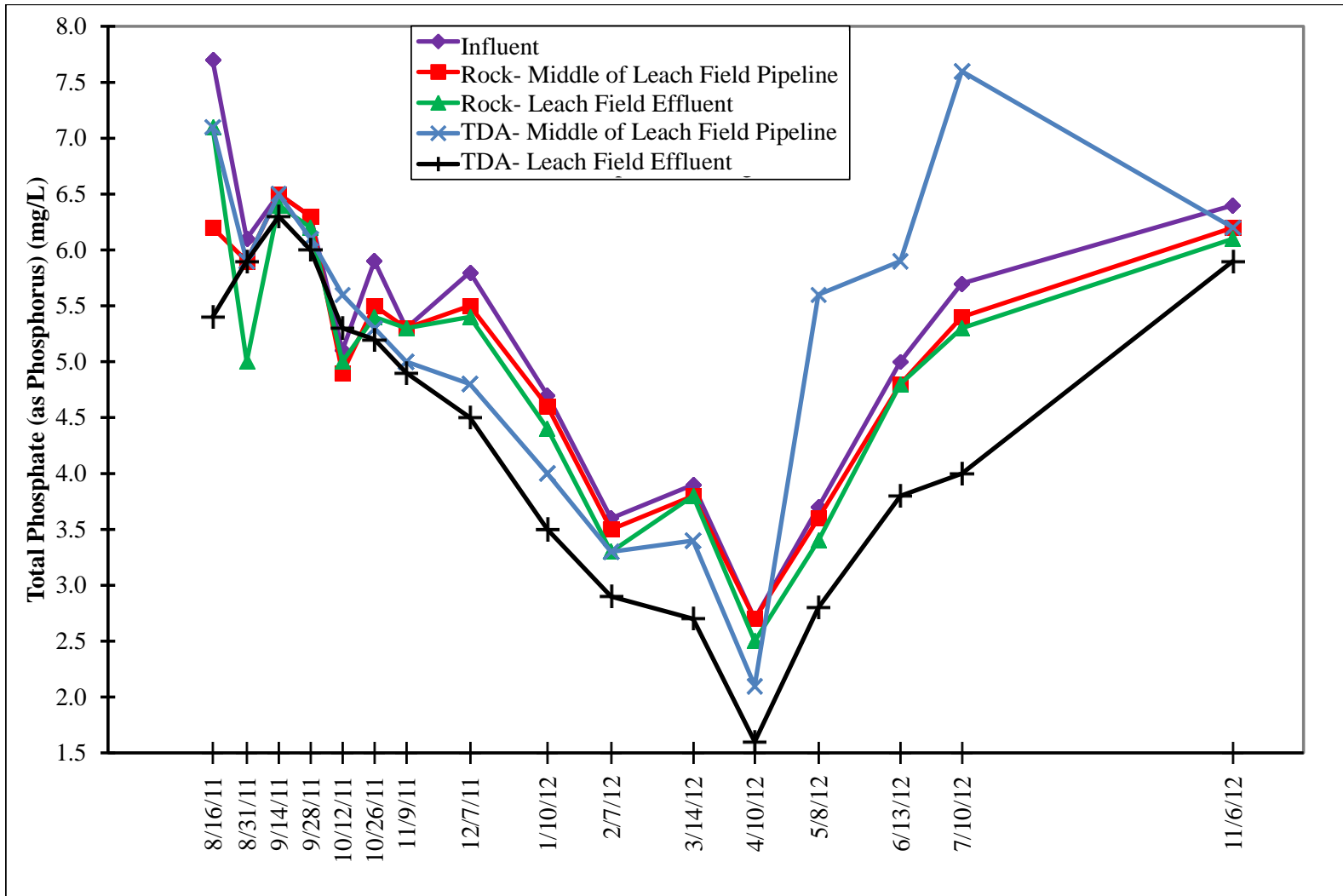


Figure C-21. Total phosphate (as P) concentrations in the rock and TDA leach fields.

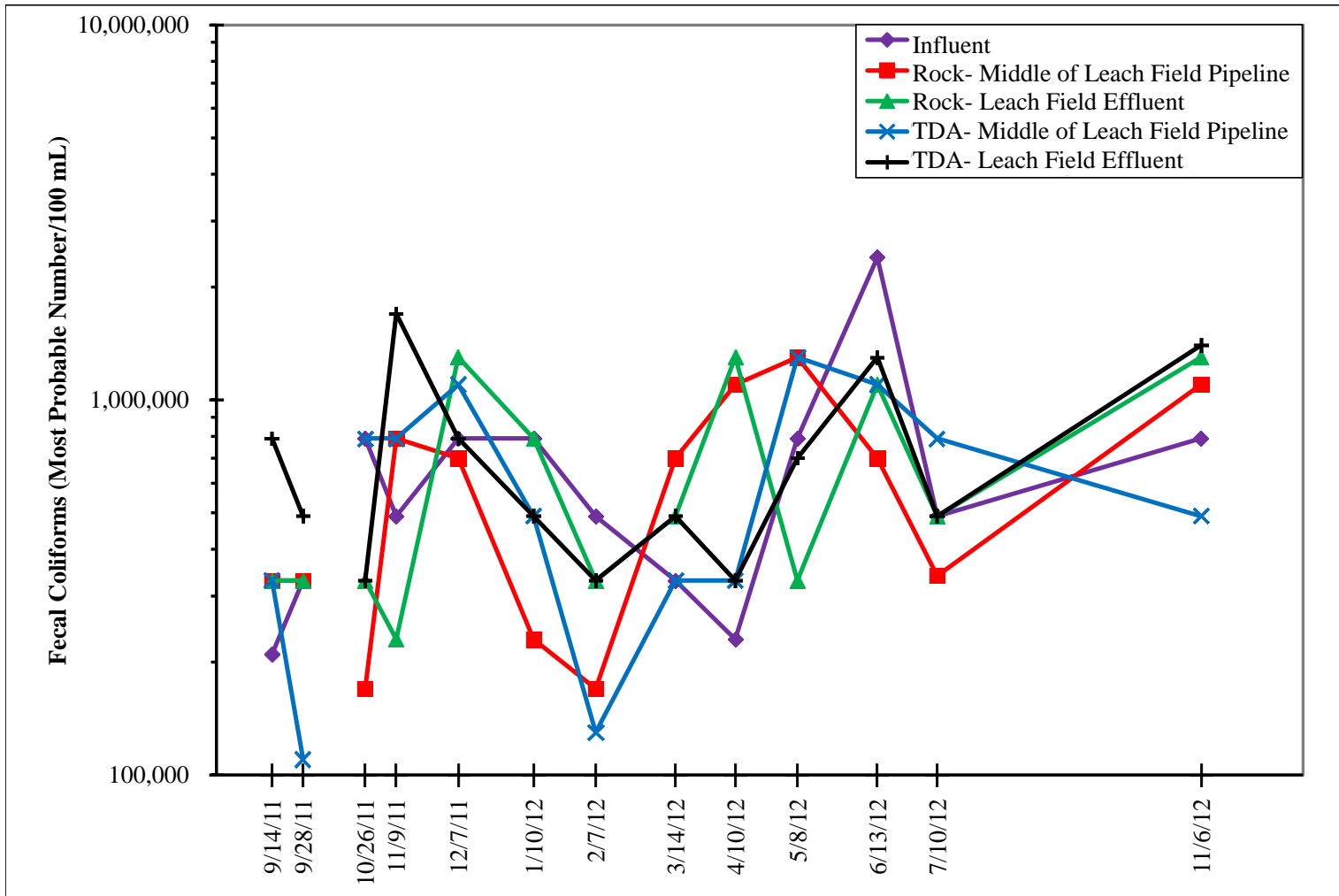


Figure C-22. Fecal coliform in the rock and TDA leach fields. Data is missing between 9/28/11 and 10/26/11 due to a laboratory dilution error.

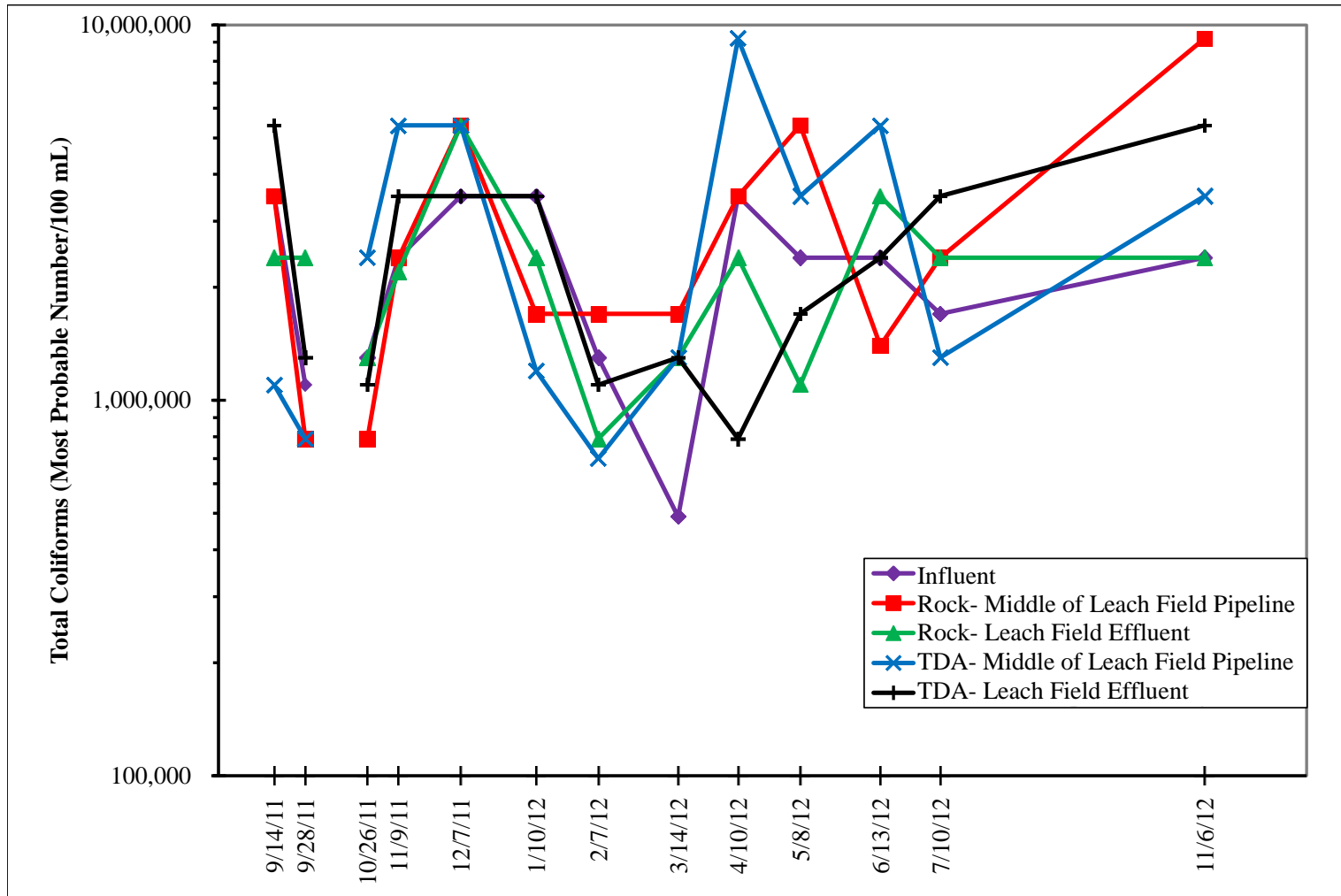


Figure C-23. Total coliform in the rock and TDA leach fields. Data is missing between 9/28/11 and 10/26/11 due to a laboratory dilution error.

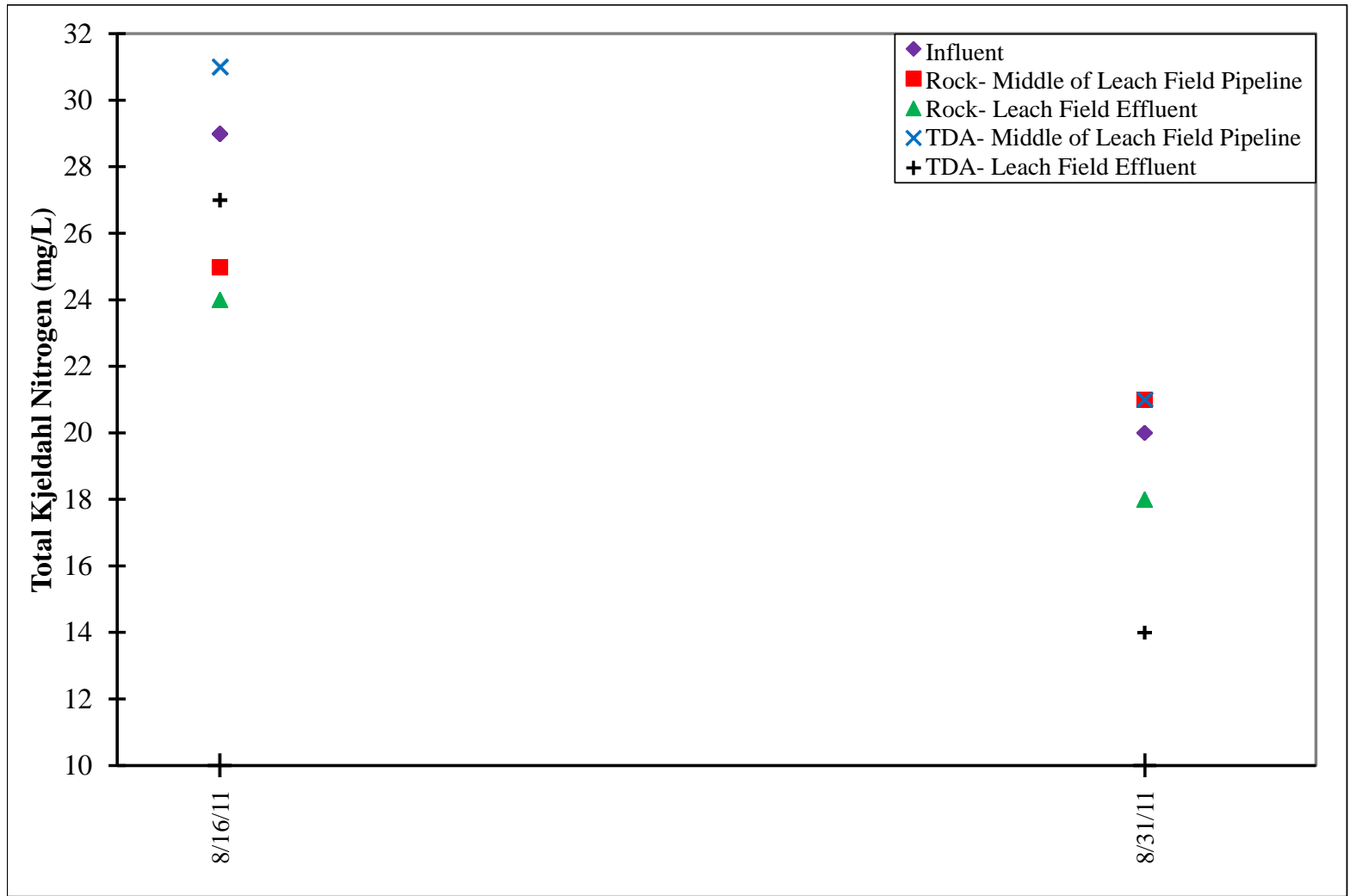
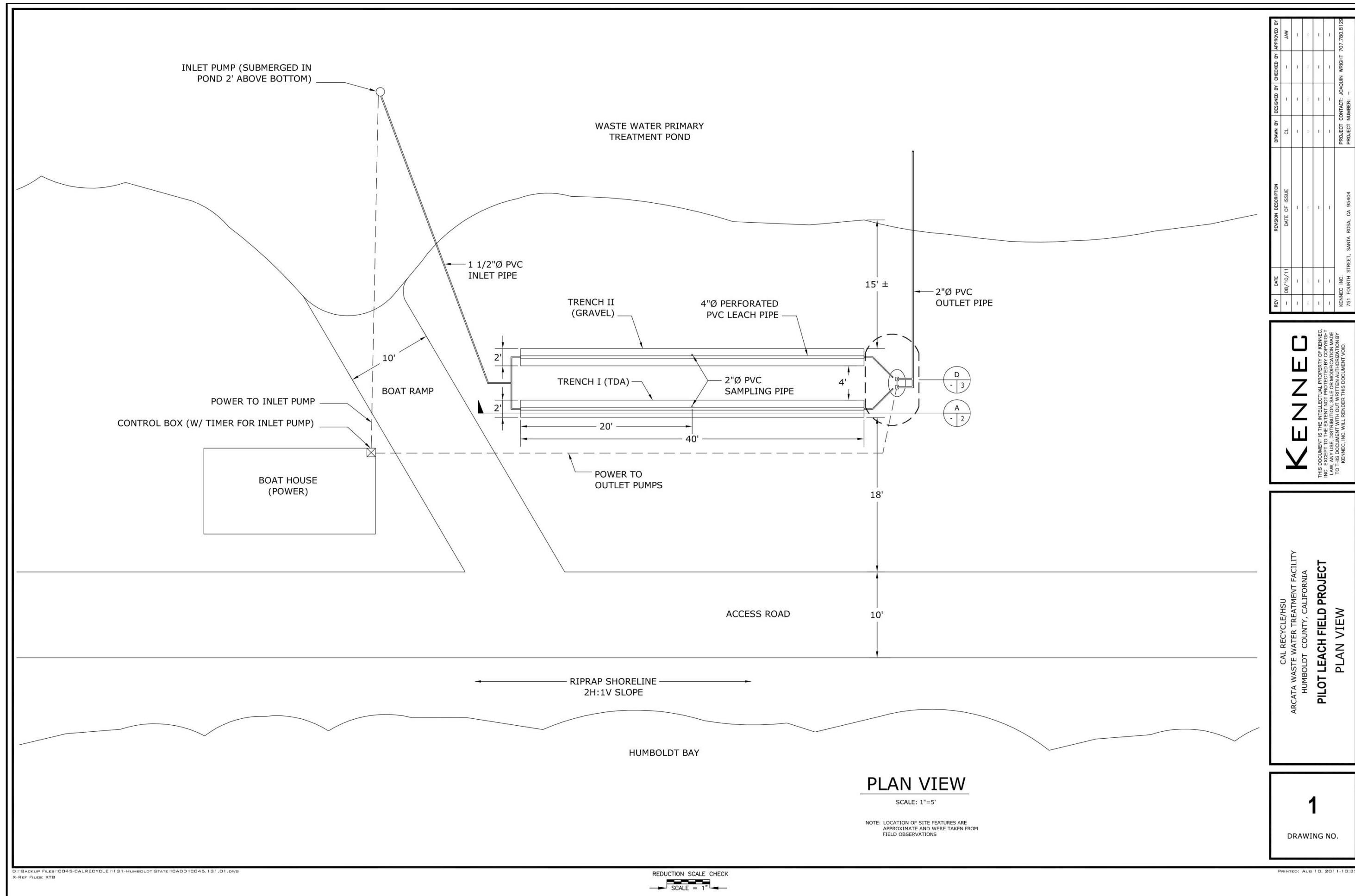


Figure C-24. Total Kjeldahl nitrogen concentrations in the rock and TDA leach fields.

Appendix D: Computer Aided Design Drawings

Computer aided drawings were created for constructing the leach fields and the temperature tower filled with type A TDA. This appendix shows the detailed as-built drawings for the leach fields (Figures D-1 through D-3) and for the TDA-filled tower (D-4 through D-5).

This page is intentionally left blank.



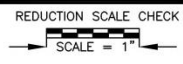
REV	DATE	REVISION DESCRIPTION	DESIGNED BY	CHECKED BY	APPROVED BY
08/10/11			CL		JAW

KENNEC
 THIS DOCUMENT IS THE INTELLECTUAL PROPERTY OF KENNEC. IT IS NOT TO BE REPRODUCED, COPIED, OR TRANSMITTED IN ANY FORM OR BY ANY MEANS, ELECTRONIC OR MECHANICAL, WITHOUT THE WRITTEN AUTHORIZATION OF KENNEC. ANY USE, DISTRIBUTION, SALE OR MODIFICATION MADE TO THIS DOCUMENT WITHOUT WRITTEN AUTHORIZATION BY KENNEC, INC. WILL RENDER THIS DOCUMENT VOID.

CAL RECYCLE/HSU
 ARCATA WASTE WATER TREATMENT FACILITY
 HUMBOLDT COUNTY, CALIFORNIA
PILOT LEACH FIELD PROJECT
PLAN VIEW

1
 DRAWING NO.

3:\Backup Files\0045-CALRECYCLE\131-HUMBOLDT\STATE\CADD\0045_131_01.dwg
 X-Ref File: XYB



Printed: Aug 10, 2011 10:35AM

Figure D-1. Plan view of the rock and tire-derived aggregate leach fields (Wright, 2011).

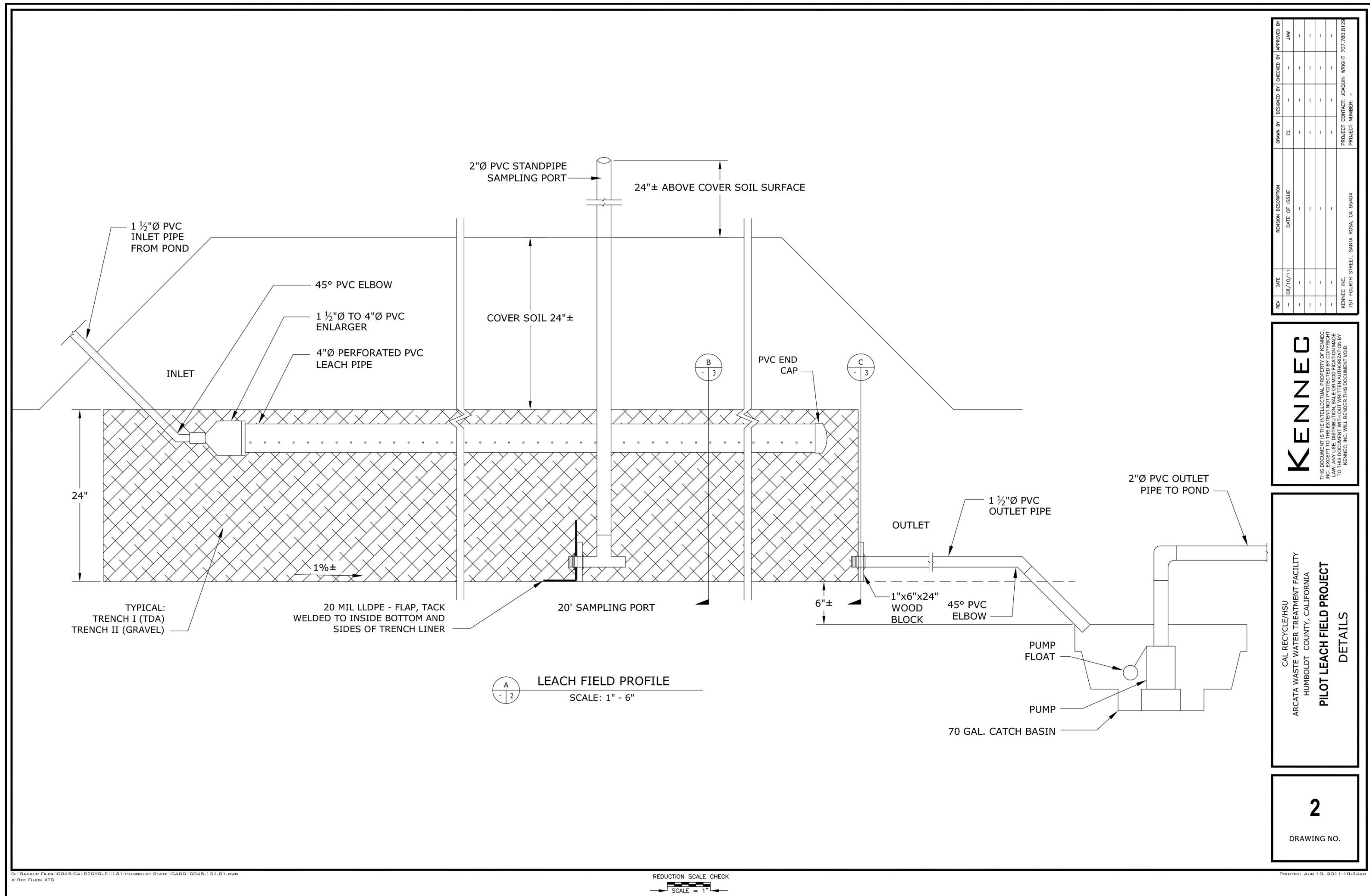


Figure D-2. Side view of the rock and TDA leach fields (Wright, 2011).

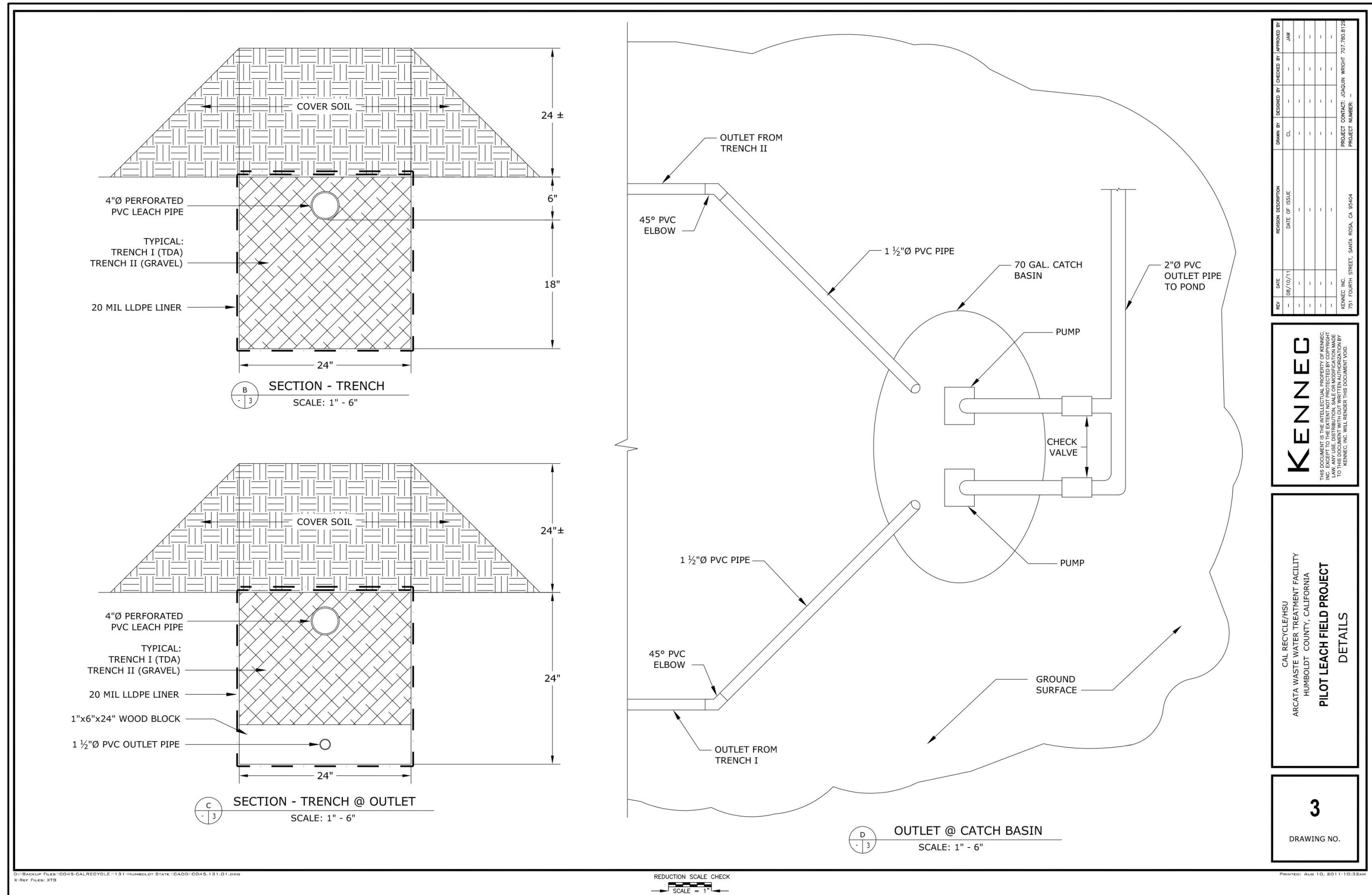


Figure D-3. Cross-sectional and plan view of the effluent setup for rock TDA leach fields (Wright, 2011).

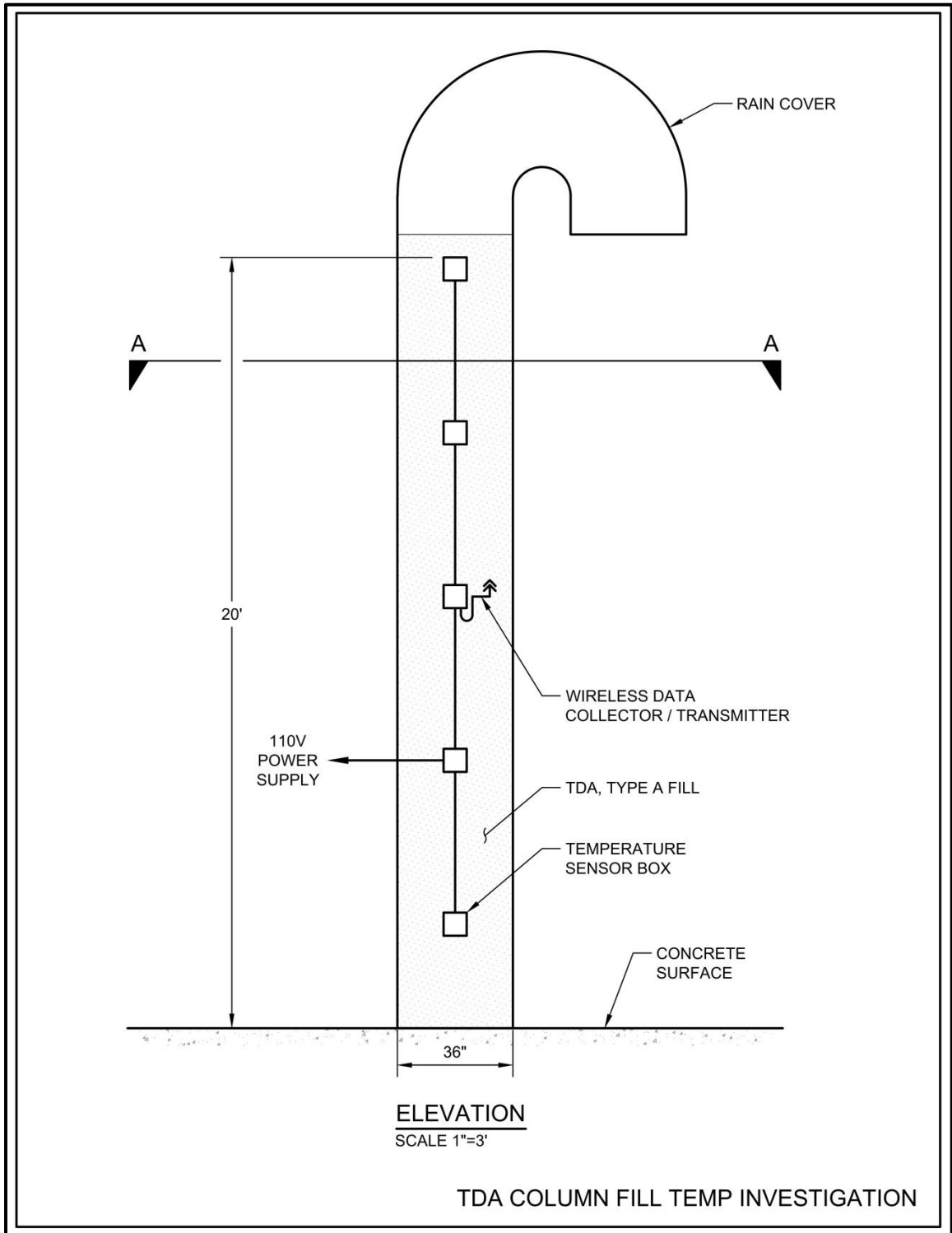


Figure D-4. Side view of the tower containing type A TDA (Wright, 2011).

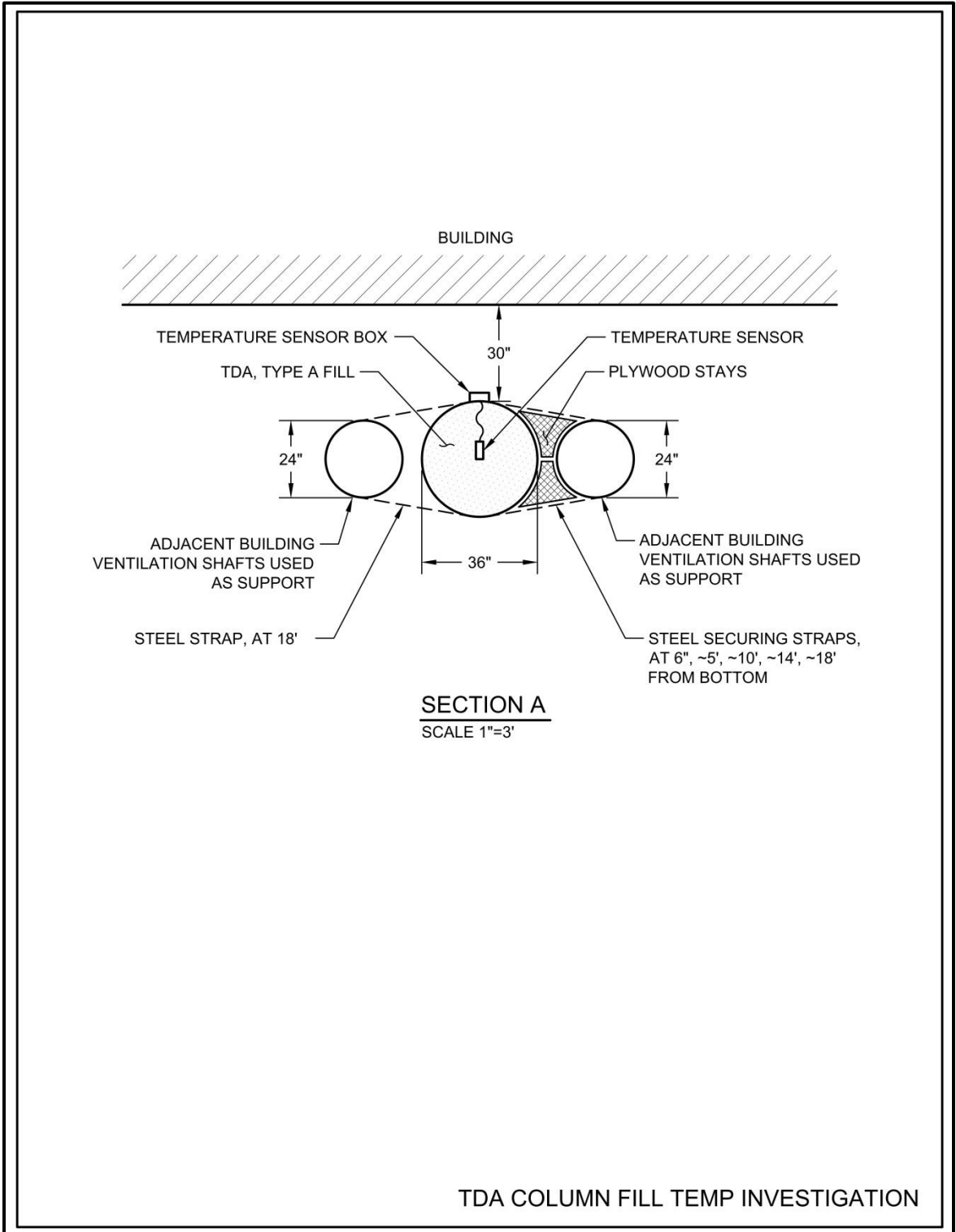


Figure D-5. Plan view of the tower containing type A TDA (Wright, 2011)

Appendix E: Temperature Results From TDA Pit

The temperature of TDA placed in an earthen pit within 12 hours of being produced was recorded for a five month period. Figure E-1 is the native soil and ambient temperature conditions at the experimental site. Figure E-2 through E-8 show temperature plots for depths ranging from 1.3 ft. to 9 ft. below the surface. Precipitation accumulations in the experimental area are plotted alongside the temperature results to determine if any significant impact occurred due to this environmental condition. For experimental setup conditions refer to Figure 11 (on page 24).

This page is intentionally left blank.

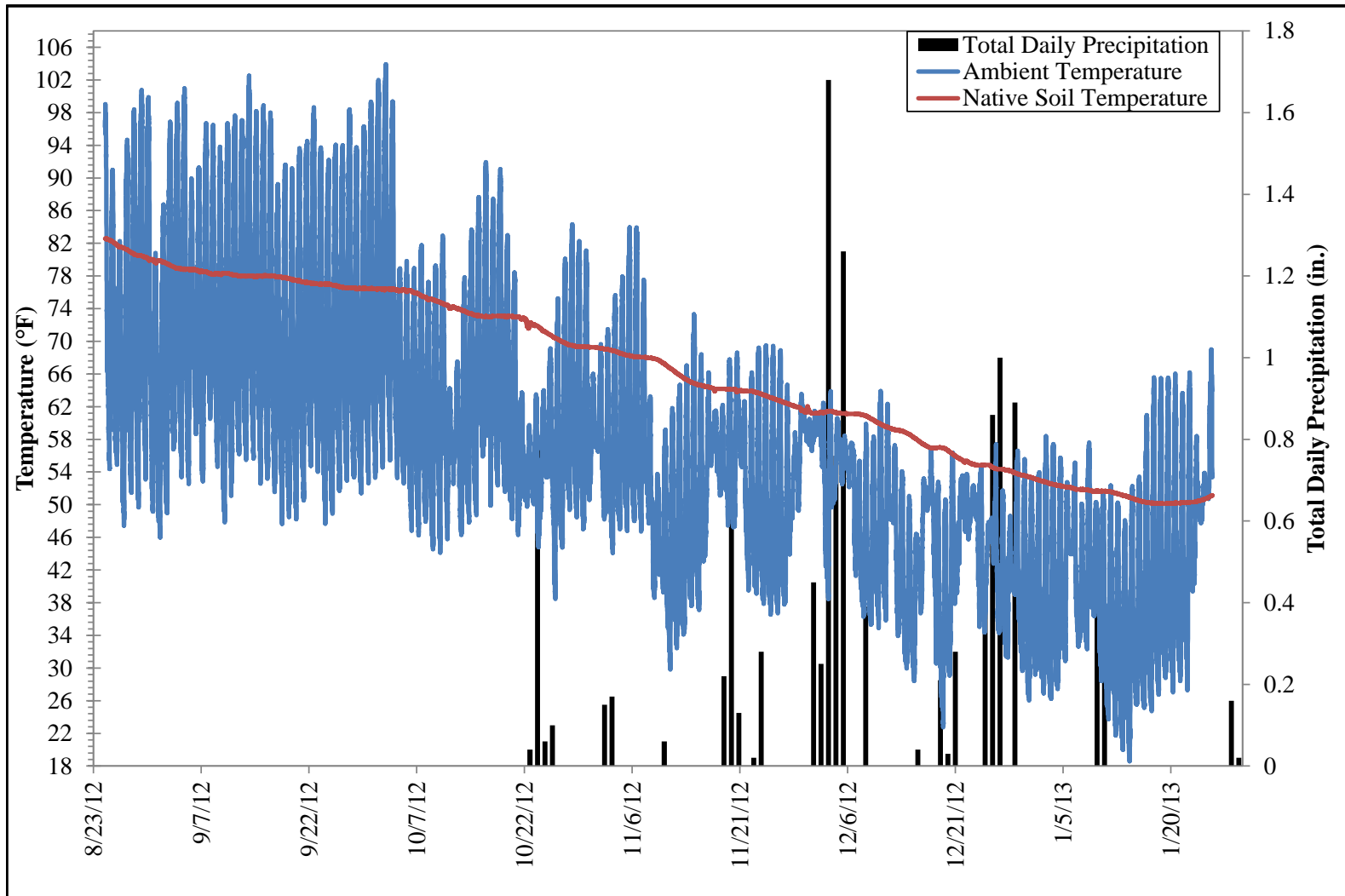


Figure E-1. Native soil and ambient temperatures for the Keifer landfill.

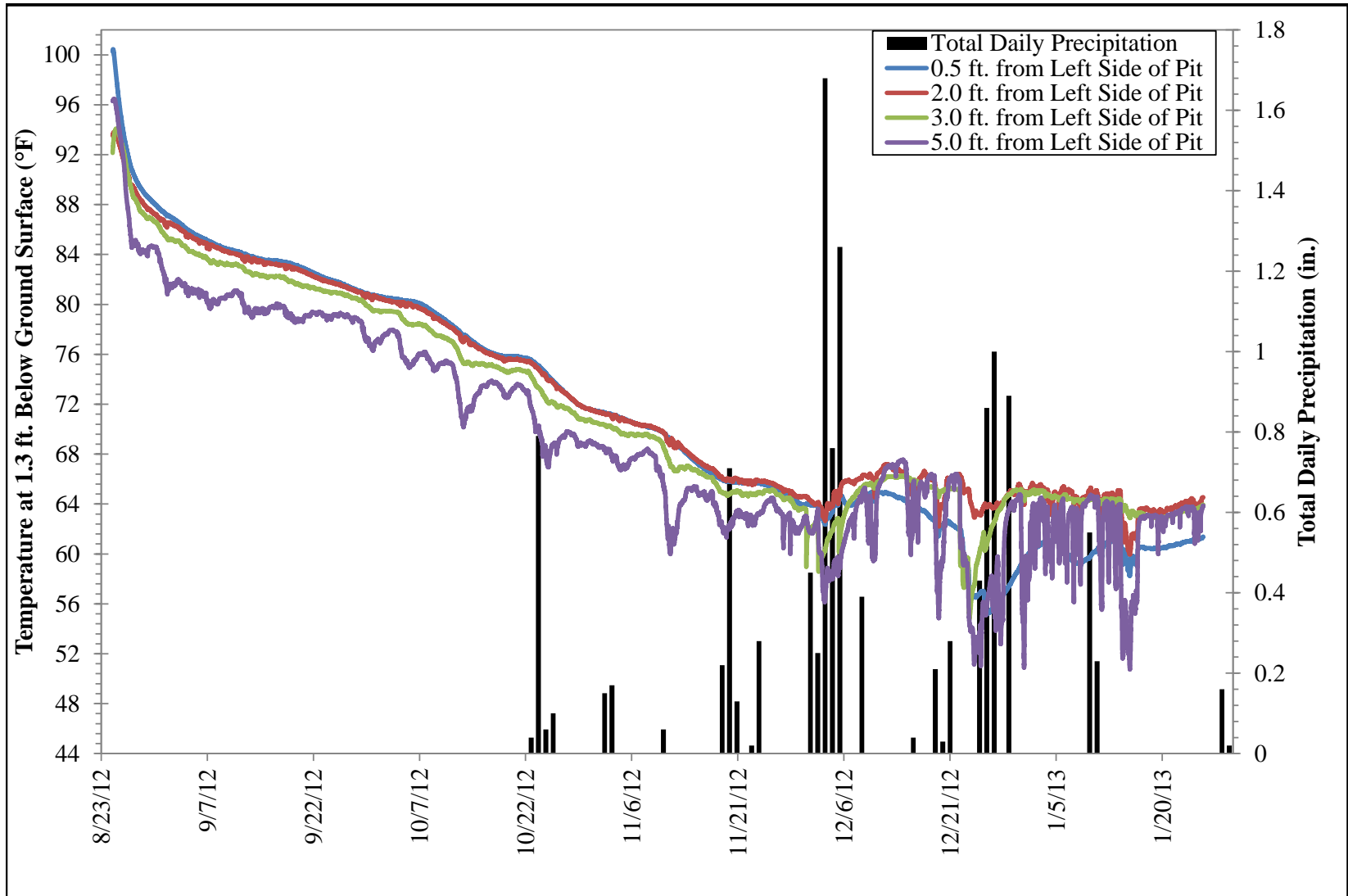


Figure E-2. Temperatures at 1.3 ft. below the ground surface in the TDA pit.

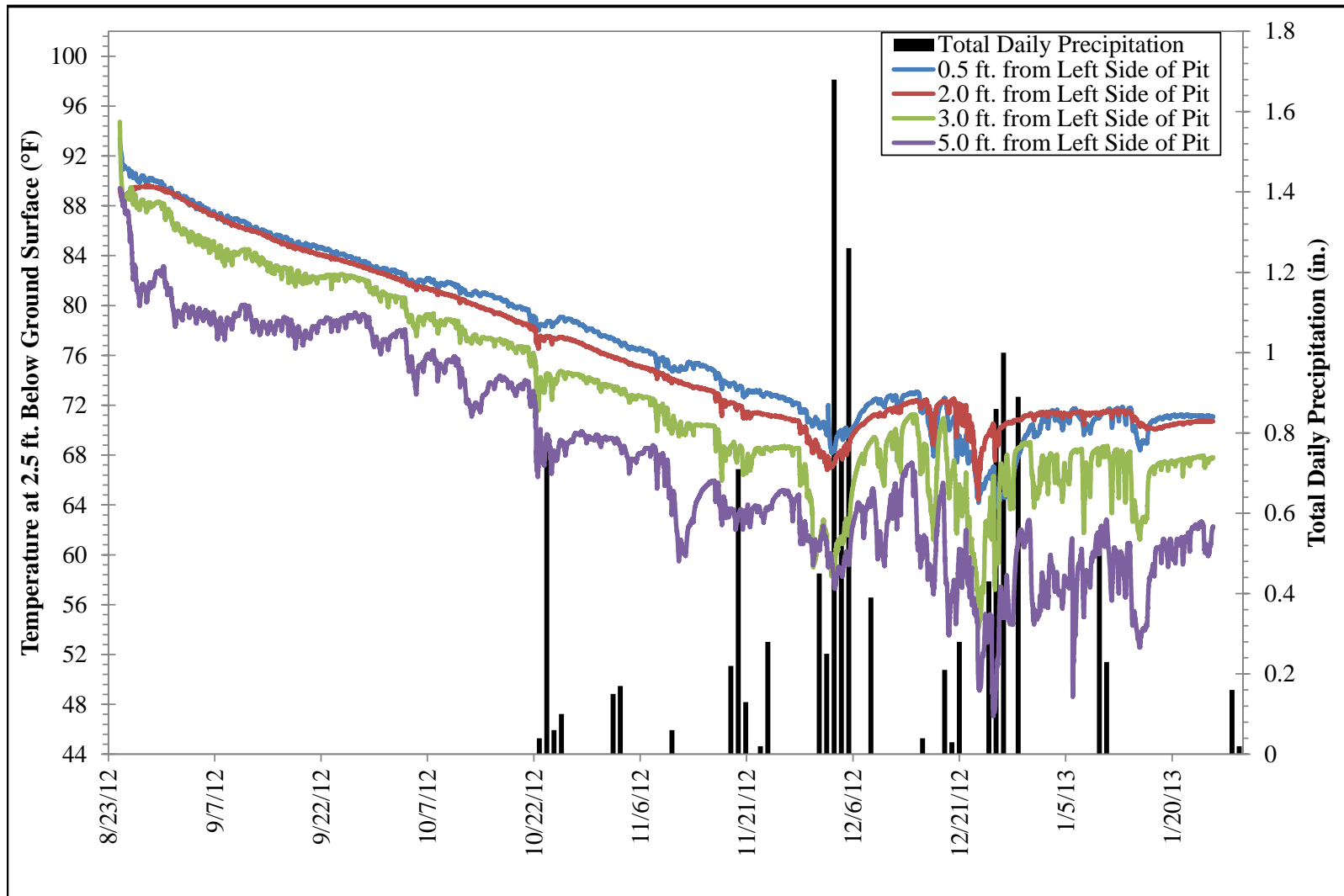


Figure E-3. Temperatures at 2.5 ft. below the ground surface in the TDA pit.

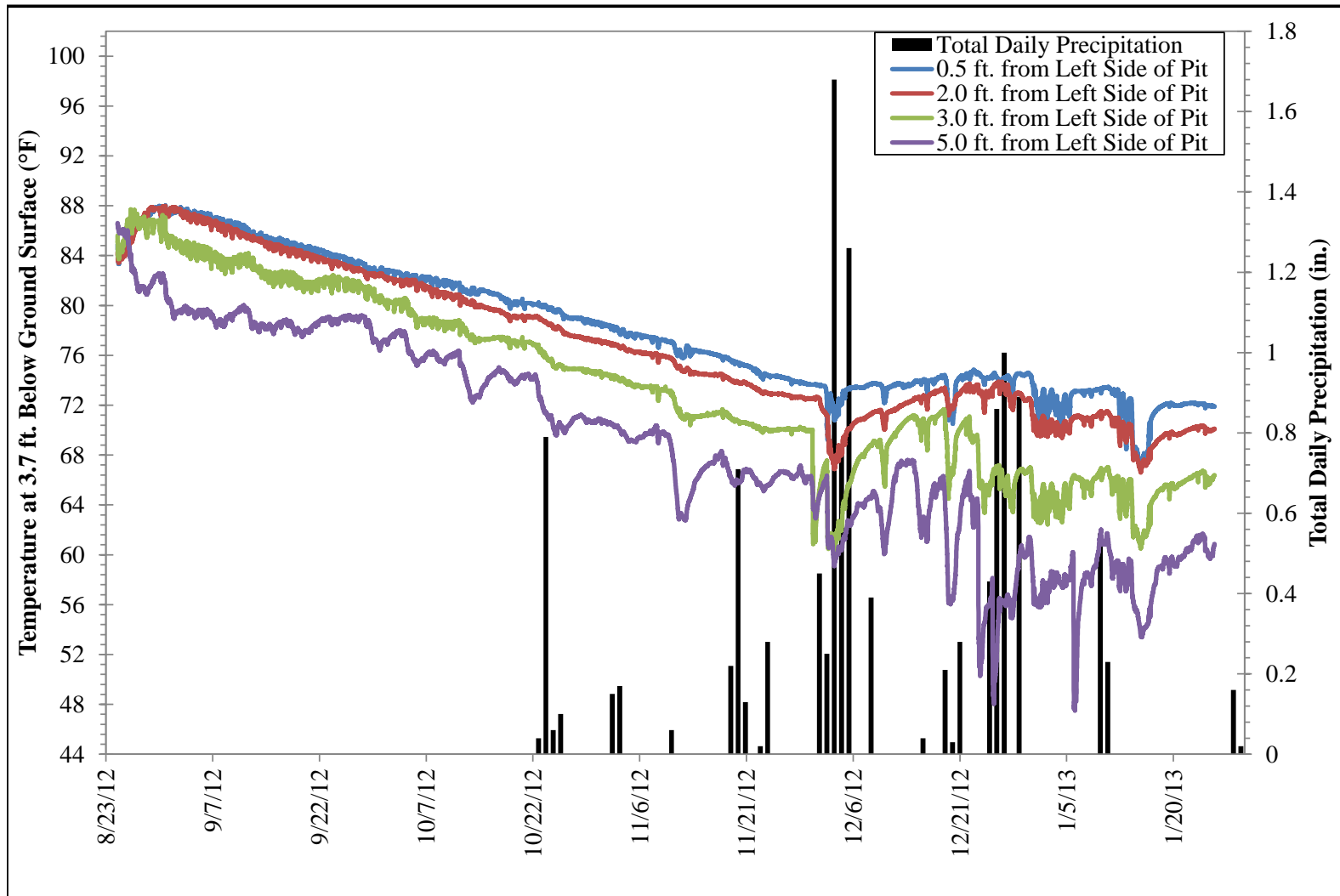


Figure E-4. Temperatures at 3.7 ft. below the ground surface in the TDA pit.

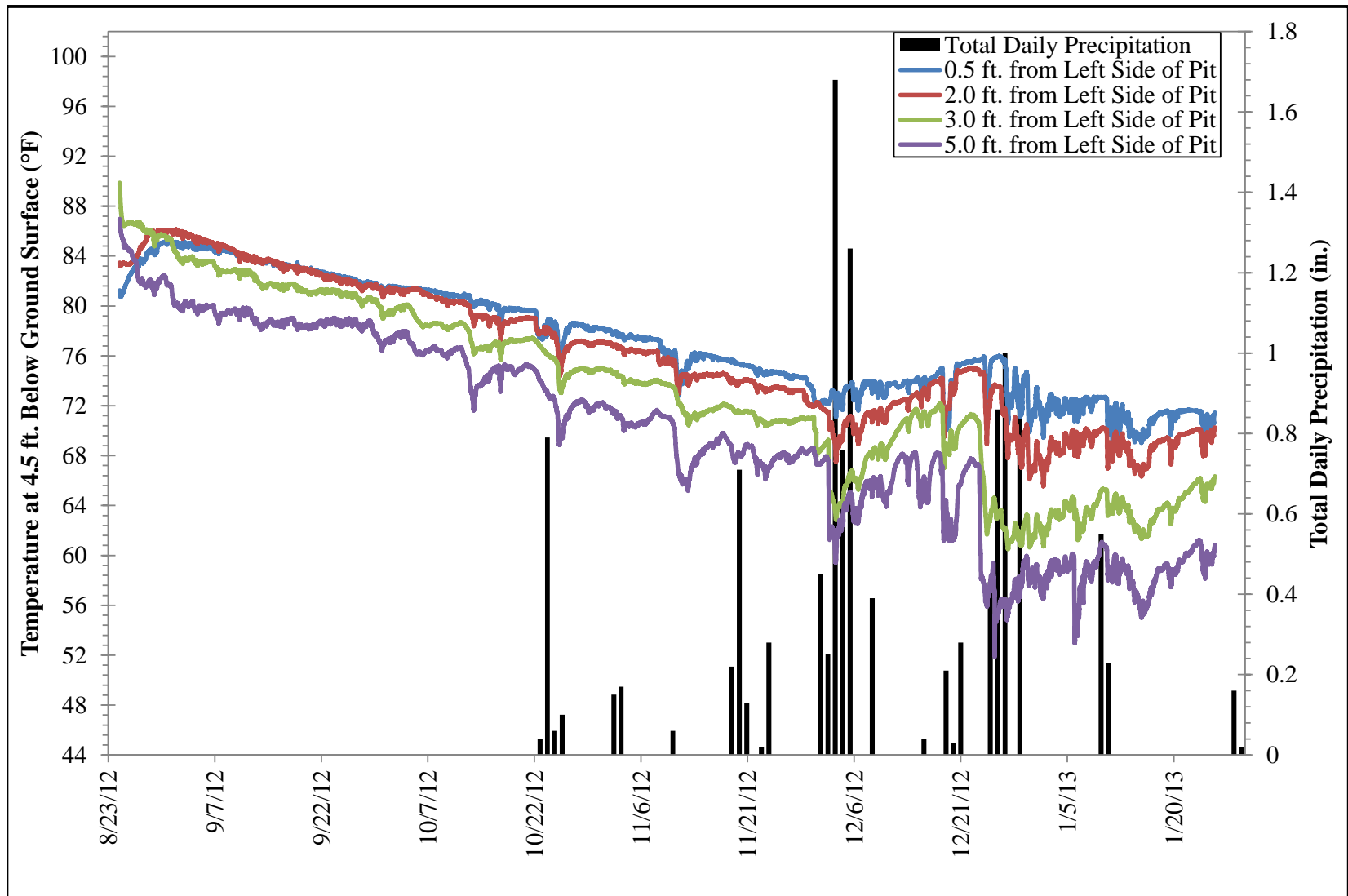


Figure E-5. Temperatures at 4.5 ft. below the ground surface in the TDA pit.

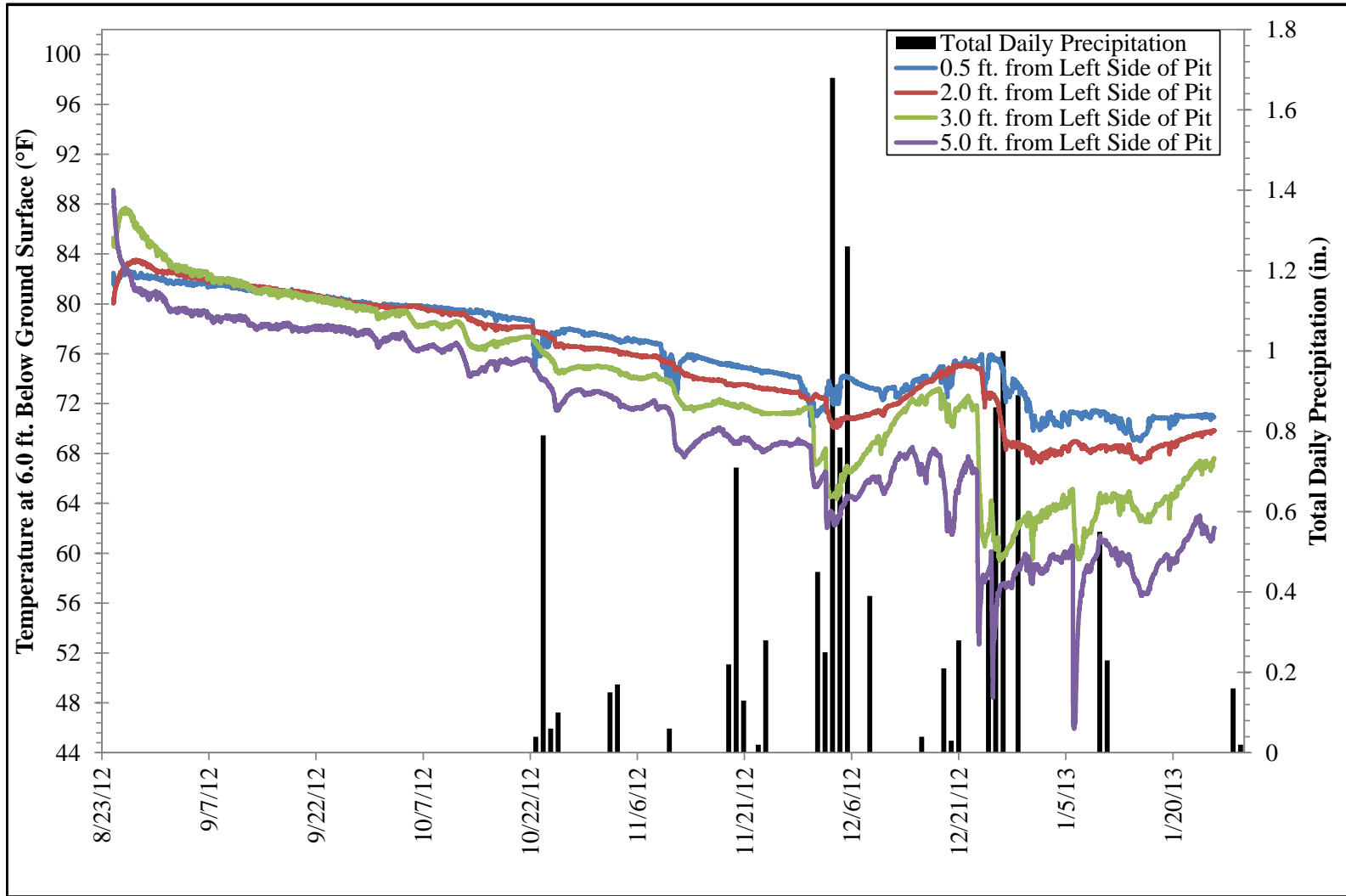


Figure E-6. Temperatures at 6.0 ft. below the ground surface in the TDA pit.

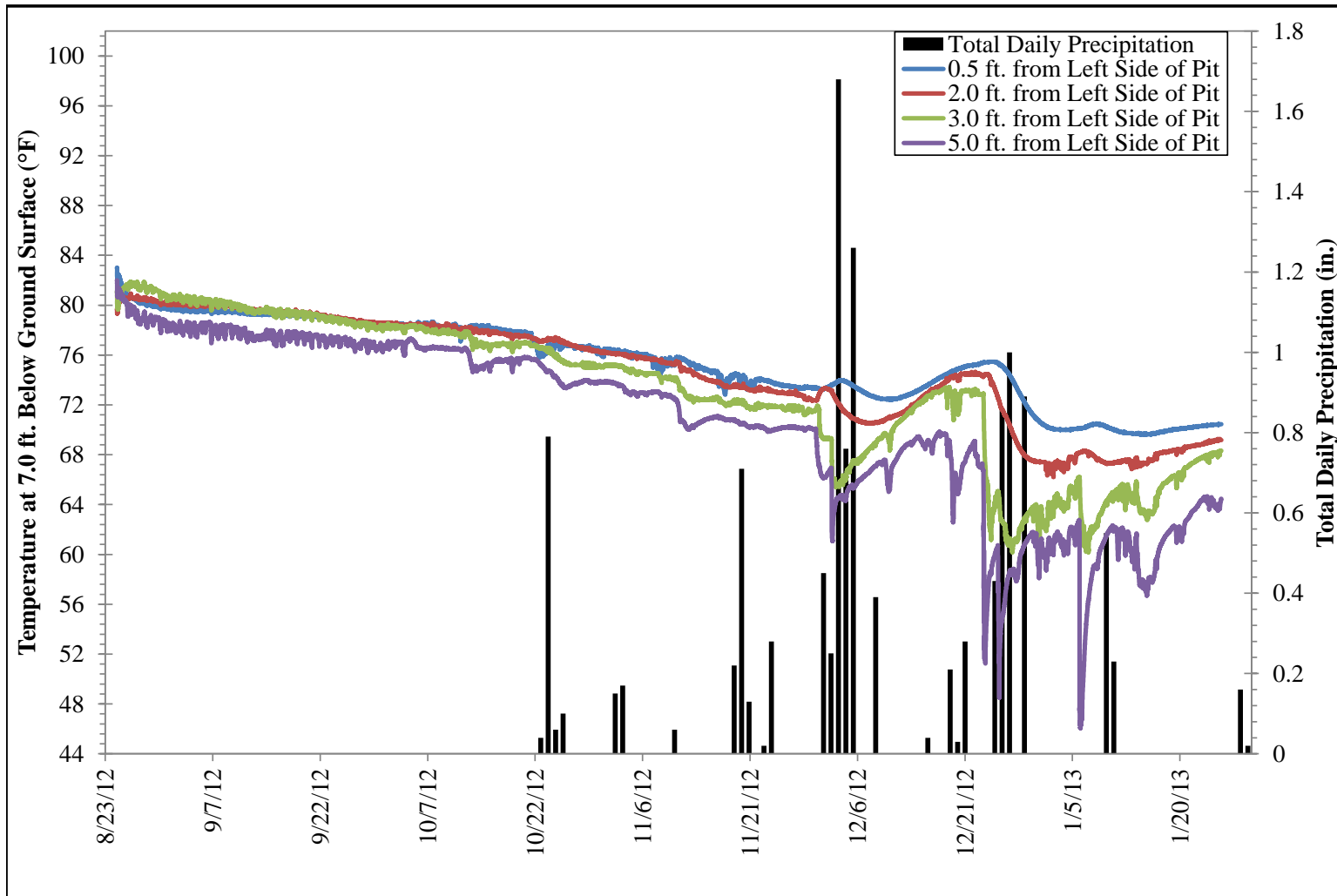


Figure E-7. Temperatures at 7.0 ft. below the ground surface in the TDA pit.

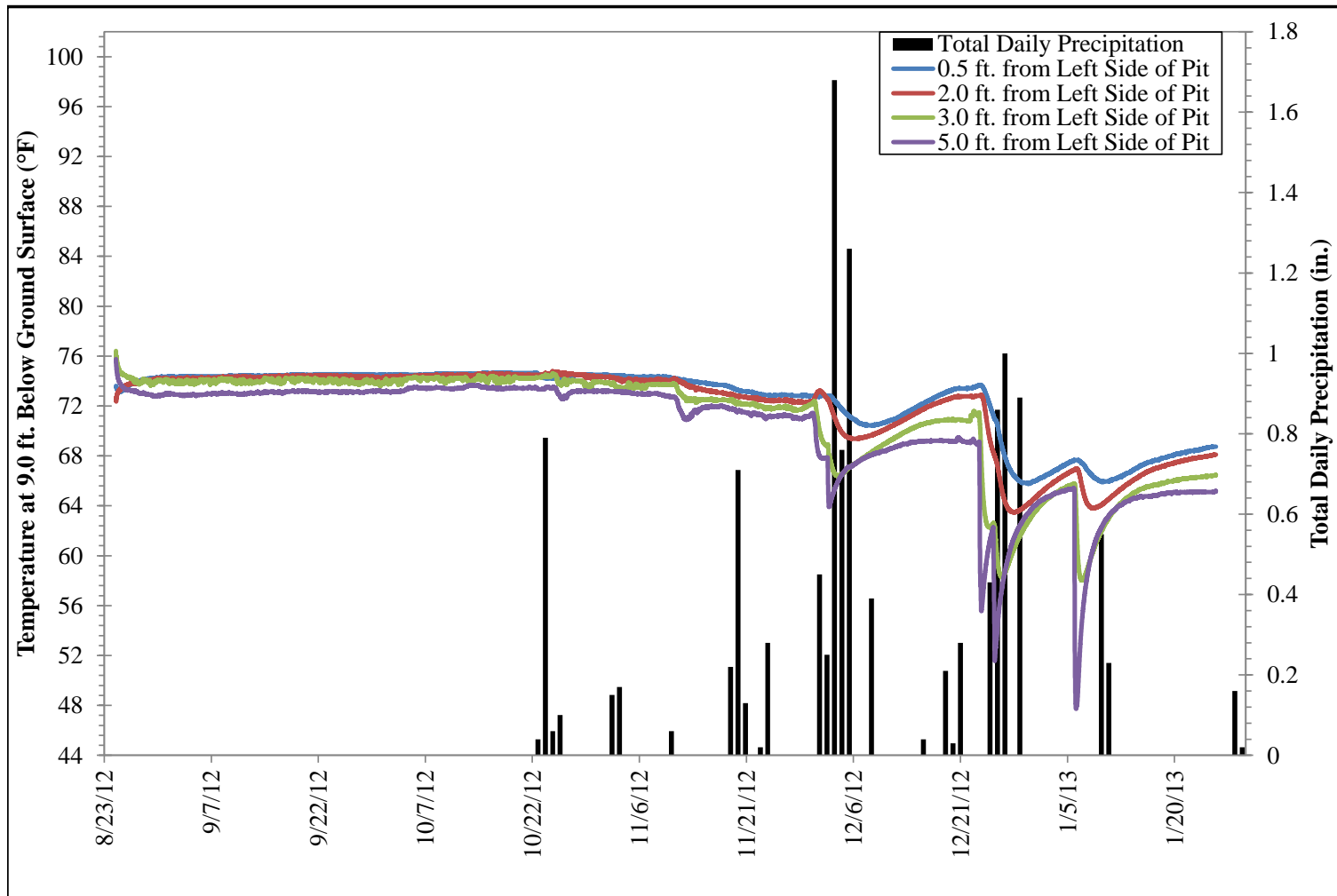


Figure E-8. Temperatures at 9.0 ft. below the ground surface in the TDA pit.